

UNIVERSITE DE YAOUNDE I

CENTRE DE RECHERCHE ET DE
FORMATION DOCTORALE EN
SCIENCE DE LA VIE, SANTE ET
ENVIRONNEMENT

UNITE DE RECHERCHE ET DE
FORMATION DOCTORALE
SCIENCES DE LA VIE

DEPARTEMENT DE BIOCHIMIE



UNIVERSITY OF YAOUNDE I

CENTRE FOR RESEARCH AND
TRAINING IN GRADUATE STUDIES
IN LIFE, HEALTH AND
ENVIRONMENTAL SCIENCE

RESEARCH AND DOCTORATE
TRAINING UNIT IN LIFE SCIENCE

DEPARTMENT OF BIOCHEMISTRY

DEPARTMENT OF BIOCHEMISTRY

DEPARTEMENT DE BIOCHIMIE

MOLECULAR PARASITOLOGY AND DISEASE VECTOR RESEARCH

LABORATOIRE DE PARASITOLOGY MOLECULAIRE ET DE VECTEURS DE MALADIES

Investigating the molecular basis and underlying
biochemical mechanisms of *CYP325A* as a pyrethroid
resistance gene in *Anopheles funestus*, a major malaria
vector across Africa

THESIS

submitted in Partial Fulfilment of the

Requirements for the Award of a Doctor of Philosophy Doctorate/Ph.D. in Biochemistry

Option: Biotechnology and Development

By

AMELIE WAMBA NDONGMO Regine

Matricule: 07R042

MSc. Biochemistry

Co-supervised by

Charles Sinclair Wondji
Professor, LSTM

Jude Daiga BIGOGA
Professor, UYI



Academic Year: 2022/2023

UNIVERSITY OF YAOUNDE I

FACULTY OF SCIENCES

Graduate Program for Life Sciences
Health and the Environment



UNIVERSITE DE YAOUNDE I

FACULTE DES SCIENCES

Centre de Recherche & de Formation Doctorale,
Science de la Vie, Sante & Environnement

DEPARTMENT OF BIOCHEMISTRY
DEPARTEMENT DE BIOCHIMIE

CERTIFICATE OF CORRECTION OF THE DOCTORAL THESIS
ATTESTATION DE CORRECTION DE LA THESE DE DOCTORAT

We, the undersigned Thesis Director, and Board of Assessors of the Doctorate/PhD thesis in Biochemistry entitled: **Investigating the molecular basis and underlying biochemical mechanisms of CYP325A as a pyrethroid resistance gene in Anopheles funestus, a major malaria vector across Africa** defended on January 6, 2022, by **Miss. AMELIE WAMBA NDONGMO Regine** - registration number 07R042, hereby certify that the candidate has completed the corrections of the above-mentioned thesis as requested by the Examiners.

We hereby certify that the Board of Assessors is satisfied with the corrections made and recommend that the Doctorate/PhD degree be awarded to the candidate.

Yaoundé, the 03 OCT 2023

Jury Member

NJIOKOU Flobert
Professor, University of
Yaoundé I

**Committee of Examiners
(Members)**

MBACHAM Wilfred FON
Professor,
University of Yaoundé I

Prof. Mbacham Wilfred Fon
MS, DS, ScD (Harvard), FAS, FCAS, FAAS
Public Health Biotechnologist

**President of Jury
Head of Biochemistry Department**

Moundipa Fewou Paul
MOUNDIPA FEWOU Paul,
Professor
University of Yaoundé I
(UYI)

**Supervisor and Thesis
Director (Rapporteurs)**


BIGOGA DAIGA Jude
Professor, UYI

WONDJI Charles Sinclair
Professor, LSTM

Charles Wondji
Professeur de Génétique / Etomologie Médicale
Liverpool School of Tropical Medicine, LSTM, Angleterre
Centre for Research in Infectious Diseases, CRID, Cameroon

GHOGOMU Stephen
Associate Professor,
University of Buea

Paul F. Moundipa
Paul F. MOUNDIPA
Professor
Enzymology & Toxicology

UNIVERSITÉ DE YAOUNDÉ I Faculté des Sciences Division de la Programmation et du Suivi des Activités Académiques		THE UNIVERSITY OF YAOUNDE I Faculty of Science Division of Programming and Follow-up of Academic Affairs
LISTE DES ENSEIGNANTS PERMANENTS		LIST OF PERMANENT TEACHING STAFF

ANNÉE ACADEMIQUE 2022/2023

(Par Département et par Grade)

DATE D'ACTUALISATION 31 MAI 2023

ADMINISTRATION

DOYEN : TCHOUANKEU Jean- Claude, *Maître de Conférences*

VICE-DOYEN / DPSAA: ATCHADE Alex de Théodore, *Professeur*

VICE-DOYEN / DSSE : NYEGUE Maximilienne Ascension, *Professeur*

VICE-DOYEN / DRC : ABOSSOLO ANGUE Monique, *Maître de Conférences*

Chef Division Administrative et Financière : NDOYE FOE Florentine Marie Chantal, *Maître de Conférences*

Chef Division des Affaires Académiques, de la Recherche et de la Scolarité DAARS : AJEAGAH Gideon AGHAINDUM, *Professeur*

1- DÉPARTEMENT DE BIOCHIMIE (BC) (43)

N°	NOMS ET PRÉNOMS	GRADE	OBSERVATIONS
1.	BIGOGA DAIGA Jude	Professeur	En poste
2.	FEKAM BOYOM Fabrice	Professeur	En poste
3.	KANSCI Germain	Professeur	En poste
4.	MBACHAM FON Wilfred	Professeur	En poste
5.	MOUNDIPA FEWOU Paul	Professeur	<i>Chef de Département</i>
6.	NGUEFACK Julienne	Professeur	En poste
7.	NJAYOU Frédéric Nico	Professeur	En poste
8.	OBEN Julius ENYONG	Professeur	En poste

9.	ACHU Merci BIH	Maître de Conférences	En poste
----	----------------	-----------------------	----------

10.	ATOUGHO Barbara MMA	Maître de Conférences	En poste
11.	AZANTSA KINGUE GABIN BORIS	Maître de Conférences	En poste
12.	BELINGA née NDOYE FOFÉ F. M. C.	Maître de Conférences	<i>Chef DAF / FS</i>
13.	DJUIDJE NGOUNOUÉ Marceline	Maître de Conférences	En poste
14.	DJUIKWO NKONGA Ruth Viviane	Maître de Conférences	En poste
15.	EFFA ONOMO Pierre	Maître de Conférences	<i>VD/FS/Univ Ebwa</i>
16.	EWANE Cécile Annie	Maître de Conférences	En poste
17.	KOTUE TAPTUE Charles	Maître de Conférences	En poste
18.	LUNGA Paul KEILAH	Maître de Conférences	En poste
19.	MBONG ANGIE M. Mary Anne	Maître de Conférences	En poste
20.	MOFOR née TEUGWA Clotilde	Maître de Conférences	<i>Doyen FS / UDs</i>
21.	NANA Louise épouse WAKAM	Maître de Conférences	En poste
22.	NGONDI Judith Laure	Maître de Conférences	En poste
23.	TCHANA KOUATCHOUA Angèle	Maître de Conférences	En poste

24.	AKINDEH MBUH NJI	Chargé de Cours	En poste
25.	BEBEE Fadimatou	Chargée de Cours	En poste
26.	BEBOY EDJENGUELE Sara Nathalie	Chargé de Cours	En poste
27.	DAKOLE DABOY Charles	Chargé de Cours	En poste
28.	DONGMO LEKAGNE Joseph Blaise	Chargé de Cours	En poste
29.	FONKOUA Martin	Chargé de Cours	En poste
30.	FOUPOUAPOUOGNIGNI Yacouba	Chargé de Cours	En poste
31.	KOUOH ELOMBO Ferdinand	Chargé de Cours	En poste
32.	MANANGA Marlyse Joséphine	Chargée de Cours	En poste
33.	OWONA AYISSI Vincent Brice	Chargé de Cours	En poste
34.	Palmer MASUMBE NETONGO	Chargé de Cours	En poste
35.	PECHANGOU NSANGOU Sylvain	Chargé de Cours	En poste
36.	WILFRED ANGIE ABIA	Chargé de Cours	En poste

37.	BAKWO BASSOGOG Christian Bernard	Assistant	En Poste
38.	ELLA Fils Armand	Assistant	En Poste
39.	EYENGA Eliane Flore	Assistant	En Poste
40.	MADIESSE KEMGNE Eugénie Aimée	Assistant	En Poste
41.	MANJIA NJIKAM Jacqueline	Assistant	En Poste
42.	MBOUCHE FANMOE Marceline Joëlle	Assistant	En poste

43.	WOGUIA Alice Louise	Assistant	En Poste
-----	---------------------	-----------	----------

2- DÉPARTEMENT DE BIOLOGIE ET PHYSIOLOGIE ANIMALES (BPA) (52)

1.	AJEAGAH Gideon AGHAINDUM	Professeur	<i>DAARS/FS</i>
2.	BILONG BILONG Charles-Félix	Professeur	<i>Chef de Département</i>
3.	DIMO Théophile	Professeur	En Poste
4.	DJIETO LORDON Champlain	Professeur	En Poste
5.	DZEUFJET DJOMENI Paul Désiré	Professeur	En Poste
6.	ESSOMBA née NTSAMA MBALA	Professeur	<i>CD et Vice Doyen/FMSB/UIYI</i>
7.	FOMENA Abraham	Professeur	En Poste
8.	KEKEUNOU Sévilor	Professeur	En poste
9.	NJAMEN Dieudonné	Professeur	En poste
10.	NJIOKOU Flobert	Professeur	En Poste
11.	NOLA Moïse	Professeur	En poste
12.	TAN Paul VERNYUY	Professeur	En poste
13.	TCHUEM TCHUENTE Louis Albert	Professeur	<i>Inspecteur de service / Coord.Progr./MINSANTE</i>
14.	ZEBAZE TOGOUET Serge Hubert	Professeur	En poste

15.	ALENE Désirée Chantal	Maître de Conférences	<i>Vice Doyen/ Uté Ebwa</i>
16.	BILANDA Danielle Claude	Maître de Conférences	En poste
17.	DJIOGUE Séfirin	Maître de Conférences	En poste
18.	GOUNOUE KAMKUMO Raceline épse FOTSING	Maître de Conférences	En poste
19.	JATSA BOUKENG Hermine épse MEGAPTCHÉ	Maître de Conférences	En Poste
20.	LEKEUFACK FOLEFACK Guy B.	Maître de Conférences	En poste
21.	MAHOB Raymond Joseph	Maître de Conférences	En poste
22.	MBENOUN MASSE Paul Serge	Maître de Conférences	En poste
23.	MEGNEKOU Rosette	Maître de Conférences	En poste
24.	MOUNGANG Luciane Marlyse	Maître de Conférences	En poste
25.	NOAH EWOTI Olive Vivien	Maître de Conférences	En poste
26.	MONY Ruth épse NTONE	Maître de Conférences	En Poste

27.	NGUEGUIM TSOFAK Florence	Maître de Conférences	En poste
28.	NGUEMBOCK	Maître de Conférences	En poste
29.	TAMSA ARFAO Antoine	Maître de Conférences	En poste
30.	TOMBI Jeannette	Maître de Conférences	En poste

31.	ATSAMO Albert Donatien	Chargé de Cours	En poste
32.	BASSOCK BAYIHA Etienne Didier	Chargé de Cours	En poste
33.	ETEME ENAMA Serge	Chargé de Cours	En poste
34.	FEUGANG YOUMSSI François	Chargé de Cours	En poste
35.	FOKAM Alvine Christelle Epse KENGNE	Chargé de Cours	En poste
36.	GONWOUO NONO Legrand	Chargé de Cours	En poste
37.	KANDEDA KAVAYE Antoine	Chargé de Cours	En poste
38.	KOGA MANG DOBARA	Chargé de Cours	En poste
39.	LEME BANOCK Lucie	Chargé de Cours	En poste
40.	MAPON NSANGOU Indou	Chargé de Cours	En poste
41.	METCHI DONFACK MIREILLE EL AIRE EPSE GHOLMO	Chargé de Cours	En poste
42.	MVEYO NDANKEU Yves Patrick	Chargé de Cours	En poste
43.	NGOUATEU KENFACK Omer Bébé	Chargé de Cours	En poste
44.	NJUA Clarisse YAFI	Chargée de Cours	<i>Chef Div. Uté Bamenda</i>
45.	NWANE Philippe Bienvenu	Chargé de Cours	En poste
46.	TADU Zephyrin	Chargé de Cours	En poste
47.	YEDE	Chargé de Cours	En poste
48.	YOUNOUSSA LAME	Chargé de Cours	En poste

49.	AMBADA NDZENGUE GEORGIA ELNA	Assistante	En poste
50.	KODJOM WANCHE Jacguy Joyce	Assistante	En poste
51.	NDENGUE Jean De Matha	Assistant	En poste
52.	ZEMO GAMO Franklin	Assistant	En poste

3- DÉPARTEMENT DE BIOLOGIE ET PHYSIOLOGIE VÉGÉTALES (BPV) (34)

1.	AMBANG Zachée	Professeur	<i>Chef de Département</i>
2.	DJOCGOUÉ Pierre François	Professeur	En poste
3.	MBOLO Marie	Professeur	En poste

AMELIE WAMBA NDONGMO Regine/Doctorate/Ph.D. Thesis/University of Yaoundé I

4.	MOSSEBO Dominique Claude	Professeur	En poste
5.	YOUMBI Emmanuel	Professeur	En poste
6.	ZAPFACK Louis	Professeur	En poste

7.	ANGONI Hyacinthe	Maître de Conférences	En poste
8.	BIYE Elvire Hortense	Maître de Conférences	En poste
9.	MAHBOU SOMO TOUKAM. Gabriel	Maître de Conférences	En poste
10.	MALA Armand William	Maître de Conférences	En poste
11.	MBARGA BINDZI Marie Alain	Maître de Conférences	<i>DAAC /UDla</i>
12.	NDONGO BEKOLO	Maître de Conférences	En poste
13.	NGALLE Hermine BILLE	Maître de Conférences	En poste
14.	NGODO MELINGUI Jean Baptiste	Maître de Conférences	En poste
15.	NGONKEU MAGAPTCHE Eddy L.	Maître de Conférences	<i>CT / MINRESI</i>
16.	TONFACK Libert Brice	Maître de Conférences	En poste
17.	TSOATA Esaïe	Maître de Conférences	En poste
18.	ONANA JEAN MICHEL	Maître de Conférences	En poste

19.	DJEUANI Astride Carole	Chargé de Cours	En poste
20.	GONMADGE CHRISTELLE	Chargée de Cours	En poste
21.	MAFFO MAFFO Nicole Liliane	Chargé de Cours	En poste
22.	NNANGA MEBENGA Ruth Laure	Chargé de Cours	En poste
23.	NOUKEU KOUAKAM Armelle	Chargé de Cours	En poste
24.	NSOM ZAMBO EPSE PIAL ANNIE CLAUDE	Chargé de Cours	<i>En détachement/UNESCO MALI</i>
25.	GODSWILL NTSOMBOH NTSEFONG	Chargé de Cours	En poste
26.	KABELONG BANAHOU Louis-Paul-Roger	Chargé de Cours	En poste
27.	KONO Léon Dieudonné	Chargé de Cours	En poste
28.	LIBALAH Moses BAKONCK	Chargé de Cours	En poste
29.	LIKENG-LI-NGUE Benoit C	Chargé de Cours	En poste
30.	TAEDOUNG Evariste Hermann	Chargé de Cours	En poste
31.	TEMEGNE NONO Carine	Chargé de Cours	En poste
32.	MANGA NDJAGA JUDE	Assistant	En poste
33.	DIDA LONTSI Sylvere Landry	Assistant	En poste

34.	METSEBING Blondo-Pascal	Assistant	En poste
-----	-------------------------	-----------	----------

4- DÉPARTEMENT DE CHIMIE INORGANIQUE (CI) (28)

1.	GHOGOMU Paul MINGO	Professeur	<i>Ministre Chargé de Mission PR</i>
2.	NANSEU NJIKI Charles Péguy	Professeur	En poste
3.	NDIFON Peter TEKE	Professeur	<i>CT MINRESI</i>
4.	NENWA Justin	Professeur	En poste
5.	NGAMENI Emmanuel	Professeur	<i>Doyen FS Univ.Ngaoundere</i>
6.	NGOMO Horace MANGA	Professeur	<i>Vice Chancellor/UB</i>
7.	NJOYA Dayirou	Professeur	En poste

8.	ACAYANKA Elie	Maître de Conférences	En poste
9.	EMADAK Alphonse	Maître de Conférences	En poste
10.	KAMGANG YOUBI Georges	Maître de Conférences	En poste
11.	KEMMEGNE MBOUGUEM Jean C.	Maître de Conférences	En poste
12.	KENNE DEDZO GUSTAVE	Maître de Conférences	En poste
13.	MBEY Jean Aime	Maître de Conférences	En poste
14.	NDI NSAMI Julius	Maître de Conférences	<i>Chef de Département</i>
15.	NEBAH Née NDO SIRI Bridget NDOYE	Maître de Conférences	<i>Sénatrice/SENAT</i>
16.	NJIOMOU C. épse DJANGANG	Maître de Conférences	En poste
17.	NYAMEN Linda Dyorisse	Maître de Conférences	En poste
18.	PABOUDAM GBAMBIE AWAWOU	Maître de Conférences	En poste
19.	TCHAKOUTE KOUAMO Hervé	Maître de Conférences	En poste
20.	BELIBI BELIBI Placide Désiré	Maître de Conférences	<i>Chef Service/ ENS Bertoua</i>
21.	CHEUMANI YONA Arnaud M.	Maître de Conférences	En poste
22.	KOUOTOU DAOUDA	Maître de Conférences	En poste

23.	MAKON Thomas Beauregard	Chargé de Cours	En poste
24.	NCHIMI NONO KATIA	Chargée de Cours	En poste

25.	NJANKWA NJABONG N. Eric	Chargé de Cours	En poste
26.	PATOUOSSA ISSOFA	Chargé de Cours	En poste
27.	SIEWE Jean Mermoz	Chargé de Cours	En Poste
28.	BOYOM TATCHEMO Franck W.	Assistant	En Poste

5- DÉPARTEMENT DE CHIMIE ORGANIQUE (CO) (37)

1.	Alex de Théodore ATCHADE	Professeur	<i>Vice-Doyen / DPSAA</i>
2.	DONGO Etienne	Professeur	<i>Vice-Doyen/FSE/UIYI</i>
3.	NGOUELA Silvère Augustin	Professeur	<i>Chef de Département UDS</i>
4.	PEGNYEMB Dieudonné Emmanuel	Professeur	<i>Directeur/ MINESUP/ Chef de Département</i>
5.	WANDJI Jean	Professeur	En poste
6.	MBAZOA née DJAMA Céline	Professeur	En poste

7.	AMBASSA Pantaléon	Maître de Conférences	En poste
8.	EYONG Kenneth OBEN	Maître de Conférences	En poste
9.	FOTSO WABO Ghislain	Maître de Conférences	En poste
10.	KAMTO Eutrophe Le Doux	Maître de Conférences	En poste
11.	KENMOGNE Marguerite	Maître de Conférences	En poste
12.	KEUMEDJIO Félix	Maître de Conférences	En poste
13.	KOUAM Jacques	Maître de Conférences	En poste
14.	MKOUNGA Pierre	Maître de Conférences	En poste
15.	MVOT AKAK CARINE	Maître de Conférences	En poste
16.	NGO MBING Joséphine	Maître de Conférences	<i>Chef de Cellule MINRESI</i>
17.	NGONO BIKOBO Dominique Serge	Maître de Conférences	<i>C.E.A/ MINESUP</i>
18.	NOTE LOUGBOT Olivier Placide	Maître de Conférences	<i>DAAC/Uté Bertoua</i>
19.	NOUNGOUE TCHAMO Diderot	Maître de Conférences	En poste
20.	TABOPDA KUATE Turibio	Maître de Conférences	En poste
21.	TAGATSING FOTSING Maurice	Maître de Conférences	En poste
22.	TCHOUANKEU Jean-Claude	Maître de Conférences	<i>Doyen /FS/ UYI</i>
23.	YANKEP Emmanuel	Maître de Conférences	En poste

24.	ZONDEGOUMBA Ernestine	Maître de Conférences	En poste
-----	-----------------------	-----------------------	----------

25.	MESSI Angélique Nicolas	Chargé de Cours	En poste
26.	NGNINTEDO Dominique	Chargé de Cours	En poste
27.	NGOMO Orléans	Chargée de Cours	En poste
28.	NONO NONO Éric Carly	Chargé de Cours	En poste
29.	OUAHOUE WACHE Blandine M.	Chargée de Cours	En poste
30.	OUETE NANTCHOUANG Judith Laure	Chargée de Cours	En poste
31.	SIELINOUE TEDJON Valérie	Chargé de Cours	En poste
32.	TCHAMGOUE Joseph	Chargé de Cours	En poste
33.	TSAFFACK Maurice	Chargé de Cours	En poste
34.	TSAMO TONTSA Armelle	Chargé de Cours	En poste
35.	TSEMEUGNE Joseph	Chargé de Cours	En poste

36.	MUNVERA MFIFEN Aristide	Assistant	En poste
37.	NDOGO ETEME Olivier	Assistant	En poste

6- DÉPARTEMENT D'INFORMATIQUE (IN) (22)

1.	ATSA ETOUNDI Roger	Professeur	<i>Chef de Division MINESUP</i>
2.	FOUDA NDJODO Marcel Laurent	Professeur	<i>Inspecteur Général/ MINESUP</i>

3.	NDOUNDAM René	Maître de Conférences	En poste
4.	TSOPZE Norbert	Maître de Conférences	En poste

5.	ABESSOLO ALO'O Gislain	Chargé de Cours	<i>Chef de Cellule MINFOPRA</i>
6.	AMINOU HALIDOU	Chargé de Cours	<i>Chef de Département</i>
7.	DJAM XAVIERA YOUH - KIMBI	Chargé de Cours	En Poste
8.	DOMGA KOMGUEM Rodrigue	Chargé de Cours	En poste
9.	EBELE SERGE ALAIN	Chargé de Cours	En poste
10.	HAMZA ADAMOU	Chargé de Cours	En poste
11.	JIOMEKONG AZANZI Fidel	Chargé de Cours	En poste
12.	KOUOKAM KOUOKAM E. A.	Chargé de Cours	En poste
13.	MELATAGIA YONTA Paulin	Chargé de Cours	En poste
14.	MESSI NGUELE Thomas	Chargé de Cours	En poste
15.	MONTHE DJIADEU Valery M.	Chargé de Cours	En poste
16.	NZEKON NZEKO'O ARMEL JACQUES	Chargé de Cours	En poste
17.	OLLE OLLE Daniel Claude Georges Delort	Chargé de Cours	<i>Sous-Directeur ENSET Ebolowa</i>
18.	TAPAMO Hyppolite	Chargé de Cours	En poste

19.	BAYEM Jacques Narcisse	Assistant	En poste
20.	EKODECK Stéphane Gaël Raymond	Assistant	En poste
21.	MAKEMBE. S . Oswald	Assistant	<i>Directeur CUTI</i>
22.	NKONDOCK. MI. BAHANACK.N.	Assistant	En poste

7- DÉPARTEMENT DE MATHÉMATIQUES (MA) (33)

1.	AYISSI Raoult Domingo	Professeur	<i>Chef de Département</i>
----	-----------------------	------------	----------------------------

2.	KIANPI Maurice	Maître de Conférences	En poste
3.	MBANG Joseph	Maître de Conférences	En poste
4.	MBEHOU Mohamed	Maître de Conférences	En poste
5.	MBELE BIDIMA Martin Ledoux	Maître de Conférences	En poste
6.	NOUNDJEU Pierre	Maître de Conférences	<i>Chef Service des Programmes & Diplômes/FS/UYI</i>
7.	TAKAM SOH Patrice	Maître de Conférences	En poste
8.	TCHAPNDA NJABO Sophonie B.	Maître de Conférences	<i>Directeur/AIMS Rwanda</i>
9.	TCHOUNDJA Edgar Landry	Maître de Conférences	En poste

10.	AGHOUKENG JIOFACK Jean Gérard	Chargé de Cours	<i>Chef Cellule MINEPAT</i>
11.	BOGSO ANTOINE Marie	Chargé de Cours	En poste
12.	CHENDJOU Gilbert	Chargé de Cours	En poste
13.	DJIADEU NGAHA Michel	Chargé de Cours	En poste
14.	DOUANLA YONTA Herman	Chargé de Cours	En poste
15.	KIKI Maxime Armand	Chargé de Cours	En poste
16.	LOUMNGAM KAMGA Victor	Chargé de Cours	En poste
17.	MBAKOP Guy Merlin	Chargé de Cours	En poste
18.	MBATAKOU Salomon Joseph	Chargé de Cours	En poste
19.	MENGUE MENGUE David Joël	Chargé de Cours	<i>Chef Dpt /ENS Université d'Ebolowa</i>
20.	MBIAKOP Hilaire George	Chargé de Cours	En poste
21.	NGUEFACK Bernard	Chargé de Cours	En poste
22.	NIMPA PEFOUKEU Romain	Chargée de Cours	En poste
23.	OGADOA AMASSAYOGA	Chargée de Cours	En poste
24.	POLA DOUNDOU Emmanuel	Chargé de Cours	<i>En stage</i>
25.	TCHEUTIA Daniel Duviol	Chargé de Cours	En poste
26.	TETSADJIO TCHILEPECK M. Eric.	Chargé de Cours	En poste

27.	BITYE MVONDO Esther Claudine	Assistante	En poste
28.	FOKAM Jean Marcel	Assistant	En poste

29.	GUIDZAVAI KOUCHERE Albert	Assistant	En poste
30.	MANN MANYOMBE Martin Luther	Assistant	En poste
31.	MEFENZA NOUNTU Thiery	Assistant	En poste
32.	NYOUMBI DLEUNA Christelle	Assistant	En poste
33.	TENKEU JEUFACK Yannick Léa	Assistant	En poste

8- DÉPARTEMENT DE MICROBIOLOGIE (MIB) (24)

1.	ESSIA NGANG Jean Justin	Professeur	<i>Chef de Département</i>
2.	NYEGUE Maximilienne Ascension	Professeur	<i>VICE-DOYEN / DSSE</i>

3.	ASSAM ASSAM Jean Paul	Maître de Conférences	En poste
4.	BOUGNOM Blaise Pascal	Maître de Conférences	En poste
5.	BOYOMO ONANA	Maître de Conférences	En poste
6.	KOUITCHEU MABEKU Epse KOUAM Laure Brigitte	Maître de Conférences	En poste
7.	RIWOM Sara Honorine	Maître de Conférences	En poste
8.	NJIKI BIKOÏ Jacky	Maître de Conférences	En poste
9.	SADO KAMDEM Sylvain Leroy	Maître de Conférences	En poste

10.	ESSONO Damien Marie	Chargé de Cours	En poste
11.	LAMYE Glory MOH	Chargé de Cours	En poste
12.	MEYIN A EBONG Solange	Chargé de Cours	En poste
13.	MONI NDEDI Esther Del Florence	Chargé de Cours	En poste
14.	NKOUDOU ZE Nardis	Chargé de Cours	En poste
15.	TAMATCHO KWEYANG Blandine Pulchérie	Chargé de Cours	En poste
16.	TCHIKOUA Roger	Chargé de Cours	<i>Chef de Service de la Scolarité</i>
17.	TOBOLBAÏ Richard	Chargé de Cours	En poste

18.	NKOUÉ TONG Abraham	Assistant	En poste
19.	SAKE NGANE Carole Stéphanie	Assistant	En poste
20.	EZO'O MENGO Fabrice Télésfor	Assistant	En poste

21.	EHETH Jean Samuel	Assistant	En poste
22.	MAYI Marie Paule Audrey	Assistant	En poste
23.	NGOUEMAM Romial Joël	Assistant	En poste
24.	NJAPNDOUNKE Bilkissou	Assistant	En poste

9. DEPARTEMENT DE PYSIQUE(PHY) (43)

1.	BEN- BOLIE Germain Hubert	Professeur	En poste
2.	DJUIDJE KENMOE épouse ALOYEM	Professeur	En poste
3.	EKOBENA FOUA Henri Paul	Professeur	<i>Vice-Recteur. Uté Ngaoundéré</i>
4.	ESSIMBI ZOBO Bernard	Professeur	En poste
5.	HONA Jacques	Professeur	En poste
6.	NANA ENGO Serge Guy	Professeur	En poste
7.	NANA NBENDJO Blaise	Professeur	En poste
8.	NDJAKA Jean Marie Bienvenu	Professeur	<i>Chef de Département</i>
9.	NJANDJOCK NOUCK Philippe	Professeur	En poste
10.	NOUAYOU Robert	Professeur	En poste
11.	SAIDOU	Professeur	<i>Chef de centre/IRGM/MINRESI</i>
12.	TABOD Charles TABOD	Professeur	<i>Doyen FSUniv/Bda</i>
13.	TCHAWOUA Clément	Professeur	En poste
14.	WOAFO Paul	Professeur	En poste
15.	ZEKENG Serge Sylvain	Professeur	En poste
16.	BIYA MOTTO Frédéric	Maître de Conférences	<i>DG/HYDRO Mekin</i>
17.	BODO Bertrand	Maître de Conférences	En poste
18.	ENYEGUE A NYAM épse BELINGA	Maître de Conférences	En poste
19.	EYEBE FOUA Jean sire	Maître de Conférences	En poste
20.	FEWO Serge Ibraïd	Maître de Conférences	En poste
21.	MBINACK Clément	Maître de Conférences	En poste
22.	MBONO SAMBA Yves Christian U.	Maître de Conférences	En poste
23.	MELI'I Joelle Larissa	Maître de Conférences	En poste

24.	MVOGO ALAIN	Maître de Conférences	En poste
25.	NDOP Joseph	Maître de Conférences	En poste
26.	SIEWE SIEWE Martin	Maître de Conférences	En poste
27.	SIMO Elie	Maître de Conférences	En poste
28.	VONDOU Derbetini Appolinaire	Maître de Conférences	En poste
29.	WAKATA née BEYA Annie Sylvie	Maître de Conférences	<i>Directeur/ENS/UII</i>
30.	WOULACHE Rosalie Laure	Maître de Conférence	<i>En stage depuis février 2023</i>
31.	ABDOURAHIMI	Chargé de Cours	En poste
32.	AYISSI EYEBE Guy François Valérie	Chargé de Cours	En poste
33.	CHAMANI Roméo	Chargé de Cours	En poste
34.	DJIOTANG TCHOTCHOU Lucie Angennes	Chargée de Cours	En poste
35.	EDONGUE HERVAIS	Chargé de Cours	En poste
36.	FOUEJIO David	Chargé de Cours	<i>Chef Cell. MINADER</i>
37.	KAMENI NEMATCHOUA Modeste	Chargé de Cours	En poste
38.	LAMARA Maurice	Chargé de Cours	En poste
39.	OTTOU ABE Martin Thierry	Chargé de Cours	Directeur Unité de production des réactifs/IMPM
40.	TEYOU NGOUPO Ariel	Chargé de Cours	En poste
41.	WANDJI NYAMSI William	Chargé de Cours	En poste
42.	NGA ONGODO Dieudonné	Assistant	En poste
43.	SOUFFO TAGUEU Merimé	Assistant	En poste

10- DÉPARTEMENT DE SCIENCES DE LA TERRE (ST) (42)

1.	BITOM Dieudonné-Lucien	Professeur	<i>Doyen / FASA /UDs</i>
2.	NDAM NGOUPAYOU Jules-Remy	Professeur	En poste
3.	NDJIGUI Paul-Désiré	Professeur	<i>Chef de Département</i>
4.	NGOS III Simon	Professeur	En poste
5.	NKOUMBOU Charles	Professeur	En poste
6.	NZENTI Jean-Paul	Professeur	En poste
7.	ONANA Vincent Laurent	Professeur	<i>Chef de Département/Uté. Eb.</i>
8.	YENE ATANGANA Joseph Q.	Professeur	<i>Chef Div. /MINTP</i>

9.	ABOSSOLO née ANGUE Monique	Maître de Conférences	<i>Vice-Doyen / DRC</i>
10.	BISSO Dieudonné	Maître de Conférences	En poste
11.	EKOMANE Emile	Maître de Conférences	<i>Chef Div./Uté Ebolowa</i>
12.	Elisé SABABA	Maitre de Conférences	En poste
13.	FUH Calistus Gentry	Maître de Conférences	<i>Sec. d'Etat/MINMIDT</i>
14.	GANNO Sylvestre	Maître de Conférences	En poste
15.	GHOGOMU Richard TANWI	Maître de Conférences	<i>Chef de Div. /Uté Bertoua</i>
16.	MBIDA YEM	Maitre de Conférences	En poste
17.	MOUNDI Amidou	Maître de Conférences	<i>CT/MINIMDT</i>
18.	NGO BIDJECK Louise Marie	Maître de Conférences	En poste
19.	NGUEUTCHOUA Gabriel	Maître de Conférences	<i>CEA/MINRESI</i>
20.	NJILAH Isaac KONFOR	Maître de Conférences	En poste
21.	NYECK Bruno	Maître de Conférences	En poste
22.	TCHAKOUNTE Jacqueline épouse NUMBEM	Maître de Conférences	<i>Chef. Cell /MINRESI</i>
23.	TCHOUANKOUE Jean-Pierre	Maître de Conférences	En poste
24.	TEMGA Jean Pierre	Maître de Conférences	En poste
25.	ZO'O ZAME Philémon	Maître de Conférences	<i>DG/ART</i>

26.	ANABA ONANA Achille Basile	Chargé de Cours	En poste
27.	BEKOA Etienne	Chargé de Cours	En poste
28.	ESSONO Jean	Chargé de Cours	En poste
29.	EYONG John TAKEM	Chargé de Cours	En poste
30.	MAMDEM TAMTO Lionelle Estelle, épouse BITOM	Chargée de Cours	En poste
31.	MBESSE Cécile Olive	Chargée de Cours	En poste
32.	METANG Victor	Chargé de Cours	En poste
33.	MINYEM Dieudonné	Chargé de Cours	<i>Chef Serv./Uté Maroua</i>
34.	NGO BELNOUN Rose Noël	Chargée de Cours	En poste
35.	NOMO NEGUE Emmanuel	Chargé de Cours	En poste
36.	NTSAMA ATANGANA Jacqueline	Chargée de Cours	En poste
37.	TCHAPTCHET TCHATO De P.	Chargé de Cours	En poste
38.	TEHNA Nathanaël	Chargé de Cours	En poste
39.	FEUMBA Roger	Chargé de Cours	En poste
40.	MBANGA NYOBE Jules	Chargé de Cours	En poste

41.	KOAH NA LEBOGO Serge Parfait	Assistant	En poste
42.	NGO'O ZE ARNAUD	Assistant	En poste
43.	TENE DJOUKAM Joëlle Flore, épouse KOUANKAP NONO	Assistante	En poste

Répartition chiffrée des Enseignants de la Faculté des Sciences de l'Université de Yaoundé I

NOMBRE D'ENSEIGNANTS

DÉPARTEMENT	Professeurs	Maîtres de Conférences	Chargés de Cours	Assistants	Total
BCH	8 (01)	15 (11)	13 (03)	7 (05)	43 (20)
BPA	14 (01)	16 (09)	18 (04)	4 (02)	52 (16)
BPV	6 (01)	12 (02)	13 (07)	3 (00)	34 (10)
CI	7 (01)	15 (04)	5 (01)	1 (00)	28 (06)
CO	6 (01)	18 (04)	11 (04)	2 (00)	37 (09)
IN	2 (00)	2 (00)	14 (01)	4 (00)	22 (01)
MAT	1 (00)	8 (00)	17 (01)	7 (02)	33 (03)
MIB	2 (01)	7 (03)	8 (04)	7 (02)	24 (10)
PHY	15 (01)	15 (04)	11 (01)	2 (00)	43 (06)
ST	8 (00)	17 (03)	15 (04)	3 (01)	43 (08)
Total	69 (07)	125 (40)	125 (30)	40 (12)	359 (89)

Soit un total de **359 (89)** dont :

- Professeurs **69 (07)**
- Maîtres de Conférences **125 (40)**
- Chargés de Cours **125 (30)**
- Assistants **40 (12)**

() = Nombre de Femmes **89**

TO

The memory of and in tribute to my father Mr. NDONGMO Joseph

DEDICATION

TO

My sweet and loving mother, Mrs. NONGNI Celine

ACKNOWLEDGEMENTS

This research work was carried out at the Centre for Research in Infectious Diseases (CRID), Yaoundé, and the Department of Vector Biology at the Liverpool School of Tropical Medicine (LSTM), Liverpool, United Kingdom with the collaboration of the Molecular Parasitology and Disease Vector Research Laboratory of the Biotechnology Centre (BTC), University of Yaoundé I. It was made possible thanks to the unwavering support of several people whom I am immensely pleased to thank here:

Prof Charles S. WONDJI, my thesis co-supervisor, for awarding me a Ph.D. scholarship from his Wellcome Trust funding and accepting me into his team at CRID where he facilitated this research work. I am especially thankful for the expertise and technical platform provided at CRID and at the LSTM in the UK where I did part of my research work with his team there. Despite his multiple responsibilities, he was always there when I needed his guidance towards the smooth running and finalization of this work. Find in these words the expression of my deep gratitude and best regards. ‘Thank you, Sir, for your energy, for your availability, for the scientific rigor, work ethic, and diligence in research work. You are a role model to me, and I have the honor to be a part of your Research Team. I will never find enough words to express my gratitude for everything you taught me and the opportunities you made available for me’.

Prof Jude D. BIGOGA, my thesis co-supervisor for accepting to supervise my Ph.D. work. I remember this sentence he said when I walked into his office after being awarded the scholarship in 2017 to ask for his supervision of my Ph.D. work, he said: “I have decided not to take more students at the moment, but I’ll make an exception for you because of your diligence in acquiring the scholarship”. He led my first steps in research during my Master's, believed in me, was patient with me, and instilled in me a deep love for research to improve living and health conditions in our communities.

Thank you to the members of the jury and external reviewers who dutifully examined this research work. Their many reviews and recommendations will improve the content, and context form of the final document.

My gratitude also goes to Dr. Mark PAINE from the Liverpool School of Tropical Medicine (LSTM), UK for providing the cytochrome P450 expression plasmid pCWori+ without which the *in vitro* part of my research work was not going to be possible.

Prof Paul FEWOU MOUNDIPA, Head of the Department of Biochemistry, and all the teachers of the said Department, for having spared no effort to ensure my academic training, for having actively participated in this work through many constructive suggestions and criticisms in the various doctoral seminars (proposal, progress report and pre-defense presentations).

Dr. Ibrahim Sadi Sulaiman (LSTM) and Dr. Michael Kusimo (Sheffield) for their precious help in the supervision of my bench work at the LSTM and CRID respectively. I am grateful for their tutelage and continue to learn from their amazing research contributions.

Miss FORGWE Kizita and Miss FORGWE Alma for their immense support in returning to school after a break which allowed the advancement and completion of my Ph.D. work.

I thank all my classmates and seniors, I am thinking of Ruth SANDEU, GHOMSI Pierre Gilbert, TCHATAT Brice, EBOGO, Mrs. KOUAMO Mersimine, DJONABAYE Desire, Dr. TCHOUAKUI Magellan, Mr. TEDJOU Arnel, Mr. BAHUN-WILSON Theodel, Dr. NAKEBANG Amen, thank you for all these moments of conviviality spent together. Our numerous discussions, seminars, and presentations at the Laboratory have enabled me to acquire other knowledge in the field of Biochemistry.

The 'OTHERS' Ph.D. students at CRID namely MAFFO Claudine, BOUAKA Calmes, SADO Francine, DJONABAYE Desire, FOTSO Yvan, ASHU Fred, NKEMGHO Francis and AMBADIANG Mae for sharing same office space and assisting me immensely especially encouraging me during difficult moments.

My brothers and sisters who have continued to support me financially and morally during all these years of research and I'd like to mention MAFFO Berthe, SONGONG Marilyne, DEMEFOR Mark, JIOKENG Blanche, MOMO Evelyne, GUEDIA Alida, and MBONGNIN Aristide. Also my maternal uncle Papa Emmanuel in Abidjan for his financial support.

My childhood and hustling friends notably Mr. NDASI Edwin, Dr. PENN Amah, Mr. ACHOMBOM George, Major FONGHA Henry, Mr. ITOE Molimo, and Dr. TOKAM Alain.

Gratitude to the entire CRID family and team with whom I spent four years during this work. I am grateful for their assistance, company, encouragement, and tutelage all through these years.

To all the people I haven't named here who have participated in some way or another in the completion of this thesis, I say thank you very much.

ABSTRACT

The overexpression and overactivity of key cytochrome P450s (CYP450) genes are major drivers of metabolic resistance to insecticides in African malaria vectors such as *Anopheles funestus* s.s. Previous RNAseq-based transcription analyses revealed elevated expression of *CYP325A* specific to Central African populations but its role in conferring resistance has not previously been demonstrated. This study used a wide range of molecular biology techniques to perform the molecular characterization (insecticidal bioassays, PCR and cloning) and functional validation of *CYP325A* as a pyrethroid resistance gene through *in silico* prediction (homology modelling and molecular docking simulations), *in vitro* (heterologous expression in *E. coli* and metabolism or depletion assays with insecticides) and *in vivo* (transgenic expression in flies and RNA interference in mosquitoes validation techniques). In this study, RT-qPCR consistently confirmed that *CYP325A* is highly over-expressed in pyrethroid-resistant *An. funestus* from Cameroon, compared with a control strain and insecticide-unexposed mosquitoes. A synergist bioassay with PBO significantly recovered susceptibility for permethrin and deltamethrin indicating P450-based metabolic resistance. Analyses of the coding sequence of *CYP325A* Africa-wide detected high levels of polymorphism, but with no predominant alleles selected by pyrethroid resistance. Geographical amino acid changes were detected notably in Cameroon. *In silico* experiments predicted that *CYP325A* binds and metabolises type I and type II pyrethroids. Heterologous expression of recombinant *CYP325A* and metabolic assays confirmed that the most-common Cameroonian haplotype metabolises both type I and type II pyrethroids with a depletion rate twice that of the DR Congo haplotype. Analysis of the 1 kb putative promoter of *CYP325A* revealed reduced diversity in resistant mosquitoes compared to susceptible ones, suggesting a potential selective sweep in this region. *In vivo* trials with transgenic flies and RNA interference have confirmed the trend implicating *CYP325A* in pyrethroid resistance. The establishment of *CYP325A* as a pyrethroid resistance metabolising gene further explains pyrethroid resistance in Central African populations of *An. funestus*. Our work will facilitate future efforts to detect the causative resistance markers in the promoter region of *CYP325A* to design field applicable DNA-based diagnostic tools and advise decision-makers on the choice of vector control tools..

Keywords: *Anopheles funestus*, malaria, pyrethroids, metabolic resistance, Cytochrome P450-CYP325A, Central Africa

RESUME

La surexpression et la suractivité des gènes clés du cytochrome P450 (CYP450) sont les principaux moteurs de la résistance métabolique aux insecticides chez les vecteurs africains du paludisme tels que *Anopheles funestus* s.s. De précédentes analyses de transcription basées sur RNAseq ont révélé une expression élevée de CYP325A spécifique aux populations d'Afrique centrale, mais son rôle dans la résistance n'a pas été démontré auparavant. Cette étude a utilisé un large éventail de techniques de biologie moléculaire pour effectuer la caractérisation moléculaire (essais biologiques insecticides, PCR et clonage) et validation fonctionnelle du CYP325A en tant que gène de résistance aux pyréthroïdes par prédiction *in silico* (modélisation d'homologie et simulations d'amarrage moléculaire), *in vitro* (expression hétérologue dans *E. coli* et essais de métabolisme ou de déplétion avec des insecticides) et *in vivo* (expression transgénique chez les mouches et interférence ARN dans les techniques de validation chez les moustiques). Dans cette étude, la RT-qPCR a systématiquement confirmé que le CYP325A est fortement surexprimé chez *An. funestus* résistant aux pyréthrinoïdes du Cameroun, par rapport à une souche témoin et à des moustiques non exposés aux insecticides. Avec le PBO, sensibilité récupérée pour la perméthrine et la deltaméthrine indiquant une résistance métabolique basée sur le P450. Les analyses de la séquence codante du CYP325A à l'échelle de l'Afrique ont détecté des niveaux élevés de polymorphisme, mais sans allèles prédominants sélectionnés par la résistance aux pyréthroïdes. Des modifications géographiques des acides aminés ont été détectées notamment au Cameroun. Des expériences *in silico* ont prédit que le CYP325A se lie et métabolise les pyréthroïdes de type I et de type II. L'expression hétérologue du CYP325A recombinant et les tests métaboliques ont confirmé que l'haplotype camerounais le plus courant métabolise les pyréthrinoïdes de type I et de type II avec un taux de déplétion deux fois supérieur à celui de l'haplotype de la RD Congo. L'analyse du promoteur putatif de 1 kb du CYP325A a révélé une diversité réduite chez les moustiques résistants par rapport aux moustiques sensibles, suggérant un balayage sélectif potentiel dans cette région. Des essais *in vivo* avec des mouches transgéniques et des interférences ARN ont confirmé la tendance impliquant le CYP325A dans la résistance aux pyréthroïdes. L'établissement du CYP325A en tant que gène métabolisant la résistance aux pyréthrinoïdes explique en outre la résistance aux pyréthrinoïdes dans les populations centrafricaines d'*An. funeste*. Notre travail facilitera les efforts futurs pour détecter les marqueurs de résistance causals dans la région promotrice du CYP325A afin de concevoir des outils de diagnostic basés sur l'ADN applicables sur le terrain et de conseiller les décideurs sur le choix des outils de lutte antivectorielle.

Mots-clés : *Anopheles funestus*, paludisme, pyréthrinoïdes, résistance métabolique, Cytochrome P450-CYP325A, Afrique centrale

TABLE OF CONTENTS

TABLE OF CONTENTS	xxii
LIST OF TABLES	xxiv
LIST OF FIGURES.....	xxvi
LIST OF APPENDICES	xxxii
LIST OF ABBREVIATIONS	xxxii
Introduction	1
Research question.....	2
Hypothesis.....	2
General Objectives	2
Specific Objectives.....	2
Chapter 1: Literature Review	4
1.1 Background	4
1.2 Vector-borne diseases	5
1.3 Malaria Epidemiology.....	7
1.4 Malaria History and Evolution.....	8
1.5 Malaria Pathogen.....	8
1.6 Malaria Vectors	10
1.7 Malaria Control Strategies	15
1.8 Chemical Use in Vector Control (Pest Control and Vector Control).....	18
1.9 Insecticide Resistance (IR).....	27
1.11 Insecticide Resistance Management.....	35
1.12 Metabolic Drivers of Insecticide Resistance	36
1.13 Action Mechanisms of Cytochrome P450s	39
1.14 Cytochrome P450 Reaction Mechanisms in Metabolic Resistance	40

1.15 Molecular Methods and Techniques in P450 Studies	44
Chapter 2: General Materials and Methods.....	59
2.1 Methods.....	59
2.2 Polymorphism survey and in silico molecular docking studies of <i>CYP325A</i> with major classes of insecticides.....	67
2.3 Molecular characterisation and functional validation of <i>CYP325A</i> as an insecticide resistance gene through <i>in vivo</i> and <i>in vitro</i> techniques.....	73
1.10 Detoxification Phases of Metabolic Resistance (MR)	76
2.3.1.7 Co-transformation of pB13::ompA+2CYP325A with pACYC-184- <i>An. gambiae</i> CPR	80
3. RESULTS.....	93
3.1 Genomic characterisation of <i>CYP325A</i> gene and investigating the role of causative mutations in the promoter region in <i>An. funestus</i> field populations across Africa	93
3.2 Perform a polymorphism survey, homology modelling, and molecular docking (in silico studies) of <i>CYP325A</i> with major classes of insecticides.....	109
3.3 Functional validation of <i>CYP325A</i> through <i>in vitro</i> and <i>in vitro</i> techniques.....	128
DISCUSSION	136
4.1. <i>CYP325A</i> over-expression is observed only in Central Africa	136
4.2. <i>CYP325A</i> metabolism of pyrethroids establishes its role in resistance in Central African <i>An. funestus</i>	137
4.3. Lack of strong signatures of selective sweep around <i>CYP325A</i>	138
CONCLUSION	140
FUTURE PERSPECTIVES	141
REFERENCES.....	143
APPENDICES.....	A
PUBLICATION	R

LIST OF TABLES

Table 1: Non-exhaustive list of vector-borne diseases.....	5
Table 2: African <i>Anopheles funestus</i> complex (Dia et al., 2013).....	13
Table 3: List of the species reported as the major and minor malaria vectors in Cameroon (Antonio-Nkondjio et al., 2019).....	15
Table 4: Comparison between thick and thin blood smear of plasmodium detection	17
Table 5: List of insecticides currently recommended by the World Health Organization (WHO) for public health applications (Thatheyus & Selvam, 2013).....	18
Table 6: Some online software used in genetic sequence analysis in molecular biology research	56
Table 7: Some offline and downloadable software used in genetic sequence analysis in molecular biology research	57
Table 8: Primers used for gene amplification and plasmid sequencing	63
Table 9: pJET1.2/Blunt ligation protocol.....	64
Table 10: Country of origin, CYP325A alleles selected for functional characterisation.....	73
Table 11: PCR reaction mix for ompA+2 intermediate linker fragment synthesis.....	75
Table 12: PCR reaction mix for fusion of ompA+2 leader sequence to CYP325A cDNA	76
Table 13: Double digestion of ompA+2CYP325A and pJET1.2::ompA+2CYP325A products	77
Table 14: Ligation of ompA+2CYP325A and pJET1.2::ompA+2CYP325A products.....	78
Table 15: Primers for sequencing of ompA+2-CYP325A in pCWOri+ and CPR in pACYC-184.....	79
Table 16: Reaction mix for HPLC metabolic assay	83
Table 17: Conditions used for Reverse-Phase HPLC Analysis. Conditions used for Reverse-Phase HPLC Analysis	84
Table 18: PCR reaction mix for amplification of <i>CYP325A</i> cDNA for transgenic analysis...	87

Table 19: List of primers used.....	88
Table 20: Nucleotide polymorphisms and amino acid substitutions between resistant alleles compared with FANG.	97
Table 21: Similarly expressed entities to CYP325A and associated function	100
Table 22: Genetic parameters of <i>CYP325A</i> in laboratory and field population.....	102
Table 23: Genetic parameters of 1 kb 5'UTR region <i>CYP325A</i> upstream region between Permethrin alive and dead samples.	104
Table 24: ChemScores of the productive binding of CYP325A Cameroon model with different insecticides.	113
Table 25: ChemScores of the productive binding of CYP325A DRC model with different insecticides.	117
Table 26: ChemScores of the productive binding of CYP325A Ghana model with different insecticides.	120
Table 27: ChemScores of the productive binding of CYP325A FANG model with different insecticides.	123
Table 28: ChemScores of the productive binding of CYP325A FUMOZ model with different insecticides.	125

LIST OF FIGURES

Figure 1: Global malaria epidemiology in (WHO, 2021)	7
Figure 2: Life cycle of the malaria parasite (Aravind et al., 2003).....	9
Figure 3: Difference between resting position of Anopheles and non-Anopheles mosquitoes	12
Figure 4: Mosquito life cycle	12
Figure 5: Global Distribution (Robinson Projection) of Dominant or Potentially Important Malaria Vectors (Kiszewski et al., 2004)	14
Figure 6: Microscopy technique to detect malaria.....	16
Figure 7: The chemical structure of the constituents of pyrethrum extracts which are collectively known as pyrethrin (Babić et al., 2012).....	19
Figure 8: Chemical structure of first and second-generation pyrethroid insecticides (Moyes et al., 2021).....	20
Figure 9: Mode of action of pyrethroids on VGSC (Kazachkova, 2007)	21
Figure 10: Some carbamates used in pest control (Kopeć et al., 2020)	21
Figure 11: Some examples of organochlorines used in pest control (Kopeć et al., 2020).....	22
Figure 12: Some examples of organophosphates used in pest control (Kopeć et al., 2020)...	23
Figure 13: Ryanoids and synthetics (Kopeć et al., 2020)	24
Figure 14: The global status of insecticide resistance to some neonicotinoid insecticides (Bass et al., 2015).....	25
Figure 15: Some examples pyrazole and pyrrole insecticides used in pest control (Ma et al., 2018).....	26
Figure 16: Layers of cuticle and impact on insecticide resistance phenotype in mosquitoes (Balabanidou et al., 2018)	29
Figure 17: Aspects of behavioural resistance that could impact insecticide resistance in mosquitoes (Wooding et al., 2020)	30
Figure 18: Major drivers of insecticide resistance	31

Figure 19: The molecular biology of knock-down resistance to pyrethroid insecticides	32
Figure 20: Mechanism of action of AChE with insect acetylcholinesterase inhibitors (left) and without the presence of acetylcholinesterase inhibitors (right) (Hematpoor et al., 2017)	33
Figure 21: RDL GABA-receptor-targeted resistance in <i>Drosophila</i>	34
Figure 22: Components of metabolic resistance in mosquitoes (Corbel & N’Guessan, 2013)	35
Figure 24: The ABC gene family in arthropods (Kumari, 2015).....	38
Figure 25: Comparison between bioavailability and bioactivity of substances in an organism (McClements et al., 2015)	39
Figure 26: Different reaction mechanisms of cytochrome P450s on different substrates (Manoj et al., 2010).....	40
Figure 27: Novel reactions catalyzed by cytochrome P450 enzymes (Munro et al., 2018) ...	41
Figure 28: The cytochrome P450 catalytic cycle, incorporating steps specific to peroxygenase activity and the formation of terminal alkenes (Munro et al., 2018)	43
Figure 29: Major steps of Sanger sequencing	48
Figure 30: Principle of restriction enzyme action. Example of EcoRI	49
Figure 31: Set-up of gel electrophoresis.....	50
Figure 32: PJET carrier plasmid for cloning.....	51
Figure 33: pCW expression plasmid for P450 protein expression.....	51
Figure 34: The principle of mass spectrophotometry (Ihling et al., 2020)	52
Figure 35: Principle and setup of HPLC	53
Figure 36: Principle and setup of ultracentrifugation	53
Figure 37: Normal inheritance compared to gene drive inheritance showing altered gene is always inherited (Perry, 2018)	54
Figure 38: Principle of RNA interference and how it inhibits gene expression (Chery, 2016)	55
Figure 39: Principle of Gal4 hybrids, balancing of strains and transgenic expression with specific phenotypes (Cabia et al., 2012)	56

Figure 40: Study sites across Africa and sites of interest in Cameroon (Wamba et al., 2021)	59
Figure 41: General scheme for the PCR-mediated fusion of bacterial leader sequences to P450 cDNAs. Adapted from (Pritchard et al., 1997).	74
Figure 42: ~ 100 bp intermediate linker product migrated on 1.5% agarose gel stained with Midori Green	75
Figure 23: Xenobiotic metabolism and disposition	77
Figure 43: Map of pB13::ompA+2CYP325A showing expression plasmid construct in circular form.	80
Figure 44: The GAL4-UAS system for directed gene expression.	86
Figure 45: Principle and steps involved in RNA interference of gene expression	90
Figure 46: Agarose gel picture of species identification PCR of the WHO bioassay F1 mosquitoes (S: Sample)	93
Figure 47: Susceptibility profile of <i>An. funestus</i> mosquitoes to insecticide.	94
Figure 48: Phusion Taq Polymerase amplification of <i>CYP325A</i> gene.	95
Figure 49: Phusion Taq Polymerase amplification of <i>CYP325A</i> 1kb putative promoter.	95
Figure 50: Kapa Taq Polymerase colony screening PCR of positive colonies with <i>CYP325A</i> insert. S: sample of PCR product.	96
Figure 51: Intron retention example of FANG sequences compared to <i>CYP325A</i> template and Ghana sequences	97
Figure 52: Expression patterns of some overexpressed CYP genes implicated in pyrethroid-based resistance across Africa.	98
Figure 53: Differential expression of <i>CYP325A</i> in the <i>An. funestus</i> s.s. Mibellon population in Cameroon.	100
Figure 54: Gene ontology (GO) for <i>CYP325A</i> entity similarity	101
Figure 55: Population studies of <i>CYP325A</i> coding and upstream putative promoter across Africa.	103
Figure 56: Genetic diversity of <i>CYP325A</i> cDNA.	104

Figure 57: Haplotype network and phylogenetic tree of putative promoter sequences for permethrin dead and alive	105
Figure 58: Genetic diversity of the 1kb putative promoter	106
Figure 59: Comparison of <i>An. funestus</i> CYP325A amino acid sequences with orthologs from <i>An. gambiae</i> , <i>An. epiroticus</i> and <i>An. stephensi</i>	107
Figure 60: Comparison of <i>An. funestus</i> CYP325A amino acid sequences from Cameroon and DRC alleles.	108
Figure 61: 3-D structural model of CYP325A cDNA constructed and viewed in PyMol software	109
Figure 62: Errat plot for the lowest energy model.	111
Figure 63: Binding modes of CYP325A_CMV with insecticide models.	114
Figure 64: The activation of lethal oxon metabolite of malathion by phase I detoxification genes.....	116
Figure 65: Binding modes of CYP325A_DRC with insecticide models.....	118
Figure 66: Binding modes of CYP325A_GHA with insecticide models.	121
Figure 67: Binding modes of CYP325A_FAN with insecticide models.	124
Figure 68: Binding modes of CYP325A_FUM with insecticide models.	126
Figure 69: Electrophoresis gel showing successful omp+2 addition to CYP325A cDNA templates.....	128
Figure 70: Colony screening PCR for positive clones with CYP325A insert omp+2-CYP325A.	129
Figure 71: Colony screening gel picture for positive clones to co-transformation of recombinant pCWori+ and CPR.	130
Figure 72: Spectrophotometer map showing P450 activation during culture and P450 expression.....	131
Figure 73: Cameroon and DRC CYP325A recombinant DNA depletion assays with permethrin, deltamethrin, and α -cypermethrin	131
Figure 74: <i>In vitro</i> assay results. Functional confirmation of the metabolic activity of CYP325A was conducted for permethrin and deltamethrin using protein membranes.....	131

Figure 75: *In vitro* assay results. Functional confirmation of the metabolic activity of CYP325A was conducted for permethrin and deltamethrin using protein membranes..... 132

Figure 76: Endonuclease digestion of transgenic expression plasmid and PJET-CYP325A recombinant plasmid 133

Figure 77: Assessment of transgenic activity of CYP325A: Contact bioassay mortality results of transgenic flies with permethrin and DDT..... 134

Figure 78: Assessment of inhibited expression of CYP325A after injection of double strand 134

Figure 79: Assessment of expression of *CYP325A* after injection of double-strand in two trial runs 135

LIST OF APPENDICES

Appendix 1: Python script used to build models using the MODELLER 9v2.0	A
Appendix 2: Errat profiles of CYP325A models and CYP3A4 (PDB:1TQN)	B
Appendix 3: Potential transmembrane segments and DAS plot of transmembrane domains of CYP325A protein sequence	B
APPENDIX 4: Binding modes of permethrin in CMRCYP325A model.	D
Appendix 5: Molecular docking scores with other docking parameters	I
Appendix 6: Preparation of CYP450 Expressing Bacterial Membranes	K
Appendix 7: Kinetic Constants of Recombinant P450 CYP325A for Pyrethroids, Bendiocarb, propoxur and DDT	N
Appendix 8: Binding parameters of the productive mode of permethrin, deltamethrin, alpha cypermethrin, bendiocarb and DDT docked to the active sites of CYP325A models	N
Appendix 9: List of some important reagents used in this study	O
Appendix 10: Intron retention phenomenon observed in CYP325A Ghana and FANG sequences (spliced out manually for in silico studies)	R

LIST OF ABBREVIATIONS

ace-1: acetylcholinesterase 1

An.: Anopheles

AChE: Acetylcholinesterase

Ae.: Aedes

BAC: Bacterial artificial chromosome

BLAST: Basic local alignment search tool

Bti: Bacillus thuringiensis

BS β P450: BS β , CYP152A1 from Bacillus subtilis

CamA/B: putidaredoxin reductase/putidaredoxin from Pseudomonas putida

cDNA: Complementary DNA

Chr: Chrysanthemum

CO: Carbon monoxide

CPR: Cytochrome P450 reductase

CYP: Cytochrome P450 monooxygenase

CYP-I: Cytochrome P450 compound I (FeIV-oxo pi-cation radical)

CYPED: Cytochrome P450 Engineering Database

Cx.: Culex

DDE: 1,1,1-dichloro-2,2-bis(4-chlorophenyl) ethane

DDT: 1,1,1-Trichloro-2,2-bis(4-chlorophenyl) ethane

dH₂O: Distilled water

DNA: Deoxyribonucleic acid

DNase: Deoxyribonuclease

AMELIE WAMBA NDONGMO Regine/Doctorate/Ph.D. Thesis/University of Yaoundé I

dNTP: Deoxyribonucleoside triphosphate

DTT: Dithiothreitol

EM: Electronic Microscopy

FAD: Flavin adenine dinucleotide

FANG: Anopheles funestus from Angola

FLD: Flavodoxin from Escherichia coli

FLDR: Flavodoxin reductase from Escherichia coli

FMN: Flavin mononucleotide

FUMOS-R: Anopheles funestus from Mozambique-Resistant

GABA: Gamma-aminobutyric acid

gDNA: Genomic DNA

GSH: Glutathione

H₂O₂: Hydrogen peroxide

HAT: Hydrogen atom transfer

HMG-CoA: 3-Hydroxy-3-methylglutaryl-coenzyme A

IPTG: Isopropyl β-D-1-thiogalactopyranoside

ITNs: Insecticide treated nets

KIE: Kinetic isotope effect

KPi: Potassium phosphate

LB: Lysogeny broth

LLINs: Long lasting insecticide treated nets

MgCl₂: Magnesium chloride

mRNA: Messenger RNA

AMELIE WAMBA NDONGMO Regine/Doctorate/Ph.D. Thesis/University of Yaoundé I

MS: Mass spectrometry

nAChR: Nicotinic acetylcholine receptor

NAD: Nicotinamide adenine dinucleotide

NADP: Nicotinamide adenine dinucleotide phosphate

NCBI: National centre for biotechnology information

NHE: Normal hydrogen electrode

NMR: Nuclear magnetic resonance

PCR: Polymerase chain reaction

P.: Plasmodium

PMSF: Phenylmethanesulfonylfluoride

qPCR : Quantitative polymerase chain reaction

qRT-PCR : Quantitative Reverse Transcriptase Polymerase Chain Reaction

r.m.s.d.: root mean square deviation

Rdl: Resistance to dieldrin

RIS: Reductase interacting site

RNA: Ribonucleic acid

RNase: Ribonuclease

RPL11: Ribosomal protein L11

RTS,S: Repeat region for T-cell epitope surface antigen of free S protein

S.: Sacchromyces

s.l.: sensu lato

S.O.C.: Super optimal broth with catabolite repression

s.s. : sensu stricto

AMELIE WAMBA NDONGMO Regine/Doctorate/Ph.D. Thesis/University of Yaoundé I

sf9 : Spodoptera frugiperda 9 cells

SET: Single electron transfer

SRS: Substrate recognition site

T.: Tribolium

TB: Terrific broth

TLC: Thin layer chromatography

T_m: Melting temperature

TSE: Tris-Sucrose –EDTA

vdW: van der Waals

VGSC: Voltage-gated sodium channel

δ-ALA : Lamda aminolevulinic acid

Introduction

Vector-borne diseases account for more than 17% of all infectious diseases causing more than 700,000 human deaths annually (Gubler, 2009). Malaria is a parasitic infectious disease transmitted by the bite of an infected mosquito. Mosquitoes constitute the major vectors of human disease and are known as the greatest killers of humans. Malaria is a major cause of death globally especially in sub-Saharan Africa which shoulders approximately 94% of the global disease burden (WHO, 2020b). Malaria is a vector-borne disease caused by a protozoan parasite of the genus *Plasmodium* transmitted by the bite of an infected female *Anopheles* mosquito during blood meal intake necessary for the maturation of its eggs (Harrison, 1978). Due to favourable climatic conditions and the abundance of breeding sites, sub-Saharan Africa remains highly endemic to malaria with an abundance of the mosquito vector (Forgash, 1984). Cameroon shoulders 3% of the global burden affecting mainly pregnant women and children below five, constituting 57% of hospitalisation cases in health centres (Antonio-Nkondjio et al., 2019).

Major malaria vectors in Africa include *Anopheles gambiae* and *Anopheles funestus* which are widely and abundantly distributed across Africa (Hemingway, 2014). Efforts to control and eliminate malaria mainly involve the use of ACTs and chemicals in vector control. Vector control is the frontline in the fight against malaria comprising the distribution of ITNs, IRS, larval source management, and adult mosquito control. Four major classes of insecticide exist but the WHO-recommended class for malaria control interventions is the pyrethroid class (WHO, 2020c). The intensive use of chemicals in vector control coupled with the uncontrolled use of chemicals in agricultural pest control now constitute a selection pressure that has led to the emergence and spread of an increasingly alarming phenomenon known as insecticide resistance which confers to some mosquitoes the ability to survive contact with insecticide through various mechanisms namely metabolic, target-site, behavioural and cuticular resistance (Sparks & Nauen, 2015).

In *Anopheles funestus*, there is no evidence of target-site resistance with respect to pyrethroid resistance implying the mechanism is mainly metabolic. The main drivers of metabolic resistance are detoxification genes mainly cytochrome P450s, glutathione-S-transferases, and esterases. Cytochrome P450s constitute the largest class of genes intervening in this phenomenon and can act through varying mechanisms (Feyereisen, 2012). The biochemical mechanisms underlying CYP-mediated insecticide resistance in *Anopheles* are still poorly

understood. However, RNAseq genome-wide transcriptomic analysis have implicated several genes in pyrethroid resistance in mosquitoes across Africa (Ibrahim et al., 2018; Weedall et al., 2019). Specifically, the upregulation or overexpression of some *CYP* genes have been found to drive resistance to some insecticides through allelic variation or rapid detoxification through increased bioavailability and bioactivity (Riveron et al., 2018).

This growing phenomenon of insecticide resistance in malaria vectors constitutes a major threat to the continued efficacy of currently implemented strategies (Tonye et al., 2018). It is now paramount in the fight against malaria to understand by which underlying mechanisms this resistance is acquired and spread across field mosquito populations across Africa and how to harness this information to ensure the continued efficacy of interventions and control strategies (Akoton et al., 2018). *CYP*-mediated metabolic resistance has been shown to be geographically specific with the example of *CYP6P9a/b* driving pyrethroid resistance in southern Africa and *CYP6P4a/b* in West Africa, Ghana (Ibrahim et al., 2016; Mugenzi et al., 2019).

In central Africa, such a mechanism has not yet been investigated leaving a huge knowledge gap which we aimed to contribute towards addressing in this study whose principal focus was to elucidate the underlying biochemical mechanisms that drive pyrethroid resistance in *Anopheles funestus* mosquitoes from Central Africa.

Research question

By which mechanisms do cytochrome p450 genes confer insecticide resistance (metabolic resistance) to *An. funestus* mosquitoes?

Hypothesis

Cytochrome p450 *CYP325A* plays no role in pyrethroid resistance observed in *An. funestus*.

General Objectives

Investigating the molecular basis and underlying biochemical mechanisms of *CYP325A* as a pyrethroid resistance gene in *Anopheles funestus*, a major malaria vector across Africa.

Specific Objectives

1. To conduct genomic characterisation of *CYP325A* gene and investigate the role in insecticide resistance of other causative mutations in the promoter region in *An. funestus* field populations from Cameroon and across Africa.

2. To perform a polymorphism survey and molecular docking (*in silico* studies) of *CYP325A* with major classes of insecticides
3. To functionally validate of *CYP325A* as an insecticide resistance gene through *in vitro* (heterologous expression in *E. coli* and enzyme kinetic studies) and *in vivo* (RNA interference in mosquitoes and transgenic expression in flies) techniques.

This thesis is presented in three chapters:

1. Chapter 1 highlights the updated scientific findings on the subject.
2. Chapter 2 presents the materials used in the first part and in the second part, the methods used to achieve the above objectives.
3. Chapter 3 presents the most pertinent results obtained and the discussion.

Chapter 1: Literature Review

1.1 Background

Infectious diseases account for 17% of diseases that affect humans globally and malaria remains a leading cause of death in tropical areas such as sub-Saharan Africa, Latin America, and South East Asia (WHO, 2020a). In 2019, 229 million malaria cases were registered in 87 malaria endemic countries with 409000 deaths 67% of which were children below five years (WHO, 2020a). Sub-Saharan Africa shoulders the bulk of the disease burden where 15 countries plus India account for over 90% of the global burden (WHO, 2020c). Cameroon bears approximately 3% of this burden with 57% of hospitalization cases registered in Health Centres being due to malaria (PNLP, 2018). Malaria is a vector-borne infectious disease caused by a protozoan parasite called *Plasmodium* transmitted by the bite of an infected female *Anopheles* mosquito during bloodmeal (Gubler, 2009). In Africa, the major malaria vectors are *Anopheles gambiae*, *Anopheles funestus*, and *Anopheles arabiensis*. Malaria treatment and prevention depend on ACT drug therapy and the use of ITNs, but eradication is made difficult by the wide distribution and abundance of these mosquitoes in tropical areas whose proliferation is favoured by climatic conditions (Antonio-Nkondjio et al., 2019). Consequently, vector control is the frontline in the fight against malaria which involves principally the use of chemicals in larval source management and indoor residual spraying (IRS) or use of ITNs. The intense and uncontrolled use of chemicals in vector control and agriculture has led to the emergence and spread of a phenomenon known as insecticide resistance (Riveron et al., 2018). Insecticide resistance has been observed for all classes of insecticides, especially to pyrethroids which are the only recommended class for impregnation of LLINs (Ibrahim, Fadel, et al., 2019). To make bad matters worse, there have been cases of cross-resistance and multiple resistance registered in several mosquito populations on the field (Ibrahim, Mukhtar, et al., 2019). The molecular basis of this phenomenon has not yet been elucidated and the mechanisms through which it is acquired and spread across mosquito populations on the field remain poorly understood (Gareth D. Weedall, 2019). Several mechanisms have been implicated in the acquisition and spread of insecticide resistance notably, target-site resistance, metabolic resistance, cuticular resistance, and behavioural resistance in mosquito populations across Africa (Hemingway et al., 2004). In *Anopheles funestus* which is one of the major malaria vectors across Africa, there is still no evidence of target-site resistance concerning pyrethroid resistance indicating that the mechanism is mainly metabolic (Hemingway, 2014). Metabolic resistance is a result of increased detoxification ability leading to faster digestion and excretion of xenobiotics such as

AMELIE WAMBA NDONGMO Regine/Doctorate/Ph.D. Thesis/University of Yaoundé I

insecticide molecules by the mosquitoes (Fadel et al., 2019; Tchouakui, Riveron Miranda, et al., 2020). The main families of detoxification enzymes involved are cytochrome P450s, glutathione-S-transferases, and carboxylesterases (Wondji et al., 2008). Several genes have been shown to contribute greatly to metabolic resistance in *An. funestus* mosquitoes in the field across Africa such as *CYP6P9a*, *CYP6P9b*, *CYP6M7*, *GSTe2*, among others (Ibrahim et al., 2015; Riveron et al., 2015; Riveron, Ibrahim, et al., 2014; Riveron, Yunta, et al., 2014). Several candidate genes have been implicated in metabolic resistance through genome-wide microarray and transcriptomic analysis of *Anopheles funestus* gene transcripts. Despite the great progress made in the detection of candidate genes and even their functional characterisation in some cases, the exact mechanism of pyrethroid resistance remains poorly understood. There is also the need for molecular markers that could allow for effective detection and tracking of metabolic resistance on the field. This study therefore aimed to fill some of the knowledge gap by investigating the role of an over-expressed cytochrome P450 known as *CYP325A* in pyrethroid resistance in field populations of *Anopheles funestus* in Cameroon and across Africa.

1.2 Vector-borne diseases

Vector-borne diseases are major contributors to the global disease burden responsible for >17% of all infectious diseases and approximately one million deaths annually. Control of insect vectors is often the best, and sometimes the only, way to protect humans from these destructive diseases. Below in Table 1 is a list of the major vector-borne diseases as recorded by the WHO (WHO, 2020c). The following table is a non-exhaustive list of vector-borne diseases, ordered according to the vector by which it is transmitted. The list also mentions the type of pathogen that causes the disease in humans.

Table 1: Non-exhaustive list of vector-borne diseases

<https://www.who.int/news-room/fact-sheets/detail/vector-borne-diseases>

Vector		Disease caused	Type of pathogen
Mosquito	<i>Aedes</i>	Chikungunya	Virus
		Dengue	Virus
		Lymphatic filariasis	Parasite
		Rift Valley fever	Virus
		Yellow Fever	Virus

		Zika	Virus
	<i>Anopheles</i>	Lymphatic filariasis Malaria	Parasite Parasite
	<i>Culex</i>	Japanese encephalitis Lymphatic filariasis West Nile fever	Virus Parasite Virus
Aquatic snails		Schistosomiasis (bilharziasis)	Parasite
Blackflies		Onchocerciasis (river blindness)	Parasite
Fleas		Plague (transmitted from rats to humans) Tungiasis	Bacteria Ectoparasite
Lice		Typhus Louse-borne relapsing fever	Bacteria Bacteria
Sandflies		Leishmaniasis Sandfly fever (phlebotomus fever)	Parasite Virus
Ticks		Crimean-Congo haemorrhagic fever Lyme disease Relapsing fever (borreliosis) Rickettsial diseases (eg: spotted fever and Q fever) Tick-borne encephalitis Tularaemia	Virus Bacteria Bacteria Bacteria Virus Bacteria
Triatome bugs		Chagas disease (American trypanosomiasis)	Parasite
Tsetse flies		Sleeping sickness (African trypanosomiasis)	Parasite

1.3 Malaria Epidemiology

To estimate the potential impact of malaria in each population it is important to understand the relationship between transmission intensity, levels of acquired immunity within a population, and manifestations of malaria illness. In 2019, there were an estimated 229 million cases of malaria worldwide (WHO, 2020c). The estimated number of malaria deaths stood at 409 000 in 2019, especially among children aged under 5 years who are the most vulnerable group affected by malaria. In 2019, they accounted for 67% (274 000) of all malaria deaths worldwide. Cameroon shoulders 3% of the global malaria burden and over 90% of Cameroonians are at risk of malaria infection, and ~ 41% have at least one episode of malaria each year. Historically, the rate of malaria infection in Cameroon has fluctuated over the years; the number of cases was about 2 million in 2010 and 2011.

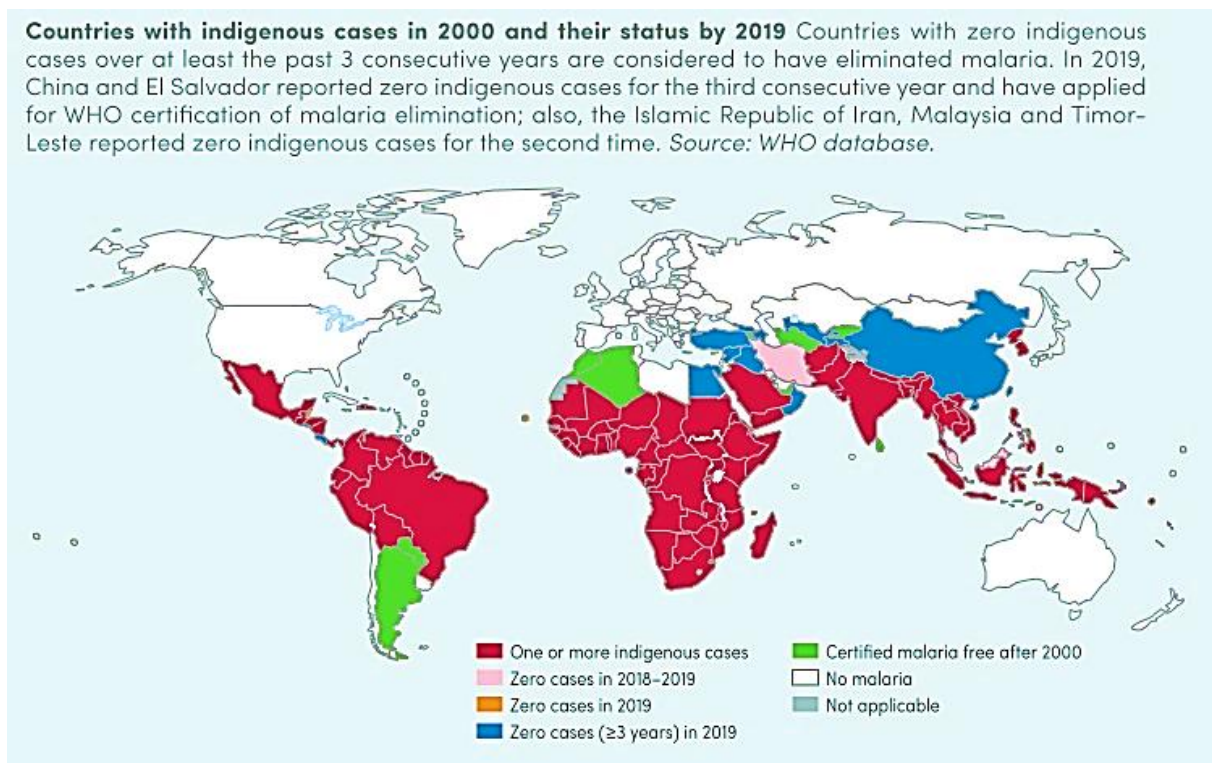


Figure 1: Global malaria epidemiology in (WHO, 2021)

1.4 Malaria History and Evolution

Ever since the early days of human civilization, people have sought to combat malaria around the world. From ancient remedies to modern pharmaceutical agents (and their noteworthy discoverers), the history of malaria and its treatment is a rich one (Harrison, 1978). Malaria has afflicted humans for thousands of years. The “Father of Medicine,” Hippocrates, described the disease in a medical text in the 4th or 5th Century BC. Even great warriors were no match for the tiny parasites as Alexander the Great may have died of malaria infection at age 30. However, it was not until 1718 that the term malaria (from Italian malaria, or “bad air”) was coined by Italian physician Francisco Torti, a title stemming from the belief perpetuated by Roman physicians that the disease was called by malignancies in the swamp air. Even into the 19th Century, how malaria was transmitted was still unclear. The tiny world of microorganisms and the role these life forms played in the spread of disease remained mysterious. The transmission of malaria was unraveled in 1880 by the French surgeon Alphonse Laveran, who, while stationed at a hospital in Algiers as a military surgeon, observed a parasite moving within a red blood cell from a malarial patient. For his discovery, Laveran was awarded the Nobel Prize in Medicine in 1907. Italian neurophysiologist Camillo Golgi was the first to describe different species of the malarial parasite (based on the frequency of attacks they caused, and the number of parasites released once the red blood cells containing them ruptured), work for which he was awarded a Nobel Prize in 1906. Italian researchers Giovanni Grassi and Raimondo Filetti first put a name to these, classifying *P. vivax* and *P. malariae*. Americans William Welch and John Stephens later contributed, respectively, the names *P. falciparum* and *P. ovale*.

1.5 Malaria Pathogen

Malaria is a vector-borne parasitic infection caused by a protozoan parasite of the genus *Plasmodium* and several species exist namely *P. falciparum*, *P. vivax*, *P. malariae*, and *P. ovale*. *Plasmodium falciparum* is responsible for approximately 96% of all malaria cases globally however this varies with respect to the geographical location. Malaria is caused by unicellular parasite which belongs to the genus *Plasmodium* (Sherman, 1979) (Kettler, 2020). The scientific classification of the genus *Plasmodium* is as follows (Wéry, 1995).

Kingdom: Animalia

Phylum: Apicomplexa

Class: Haemosporidea

Sub-class: Heamotzoae

AMELIE WAMBA NDONGMO Regine/Doctorate/Ph.D. Thesis/University of Yaoundé I

Order: Haemosporida

Family: Plasmodidae

Genus: *Plasmodium*

This pathogen goes through a cyclical infection of humans and Anopheles mosquitoes (Figure 2). In humans, the parasite grows and multiplies in the liver cells and then in the red blood cells (RBCs) of the blood. Subsequently, they lyse the RBCs to release daughter parasites called merozoites that continue to invade other RBCs. The blood-stage parasites are responsible for the symptoms of malaria and the male and female gametocytes ingested by the female Anopheles mosquito during the blood meal mate in the gut of the mosquito and begin the cycle of growth and multiplication in the mosquito. After 10 – 18 days, the sporozoite form of the parasite migrates to the mosquito salivary glands where they reside until they are injected into a human with anticoagulants during the next blood meal of the mosquito and migrate to the liver to continue the cycle of development (Aravind et al., 2003).

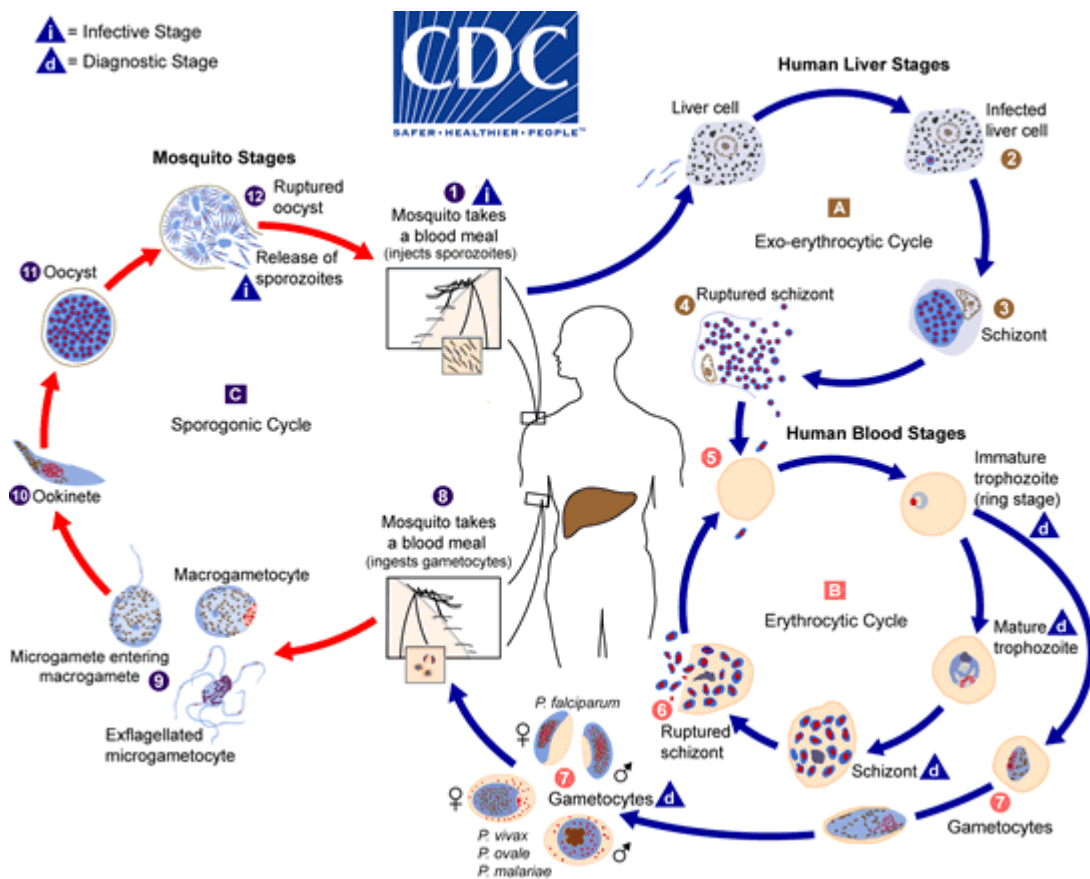


Figure 2: Life cycle of the malaria parasite (Aravind et al., 2003).

The malaria parasite life cycle involves two hosts. During a blood meal, a malaria-infected female *Anopheles* mosquito inoculates sporozoites into the human host. Sporozoites infect liver cells and mature into schizonts, which rupture and release merozoites. (Of note, in *P. vivax* and *P. ovale* a dormant stage [hypnozoites] can persist in the liver (if untreated) and cause relapses by invading the bloodstream weeks, or even years later.) After this initial replication in the liver (exo-erythrocytic schizogony), the parasites undergo asexual multiplication in the erythrocytes (erythrocytic schizogony). Merozoites infect red blood cells. The ring stage trophozoites mature into schizonts, which rupture releasing merozoites. Some parasites differentiate into sexual erythrocytic stages (gametocytes). Blood stage parasites are responsible for the clinical manifestations of the disease. The gametocytes, male (microgametocytes) and female (macrogametocytes), are ingested by an *Anopheles* mosquito during a blood meal. The parasites' multiplication in the mosquito is known as the sporogonic cycle. While in the mosquito's stomach, the microgametes penetrate the macrogametes generating zygotes. The zygotes in turn become motile and elongated (ookinetes) which invade the midgut wall of the mosquito where they develop into oocysts. The oocysts grow, rupture, and release sporozoites, which make their way to the mosquito's salivary glands. Inoculation of the sporozoites into a new human host perpetuates the malaria life cycle (Aravind et al., 2003).

1.6 Malaria Vectors

Infected female *Anopheles* mosquitoes carry *Plasmodium* from one human to another (acting as a "vector"), while infected humans transmit the parasite to the mosquito. In contrast to the human host, the mosquito vector does not suffer from the presence of the parasites. These parasites infest the salivary glands of mosquitoes during a blood meal on an infected individual where they proliferate and can be transmitted to another individual during the next blood meal. Only female *Anopheles* mosquitoes transmit malaria because they need the blood meal for the maturation of their eggs while the males feed on nectar and play a major role in pollination. There are nearly 500 species in the *Anopheles* genus and over 70 species have been established as vectors of human and animal diseases. The species and distribution of *Anopheles* in each location influence the intensity of malaria transmission as not all *Anopheles* species are equally efficient to transmit malaria. The mosquitoes which are more prone to bite humans frequently and indoors tend to be more implicated in malaria transmission. Africa bears the brunt of the malaria burden because it has the most effective and efficient dominant vector species (DVS) of human malaria (Gillies & Coetzee, 1987; Sinka et al., 2010). *An. gambiae* s.s. (Guerra et al., 2008), with its sibling *An. arabiensis* (Gillies & Coetzee, 1987) and *An. funestus* (Sinka et al., 2008).

2012) whose distribution has increased greatly and rapidly over the past decade making it a major malaria vector across Africa today. Mosquitoes cause well known human diseases such as malaria, filariasis, encephalitis, yellow fever, and dengue which are especially severe in developing regions of the tropics where they cause early death and chronic debilitation that can strain the resources of health services and reduce human productivity thereby perpetuating economic hardship.

1.6.1 Mosquito Vectors of Malaria in Africa

Malaria vectors, *Anopheles* are invertebrate animals possessing a chitinous exoskeleton, three body parts: head, thorax, and abdomen; three pairs of jointed legs, compound eyes, and a pair of antennae. Anopheline mosquitoes belong to the Arthropod Phylum. The scientific classification of the genus *Anopheles* are given below (Harbach & Kitching, 2016). There are three types of malaria carrying mosquitoes. The top three malaria transmitters in Africa are *Anopheles gambiae*, *Anopheles funestus* and *Anopheles arabiensis*. The first two live in areas of Africa where there is higher rainfall while the third, *Anopheles arabiensis*, is a more savanna-based, arid zone species.

Kingdom: Animal

Phylum: Arthropoda

Class: Insecta

Sub-class: Pterygota

Order: Diptera

Suborder: Nematocera

Family: Culicidae

Subfamily: Anophelinae

Genus: *Anopheles*

There are three important mosquito genera. *Anopheles*, the only known carrier of malaria, also transmits filariasis and encephalitis. *Anopheles* mosquitoes are easily recognized in their resting position, in which the proboscis, head, and body are held in a straight line to each other but at an angle to the surface (Coetzee, 2020). See Figure 3 below.

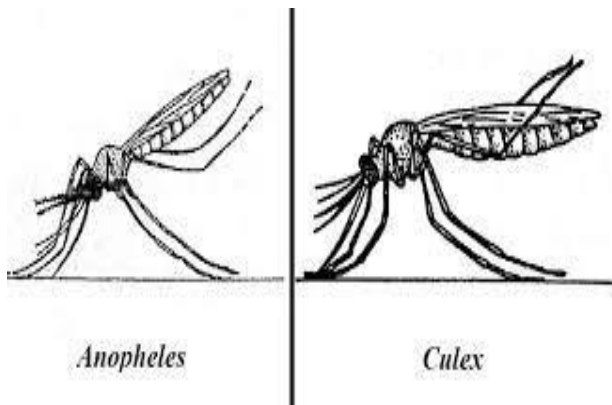


Figure 3: Difference between resting position of *Anopheles* and non-*Anopheles* mosquitoes <https://onlinesciencenotes.com/differences-anopheles-culex/>

The spotted colouring on the wings results from coloured scales. Egg laying usually occurs in water containing heavy vegetation. The female deposits her eggs singly on the water surface. *Anopheles* larvae lie parallel to the water surface and breathe through posterior spiracular plates on the abdomen instead of through a tube, as do most other mosquito larvae. The life cycle is from 18 days to several weeks (Harrison, 1978) as shown in Figure 4 below.

Mosquito life cycle

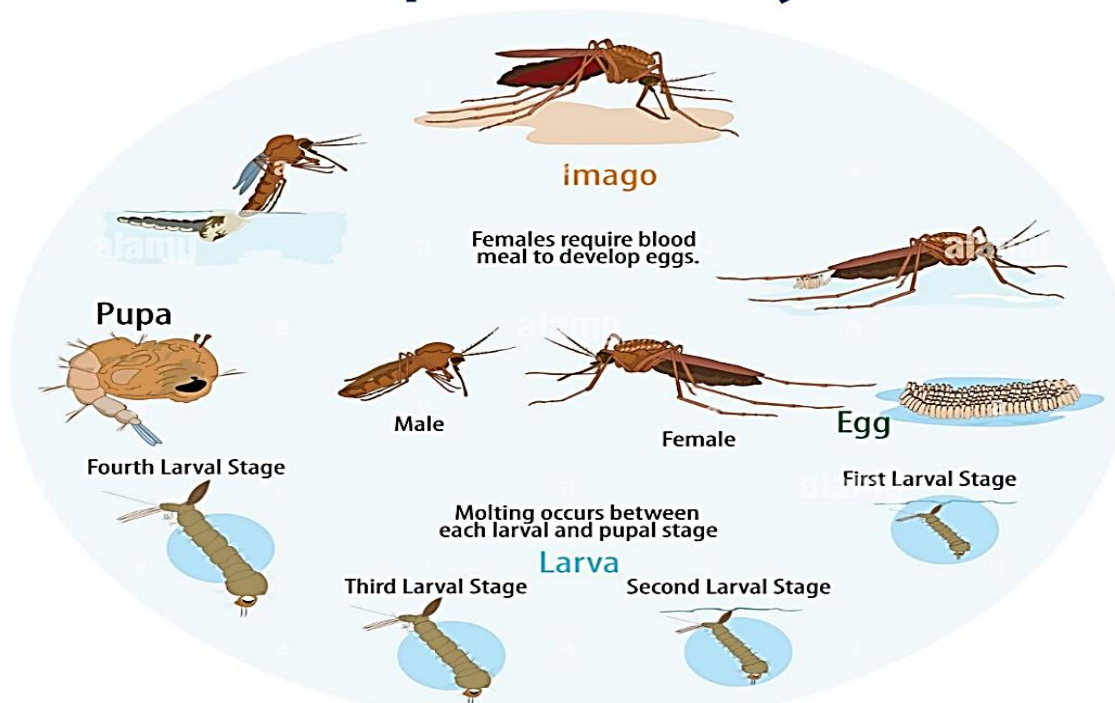


Figure 4: Mosquito life cycle (<https://www.alamy.com/stock-photo-vector-illustration-of-mosquito-life-cycle-126216933.html>)

1.6.2 *Anopheles funestus* s.s.

An. funestus is one of the major malaria vectors due to its wide distribution and abundance in sub-Saharan Africa wherever suitable breeding sites are available (Coetzee & Koekemoer, 2013). *An. funestus* belongs to a group of thirteen species (Dia et al., 2013) that are very similar morphologically at the adult stage (Coetzee & Fontenille, 2004). Four species, *An. funestus*, *An. vaneedeni*, *An. parensis* and *An. aruni* possess identical morphology at all stages of life (Gillies & Coetzee, 1987; Gillies & De Meillon, 1968) and together with *An. confusus*, *An. longipalpis* type C and *An. funestus-like* are known as the Funestus sub-group (Dia et al., 2013). Another sub-group known as the Minimus sub-group exists and is composed of the species *An. leesoni* and *An. longipalpis* Type A. The third sub-group is the Rivulorum sub-group which comprises of *An. rivulorum*, *An. rivulorum-like*, *An. brucei* and *An. fuscivenosus*. The most distinct species at both the egg and larval stages is *An. leesoni* but *An. confusus* is easily identified through larval characteristics. *An. rivulorum* and *An. brucei* also possess very distinct features at the larval stage although they are virtually indistinguishable from each other (Coetzee & Fontenille, 2004). Besides *An. funestus* which is highly anthropophilic, the rest of the group is mainly zoophilic. Nonetheless, *An. rivulorum* has been implicated as a minor malaria vector in a locality in Tanzania (Wilkes et al., 1996). The *Anopheles funestus* complex is tabulated below (Table 2) *An. funestus*, *An. leesoni* and *An. rivulorum* are the most widely distributed (Dia et al., 2013) and are traditionally represented in the whole of sub-Saharan Africa (Dia et al., 2013; M. Gillies & Coetzee, 1987; M. T. Gillies & De Meillon, 1968). *An. funestus* is present all over the African continent (Figure 5) while the other species exhibit local distribution across the continent (Dia et al., 2013). While *An. gambiae* typically breeds in small temporary rain-dependent pools and puddles, *An. funestus* exploits larger permanent or semi-permanent bodies of water containing emergent vegetation.

Table 2: African *Anopheles funestus* complex (Dia et al., 2013).

African species of the <i>Funestus</i> group				
Sub-group	Species	Geographical distribution	Host preference	Vector role
Funestus	<i>An. funestus</i>	Continental	Anthropophilic	Major
	<i>An. funestus-like</i>	Local	Unknown	Unknown
	<i>An. aruni</i>	Local	Unknown	Unknown
	<i>An. confuses</i>	Regional	Zoophilic	Unknown

Funestus	<i>An. parensis</i>	Regional	Unknown	Minor
	<i>An. vaneedeni</i>	Local	Unknown	Unknown
	<i>An. logipalpis</i> type C	Local	Zoophilic	Unknown
Minimus	<i>An. leesoni</i>	Continental	Zoophilic	Minor
	<i>An. longipalpis</i> type A	Local	Zoophilic	Unknown
Rivulorum	<i>An. rivulorum</i>	Continental	Zoophilic	Minor
	<i>An. rivulorum-like</i>	Local	Unknown	Unknown
	<i>An. brucei</i>	Local	Unknown	Unknown
	<i>An. fuscavenosus</i>	Local	Unknown	Unknown

Anopheles mosquitoes are found worldwide except in Antarctica and so malaria vectors are not only found in malaria-endemic regions but also in areas where malaria has already been eliminated shown in Figure 5 below. These areas therefore remain at risk of re-introduction of malaria.

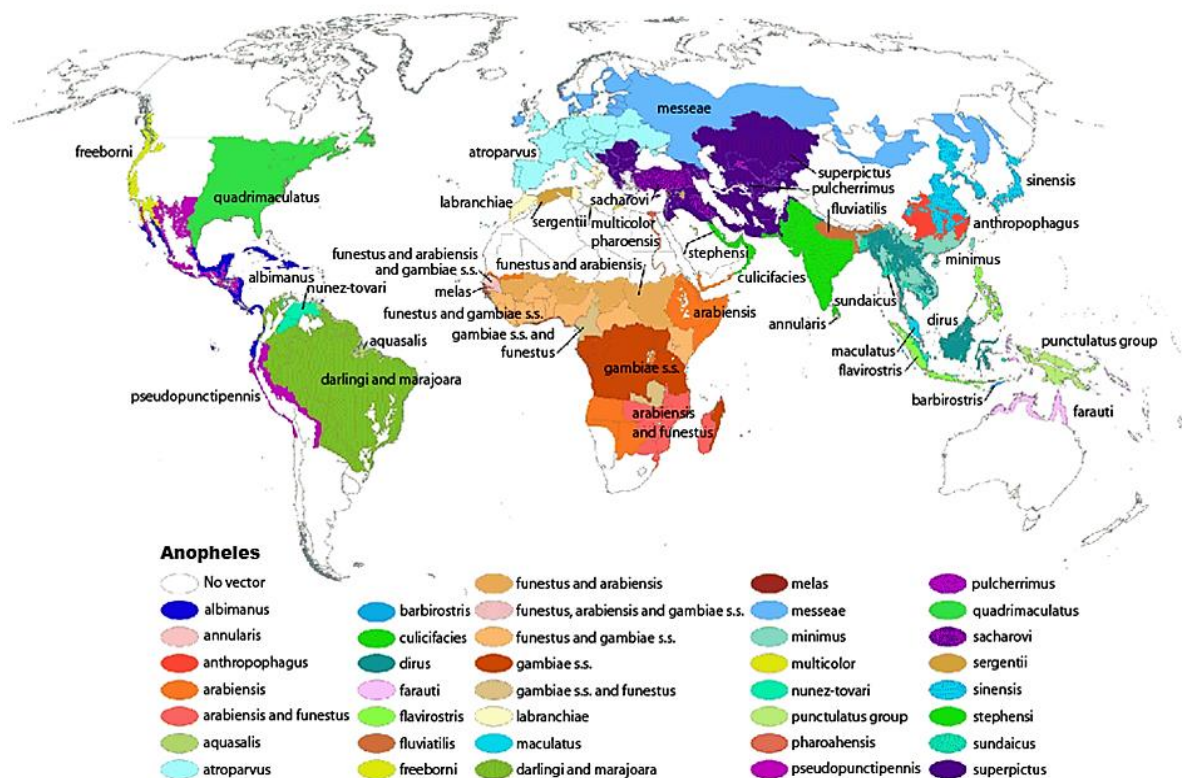


Figure 5: Global Distribution (Robinson Projection) of Dominant or Potentially Important Malaria Vectors (Kiszewski et al., 2004)

Due to the high endemicity of malaria and the public health burden it represents, a variety of interventions have been implemented ranging from diagnosis, prevention, and treatment. In Cameroon, malaria vectors exist, and their presence has been pointed out by numerous field studies highlighting the anopheline fauna that could be considered one of the most diverse in Africa accounting more than 50 species reported (Antonio-Nkondjio et al., 2019).

Table 3: List of the species reported as the major and minor malaria vectors in Cameroon (Antonio-Nkondjio et al., 2019)

Species	Authors	Year of publication
<i>Anopheles gambiae</i>		Giles, 1902
<i>Anopheles coluzzii</i>		Coetzee & Wilkerson, 2013
<i>Anopheles arabiensis</i>		Patton, 1905
<i>Anopheles funestus</i>		Giles, 1900
<i>Anopheles lesoni</i>		Evans, 1931
<i>Anopheles nili</i>		Theobald, 1904
<i>Anopheles carnevalei</i>		Brunhes et al., 1999
<i>Anopheles ovengensis</i>		Awono - Ambene et al., 2004
<i>Anopheles moucheti</i>		Evans, 1925
<i>Anopheles pharoensis</i>		Theobald, 1901
<i>Anopheles paludis</i>		Theobald, 1900
<i>Anopheles ziemanni</i>		Grünberg, 1902
<i>Anopheles coustanni</i>		Laveran, 1900
<i>Anopheles rufipes</i>		Gough, 1910
<i>Anopheles hancocki</i>		Edwards, 1929
<i>Anopheles wellcomei</i>		Theobald, 1904

1.7 Malaria Control Strategies

Malaria remains a major public health concern globally and many strategies have been put in place towards malaria elimination. These strategies include an integrated strategy in vector control because the mosquitoes that transmit malaria are also vectors of other human diseases of great public health importance. Since 2000, progress in malaria control has resulted primarily from expanded access to vector control interventions, particularly in sub-Saharan Africa.

Malaria prevention and control have three principal components: reduction of contact between vector and human host, prevention of disease through prophylactic use of the antimalarial drug, and adequate treatment of malaria episodes to minimize the risk of transmission. Currently, no vaccines to protect against malaria are licensed but promising candidates are in development. For example, in January 2016, the RTS²S/AS01 vaccine that acts against only *P. falciparum* was recommended by WHO for pilot introduction in three selected African countries: Ghana, Malawi, and Kenya. Recent increases in resources (US\$ 3.2 billion in 2017 and US\$ 2.7 billion in 2018), political will, and commitment have led to the discussion of the possibility of malaria elimination and, ultimately eradication (WHO, 2020c).

1.7.1 Malaria Diagnosis

Several methods exist to diagnose malaria, and these range from microscopy to molecular methods. The most used method nowadays is molecular through rapid diagnosis testing kits. RDTs are used to detect specific malaria antigens in the patient's blood to establish a rapid diagnosis.

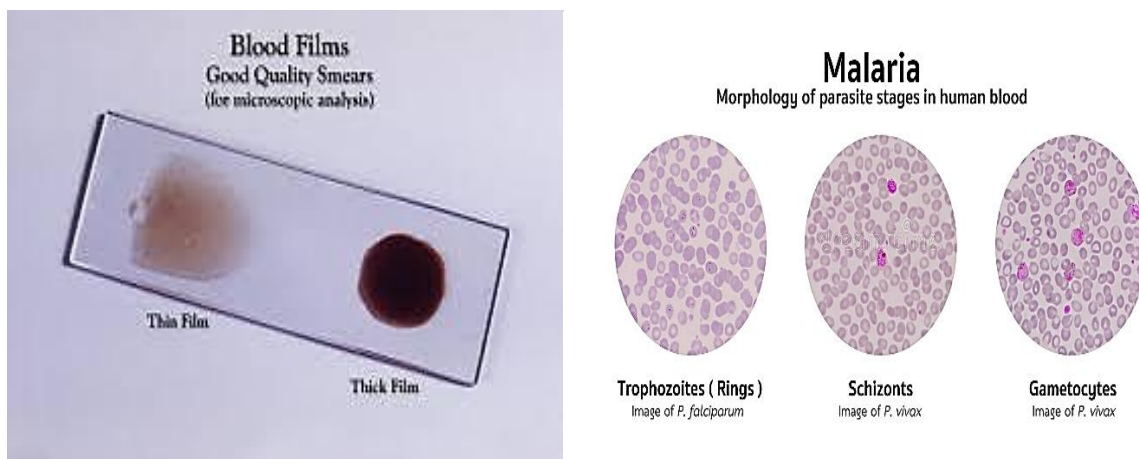


Figure 6: Microscopy technique to detect malaria.

Left: Thick and thin blood smears (<https://travelklinix.com/diagnosing-malaria/malaria-slide/>)
Right: Morphological identification of plasmodium parasite stages (<https://www.shutterstock.com/image-photo/microscopic-examination-blood-films-malaria-infected-500225857>)

However, RDT test are not always reliable and need to be confirmed by other techniques usually microscopy. Microscopy involves the identification under the microscope of the malaria parasite in a drop of the patient's blood spread out as a 'blood smear' on a microscope slide. Prior to examination, the specimen is stained (most often with the Giemsa stain) to give the parasites a distinctive appearance.

Table 4: Comparison between thick and thin blood smear of plasmodium detection (<https://www.slideshare.net/iyerbk/malaria-diagnostics>)

Microscopy thick smear	Microscopy thin smear
Lysed RBCs, many layers	Fixed RBCs, single layer
Large volume; 0.25µl blood/100 fields	Small volume; 0.005µl blood/100 fields
Good screening test (positive or negative)	Good species differentiation
Saves time in examination	Requires more time to read
Low density infection can be detected as blood elements are more concentrated	Low density infections can be missed
More sensitive	Less sensitive

1.7.2 Drug Therapy and Treatment

The WHO-recommended first-line treatment for uncomplicated *P. falciparum* malaria is the Artemisinin-based Combination Therapies (ACTs). ACT is a combination of two or more drugs that work against the malaria parasite in different ways. This is usually the preferred treatment for chloroquine-resistant malaria. Examples include artemether-lumefantrine (Coartem) and artesunate-mefloquine.

1.7.3 Vaccines and Vaccine Candidates for Malaria

RTS,S/AS01 (RTS,S) is a vaccine that acts against Plasmodium falciparum, the deadliest malaria parasite globally and the most prevalent in Africa. The vaccine significantly reduces malaria and life-threatening severe malaria in children. On 6 October 2021, WHO recommended widespread use of the RTS,S malaria vaccine. It was named RTS because it was engineered using genes from the repeat ('R') and T-cell epitope ('T') of the pre-erythrocytic circumsporozoite protein (CSP) of the Plasmodium falciparum malaria parasite together with a viral surface antigen ('S') of the hepatitis B virus (HBsAg). Malaria elimination requires a combination of complementary innovative tools and approaches tailored to local contexts to avoid a one-size fits all approach. This breakthrough is built on more than 30 years of research and development by technical partners with the collaboration of in-country and international partners.

1.7.4 Vector Control and Malaria Prevention

Vector control is frontline in the fight against malaria especially in sub-Saharan Africa where the favourable climate and abundance of breeding sites greatly favour mosquito proliferation and abundance. Several interventions in the fight against malaria target the mosquitoes such as Indoor Residual Spraying (IRS), Insecticide Treated Nets (ITNs).

1.7.5 Pest Control and Management in Agriculture

Pest control is the regulation or management of a species defined as a pest, a member of the animal kingdom that impacts adversely on human activities such as agriculture. This can be achieved by monitoring the crop, only applying insecticides when necessary, and by growing varieties and crops which are resistant to pests.

1.8 Chemical Use in Vector Control (Pest Control and Vector Control)

Today, integrated vector control strategies and interventions are recommended using the recommended classes of insecticides against disease vectors and agricultural pests (van den Berg et al., 2012). Insecticides are of chemical and biological origins and are used in agriculture, horticulture, forestry, gardens, homes, and offices. They are also used to control vectors, such as mosquitoes and ticks, which are involved in spreading human and animal diseases (Gupta et al., 2019). The WHO-recommended classes of insecticides for vector control are pyrethroids, organophosphates, organochlorines, and carbamates.

Table 5: List of insecticides currently recommended by the World Health Organization (WHO) for public health applications (Thatheyus & Selvam, 2013)

Insecticide	Class	Recommended Use	WHO Hazard Classification
Bendiocarb	Carbamate	IRS	II
Propoxur	Carbamate	IRS	II
DDT	Organochlorine	IRS	II
Fenitrothion	Organophosphate	IRS, Space spray	II
Malathion	Organophosphate	IRS, Space spray	III
Pirimiphos-methyl	Organophosphate	IRS, Space spray	III
A-Cypermethrin	Pyrethroid	IRS, LLIN	II
Bifenthrin	Pyrethroid	IRS	II

Cyfluthrin	Pyrethroid	IRS, LLIN, Space spray	II
Deltamethrin	Pyrethroid	IRS, LLIN, Space spray	II
Etofenprox	Pyrethroid	IRS, LLIN, Space spray	U
λ -Cyhalothrin	Pyrethroid	IRS, LLIN, Space spray	II
Permethrin	Pyrethroid	LLIN, Space spray	II
D-Phenothrin	Pyrethroid	Space spray	U
Resmethrin	Pyrethroid	Space spray	III

1.8.1 Pyrethroids

Pyrethroids are synthetic chemicals with a more refined action similar to the pyrethrum extracts of the chrysanthemum flower. The term ‘pyrethrum’ refers to the dried and powdered flower heads of the daisy-like plant belonging to the *Chrysanthemum* genus (Schleier III & Peterson, 2012). Pyrethrin shown in Figure 7, the insecticidal ingredient occurring in the flowers of *Tanacetum cinerariaefolium* (also known as *Chr. cinerariaefolium* or *Pyr. cinerariaefolium*), has been used widely for human and animal health protection by controlling indoor insect pests such as cockroaches, houseflies, and mosquitoes since ancient times (Krieger, 2010).

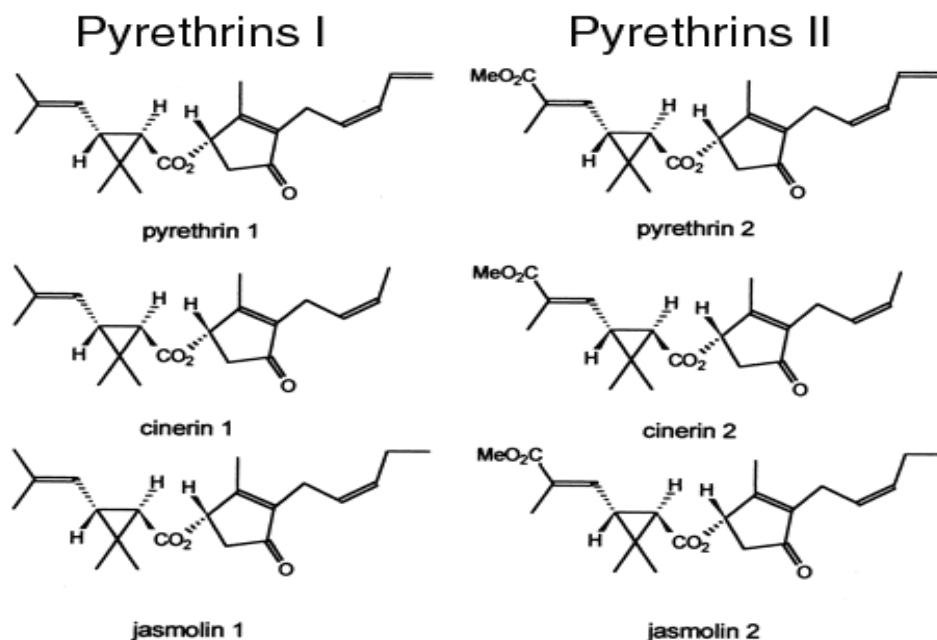


Figure 7: The chemical structure of the constituents of pyrethrum extracts which are collectively known as pyrethrin (Babić et al., 2012).

However, one of the limitations of pyrethrin, which is a mixture of six lipophilic esters was found to be a high rate of photodegradation and short "knockdown" (rapid paralysis) effect (Schleier III & Peterson, 2011). Thereafter, less photodegradable derivatives were synthesized known as pyrethroids. The dose recommended for their application is less than 1.5g, or at most 30g per 1000m², of land. The prominent advantages of pyrethroids are that they are highly lipophilic, easily biodegradable (environment-friendly), have low toxicity to terrestrial vertebrates, and do not bio-magnify like older chemical classes, such as organochlorines. Pyrethroids are widely applied in different domains especially in agriculture for pest control and public health for the control of disease vectors as described by Gupta concerning their impact on the environment (Kaviraj et al., 2014).

Pyrethroid insecticides are still the only WHO-recommended class for mosquito net impregnation. Several synthetic pyrethroids are currently available and widely used and classified as type I or II. The major difference between the two groups is the cyano-group (-CN) in the type II pyrethroids (Figure 8).

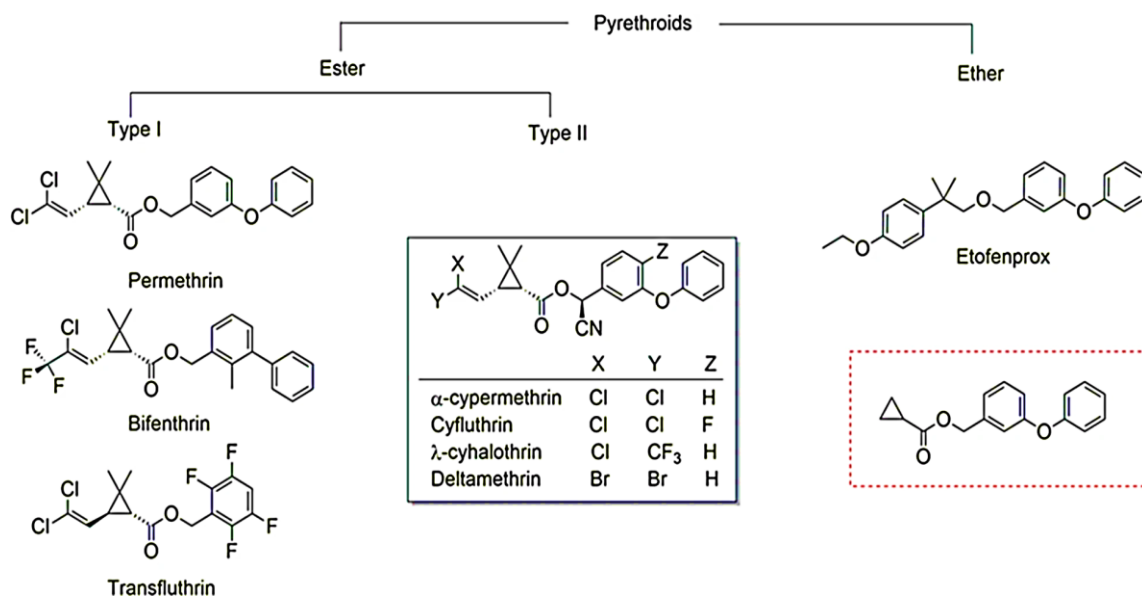


Figure 8: Chemical structure of first and second-generation pyrethroid insecticides (Moyes et al., 2021)

Pyrethroids have a rapid and efficient mode of action by acting on the nerve impulse at the level of the VGSC where they cause hyperexcitation and subsequently the death of the organism (Figure 9).

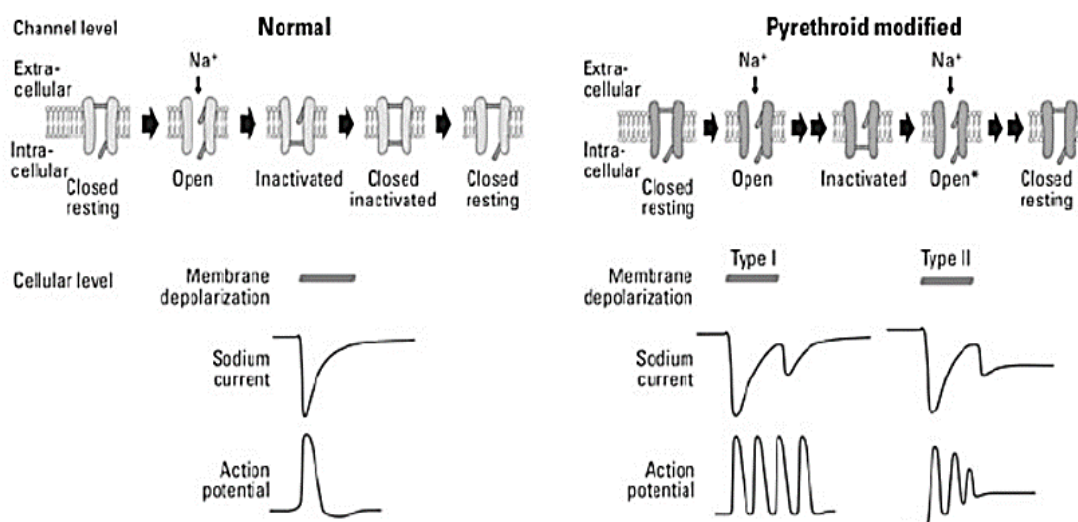


Figure 9: Mode of action of pyrethroids on VGSC (Kazachkova, 2007)

1.8.2 Carbamates

Carbamates are N-substituted esters of carbamic acid (Gupta et al., 2011). The inhibition of AChE by a carbamate insecticide occurs by a mechanism identical to that described for an organophosphate (Fukuto, 1990). The first step in the inhibition process involves the formation of the enzyme-inhibitor complex with subsequent carbamylation of the serine hydroxyl group of acetylcholinesterase at neuronal synapses and neuromuscular junctions as well as the inhibition of the enzyme (Graziadei & Metcalf, 1971; Metcalf et al., 1971). Examples of carbamates are carbaryl (SEVIN), oxamyl (VYDATE), carbofuran (FURADAN), thiodicarb (LARVIN) (Singh et al., 2012), bendiocarb (Turcam), propoxur (BAYGON), etc.

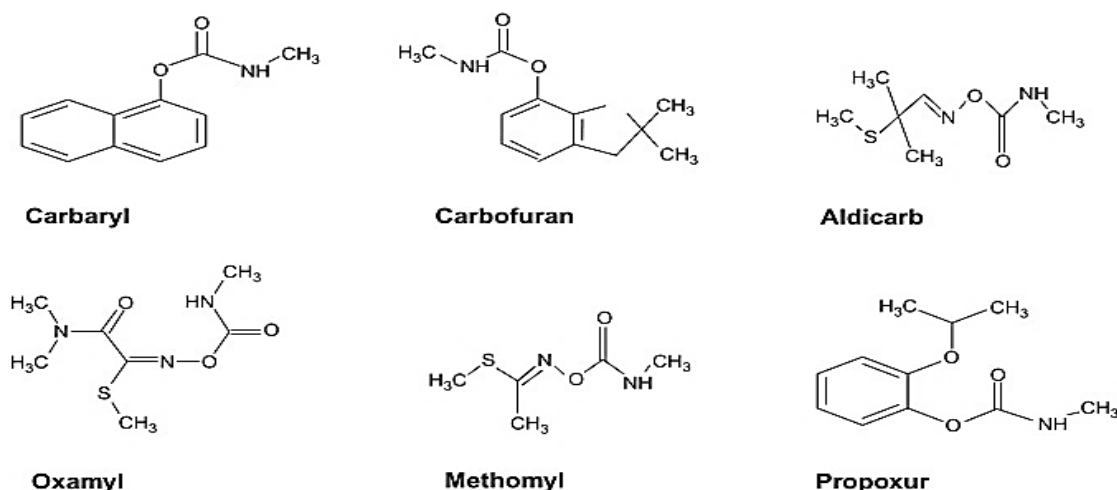


Figure 10: Some carbamates used in pest control (Kopeć et al., 2020)

1.8.3 Organochlorines

Organochlorine pesticides are chlorinated hydrocarbons used extensively from the 1940s through the 1960s (Elbashir et al., 2015). Representative compounds in this group include DDT, methoxychlor, dieldrin, chlordane, toxaphene, mirex, kepone, lindane, and benzene hexachloride. Since the 1970s, DDT and most other chlorinated hydrocarbon compounds have been restricted or banned for agricultural use in most countries, due in part to their unacceptably long persistence in the environment and because of increased concerns arising from their fat solubility (having a high partition coefficient in lipids versus water) and resultant long-term accumulation in fatty tissues of non-target organisms (Mellanby, 1992). However, DDT continues to be used in limited quantities in the control of insect vectors for public health purposes, as it was approved by WHO in 2006 for IRS (Sadasivaiah et al., 2007) DDT affects the peripheral nervous system; initial contact with the insecticide causing neurons to fire spontaneously causing muscles to twitch, with resulting tremors throughout the body and appendages, the so-called ‘DDT jitters’ (Davies et al., 2007). Over the course of a few hours or days, DDT exposure leads to excitatory paralysis and consequent death of the insect.

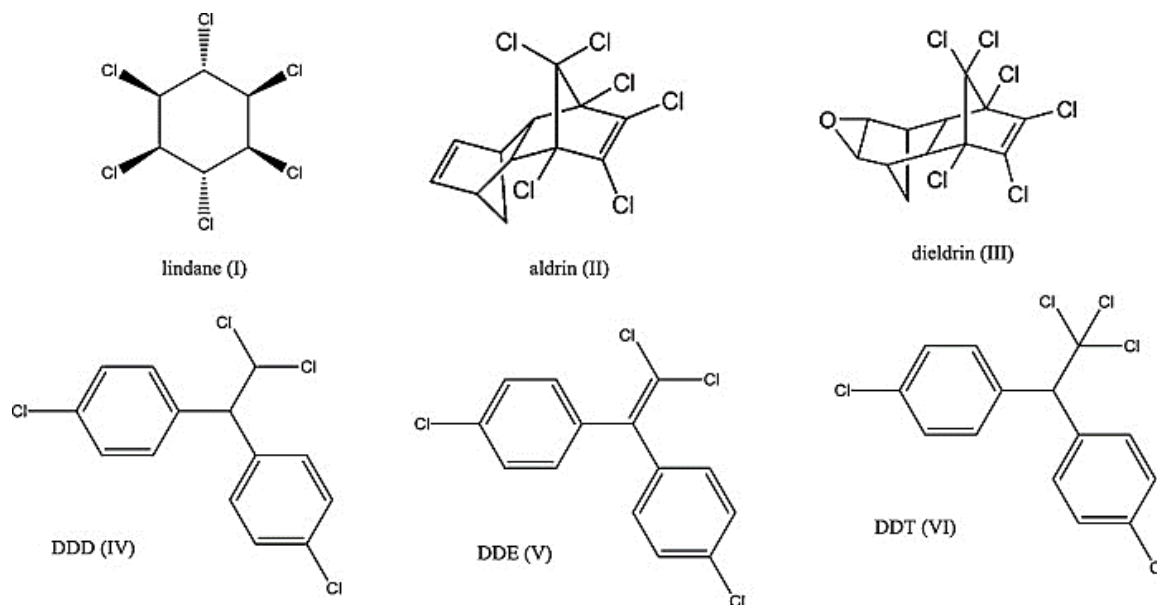


Figure 11: Some examples of organochlorines used in pest control (Kopeć et al., 2020)

1.8.4 Organophosphates

The toxicity of insecticidally active organophosphorus and carbamate esters to animals is attributed to their ability to inhibit acetylcholinesterase (AChE), a class of enzymes that catalyzes the hydrolysis of the neurotransmitter acetylcholine (ACh) (Fukuto, 1990). The

binding of OPs to AChE results in disruption of nerve impulses, killing the insect, or interfering with normal activities. OPs are normally esters, amides, or thiol derivatives of phosphoric, phosphonic, phosphorothioic, or phosphonothioic acids (Singh et al., 2012). The OPs are a very important group of compounds that vary tremendously in chemical structure and chemical properties (Bloomquist, 1996). The OP compounds can be miscible with water, but more typically are miscible in organic solvents. Generally, OPs react with a serine hydroxyl group within the enzyme active site, phosphorylating the serine hydroxyl group and yielding a hydroxylated "leaving group". This process inactivates the enzyme and blocks the degradation of the neurotransmitter, acetylcholine. There are at least 13 types of OPs (Gupta, 2011); of these malathion belongs to phosphorodithioates, sarin belongs to phosphorofluoridates, diazinon, parathion and pirimiphos-methyl belong to phosphorothioates, and dichlorvos belongs to phosphonates. OPs used in mosquito control programmes include: fenthion (bytex), temephos (abate), chlorpyrifos (dursban), fenitrothion (sumithion), pirimiphos-methyl (actelic), malathion, etc.

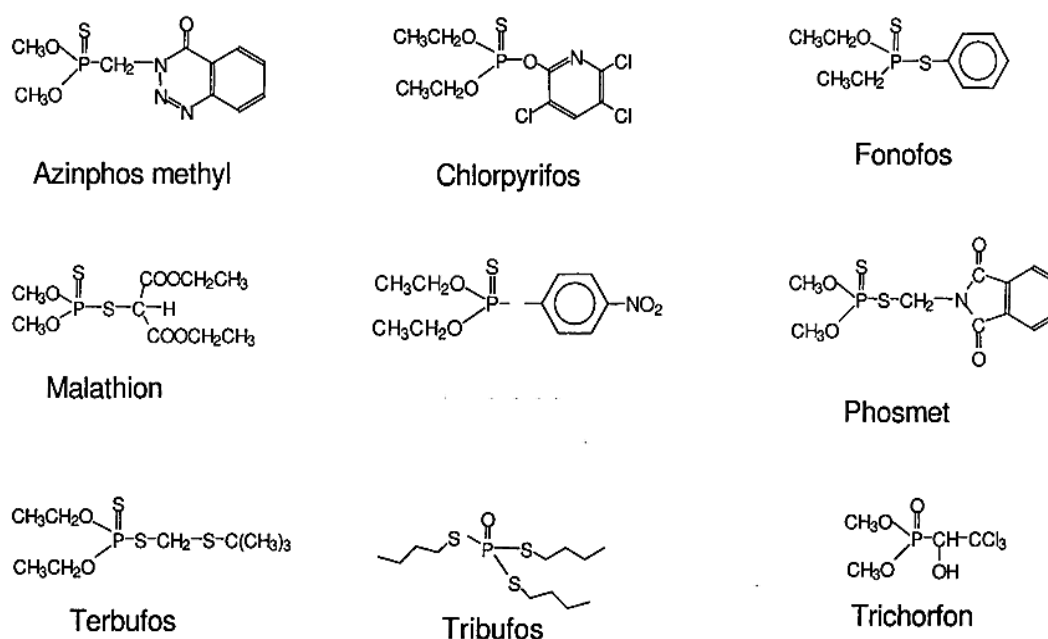


Figure 12: Some examples of organophosphates used in pest control (Kopeć et al., 2020)

1.8.5 Other Insecticides

Other compounds with insecticidal activities used for the control of insect pests include neonicotinoids and ryanoids. Neonicotinoids possess either a nitromethylene, nitroimine, or cyanoimine group (Matsuda et al., 2001) and important neonicotinoids, such as imidacloprid, nitenpyram, and acetamiprid, all contain a 6-chloro-3-pyridyl moiety and therefore resemble

AMELIE WAMBA NDONGMO Regine/Doctorate/Ph.D. Thesis/University of Yaoundé I

nicotine and epibatidine, both of which are potent agonists of nicotine acetylcholine receptors (nAChRs). Imidacloprid and other nitromethylene compounds like 1-(pyridine-3-yl-methyl)-2-nitromethyleneimidazoline (PMNI) are increasingly used worldwide as an insecticide (Bai et al., 1991). Ryania insecticide is the powdered stem wood of *Ryania speciosa* Vahl., a small shrub growing extensively in South America, and noted for its pest control properties (Jefferies et al., 1991). The major insecticidal and toxic constituents are ryanodine (Jefferies et al., 1992) and 9,12-didehydroryanodine (Waterhouse et al., 1985), which have attracted much attention as natural but expensive insecticides and for their action on the Ca^{2+} -ryanodine receptor complex of muscle (Lai et al., 1989). Ryanodine has been described in several studies to induce paralysis in insects and vertebrates by causing a sustained contracture of skeletal muscle without depolarizing the muscle membrane (Bloomquist, 1996).

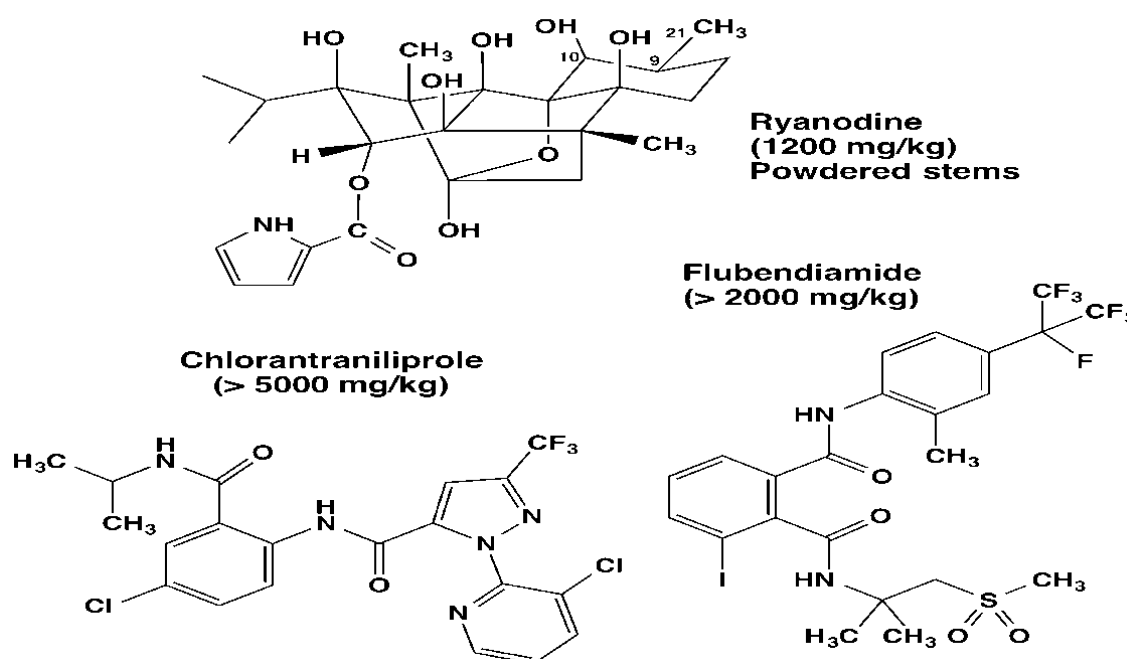


Figure 13: Ryanoids and synthetics (Kopeć et al., 2020)

1.8.5.1 Neonicotinoids

Neonicotinoid pesticides were discovered in the late 1980s and have since a widespread use in veterinary medicine and crop production (Simon-Delso et al., 2015). The neonicotinoid insecticide includes imidacloprid, acetamiprid, dinotefuran, thiamethoxan, and clothianidin. Neonicotinoids have a high target specificity to insects, and a relatively low risk for nontarget mammalian species and the environment. Among all neonicotinoids, clothianidin is the first manufactured compound used as a new alternative insecticide for IRS with long-lasting residual

activity for public health. The two IRS formulations that have been evaluated and prequalified by the WHO are SumiShield 50WG® (50% clothianidin) industrialized by Sumitomo Chemical and Fludora®Fusion (Bayer Environmental Science) which is a mixture of 500 g/kg clothianidin and 62.5 g/kg deltamethrin ((WHO, 2020c).

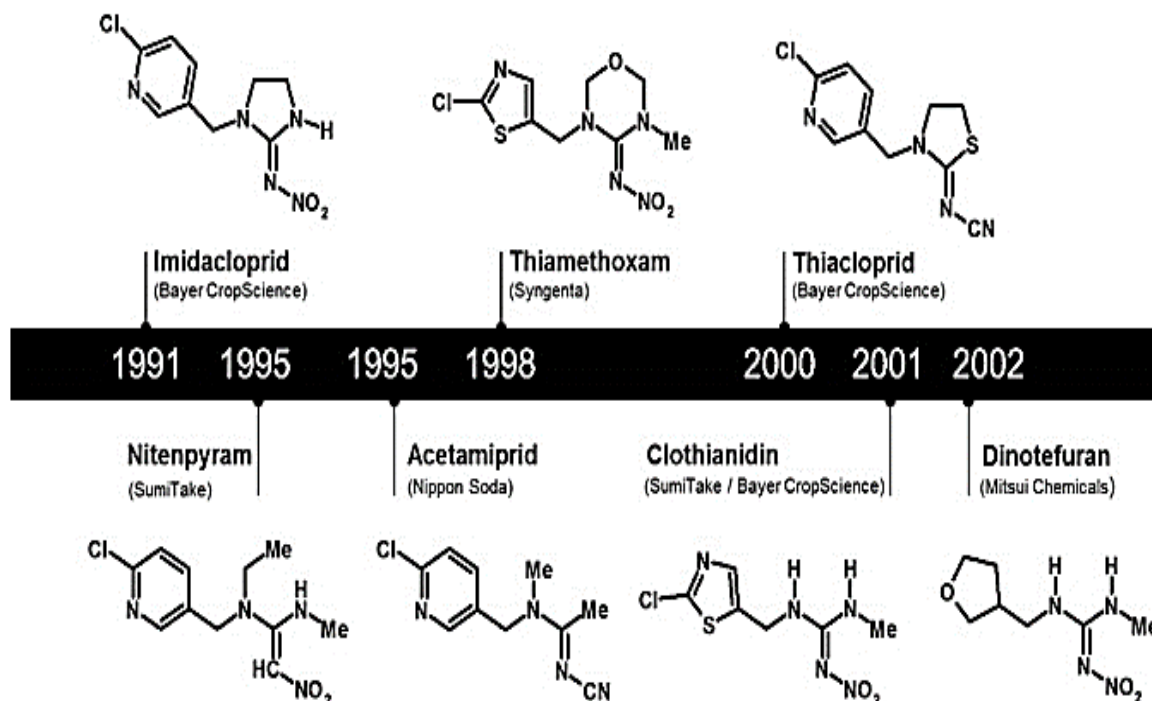


Figure 14: The global status of insecticide resistance to some neonicotinoid insecticides (Bass et al., 2015)

1.8.5.2. Pyrroles

Pyrroles are broad-spectrum insecticides and acaricides originally used in agriculture and cattle industry and later approved by WHO as new alternative chemical compounds for vector control in public health use (WHO, 2020c). They are pro-insecticides that require initial activation by mixed-function oxidases to produce the active compound. Pyrroles act at the cellular level and disrupt respiratory pathways and proton gradients through the uncoupling of oxidative phosphorylation in mitochondria (Black et al., 1994). Chlorfenapyr was the first pyrrole insecticide examined for its efficacy and personal protection potential against pyrethroid insecticide-resistant and susceptible malaria vectors when mixed with pyrethroids (Bayili et al., 2017). A new LLIN based on chlorfenapyr named Interceptor G2 is currently commercially available and recommended by the WHO.

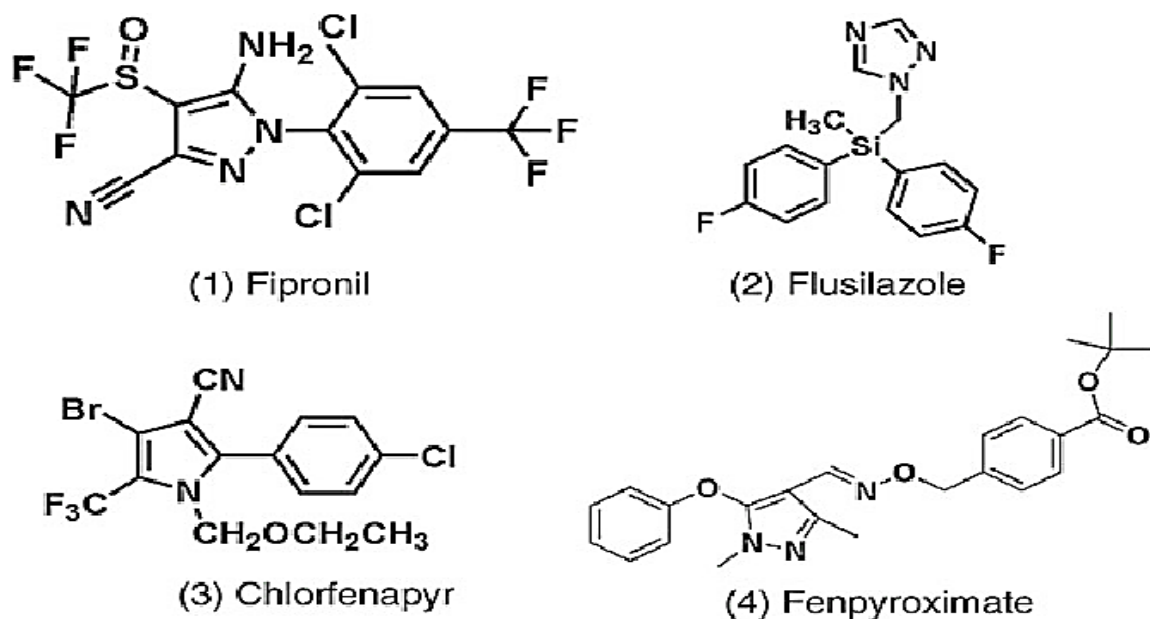


Figure 15: Some examples pyrazole and pyrrole insecticides used in pest control (Ma et al., 2018)

The intensive use of chemicals in the fight against malaria vectors coupled with an uncontrolled use in agricultural pest control has constituted a selection pressure resulting in the emergence and dissemination of insecticide resistance (IR) in mosquitoes now posing a major threat to the continued efficacy of implemented vector control strategies.

1.9 Insecticide Resistance (IR)

1.9.1 Introduction

The term resistance is defined as the ability of an insect (population) to withstand the effects of an insecticide by becoming resistant to its toxic effects by means of natural selection and mutations (Davidson, 1957). Also, it can be defined as a heritable change in the sensitivity of a pest population that is reflected in the repeated failure of a product to achieve the expected level of control when used according to the label recommendation for that pest population. Repeated exposure to insecticides can select individuals possessing biochemical machineries that can detoxify the insecticides more rapidly or are less sensitive to it (Riveron et al., 2018). These individual survivors could then pass the resistance traits to the succeeding generations resulting in pest populations being more resistant until ultimately a situation is reached whereby the pests become completely resistant to the insecticide. In a review (Corbel & N'Guessan, 2013) resistance has been described to be present in more than 500 insect species worldwide and that to date malaria vectors have developed resistance to the main chemical classes used in public health, the pyrethroids, organochlorines, carbamates, and organophosphates (Riveron et al., 2018).

1.9.2 Overview of Insecticide Resistance in Cameroon

In Cameroon, malaria vectors are highly resistant to all chemical compounds belonging to organochlorines. According to studies carried out on *An. gambiae* s.l. and *An. funestus*, this profile of resistance to organochlorine varies in time across the country (Wondji et al., 2005) (Antonio-Nkondjio et al., 2017; Bigoga et al., 2012; Menze et al., 2018; Nkemngo et al., 2020). Depending on the three epidemiological facies of malaria in Cameroon, the progressive increase of resistance profiles to pyrethroids is found variable during the periods 2000- 2007 and 2008 to 2021. Globally, a significant increase in pyrethroid resistance in *An. gambiae* s.l. in forest facies was observed over time, for both type I (permethrin) and type II (deltamethrin) pyrethroids (Bamou et al., 2019; Etang et al., 2007; Menze et al., 2018; Nwane et al., 2009; Tchakounte et al., 2019).

More recently, growing resistance to carbamates has been reported in malaria vectors in Cameroon. Five collected field populations of *An. gambiae* s.l. located in forest facies showed confirmed resistance to bendiocarb (Bamou et al., 2019). Another study with field-collected *An. gambiae* from Bankeng, a locality in southern Cameroon, showed high resistance to

bendiocarb and propoxur (Elanga-Ndille et al., 2019). No resistance to organophosphates has been reported in malaria vectors from Cameroon, and also very few studies have been conducted to test organophosphates compared to other main insecticides classes. However, prior to 2007, all populations of *An. gambiae* s.l. and *An. funestus* tested exhibit a full susceptibility to insecticides of this class. This trend remains unchanged during the period from 2008 to 2019 for malathion, fenitrothion or chlorpyrifos-methyl (Nkemngo et al., 2020; Tchakounte et al., 2019).

1.9.3 Types of Insecticide Resistance Mechanisms

The various mechanisms that enable insects to resist insecticides can be grouped into four distinct categories including metabolic resistance, target-site resistance, reduced penetration, and behavioural avoidance, as aptly reviewed in (Corbel & N'Guessan, 2013). However, increased excretion of the insecticides by some pests is also termed another mechanism of resistance

1.9.3.1 Cuticular Resistance

Modifications in the cuticle or digestive tract of insects can prevent, slow down absorption, or reduce the penetration of insecticides (Corbel & N'Guessan, 2013). Reduced uptake of insecticides (cuticular resistance) has been observed in some insect pests especially ones where the major route of exposure is through ingestion (Figure 16). For mosquito control, where insecticides are applied onto bed nets and on wall surfaces, uptake is primarily through the appendages. Therefore, increase in the thickness of the tarsal cuticle, or a reduction in its permeability to insecticide could lipophilic insecticide could have a major impact on the bioavailability of an insecticide *in vivo* (Corbel & N'Guessan, 2013). Decreased penetration of insecticides would allow sufficient time for detoxifying enzymes to metabolise the chemical and therefore make it less effective (Plapp & FW, 1976). Microarray studies have identified two genes encoding cuticular proteins that were upregulated in pyrethroid-resistant strains of *An. stepensi* (Vontas et al., 2007) and *An. gambiae* (Awolola et al., 2009). Also, it has been established using scanning by electron microscopy that in a laboratory strain of *An. funestus*, the mean cuticular thickness was significantly greater in pyrethroid-tolerant mosquitoes than in their susceptible counterparts (Balabanidou et al., 2018; Wood et al., 2010).

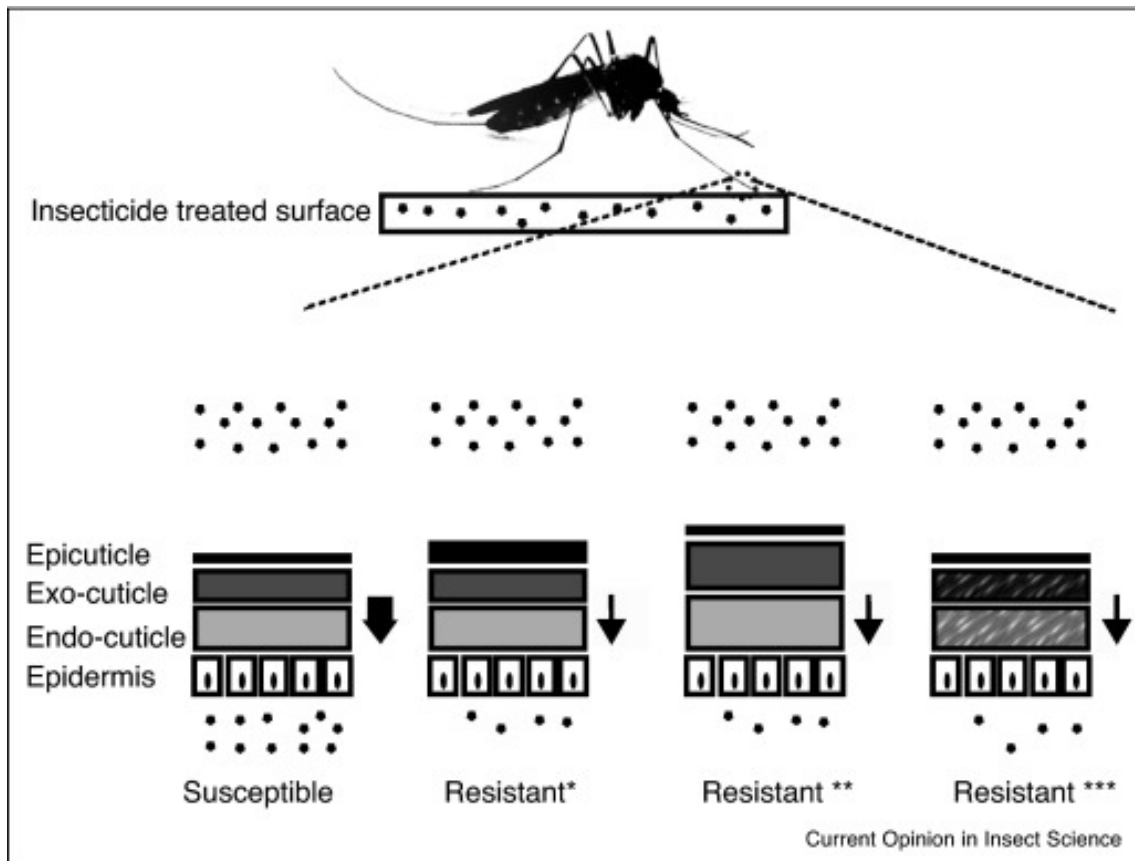


Figure 16: Layers of cuticle and impact on insecticide resistance phenotype in mosquitoes (Balabanidou et al., 2018)

1.9.3.2 Behavioural Resistance

Continued exposure to chemicals may trigger a change in the response and behaviour of insect pests (Corbel & N'Guessan, 2013) that could result in an ability to avoid lethal doses of insecticides (Chandre et al., 2000). This type of response could either be direct contact excitation (or 'irritancy') and non-contact spatial repellence that is used when insects move away from the insecticide-treated area before making direct contact (Roberts et al., 1997). In *An. funestus*, behavioural resistance has been identified as a shift from indoor to outdoor biting preference in Tanzania in relation to increasing coverage of pyrethroid-impregnated net (Russell et al., 2011) as well as significant changes in the host-seeking behaviour of the *An. funestus* population from Benin (West Africa) where scaling up LLINs at the community level induced a change from night biting to early-morning biting behaviour (Moiroux et al., 2012). These changes could impact the mating, laying, feeding and host-seeking abilities of mosquitoes and hence their survival (Figure 17).

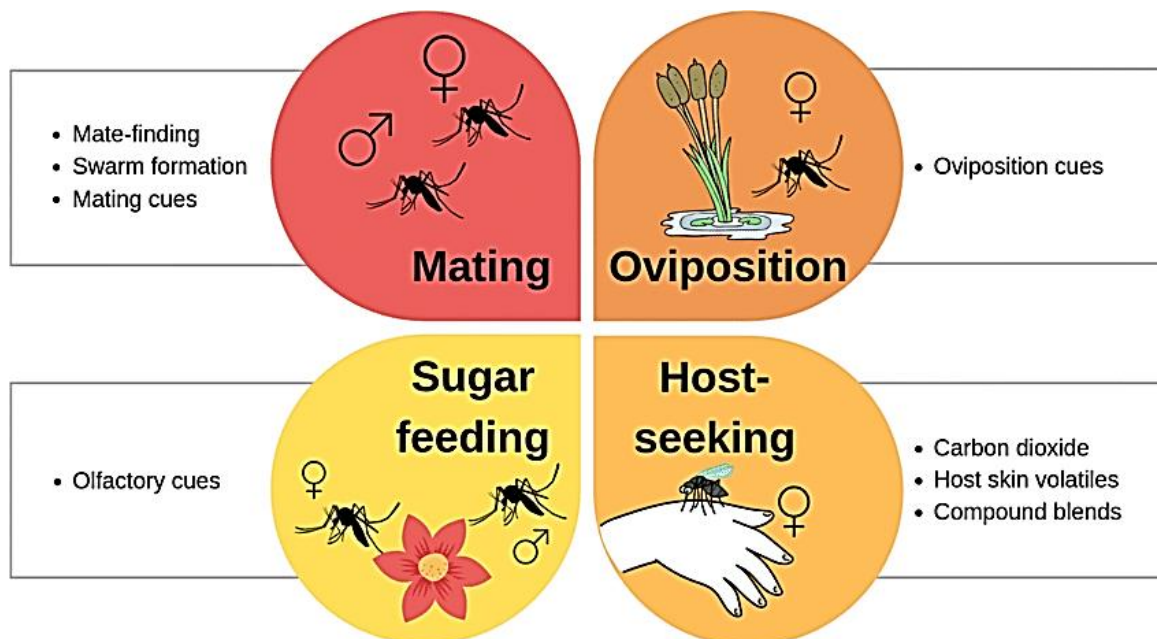


Figure 17: Aspects of behavioural resistance that could impact insecticide resistance in mosquitoes (Wooding et al., 2020)

1.9.3.3 Biochemical Mechanisms of Insecticide Resistance

In biochemical resistance, an insecticide is detoxified by one or more enzymes before it can reach its site of action and for example reduced neuronal sensitivity to insecticides as observed with knockdown resistance (*kdr*) in house flies to DDT and pyrethroids. If the target is unmodified, the efflux rate of the insecticide molecules could be affected by transporter molecules such as ABC transporters determining the quantity of active insecticide molecules reaching the target. Also, a thickening of the cuticle could impact greatly on the amount of insecticide reaching the target in the cell. Even when the molecules reach the target, an increase in detoxification enzyme activity, rate and quality could prevent the insecticide to fulfil its intended function. Besides these intra cellular and extracellular factors, there could also be the role of symbionts such as *Wolbachia* and *Asaia* which can contribute to the ability of mosquitoes to evade insecticide action (Figure 18).

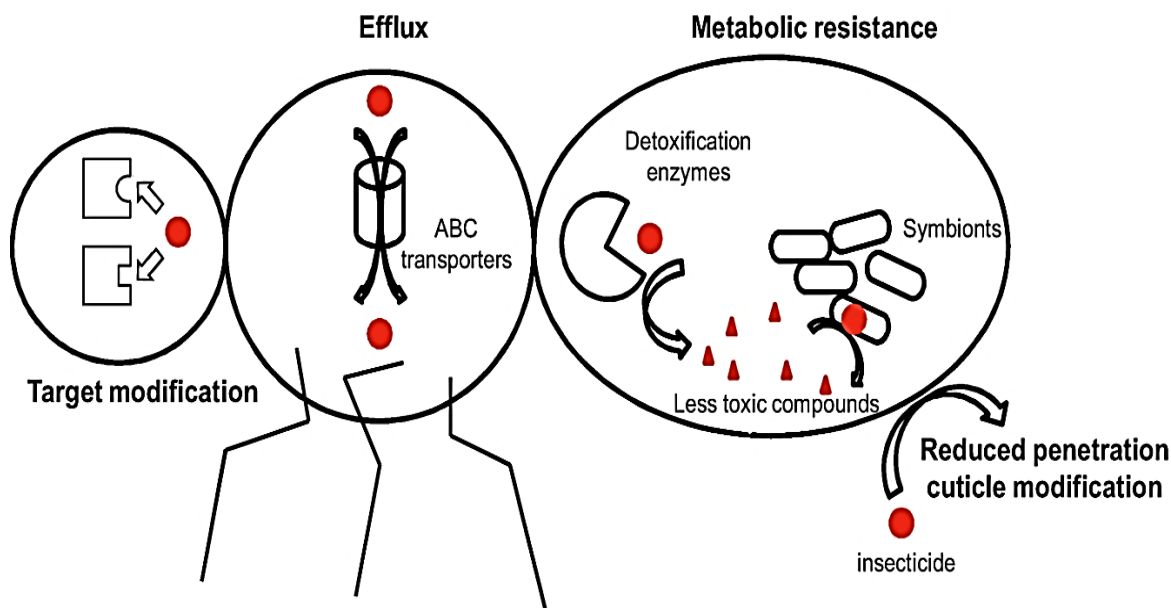


Figure 18: Major drivers of insecticide resistance

1.9.3.3.1 Target-site Resistance

Insecticides generally act in a specific manner within the insect, typically within the nervous system (for example OPs, carbamates, DDT and pyrethroid insecticides) (Corbel & N’Guessan, 2013) and modifications in resistant mosquito strains of such targets result in the inability of the insecticide molecule to bind effectively, making it inefficient (Ranson et al., 2000). Reduced sensitivity of target receptors to insecticide results from non-synonymous point mutations in the gene encoding the protein.

1.9.3.3.1.1 Knockdown Resistance (kdr)

Mutations in the amino acid sequence in the VGSC of nerve cell membranes lead to a reduction in the sensitivity of the channel to the binding of DDT and pyrethroids (Davies et al., 2007). Alterations in the target site that results in resistance in insects are often termed kdr with regards to the ability of insects with these modifications to withstand prolonged exposure to insecticides without being ‘knocked-down’ (Corbel & N’Guessan, 2013) (Figure 19).

Kdr was first identified in houseflies (Busvine, 1951) and the kdr factor is now known to be a recessive allele conferring cross resistance to the entire class of pyrethroids as well as DDT and its analogues (Davies et al., 2007). More than 20 unique VGSC sequence polymorphisms have been identified in association with pyrethroid resistance and reported in many important pest species usually accompanied by a second recessive resistance trait designated super-kdr which confers much greater resistance to pyrethroids (Farnham et al., 1987).

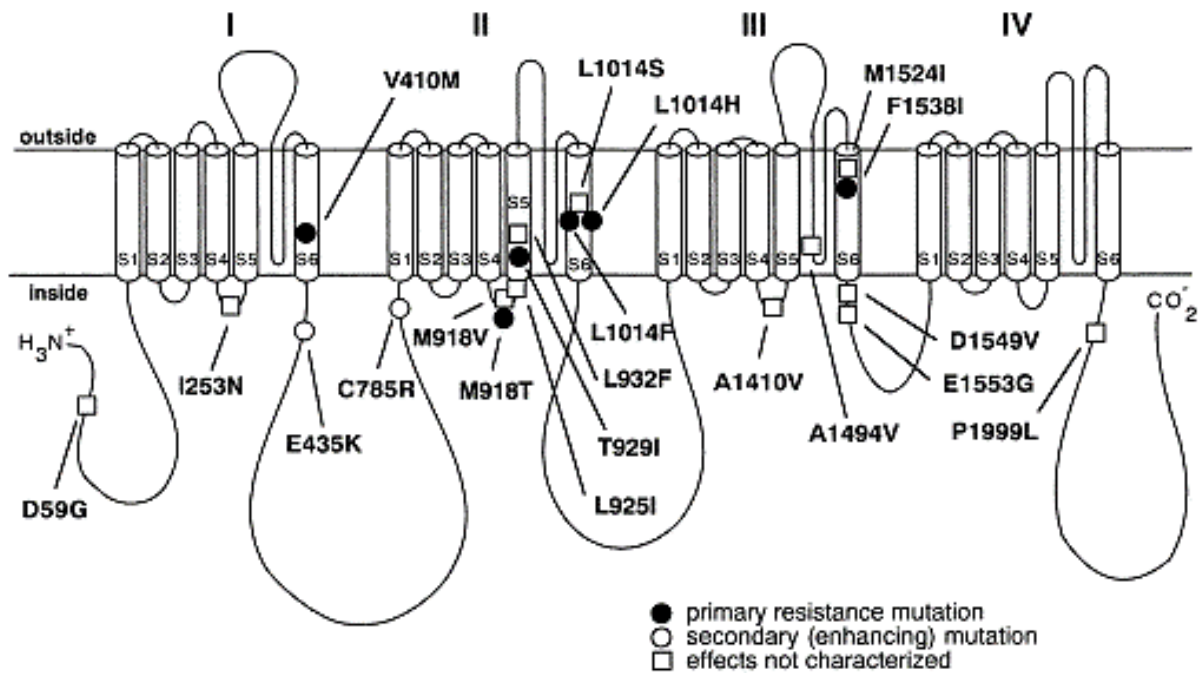


Figure 19: The molecular biology of knock-down resistance to pyrethroid insecticides

Czeher, Cyrille. (2010). Nation wide Insecticide-treated bednets distribution in Niger : effects on malaria vectors.

A very common amino acid substitution associated with pyrethroid resistance in malaria vectors especially *An. coluzzii*, *An. gambiae* Giles and *An. arabiensis* is a substitution of the leucine residue found in codon 1014 with either phenylalanine (1014F) (Martinez- Torres et al., 1998) or Serine (1014S) (Ranson et al., 2000) in the VGSC. So far, no *kdr* mutation has been discovered in the VGSC of *An. funestus* and associated with insecticide resistance.

1.9.3.3.1.2 Insensitivity to Acetylcholinesterase

Several mutations in the gene encoding AChE have been found in insects (Fournier, 2005) and the mutations result in reduced sensitivity to inhibition by insecticides (Weill et al., 2003). Gly¹¹⁹Ser mutation responsible for carbamate and OP resistance has been reported in *An. gambiae* and *Cx. Papiens* (Weill et al., 2004). Overexpression of the AchE gene, partially due to gene duplication of Gly¹¹⁹Ser copies confer carbamate resistance in *An. gambiae* from West Africa (Edi et al., 2014).

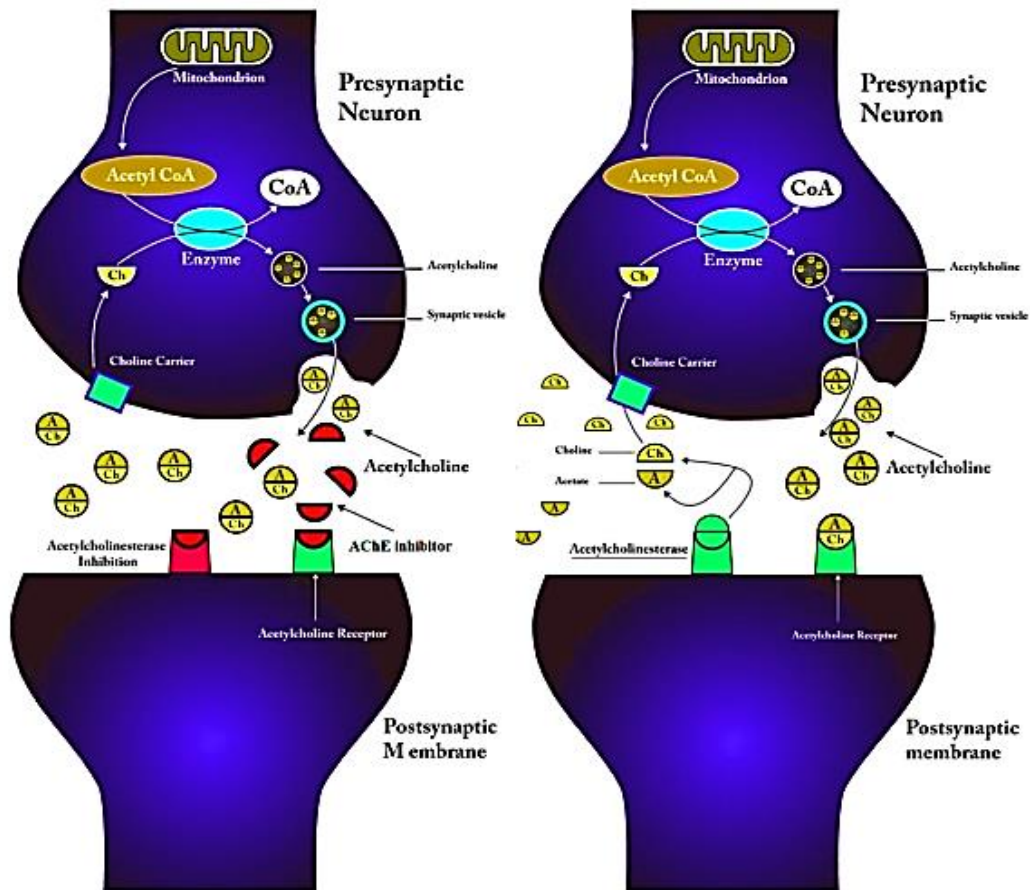


Figure 20: Mechanism of action of AChE with insect acetylcholinesterase inhibitors (left) and without the presence of acetylcholinesterase inhibitors (right) (Hematpoor et al., 2017)

1.9.3.3.1.3 GABA Receptor *rdl* Mutation

In insects, the GABA receptor is an action site for cyclodienes (Hemingway & Ranson, 2000). Several mutations in this receptor associated with resistance have been described for insects (Corbel & N'Guessan, 2013). In *An. gambiae*, substitutions of conserved Ala³⁰² in the Rdl locus with serine or glycine have been associated with resistance to dieldrin (Du et al., 2005).

Dieldrin resistance was first detected in *An. funestus* populations from West (Burkina Faso) and Central (Cameroon) Africa (Wondji et al., 2011). The Ala²⁹⁶Ser mutation in *An. funestus* has been associated with dieldrin resistance and is widely distributed in West and Central Africa (Wondji et al., 2011) but absent in southern African *An. funestus* populations. East (Uganda) and southern (Malawi and Mozambique) African populations were found to be susceptible to dieldrin.

Effects of mutations on inhibitory activity of *meta*-diamides

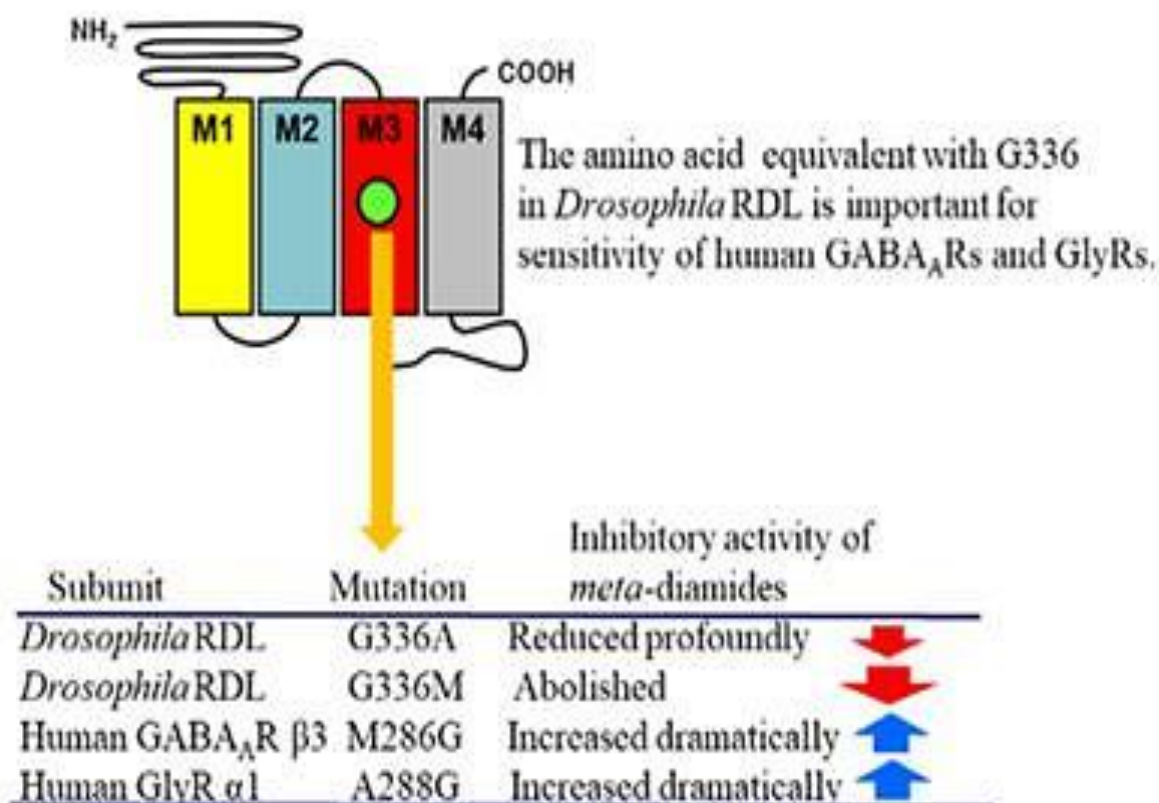


Figure 21: RDL GABA-receptor-targeted resistance in *Drosophila*

1.9.3.3.2 Metabolic-based Resistance

In major malaria vector *An. funestus*, the insecticide resistance mechanism is mainly metabolic involving major detoxification genes such as esterases, glutathione-S-transferases, and cytochrome P450s. These genes are involved in underlying biochemical mechanisms driving resistance in mosquitoes either through increased bioavailability (overexpression) or polymorphisms (allelic variation). Several components of cellular function vary between susceptible and resistant mosquitoes which determine the survival of the mosquitoes (Figure 22).

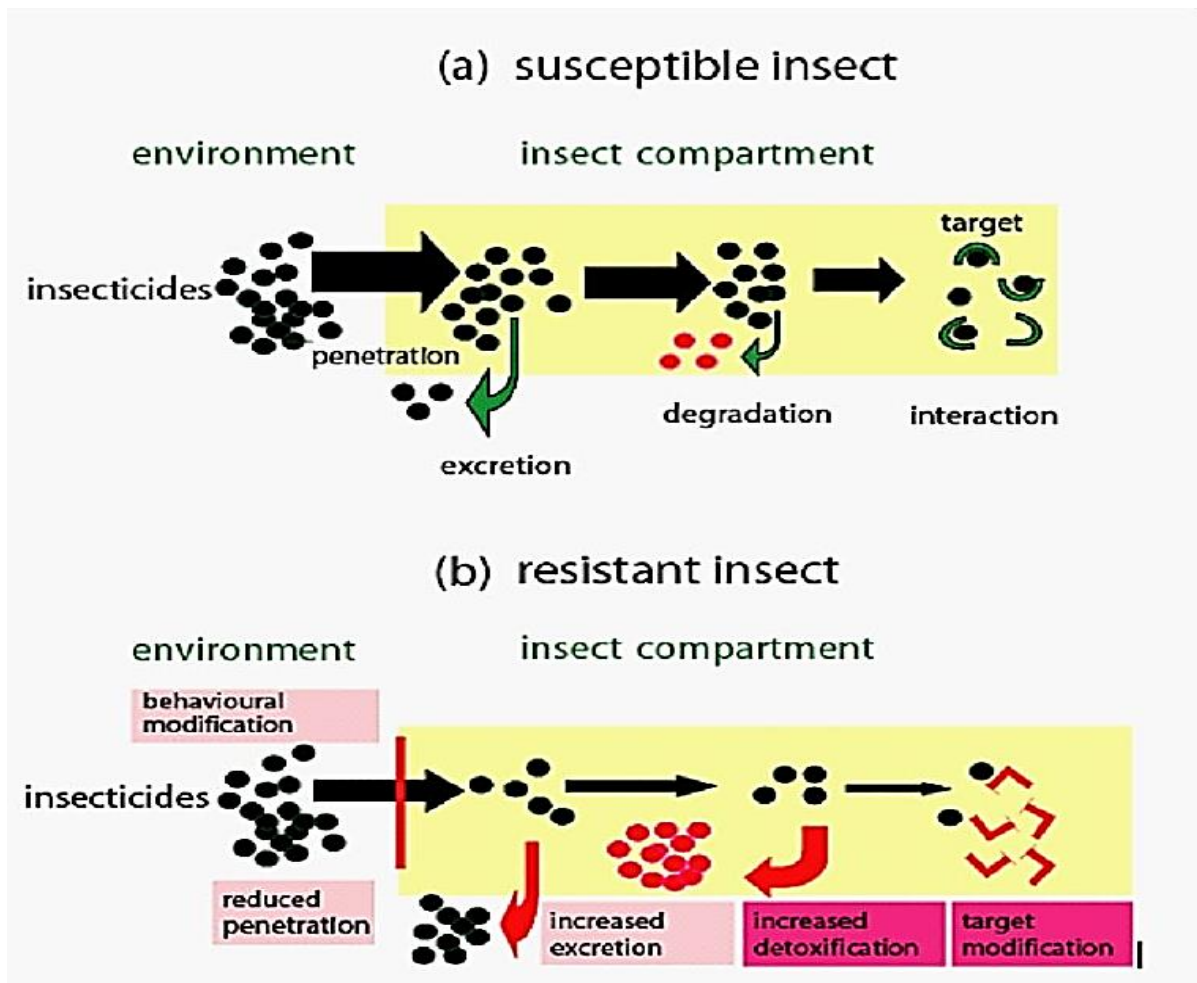


Figure 22: Components of metabolic resistance in mosquitoes (Corbel & N’Guessan, 2013)

1.11 Insecticide Resistance Management

Insecticide resistance management can follow the principle of moderation, saturation, or multiple attack (Curtis & Hill, 1993). This involves an integrated approach for vector control where different insecticides used are tracked and monitored for the emergence of resistance. Smart use of insecticides coupled to timely rotation from one insecticide to another could be useful in curbing the emergence and spread of insecticide resistance in malaria vectors. The WHO has frequently made and updated guidelines on insecticide resistance management. Chemical manufacturer’s are also keenly observing this phenomenon which now drives a huge quest for novel tools and new insecticides that could help fight the spread of insecticide resistance in malaria vectors which is posing a major threat to malaria elimination goals.

1.12 Metabolic Drivers of Insecticide Resistance

1.12.1 Cytochrome P450 - based Metabolic Resistance

The P450 enzymes (mixed function oxidases, cytochrome P450 monooxygenases), a diverse class of enzymes found in virtually all insect tissues, fulfil many important tasks, from the synthesis and degradation of ecdysteroids and juvenile hormones to the metabolism of foreign chemicals of natural or synthetic origin. Cytochrome P450s have been fundamental to the successful adaptation of insects to diverse habitats and contribute greatly to the detoxification of xenobiotics and toxins. Now, P450s are grouped into four major families: *CYP2*, *CYP3*, *CYP4* and the mitochondrial P450 clade which all intervene in the detoxification of endogenous and exogenous xenobiotics. In mosquitoes, the rate at which a particular substrate is oxidized differs from one P450 to another, so that the overall metabolism of a specific substrate depends on the different forms present and varies between tissues, life stages, and sexes. Because of the multiple cytochrome P450s expressed in each organism and the broad substrate specificity of some of these isoforms, P450s can oxidize a bewildering array of xenobiotics. While the importance of P450s in insect physiology and toxicology is widely recognized, it is not yet clear how many P450 genes precisely are involved in insecticide resistance in a single insect such as the mosquito. There are two very important and widespread mechanisms of resistance that have been uncovered by insect toxicology researchers: (1) enhanced rates or pathways of detoxification by the insect, and (2) altered target site.

1.12.2 Esterase-based Metabolic Resistance

Increase in the expression levels of esterase genes have been associated to organophosphate, pyrethroid and carbamate resistance in several pests (Farnsworth et al., 2010). Esterases are associated with resistance to insecticidal esters in mosquitoes, especially OPs and pyrethroids (Hemingway & Ranson, 2000). In some malaria vectors, qualitative change in an esterase occurs when a mutation of the gene results in an enzyme with heightened affinity for insecticide substrates. However, in mosquito vectors, these genes have not yet been characterized and more work is necessary to understand the molecular basis and underlying biochemical mechanisms of esterase-based metabolic resistance.

1.12.3 Glutathione-S-Transferases (GSTs)-mediated Metabolic Resistance

Glutathione-S-Transferases (GST) are a family of phase II detoxification enzymes that function to protect cellular macromolecules from attack by reactive electrophiles. GSTs catalyse the conjugation of glutathione (GSH) to a variety of endogenous and exogenous electrophilic compounds. There are more than 30 GST genes in mosquitoes involved in a wide range of biological processes principally conjugation and many studies have focused on their role in insecticide metabolism. This is due to elevated levels of GST activity which have been associated with resistance to all the major classes of insecticides (Ranson & Hemingway, 2005). GSTs confer metabolic resistance through direct metabolism or sequestration of insecticides as well as indirectly through protection against oxidative stress induced by exposure to insecticides. Many studies have shown that multiple, complex resistance mechanisms-increased metabolic detoxification of insecticides and decreased sensitivity of the target proteins-or genes are likely responsible for insecticide resistance. Recent advances in genome and transcriptomic sequencing together with modern genetic, functional, and biochemical techniques have facilitated the unravelling of specific GST-mediated resistance mechanisms. In *Anopheles funestus*, the identification of the first DNA-based metabolic marker of GST-based metabolic resistance caused by a leucine to phenylalanine amino acid change at codon 119 in the glutathione S-transferase epsilon 2 (L119F- GSTe2) has been reported and confirmed by many studies and associated with a fitness cost translated in lower fecundity rates, reduced larval development but an increased adult longevity.

1.12.4 Other Molecular Drivers of Insecticide Resistance

1.12.4.1 UDPs

Uridine diphosphate glycosyltransferases (UGTs) are multifunctional detoxification enzymes, which are involved in metabolizing various chemicals and contribute to the development of insecticide resistance. Recent advances in genome sequencing have permitted the assessment of the role of the multigene UGT family in insecticide resistance in mosquitoes (Huang et al., 2017). In mosquitoes, exposure to insecticides causes stress which disrupts the homeostasis leading to excessive production and accumulation of reactive oxygen species (ROS). Therefore, to defend against oxidative damage, mosquitoes implicate many complex mechanisms to maintain cellular homeostasis (Zhang et al., 2013). UDP-glucosyltransferases are a part of the critical detoxification mechanisms (Ahn et al., 2012) however, the specific way they effect this function remains to be elucidated. They are known to act through glycosylation reactions

through which they catalyse the conjugation of a small range of lipophilic compounds with sugars to produce glycosides.

1.12.4.2 ABC Transporters

Insect ATP-Binding Cassette (ABC) transporters are a large class of transmembrane proteins and play an important role in the transport and detoxification of xenobiotics. Insect ABC transporters are involved in insecticide detoxification and *Bacillus thuringiensis* (Bt) toxin perforation. The complete ABC transporter is composed of two hydrophobic transmembrane domains (TMDs) and two nucleotide binding domains (NBDs). Conformational changes that are needed for their action are mediated by ATP hydrolysis. According to the similarity among their sequences and organization of conserved ATP-binding cassette domains, insect ABC transporters have been divided into eight subfamilies (ABCA–ABCH). The upregulation of ABC transporter genes has been associated to insecticide resistance in insects especially to pyrethroids.

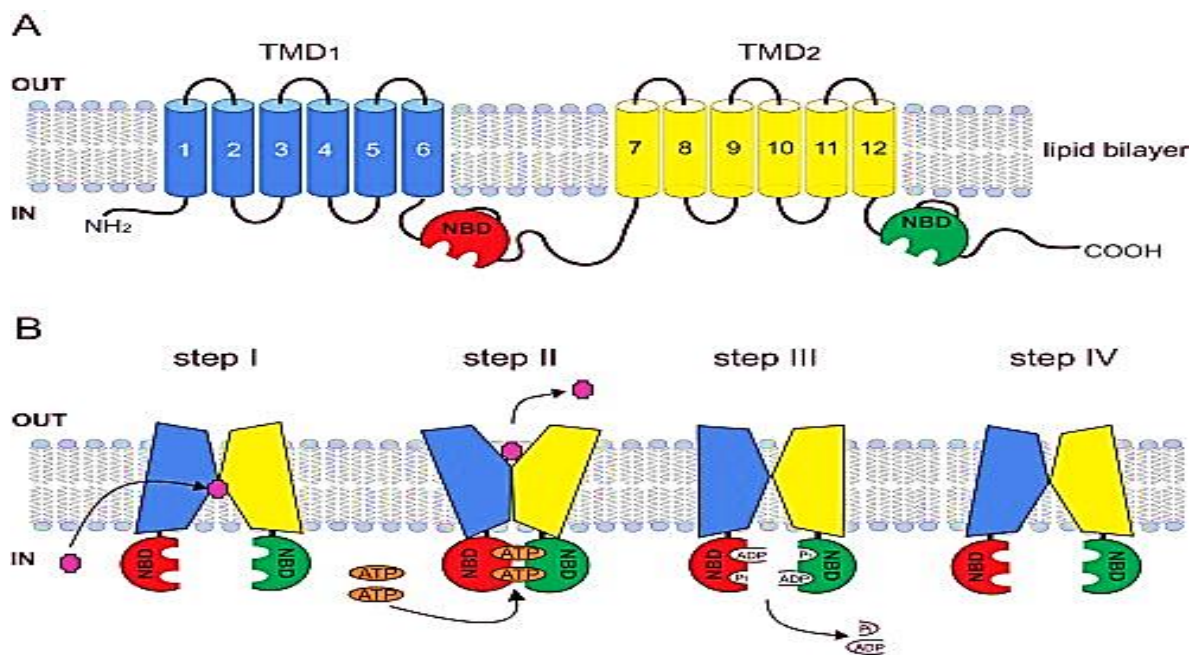


Figure 23: The ABC gene family in arthropods (Kumari, 2015)

1.13 Action Mechanisms of Cytochrome P450s

1.13.1 Allelic Variation

Allelic variation describes the presence or number of different allele forms at a particular locus (locus or loci = place) on a chromosome. Genetic variation can be caused by mutation (which can create entirely new alleles in a population), random mating, random fertilization, and recombination between homologous chromosomes during meiosis (which reshuffles alleles within an organism's offspring). In *Anopheles funestus*, a genome-wide survey of genetic diversity revealed that gene flow greatly impacts the flow of insecticide resistance, and one example is the *CYP6P9*-driven signatures of selective sweep metabolic resistance in southern Africa due to alleles *CYP6P9a* and *CYP6P9b* of the *CYP6P9* gene.

1.13.2 Increased Bioavailability and Bioactivity

Bioavailability is a key step in ensuring bio efficacy of bioactive compounds or oral drugs. Bioavailability is a complex process involving several different stages: liberation, absorption, distribution, metabolism, and elimination phases (LADME). Bio efficacy may be improved through enhanced bioavailability.

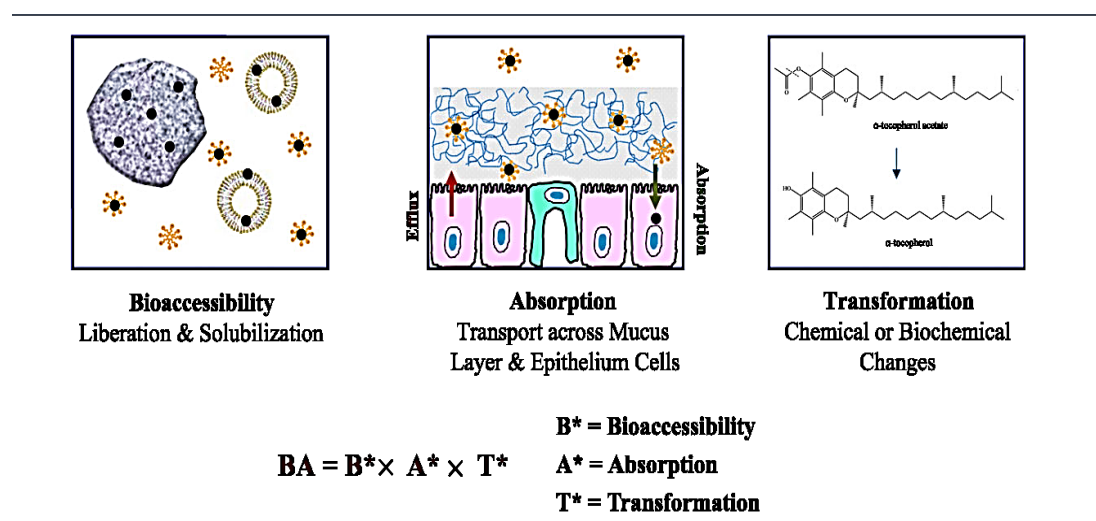


Figure 24: Comparison between bioavailability and bioactivity of substances in an organism (McClements et al., 2015)

1.14 Cytochrome P450 Reaction Mechanisms in Metabolic Resistance

Cytochrome P450 (P450) is a haemoprotein which acts as the terminal oxidase in mono oxygenase systems, and there are multiple P450 isoforms in eukaryotic species. Monooxygenases are remarkable in that they can oxidize widely diverse substrates and are capable of producing a bewildering array of reactions (Kulkarni & Hodgson, 1980; Mansuy et al., 1998; Rendic & Carlo, 1997; Winder et al., 1998).

a)



b)

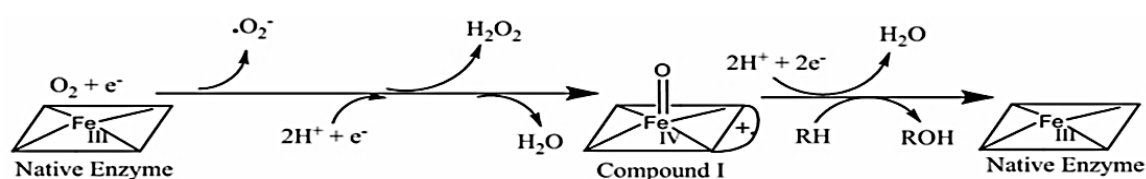


Figure 25: Different reaction mechanisms of cytochrome P450s on different substrates (Manoj et al., 2010)

CYP450s are central in biological systems for their ability to activate inert C - H bonds (Shaik et al., 2005). The ability to catalyse regiospecific and stereospecific oxidative attack on 35 non-activated hydrocarbons at physiologic temperatures make these enzymes to be compared to a nature's 'blowtorch' (Werck-Reichhart & Feyereisen, 2000). As a nanomachine P450 uses dioxygen and two reducing equivalents to catalyse a variety of stereospecific and regioselective oxygen insertion into diverse organic compounds (De Montellano, 2005). There are some structural features that are common to all P450 isoforms. The active species of the enzyme is an iron ion ligated to a protoporphyrin IX macrocycle and two additional axial ligands: one, called proximal, is a thiolate from a cysteinate side residue of the protein, and the other, called distal, is a variable ligand which changes during the catalytic cycle of the enzyme and thereby activates the enzyme's main function (Shaik et al., 2005).

The oxidized P450 is a mixture of a low spin (Fe^{III}) form with water as the sixth coordinated ligand on the opposite side of the Cys thiolate ligand and a high spin (Fe^{II}) pentacoordinate form (Feyereisen, 2012). P450 cycle has a multi-step and cyclical nature comparable to a ticking clock (Munro et al., 2018).

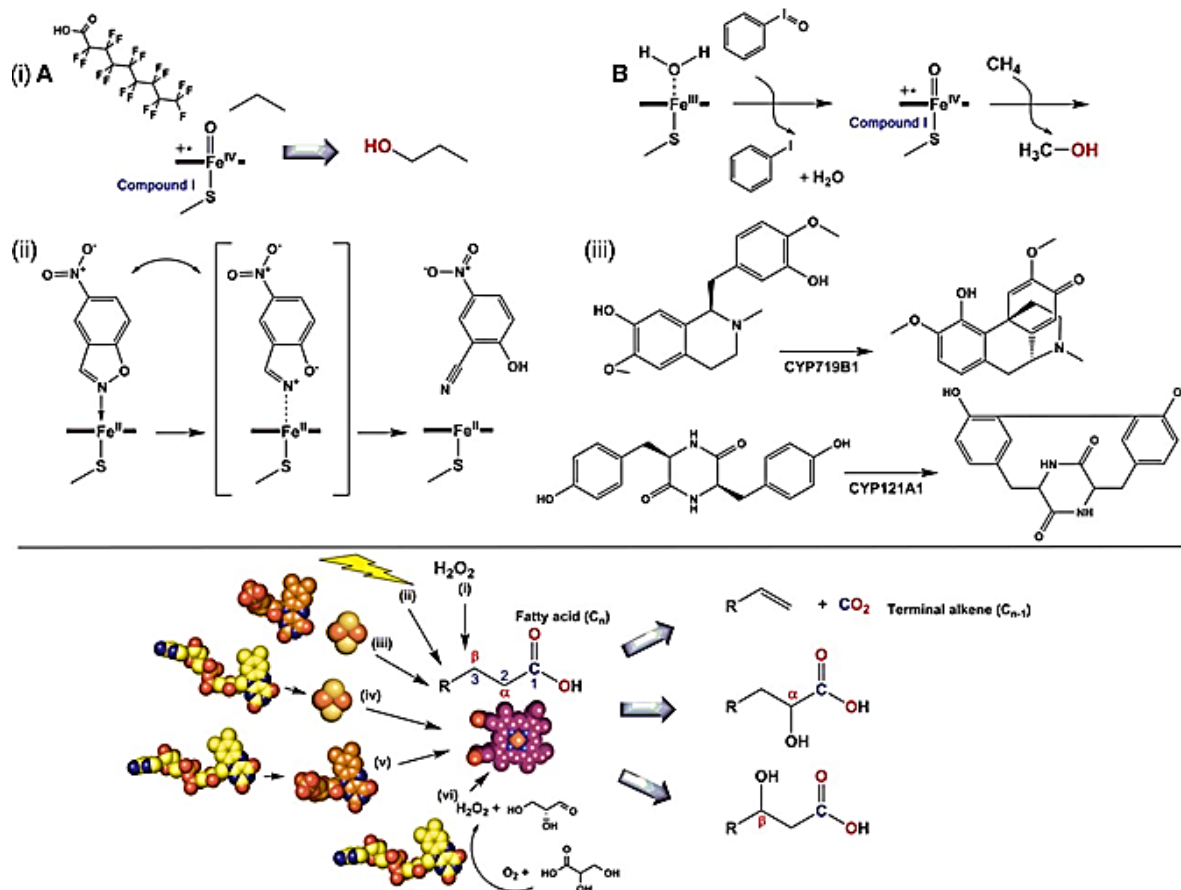


Figure 26: Novel reactions catalyzed by cytochrome P450 enzymes (Munro et al., 2018)

(A) and routes to driving catalysis in peroxygenase P450 enzymes (B). (A) A series of unusual reactions catalyzed by cytochrome P450 enzymes. (i) The hydroxylation of short chain alkanes using (a) the high-activity P450–CPR fusion enzyme P450 BM3 (*CYP102A1*) from *Bacillus megaterium* to produce propanol from propane in the presence of the ‘decoy’ molecule perfluoro-nonanoic acid (where the decoy molecule acts as a ‘dummy’ substrate to activate the enzyme and to facilitate the binding and oxidation of propane bound in the P450 active site) (Onoda et al., 2015; Shoji et al., 2010) and (b) using wild-type and evolved forms of the CYP153A6 enzyme from *Mycobacterium* sp. HXN-1500 and employing iodosyl benzene to drive oxidation of methane to methanol in small amounts (Chen et al., 2012; Funhoff et al., 2006; Zilly et al., 2011); (ii) a Kemp elimination reaction involving the conversion of 5-nitrobenzisoxazole into 2-cyano-4-nitrophenol, in which wild-type and mutant forms of P450 BM3 catalyze the reaction by a redox mechanism predicted [by QM–MM (quantum mechanics–AMELIE WAMBA NDONGMO Regine/Doctorate/Ph.D. Thesis/University of Yaoundé I

molecular mechanics simulations)] to involve a reaction in which the isoxazole nitrogen becomes coordinated to the heme iron (Li et al., 2017) and (iii) C–C bond coupling reactions in the formation of salutaridine from R-reticuline by *CYP179B1* in the morphine synthesis pathway (Yamauchi et al., 2003) and in the production of the Mycobacterium tuberculosis secondary metabolite mycocyclosin from the cyclic dipeptide cyclo-l-Tyr-l-Tyr by M. tuberculosis *CYP121A1* (McLean et al., 2008) [31,32].tuberculosis *CYP121A1* (Belin et al., 2009; McLean et al., 2008). The schematic in (B) shows different methods for driving the catalytic function of P450 peroxygenase enzymes, using the peroxygenase heme prosthetic group (in purple) to transform fatty acids to terminal alkenes and α - and β -hydroxylated fatty acids. (i) Direct formation of P450 compound 0 by reaction with H_2O_2 . (ii) Formation of H_2O_2 using light-mediated excitation of flavin cofactors in the presence of EDTA as an electron donor (Girhard et al., 2013). NAD(P)H-dependent electron transfer to the P450 using (iii) a phthalate dioxygenase-type enzyme (FMN and 2Fe–2S cluster-binding) (Liu et al., 2014), (iv) the FAD-binding putidaredoxin reductase and its 2Fe–2S cluster-binding putidaredoxin partner from P. putida (Dennig et al., 2015) and (v) the E. coli flavodoxin reductase (FAD-binding) and flavodoxin (FMN-binding) to reduce the P450 partner (Fujita et al., 2007). (vi) The FAD-binding alditol oxidase which produces H_2O_2 for peroxygenase catalysis when provided with glycerol or an alternative alditol substrate (Matthews et al., 2017).

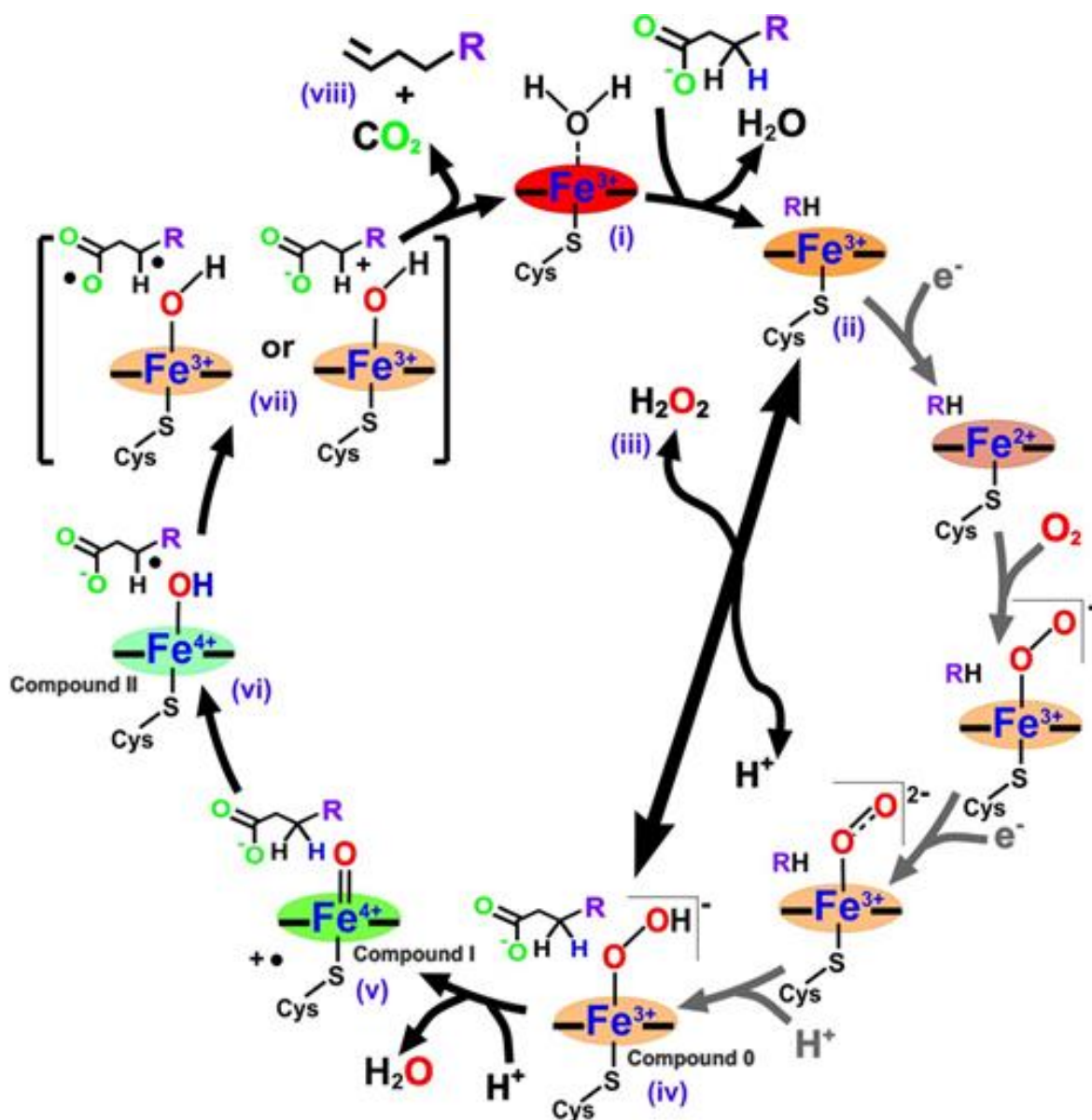


Figure 27: The cytochrome P450 catalytic cycle, incorporating steps specific to peroxygenase activity and the formation of terminal alkenes (Munro et al., 2018)

The cytochrome P450 catalytic cycle, incorporating steps specific to peroxygenase activity and the formation of terminal alkenes. (i) The P450 is in a low-spin ferric resting form with its heme iron axially coordinated by cysteine thiolate and a H_2O molecule. (ii) Substrate (fatty acid) binding displaces the axial water and converts the heme iron from low-spin to a high-spin form. (iii) Peroxygenase P450s use the peroxide shunt pathway that bypasses the need for external electrons, and interaction with H_2O_2 facilitates direct conversion of the substrate-bound, high-spin P450 to the ferric-hydroperoxo species (compound 0) (iv). Subsequent protonation and dehydration steps yield the reactive ferryl (Fe^{IV})-oxo porphyrin radical cation (compound I) (v), as observed in rapid mixing

studies of OleT with perdeuterated arachidic acid substrate (Grant et al., 2015). (vi) Compound I abstracts a hydrogen atom from the C_β position, resulting in formation of a substrate radical and the ferryl (Fe^{IV})-hydroxo species (compound II) (Grant et al., 2016). (vii) Decarboxylation of the fatty acid occurs through subsequent one-electron oxidation of the substrate by compound II to generate a substrate diradical species or a carbocation. (viii) The reactive species can readily eliminate CO₂, with formation of the C_α-C_β double bond and generation of a terminal alkene. The simultaneous recruitment of a proton to the heme restores the resting, distal water-ligated state of the P450. There is competition between the ‘radical rebound’ reaction in which (a) compound II transfers a hydroxyl radical to the substrate radical to form a hydroxylated fatty acid and the alkene-producing reaction in which (b) compound II abstracts a substrate electron to initiate fatty acid decarboxylation. The decarboxylase reaction dominates in OleT for longer chain substrates, although significant levels of hydroxylation are seen with short chain fatty acids. The P450 heme (illustrated by the iron in the relevant oxidation state and equatorial/axial bonds) is shaded to approximate the color of the relevant heme intermediate species.

1.15 Molecular Methods and Techniques in P450 Studies

Progress has been made recently in molecular genetics and bioinformatics which has provided medical entomologists with new tools to understand the biology, ecology, and epidemiology of vector-borne pathogens. The development of molecular tools has opened many exciting avenues for research on vector-borne diseases from the scale of individual organisms to populations. Parasite infections trigger a cascade of molecular processes that are governed primarily by the genetics of the parasite and its vector or host. Also, vectorial capacity, entomological inoculation rate, and related modelling concepts provide an excellent conceptual framework for understanding the parameters that regulate transmission.

1.15.1 Introduction

In molecular biology work and specifically P450 studies, several complementary approaches and techniques have been adopted to characterize and validate the role of different CYP genes in diverse phenomena such as insecticide resistance. These include in silico methods conducted in dry-lab or in a computer, in vitro studies conducted in the wet-lab or in the test-tube and in vivo studies conducted in living cells and living organisms such as lab rats, mosquitoes, or flies. Some of these techniques relevant to P450 studies are mentioned below:

1.15.2 *In Silico* Techniques

The term '*in silico*' is a modern word usually used to mean experimentation performed by computer and is related to the more commonly known biological terms *in vivo* and *in vitro*. In biology and other experimental sciences, an *in silico* experiment is one performed on computer or via computer simulation. The phrase is pseudo-Latin for 'in silicon' (in Latin it would be *in silico*), referring to silicon in computer chips. It was coined in 1987 as an allusion to the Latin phrases *in vivo*, *in vitro*, and *in situ*, which are commonly used in biology (especially systems biology). The latter phrases refer, respectively, to experiments done in living organisms, outside living organisms, and where they are found in nature. In molecular biology, many analytical studies are conducted such as:

PoolSeq Analysis: Pool-seq is an alternative cost- and time-effective option in which DNA from several individuals is pooled for sequencing. However, pooling of DNA creates new problems and challenges for accurate variant call and allele frequency (AF) estimation.

SureSelect Target Enrichment Analysis: Available for the Illumina, SOLiD, and 454 NGS sequencing platforms, Sureselect is a highly robust, customizable, and scalable system that focuses analyses on specific genomic loci by in-solution hybrid capture

Gene Ontology Transcript Detection: The Gene Ontology (GO) knowledgebase is the world's largest source of information on the functions of genes. This knowledge is both human-readable and machine-readable and is a foundation for computational analysis of large-scale molecular biology and genetics experiments in biomedical research.

Amino Acid Characterization or Amino Acid Profile Analysis: This could be performed to study the degree of difference between two closely related species. This analysis highlights the zones of similarity and difference in the amino acid sequence alignment of both species. The conserved regions in both species could depict essential amino acids combinations such as active sites.

Homology Modelling (HMM): Homology modelling, also known as comparative modelling of protein, refers to constructing an atomic-resolution model of the "target" protein from its amino acid sequence and an experimental three-dimensional structure of a related homologous protein (the "template"). Homology modelling is the most accurate computational method to

create reliable structural models and is commonly used in many biological applications. Homology modelling predicts the 3D structure of a query protein through the sequence alignment of template proteins.

Molecular Docking Simulations: Molecular docking is a kind of bioinformatic modelling which involves the interaction of two or more molecules to give the stable adduct. Depending upon binding properties of ligand and target, it predicts the three-dimensional structure of any complex.

Gene Flow, Population Structure and Genetic Diversity

Gene flow is the transfer of genetic material from one population to another. Gene flow can take place between two populations of the same species through migration and is mediated by reproduction and vertical gene transfer from parent to offspring. Gene flow is the movement of genes into or out of a population. Such movement may be due to migration of individual organisms that reproduce in their new populations, or to the movement of gametes (e.g., because of pollen transfer among plants).

Population structure is defined by the organization of genetic variation and is driven by the combined effects of evolutionary processes that include recombination, mutation, genetic drift, demographic history, and natural selection.

The variation in the amount of genetic information within and among individuals of a population, a species, an assemblage, or a community. “Genetic” means related to traits passed from parent to offspring. “Diversity” means having a range of different things. Genetic Diversity refers to the range of different inherited traits within a species. In a species with high genetic diversity, there would be many individuals with a wide variety of different traits. Genetic diversity is critical for a population to adapt to changing environments. If a highly selected and low diversity strain, like fish populations grown for aquaculture, is introduced into the wild population, it will reduce the population’s ability to adapt to changes.

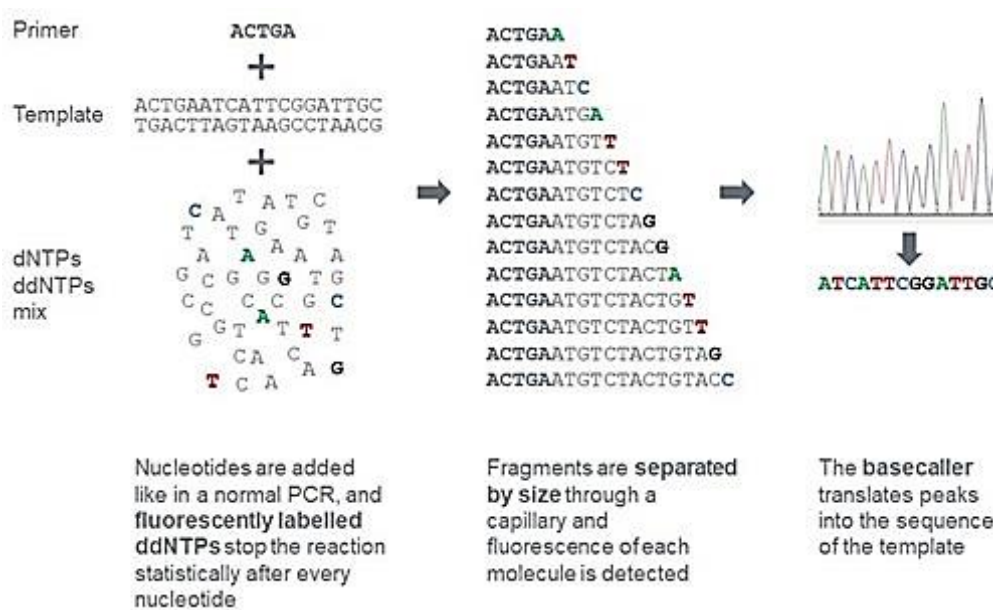
1.15.2 *In Vitro* Techniques

In vitro (meaning in glass, or in the glass) studies are performed with microorganisms, cells, or biological molecules outside their normal biological context. Colloquially called "test-tube experiments", these studies in biology and its subdisciplines are traditionally done in labware such as test tubes, flasks, Petri dishes, and microtiter plates. Studies are usually done *in vitro*

first for ethical reasons. In vitro studies allow a substance to be studied safely, without subjecting humans or animals to the possible side effects or toxicity of a new drug. In molecular biology and P450 studies, several in vitro techniques have been adapted to understand the role of many CYP genes. Some of the most frequently used are mentioned below:

RNAseq: RNA-seq (RNA-sequencing) is a technique that can examine the quantity and sequences of RNA in a sample using next-generation sequencing (NGS). It analyses the transcriptome, indicating which of the genes encoded in our DNA are turned on or off and to what extent. As RNA-Seq is quantitative, it can be used to determine RNA expression levels more accurately than microarrays. In principle, it is possible to determine the absolute quantity of every molecule in a cell population, and directly compare results between experiments. As RNA-Seq is quantitative, it can be used to determine RNA expression levels more accurately than microarrays. In principle, it is possible to determine the absolute quantity of every molecule in a cell population, and directly compare results between experiments.

SANGER Sequencing: Sanger sequencing, also known as the “chain termination method”, is a method for determining the nucleotide sequence of DNA. The method was developed by two-time Nobel Laureate Frederick Sanger and his colleagues in 1977, hence the name the Sanger. In the first step, the double-stranded DNA (dsDNA) is denatured into two single-stranded DNA (ssDNA), a primer that corresponds to one end of the sequence is attached, Four polymerase solutions with four types of dNTPs but only one type of ddNTP are added, The DNA synthesis reaction initiates and the chain extends until a termination nucleotide is randomly incorporated, the resulting DNA fragments are denatured into ssDNA and lastly, the denatured fragments are separated by gel electrophoresis and the sequence is determined.



©EurofinsGenomics

Figure 28: Major steps of Sanger sequencing

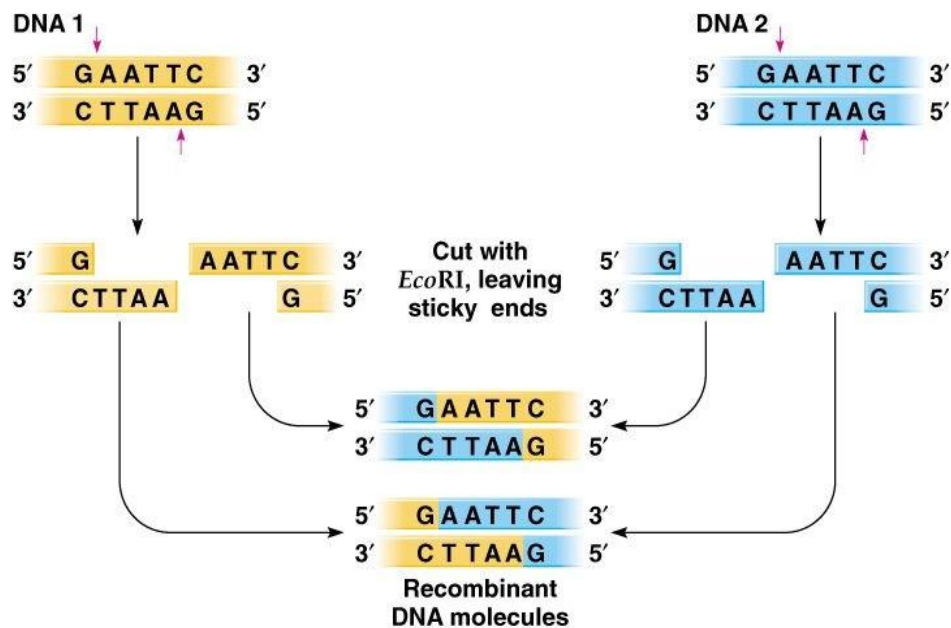
<https://eurofinsgenomics.eu/en/eurofins-genomics/material-and-methods/sanger-sequencing/>

In P450 studies, amplified genes in carrier vector PJET are sequenced by the Sanger sequencing method to determine the nucleotide sequence of the gene of interest for different samples.

PCR and qRT-PCR: The polymerase chain reaction (PCR) is a laboratory technique used for the amplification of a specific DNA fragment in a simple enzyme reaction. The basic PCR method has been modified to expand its application. Development of quantitative PCR (qPCR) has enabled detection and quantification of the target sequence in real time, while it is being synthesized. Another popular variation is reverse transcription polymerase chain reaction (RT-PCR), a technique used to detect and measure RNA. PCR technology has revolutionized the field of molecular biology and medical research. Because of its widespread use, it is important to understand the scientific principles of PCR. The aim of this chapter is to explain the concepts underlying this method and to explore the clinical usefulness and potential of this technique. The chapter also provides detailed protocols on how to undertake PCR in the laboratory, including techniques for RNA isolation, cDNA synthesis, and data analysis. A scenario in which PCR is utilized to answer a research question is also described, as well as guidance on how to troubleshoot experimental problems.

Restriction Enzyme Digestion: Restriction digestion is usually used to prepare a DNA fragment for subsequent molecular cloning, as the procedure allows fragments of DNA to be pieced together like building blocks via ligation. Restriction Digestion involves fragmenting DNA molecules into smaller pieces with special enzymes called Restriction Endonucleases

commonly known as Restriction Enzymes (RE). Because of this property the restriction enzymes are also known as molecular scissors.



Peter J. Russell, *iGenetics*. Copyright © Pearson Education, Inc., publishing as Benjamin Cummings.

Figure 29: Principle of restriction enzyme action. Example of EcoRI

https://www.researchgate.net/publication/321682682_Techniques_used_in_Molecular_Biology

Gel electrophoresis: Gel electrophoresis is a laboratory method used to separate mixtures of DNA, RNA, or proteins according to molecular size. In gel electrophoresis, the molecules to be separated are pushed by an electrical field through a gel that contains small pores. Electrophoresis is based on the phenomenon that most biomolecules exist as electrically charged particles, possessing ionizable functional groups. Biomolecules in a solution at a given pH will exist as either positively or negatively charged ions. In this manner, DNA fragments in a solution are separated based on size. There are several basic steps to performing gel electrophoresis that will be described below; 1) Pouring the gel, 2) Preparing your samples, 3) Loading the gel, 4) Running the gel (exposing it to an electric field) and 5) Staining the gel.

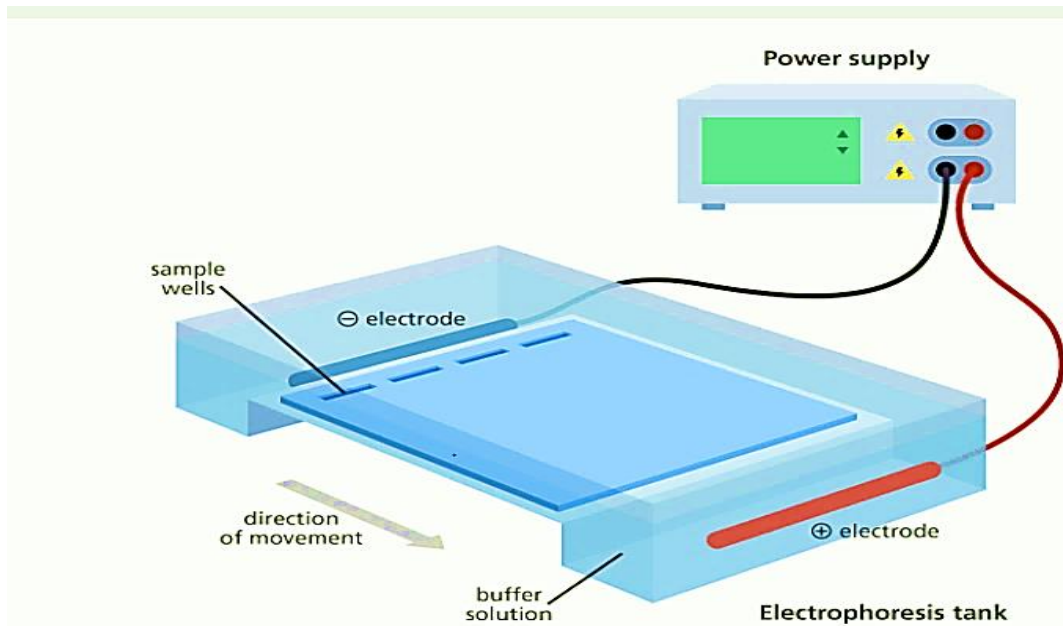
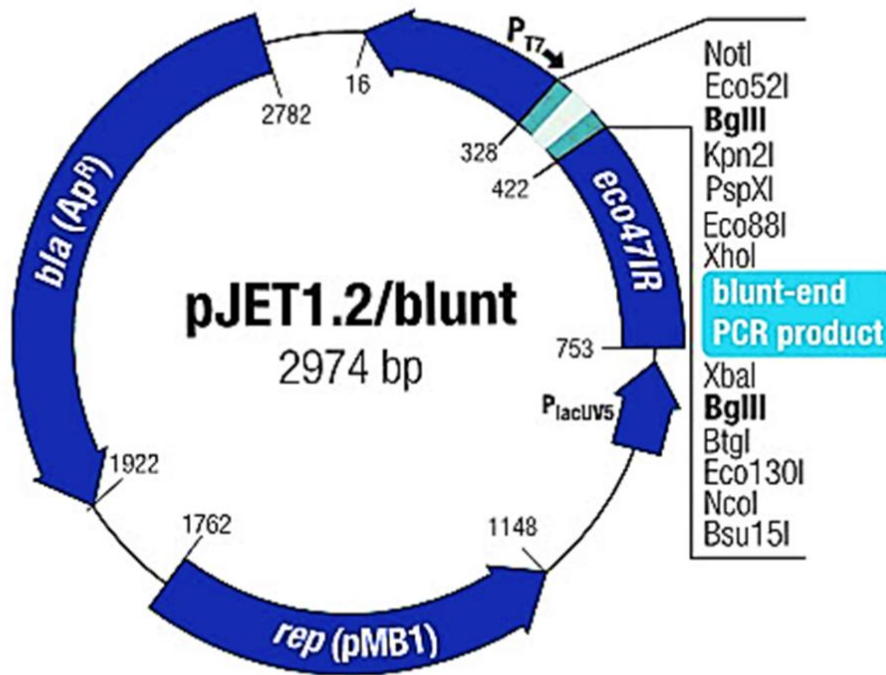


Figure 30: Set-up of gel electrophoresis

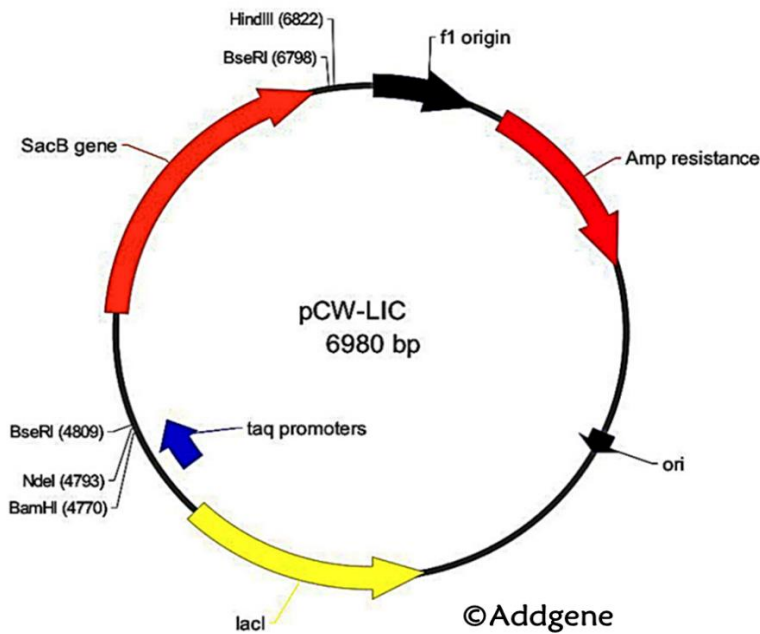
<https://blogs.baylor.edu/cili-cure-spring2017/2017/04/30/lab-14-gel-electrophoresis-8/>

Cloning and Sub-cloning: PCR cloning and subcloning are two main approaches to amplifying DNA sequences. The combination of the DNA synthesis tool and the cloning technology allows us to insert the requested genetic sequence into any customer specific vector for cloning. Cloning is the procedure which produces genetically identical organisms or cells. Subcloning is a procedure of moving a gene of interest from one vector to another vector to see the expression of the gene to gain the desired functionality of the gene. The main difference between cloning and subcloning is that cloning is the production of clones of organisms or copies of cells or DNA fragments whereas subcloning is a technique used to move a particular DNA sequence from a parent vector to a destination vector.



©Thermo Fisher Scientific

Figure 31: PJET carrier plasmid for cloning



©Addgene

Figure 32: pCW expression plasmid for P450 protein expression

<https://www.addgene.org/26098/>

Mass Spectrophotometry (MS): Spectrophotometry is a method to measure how much a chemical substance absorbs light by measuring the intensity of light as a beam of light passes through sample solution. The basic principle is that each compound absorbs or transmits light over a certain range of wavelength. Spectrophotometry is a method to measure how much a chemical substance absorbs light by measuring the intensity of light as a beam of light passes through sample solution. The basic principle is that each compound absorbs or transmits light over a certain range of wavelength. This measurement can also be used to measure the amount of a known chemical substance. Spectrophotometry is one of the most useful methods of quantitative analysis in various fields such as chemistry, physics, biochemistry, material and chemical engineering and clinical applications. Spectrophotometry is widely used for quantitative analysis in various areas (e.g., chemistry, physics, biology, biochemistry, material and chemical engineering, clinical applications, industrial applications, etc). Any application that deals with chemical substances or materials can use this technique. In biochemistry, for example, it is used to determine enzyme-catalysed reactions. In clinical applications, it is used to examine blood or tissues for clinical diagnosis. There are also several variations of the spectrophotometry such as atomic absorption spectrophotometry and atomic emission spectrophotometry.

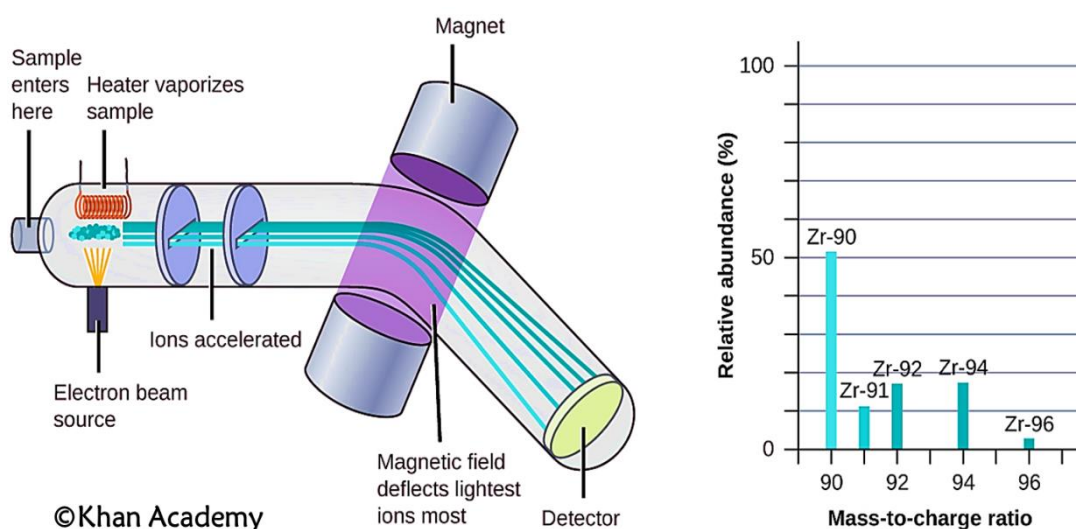


Figure 33: The principle of mass spectrophotometry (Ihling et al., 2020)

HPLC: High performance liquid chromatography or commonly known as HPLC is an analytical technique used to separate, identify, or quantify each component in a mixture. The mixture is separated using the basic principle of column chromatography and then identified and quantified by spectroscopy. The separation principle of HPLC is based on the distribution

AMELIE WAMBA NDONGMO Regine/Doctorate/Ph.D. Thesis/University of Yaoundé I

of the analyte (sample) between a mobile phase (eluent) and a stationary phase (packing material of the column). Depending on the chemical structure of the analyte, the molecules are retarded while passing the stationary phase.

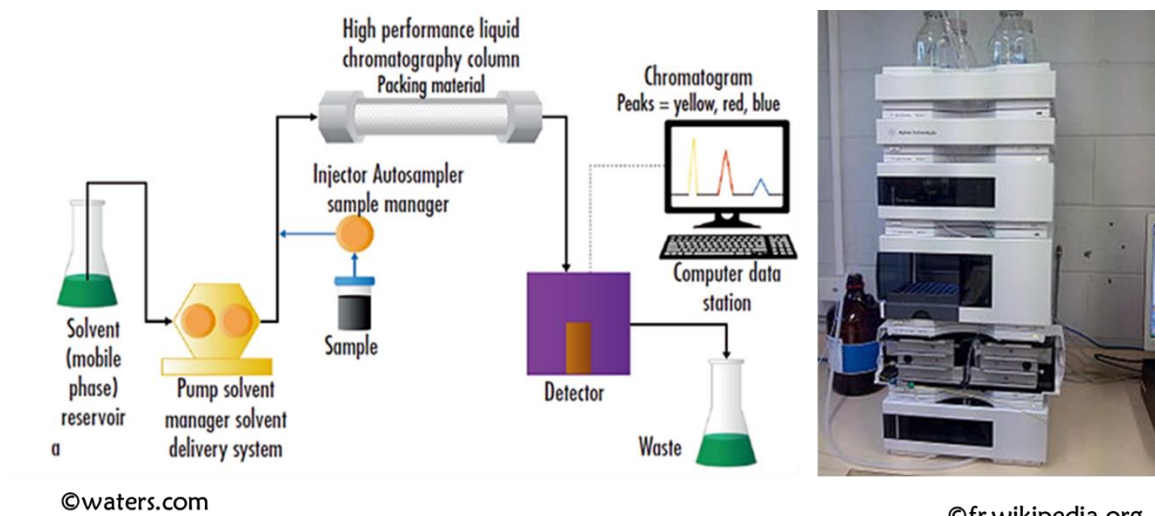


Figure 34: Principle and setup of HPLC
<https://www.waters.com/nextgen/us/en/education/primers/beginner-s-guide-to-uplc/bands-peaks-and-band-spreading.html>

Ultracentrifugation: Analytical ultracentrifugation (AUC) is the study of the behaviour of macromolecules in solution under the influence of a strong gravitational force. Most macromolecules have a different density from the solvent surrounding them and so will sink (or float) in a strong enough field. Ultracentrifuges are commonly used in molecular biology, biochemistry, and cell biology. Applications of ultracentrifuges include the separation of small particles such as viruses, viral particles, proteins and/or protein complexes, lipoproteins, RNA, and plasmid DNA.

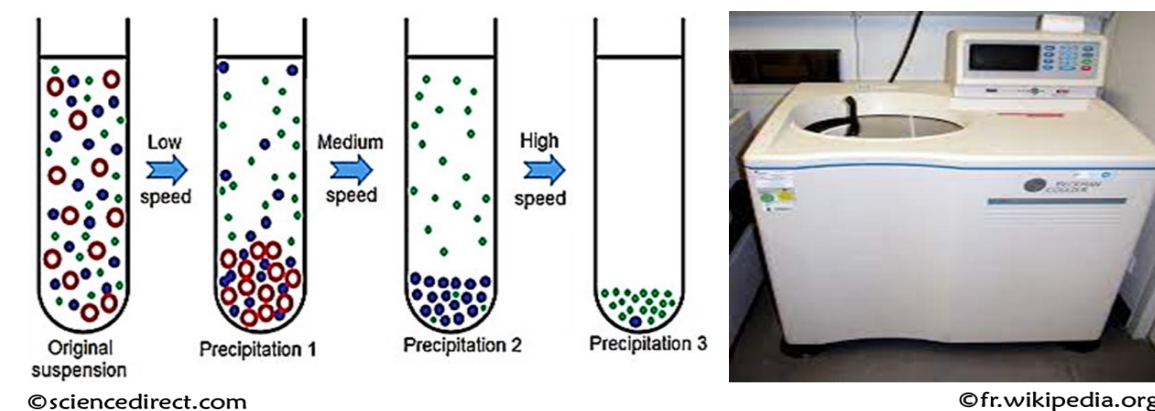


Figure 35: Principle and setup of ultracentrifugation
<https://www.medwrench.com/equipment/2402/beckman-coulter-optima-l-100k>

Molecular *in vitro* assays: Many different assays could be performed to assess the metabolic and kinetic parameters of proteins for example metabolism depletion assays (used to identify metabolic stability in chemical structures and evaluates the rate of clearance of a chemical substrate using the enzyme of interest. The disappearance or depletion rate of the parent chemical with time is an example of a change), inhibition assays (This is a measure of the amount of active enzyme, calculated by e.g., titrating the number of active sites present by employing an irreversible inhibitor. The specific activity should then be expressed as $\mu\text{mol min}^{-1} \text{mg}^{-1}$ active enzyme), fluorescent probe assays (fluorescent probes are molecules that absorb light of a specific wavelength and emit light of a different, typically longer, wavelength (a process known as fluorescence), and are used to study biological samples).

Also, more innovative techniques have been developed and now allow for more exact research and precision. Genome editing through CRISPR-Cas9 is widely used in studies in a variety of organisms especially in the study of cancer cells and now finding a promising application in vector control of human diseases. Gene drive technology using CRISPR allows for the spread of engineered traits through populations of sexually reproducing organisms at a rate more rapid than what occurs in natural evolution. In malaria research, CRISPR could also be used in site-directed mutagenesis of specific genes to predict, and study anticipated mutations.

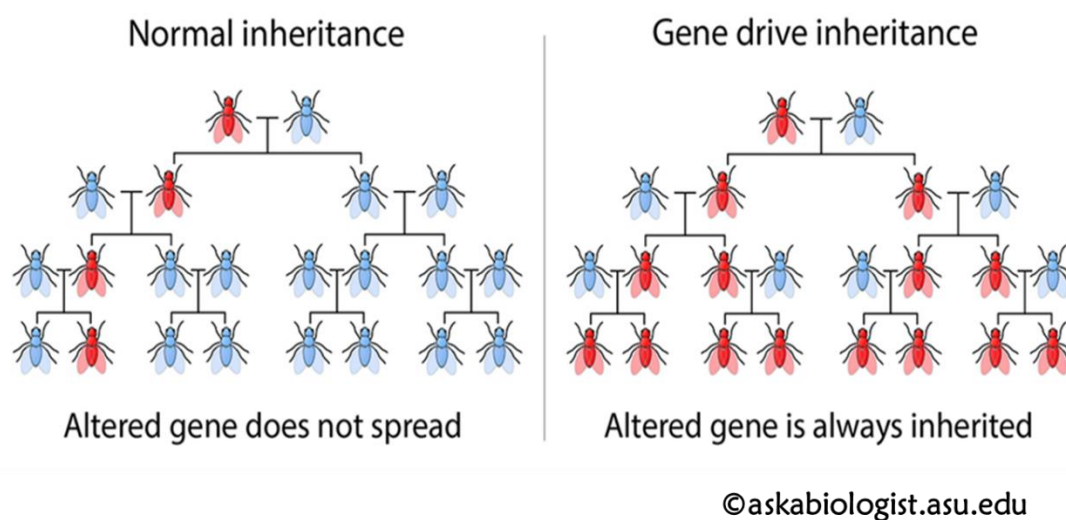


Figure 36: Normal inheritance compared to gene drive inheritance showing altered gene is always inherited (Perry, 2018)

1.15.3 *In vivo* methods

RNAi may be used for large-scale screens that systematically shut down each gene in the cell, which can help to identify the components necessary for a particular cellular process or an event such as cell division. The pathway is also used as a practical tool in biotechnology, medicine and insecticides. RNA interference (RNAi) is a regulatory mechanism of most eukaryotic cells that uses small double-stranded RNA (dsRNA) molecules as triggers to direct homology-dependent control of gene activity. RNAi is short for “RNA interference” and it refers to a phenomenon where small pieces of RNA can shut down protein translation by binding to the messenger RNAs that code for those proteins. RNA interference is a natural process with a role in the regulation of protein synthesis and in immunity. The silencing of a gene is a consequence of degradation of RNA into short RNAs that activate ribonucleases to target homologous mRNA.

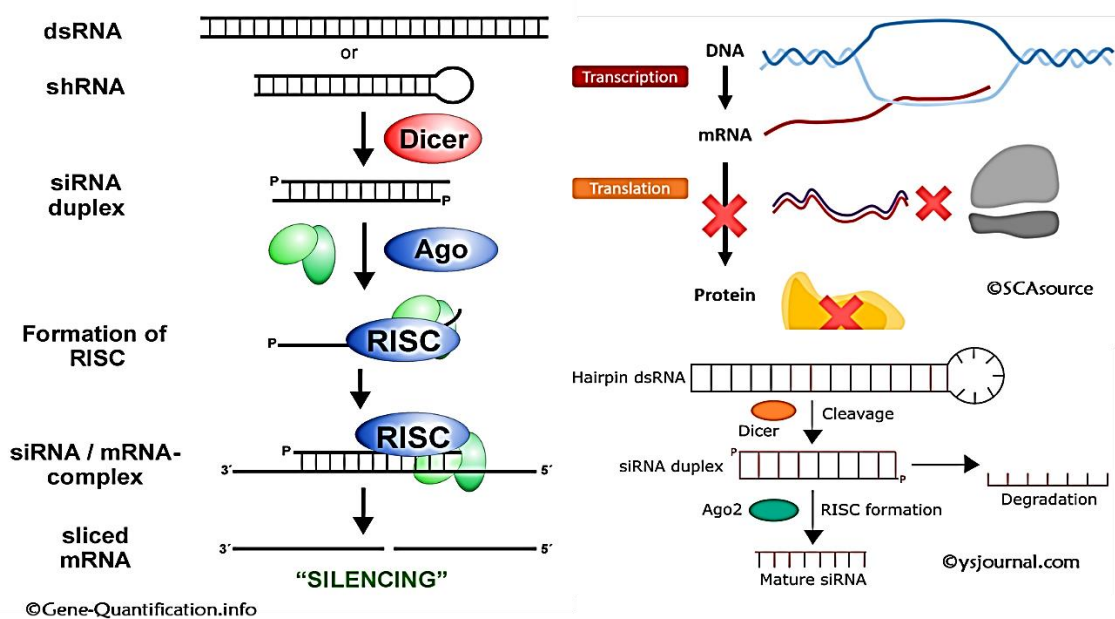


Figure 37: Principle of RNA interference and how it inhibits gene expression (Chery, 2016)

The introduction of a transgene, in a process known as transgenesis, has the potential to change the phenotype of an organism. Transgene describes a segment of DNA containing a gene sequence that has been isolated from one organism and is introduced into a different organism. Genetic manipulations are so much easier in fruit flies because they have a smaller genome which was fully sequenced in March 2000. Their short life cycle and large number of offspring are also advantageous for genetic research because new fly lines are quick and easy to make. *Drosophila melanogaster*, known colloquially as the fruit fly, remains one of the most used

AMELIE WAMBA NDONGMO Regine/Doctorate/Ph.D. Thesis/University of Yaoundé I

model organisms for biomedical science. These tools allow researchers to maintain complex stocks with multiple mutations on single chromosomes over generations, an advance that makes flies the premier genetic system. The method involves targeting integration of an exogenous plasmid (containing the transgene and sequences to facilitate integration) to a preplaced recipient site in the *Drosophila* genome. The plasmid is co-injected into embryos with mRNA encoding the ϕ C31 integrase, the enzyme that catalyses the integration reaction.

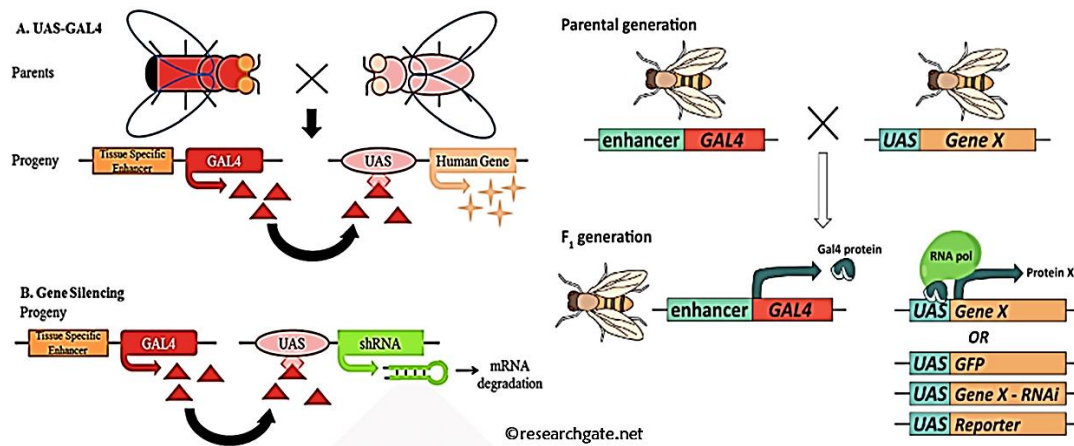


Figure 38: Principle of Gal4 hybrids, balancing of strains and transgenic expression with specific phenotypes (Cabia et al., 2012)

1.15.4 Data analyses and statistics

Genomic analysis is the identification, measurement, or comparison of genomic features such as DNA sequence, structural variation, gene expression, or regulatory and functional element annotation at a genomic scale. This could be done online using different software and programs some of which are listed below:

Table 6: Some online software used in genetic sequence analysis in molecular biology research

Software	Purpose	Link
Swiss-Model	Server for automated comparative modelling of three-dimensional (3D) protein structures	https://swissmodel.expasy.org/
CYPED	Cytochrome P450 Engineering Data base. Web accessible version contains multisequence alignments, phylogenetic trees and HMM profiles.	http://www.cyped.uni-stuttgart.de/

ERRAT	ERRAT is a program for verifying protein structures determined by crystallography. Error values are plotted as a function of the position of a sliding 9-residue window	https://servicesn.mbi.ucla.edu/ERRAT/
NEB-CUTTER	Use this tool to identify the restriction sites within your DNA sequence.	http://nc2.neb.com/NEBcutter2/
Primer 3 Design	Primer3 is a widely used program for designing PCR primers	Primer3
MultAlin	Multiple sequence alignment by Florence Corpet. INRA	Multalin interface page (inra.fr)
Gene Bank	Gene banks are a type of biorepository that preserves genetic material.	https://www.ncbi.nlm.nih.gov/genbank/
Vector Base	VectorBase is one of the five Bioinformatics Resource Centres (BRC) funded by the National Institute of Allergy and Infectious Diseases (NIAID)	VectorBase

Besides the online software, many others can be downloaded and used for various analyses. Some commonly used examples are listed below:

Table 7: Some offline and downloadable software used in genetic sequence analysis in molecular biology research

Software	Purpose	Link
BioEdit	BioEdit is a software program that embeds the tools that scientists and technicians need so they perform specific tasks.	https://bioedit.software.informer.com/7.2/
DnaSP	DnaSP, DNA Sequence Polymorphism, is a software package for the analysis of nucleotide polymorphism from aligned DNA sequence data.	http://www.ub.edu/dnasp/index_v5.html

Mega X	Molecular Evolutionary Genetic Analysis. Computer software for conducting statistical analysis of molecular evolution and for constructing phylogenetic trees. It includes many sophisticated methods and tools for phylogenomics and phylomedicine	Home (megasoftware.net) https://www.megasoftware.net/show_eua
GraphPad Prism	combines scientific graphing, comprehensive curve fitting (nonlinear regression), understandable statistics, and data organization. Allows to easily perform basic statistical tests commonly used by laboratory and clinical researchers.	https://www.graphpad.com/scientific-software/prism/
TCS	Java computer program to estimate gene genealogies including multifurcations and/or reticulations (i.e. networks).	http://cibio.up.pt/software/tcsBU/
Microsoft Office	Family of client software, server software, and services developed by Microsoft	https://www.office.com/
Molegro Virtual Docker	Integrated platform for predicting protein – ligand interactions	http://molexus.io/molegro-virtual-docker/
Modeller	Used for homology or comparative modelling of protein three-dimensional structures	https://salilab.org/modeller/
PyMol	User-sponsored molecular visualization system on an open-source foundation, maintained and distributed by Schrödinger	https://pymol.org/2/

Chapter 2: General Materials and Methods

2.1 Methods

2.1.1 Mosquito Strains

Mosquito strains from different regions of Africa with different resistance profiles and the fully susceptible, laboratory strain, FANG (*An. funestus* from Angola) were used in this study. The FANG strain originated from Calueque, southern Angola: 16°45'S, 15°7'E and had been colonised in laboratory since 2002 (Hunt et al., 2005; Wondji et al., 2005). The field strains were collected from Pahou (6°23'N, 2°13'E), southern Benin Republic (Djouaka et al., 2011), Tororo district (0°45'N, 34°5'E), eastern Uganda (Morgan et al., 2010), Tihuquine, Chikwawa (12°19'S, 34°01'E), Malawi (Wondji et al., 2012) and Mibellon, Cameroon (6°46'N, 11°70'E) (D Menze et al., 2018). Details of resistance profile of these mosquitoes and transcriptional analysis of *CYP6P9a* and *CYP6P9b* alleles were already established in the studies cited above where *CYP325A* was implicated as a pyrethroid resistance gene in *An. funestus* (Mugenzi et al., 2019; Wamba et al., 2021).

2.1.2 Mosquito Collection

Female *Anopheles funestus* mosquitoes were collected by the indoor aspiration method in the localities of interest and placed in cages in rearing which they were transported to the insectary at CRID for mosquito identification and rearing.

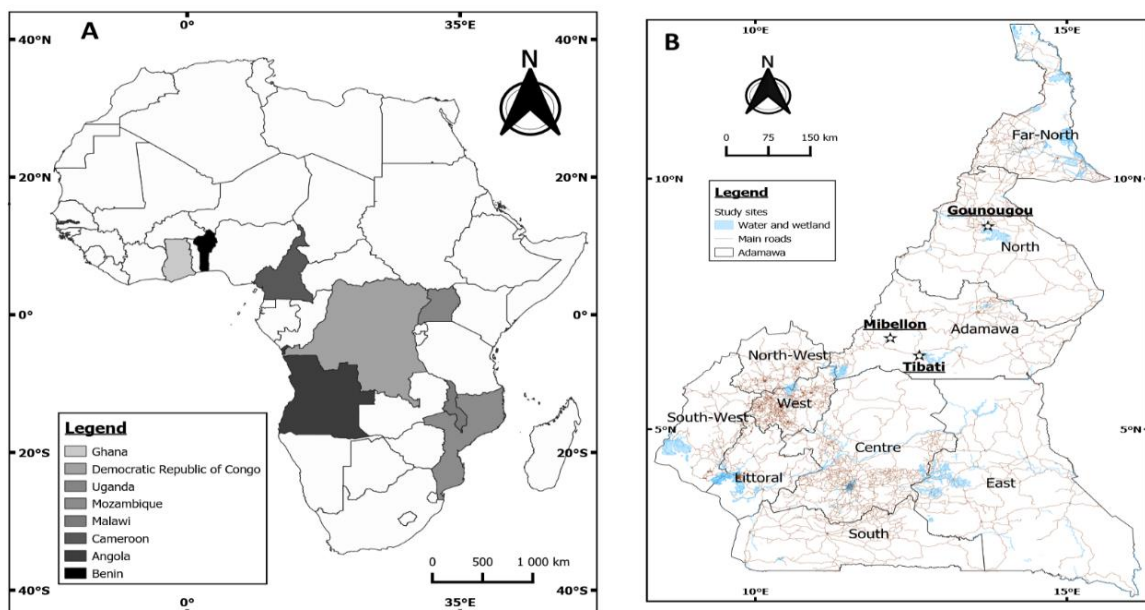


Figure 39: Study sites across Africa and sites of interest in Cameroon (Wamba et al., 2021)

2.1.3 Mosquito Identification

All female mosquitoes used for individual ovipositing were morphologically identified as belonging to the *An. funestus* group according to the identification key of Coetzee (Coetzee, 2020). The genomic DNA was extracted using the Livak method (Livak & Schmittgen, 2001) and a cocktail PCR assay (Koekemoer et al., 2002) was used to confirm that all females that laid eggs were *An. funestus* sensu stricto.

2.1.4 Mosquito Rearing

Gravid female blood-fed *An. funestus* mosquitoes were then placed individually in 1.5ml Eppendorf tubes containing mineral water-imbibed cotton and filter paper for the forced-egg laying process. Filter papers containing mosquito eggs were placed in half-full water-containing cups and fed with tetramine biscuit until they reached larval stage 2. The larvae were then transferred into mineral water-containing plastic trays where the rearing was continued until pupal stage. The pupae were transferred into mineral water-containing bowls and placed in cages for mosquito emergence. The F₁ were collected as they emerged and prepared to be used for insecticidal bioassays or RNA interference.

2.1.5 Insecticidal Bioassays

Insecticide susceptibility bioassays were conducted using 2- to 5-day-old F₁ adult female mosquitoes from pooled F₁ mosquitoes, following the WHO protocol (WHO, 2016). For each insecticide approximately 20 to 25 female mosquitoes per tube were exposed to either permethrin (0.75%) or deltamethrin (0.05%) impregnated papers for 30 min, 1 h and 1.5 h, and transferred to a clean holding tube immediately, supplied with 10 % sugar solution, and mortality determined 24 h later. For each test, mosquitoes exposed to untreated papers were used as controls. The assay was carried out at temperatures of 25 °C ± 2 and 80 % ± 10 relative humidity. As P450 monooxygenases have previously been involved in pyrethroid resistance in *An. funestus* (Riveron et al., 2013) their potential involvement in resistance was assessed in the Mibellon mosquito population using PBO (piperonyl butoxide), a synergist/inhibitor of P450s (D Menze et al., 2018; Feyereisen, 2012). 100 female mosquitoes were pre-exposed to 4 % PBO papers for 1 h and immediately exposed to 0.75 % permethrin or 0.05 % deltamethrin for 1 h. Mortality was assessed after 24 h and compared to the results obtained without PBO (D Menze et al., 2018). Significance levels were assessed using the chi-squared test at $p < 0.05$ (McHugh, 2013).

2.1.6 Extraction Methods

2.1.6.1 RNA Extraction and cDNA Synthesis

All mosquitoes used for RNA extraction were previously confirmed to be *An. funestus* s.s. using cocktail PCR (Koekemoer et al., 2002). Total RNA was extracted from pools of 10 females from resistant populations, as well as from FANG using the PicoPure RNA Extraction Kit from Arcturus (Life Technologies, CA, USA) according to manufacturer's protocol. RNA was extracted using Extraction Buffer (XB) and Conditioning Buffer (CB); isolated using 70% Methanol, Wash Buffers W1 and W2 and eluted using Elution Buffer (EB). To enhance quality, RNA was DNase-treated following washing with W1. Quantity and quality of isolated RNA were determined with NanoDrop ND1000 Spectrophotometer (Thermo Fisher) and Agilent 2100 Bioanalyzer. 2.3.2.2 cDNA Synthesis (RT-PCR) 1µg of total RNA from resistant and susceptible (FANG) mosquitoes was used as a template for cDNA synthesis using the SuperScript® III First Strand Synthesis Kit (Invitrogen) according to the manufacturer's instructions. 13µl reaction mix consisting of 1µl (1µg) RNA diluted in 8µl DEPC-treated water, 1µl of Oligo(dT)20 (50mM), 3µl DEPC-treated water and 1µl of 10mM dNTP mix was initially incubated for 5 min at 65° C. 4µl of 5X first strand buffer, 1µl of 0.1M DTT, 1µl of RNase Out (40U/µl) and 1.5µl of SuperScript® III Reverse Transcriptase (200U/µl) was added to make the total volume to 20.5µl. The mix was then incubated at 25° C for 5min, and then 50° C for 60min, followed by 70° C for 15min. 1µl of *E. coli* RNase H was added to the newly synthesized cDNA and incubated at 37° C for 20min to remove residual RNA. Quantity and quality of the DNA was finally assessed using NanoDrop ND1000 Spectrophotometer (Thermo Fisher).

2.1.6.2 DNA Extraction

Whole genome DNA was extracted from individual female *An. funestus* mosquitoes using the Livak DNA extraction technique following the protocol. The quality of the DNA was assessed using NanoDrop ND1000 Spectrophotometer (Thermo Fisher). The steps of DNA extraction involved: cell lysis by grinding and vortexing to release the genetic material. The addition of a salt like potassium acetate with positively charged potassium ions helps protect the negatively charged phosphate groups that run along the DNA backbone. A detergent is then added. The detergent breaks down the lipids in the cell membrane and nuclei. DNA is released as these membranes are disrupted. Next was to separate the DNA from proteins and other cellular debris by filtration, precipitating the DNA with an alcohol (ethanol). DNA is soluble in water but

insoluble in the presence of salt and alcohol therefore, by gently stirring the alcohol layer with a sterile pipette, a precipitate becomes visible and can be spooled out. If there is lots of DNA, it may be seen as a stringy, white precipitate. The cleaning of the DNA was done, and the precipitate was resuspended in distilled water. At the end of the optical density readings taken by a spectrophotometer and used to determine the concentration and purity of DNA in each sample. The DNA was then stored at -20°C for molecular analyses including PCR, electrophoresis, sequencing, fingerprinting, and cloning.

2.1.7 Species Identification PCR

A representative number of samples from the genomic DNA extracted was used to perform species identification PCR for the molecular confirmation that the mosquitoes used are affectively *An. funestus* ss. The PCR mix included a buffer A, 25mM dNTPs, Kapa Taq polymerase, 25mM MgCl₂, specific primers of the Funestus complex (UVF, FunR, VAN, RIV, PAR, RIVLIK, LEES), distilled water and gDNA. The PCR conditions were initiation at 94°C for 2min, elongation at 94°C for 30s, 45°C for 30s and 72°C for 40s with 35 cycles of elongation, extension at 72°C for 5min then hold at 10°C. The product size for positive *An. funestus* s.s was a sharp band at 500bp.

2.1.8 CYP325A Gene Amplification

To amplify the CYP325A full-length gene, specific primer sets were designed with respect to different purposes. Restriction sites were added to the primers to add restriction sites to the gene's 5' and 3' extremities which were very useful for subsequent work. The amplification was done using Phusion Taq polymerase yielding a product size of approximately 1.5kb as seen on agarose gel after revealing with Midori green. The full-length coding sequences of CYP325A alleles were amplified from cDNA sets from Cameroon, Uganda, Malawi, Congo, Ghana, Benin, FUMOZ and the FANG, using the primers listed in Table 8. To 14µl PCR mix made up of 3µl 5X Phusion HF Buffer (with 1.5mM MgCl₂ in final reaction), 0.12µl dNTP mix (85.7µM), 0.51µl each of forward and reverse primers (0.34µM), 0.15µl (0.015U) of Phusion High-Fidelity DNA Polymerase (Fermentas) and 10.71µl of dH₂O, 1µl cDNA was added. Amplification was carried out using the following conditions: one cycle at 95°C for 5 min; 35cycles of 94°C for 20s (denaturation), 58°C for 30s (annealing), and extension at 72°C for 90s; and one cycle at 72°C for 5min (final elongation). 3µl PCR products were separated on

1.5% agarose gel stained with Midori Green (0.5µg/µl) and visualized using transilluminator to confirm products size.

Table 8: Primers used for gene amplification and plasmid sequencing

Primer	Forward Sequence	Reverse Sequence	Size (bp)
CYP325A_Full	5'- ATGTTCTTCTACCAGCGTTCA -3'	5'TCACTGCAAAACATTTCGGTCTACG -3'	1532
CYP325A-Promoter	5' - CGCATCAATGAAGGTGCGAA -3'	5'- GGGCACTGTCTCTTACCAGT-3'	1061
pJET1.2	5'-CGACTCACTATAGGGAGAGCGGC-3'	5'AAGAACATCGATTTTCCATGGCAG-3'	~1727
pJET725	5'- CCGAAAAGTGCCACCTGAACGTCTAA-3'	5'TCCTGTCTCAGTTTCTGAAGCTTGCTC-3'	~2277
CYP325A-qPCR	5'- GGATACCGATACGGCATGTT-3'	5'- TCGGTATTTGATGCCTACA-3'	~126

2.1.9 Gel extraction purification method: Purification of PCR Product Ligation into pJET1.2 Blunt Vector

PCR products obtained from amplification were purified using the gel extraction kit as described in the manufacturer's manual. This method makes use of gel electrophoresis to separate DNA fragments on an agarose gel. The DNA fragment of interest is then excised and extracted from the agarose gel. The steps specifically involve running the PCR product on a standard agarose gel and excise the band of interest. Next was to dissolve the DNA-containing gel in excess buffer and heat at 50°C until completely dissolved and maintaining the acidic pH to enhance DNA adsorption to the membrane. Silica membranes bind DNA molecules in the presence of high ionic-salt buffers that drive hydrogen bond formation between silica and DNA. DNA binds the silica membrane as the sample is passed through the column by centrifugation. While the DNA remains bound to the silica membrane, contaminants such as nucleotides, proteins and other impurities are removed by alcohol-based washes. During several washes, salts are also removed, which sets the stage for elution of DNA. DNA is released from the silica membrane by eluting with a low-ionic solution, such as TE or water. Low salt solutions disrupt the hydrogen bonds that hold DNA on the membrane. Elution is most efficient under basic conditions, between the pH of 8 and 9, so if your water is acidic, you might want to make sure you use TE. Moreover, it is recommended to heat up the elution buffer and let it sit on the membrane for up to five minutes to release more DNA molecules. PCR products were cleaned individually with QIAquick® PCR Purification Kit (Qiagen) according to the manufacturer's

instructions and cloned into pJET1.2/blunt cloning vector using the CloneJET PCR Cloning Kit (Fermentas) as described in Table 9.

Table 9: pJET1.2/Blunt ligation protocol

Component	Quantity (µl) = 10
Blunting Reaction	
2X Reaction Buffer	05
Purified PCR Product	3.5
DNA Blunting Enzyme	0.5
Vortex briefly and microfuge for 5 seconds	-
Incubate blunting mix at 70°C for 5 min	-
Chill on ice	-
Ligation Reaction	
pJET1.2/Blunt Cloning Vector (50ng/µl)	0.5
T4 DNA Ligase	0.5
Vortex briefly and microfuge for 5seconds	-
Incubate mix at 22°C for 30 min	-

2.1.10 Transformation of CYP325A and Small-scale Plasmid Isolation

4µl (~5-10ng) of ligation product was added to 40µl Subcloning Efficiency™ DH5α Competent Cell (Invitrogen), chilled in sterile 1.5ml microcentrifuge tube. Reaction was mixed by gently flicking the bottom of the tube and left on ice for 30min. The cells were shocked for 45s at 42°C and then chilled immediately on ice for 2min. 950µl of pre-warmed S.O.C. medium was added, and the tubes incubated at 37°C and 200 rpm for 1hour. 50-100µl of transformants were spread onto LB plates containing 100mg/ml ampicillin and allowed to grow overnight at 37°C. Colonies were suspended separately in 20µl dH₂O and screened for presence of the gene in a PCR reaction using Kappa Taq DNA Polymerase (KAPABIOSYSTEMS) and the pJET1.2 primers listed in Table 8. 1.5µl of 10X Taq Buffer A, 0.75µl of MgCl₂ (25mM), 0.12µl of dNTP mix (10mM), 0.4µl each of forward and reverse primers, 0.12µl of 5U/µl KAPA Taq DNA Polymerase and 10.71µl dH₂O were mixed in total volume of 14µl, to which 1µl of colony was added. PCR was conducted using the following conditions: one cycle of 95°C for 3min; 25 cycles each of initial denaturation (94°C for 30seconds), annealing (57-60°C for 30seconds)

and extension (72°C for 90seconds); one cycle of final extension for 90seconds at 72°C. PCR product was run on 1.5% agarose gel stained with Midori Green to confirm products size.

4µl of positive colonies were grown (miniprep) at 37°C for 16hours in a 6ml LB medium containing 3µl ampicillin (100mg/ml), with shaking at 200rpm. Plasmids were isolated using the QIAprep® Spin Miniprep Kit (QIAGEN) according to the manufacturer's protocol. Quantity and quality of plasmid DNA was determined using NanoDrop ND1000 Spectrophotometer (Thermo Fisher). The isolated plasmids were sequenced on both strands using the pJET725 primers (Table 8).

2.1.11 CYP325A amplification, cloning and sequencing.

Blood fed indoor resting female *An. funestus* mosquitoes collected by the aspiration method from different localities across Africa were identified morphologically and confirmed by species identification PCR. After forced egg-laying, the eggs were reared in the insectary to adult emergence and then used to conduct insecticidal bioassays for type I (permethrin) and type II (deltamethrin) pyrethroids. Three pools of ten female mosquitoes were used for RNA extraction: highly susceptible (dead at 30min exposure), highly resistant (alive at 90min exposure), F₁ unexposed for control. cDNA was synthesized for each group, amplified using Phusion Taq polymerase, gel extracted and cloned into PJET725. The recombinant DNA containing *CYP325A* full-length gene was purified, miniprepped and sent for SANGER sequencing.

To further assess the role of polymorphisms in the non-coding region, a 1kb putative promoter upstream of *CYP325A* ATG codon was amplified in permethrin-dead and permethrin-alive mosquitoes from Mibellon, Cameroon where permethrin resistance was found to be very high. The goal being to assess the difference in *CYP325A* polymorphisms between the two groups which could be associated to observed resistance. The amplification was done using specifically designed primers (Table 8) and the cloning was performed as described earlier for the cDNA cloning into PJET and transformation in DH5α competent cells before sending for sequencing.

2.1.12 Sequence Analysis and Mapping of Polymorphisms

Analysis of sequences was conducted by detection of polymorphic positions through manual examination of sequence traces using BioEdit version 7.2.3.0 (Hall, 1999) and nucleotides differences in multiple alignments using CLC Sequence Viewer 6.8 (<http://www.clcbio.com/>). DnaSP 5.10.01 (Rozas et al., 2003) was used to analyse intra-allelic genetic variation such as AMELIE WAMBA NDONGMO Regine/Doctorate/Ph.D. Thesis/University of Yaoundé I

nucleotides and haplotypes diversity. Phylogenetic neighbour-joining trees of all haplotypes of *CYP325A* alleles were constructed using MEGA X 10.0 (Kumar et al., 2018). After sequence analyses, the predominant haplotype of each gene from each country was selected for further analysis. Amino acids sequences were generated in silico using the CLC Sequence Viewer nucleotides analysis module and used for further analyses and identification of mutations.

2.1.13 Africa-wide Genetic Polymorphism Analysis of *CYP325A*

cDNA of permethrin-resistant samples from Cameroon, Benin, Uganda, Malawi, DRC, the resistant FUMOS laboratory colony and the susceptible FANG laboratory colony were used to assess the role of allelic variation in resistance. The amplification was done on cDNA synthesized for qRT-PCR using Phusion Taq polymerase then the PCR product was cloned in PJET1.2 blunt end vector. The sequences were cleaned using Chromas version 2.6.2 (Joó & Clark, 2012) and BioEdit (Hall, 1999) then aligned in multiple alignments using ClustalW (Thompson et al., 2003). The genetic parameters such as nucleotide diversity and haplotype diversity were assessed using DnaSP version 6.12.03 (Rozas et al., 2003). A haplotype network was built using the TCS program (Clement et al., 2000) and a maximum likelihood phylogenetic tree was constructed using MEGA X (Kumar et al., 2018) to assess any ongoing selection.

In addition, to assess the potential association between promoter polymorphisms and pyrethroid resistance, a 1kb genomic fragment upstream of *CYP325A* was amplified, cloned, and sequenced in 19 susceptible (dead after 30min exposure to permethrin) and 16 resistant (alive after 1hour 30minutes exposure to 0.75% permethrin) mosquitoes from Cameroon. The primers used are listed in Table 8.

2.1.14 Comparative investigation of expression profile of *CYP325A* using qRT-PCR

The expression profile of *CYP325A* was investigated by qRT-PCR using mosquitoes from six different locations in Africa, to confirm its higher overexpression in Central Africa (Cameroon and DRC) compared with East (Uganda) and southern Africa (Malawi) (Weedall et al., 2019). Primers used are listed in Table 8. Total RNA was extracted from three biological replicates (three pools of 10 females) of the mosquitoes that survived exposure following the WHO test procedures for insecticide resistance monitoring in malaria vector mosquitoes (WHO, 2016) to permethrin and DDT from Cameroon, Malawi, Uganda, Ghana, and Benin; and bendiocarb from Malawi and Ghana. For each insecticide/location a control of same replicates of unexposed females were used. The FANG susceptible strain was used as control

susceptible *An. funestus* population. One microgram of the RNA was used for cDNA synthesis using SuperScript III (Invitrogen) with oligo-dT20 and RNAase H following the manufacturer's instructions. Using the standard protocol (Kwiatkowska et al., 2013; Riveron et al., 2013) for qRT-PCR, the amplification was conducted after establishing the standard curve for *CYP325A*. Relative expression and fold change of *CYP325A* for the test sample and control were established by comparisons to expression levels from FANG susceptible colony, after normalization with the housekeeping genes ribosomal protein S7 (RSP7; AFUN007153) and actin 5C (AFUN002505).

2.2 Polymorphism survey and in silico molecular docking studies of *CYP325A* with major classes of insecticides.

2.2.1 Modelling of *CYP325A* alleles by Satisfaction of Spatial Restraints

Homology modelling (HMM) is simply a computational approach for 3D prediction of protein structure. It involves construction of an atomic-resolution model of the "target" protein (query) from its amino acid sequence using experimental, 3D structure of a related homologous protein ("template" also referred to as a reference). The profound success of HMM is because the 3D structure of proteins from the same family is more conserved than their primary sequences (Lesk & Chothia, 1980) and proteins that share low sequence similarity often possess similar structures (Fiser & Sali, 2003; Fiser & Šali, 2003b).

2.2.2 Template Selection

The program BLASTp (Altschul et al., 1990) from NCBI (<http://blast.ncbi.nlm.nih.gov/Blast.cgi>) was used to search for the best template structure available in the protein data bank (PDB) database (Berman et al., 2002). A pairwise sequence alignment with the query protein sequences of *CYP325A* recovered as top hit a crystal structure of human microsomal 450 CYP3A4 (PDB:1TQN), with sequence similarities of 25% and lowest expectation value (E-value) of 1.0e67 for *CYP325A*. 1TQN is a crystal structure of *CYP3A4* resolved to 2.05Å without the N-terminal transmembrane leader sequence amino acids 3-23 (Yano et al., 2004) and deposited in protein database (<http://www.rcsb.org/pdb/>).

2.2.3 Template-Target Alignment

To maximise the alignment score between the template and the queries, pair-wise alignment of protein sequences (FASTA format) was done using T-Coffee (Notredame et al., 2000). The 3D-

Coffee Espresso (<http://tcoffee.org.cat/apps/tcoffee/do:expresso>) algorithm (Armougom et al., 2006) using sequence-structure threading (Fugue) generated a multisequence alignment by identifying template structure using a BLAST and substitution matrix of scores for each aligned pair of residues minus the penalties assigned to gaps, as explained elsewhere (Iorio et al., 2010). Residues present in the template and absent in the query were deleted, because misalignment of even a single residue can result in an error of about 4.0Å in the final model generated (Fiser & Šali, 2003a).

2.2.4 Model Building

MODELLER is a standalone computer program that models 3D structures of proteins and their assemblies by satisfaction of spatial restraints (Šali & Blundell, 1993). The alignment files of a sequence to be modelled with known related structures is used by the MODELLER to automatically calculate a model with all non-hydrogen atoms. The input to the program is restraints on the spatial structure of the amino acid sequence(s) and ligands to be modelled and the output is a 3D structure that satisfies these restraints as well as possible. *CYP325A* models were created using the MODELLER 9.0v2 (<https://salilab.org/modeller/>) and human *CYP3A4* (PDB:1TQN) as a template. MODELLER uses its SALIGN3D module to carry out template-query alignments and then extract spatial restraints from two sources: (i) homology-derived restraints on the distances and dihedral angles in the target sequence extracted from its alignment with template structure (Šali & Blundell, 1993); (ii) stereochemical restraints such as bond length and bond angle preferences are obtained from the molecular mechanics force field of CHARMM-22 (MacKerell Jr et al., 1998). Statistical preferences of main chain dihedral angles and non-bonded atomic distances are calculated by comparing the sequences of the target to the template, and a model calculated by optimisation employing methods of conjugate gradients and molecular dynamics (Braun & Gö, 1985) with simulated annealing in Cartesian space. The loop-module in the MODELLER automatically models all the loops in the query by energy optimisation approach as well (Fiser et al., 2000). The software refines the models by tuning alignments and side chains automatically and then relaxes the backbone. The script used for template query alignments and model building is given in Appendix 1.

2.2.5 Models Assessment (Validation)

Models generated using the MODELLER were assessed by comparing the PROSAIL Z score of the models and the template structure(s) (Sippl, 1993). The PROSAIL Z score (scoring function) of a model is a measure of compatibility between its sequences and the structure and AMELIE WAMBA NDONGMO Regine/Doctorate/Ph.D. Thesis/University of Yaoundé I

ideally the Z score of the model should be comparable to that of the template. One of the shortcomings of the Z score is that it is an internal evaluation between the modelled structure and the template to determine whether the model satisfies the spatial restraints imposed. Because of this an independent assessment tool, Errat was used to further validate the models.

2.2.6 Errat

For each query sequence 50 models were iteratively generated and externally assessed individually using Errat v2.0 (<http://nihserver.mbi.ucla.edu/ERRAT/>) to determine incorrectly determined structures. Errat analyses the statistical patterns of non-bonded interactions between different atom types (Colovos & Yeates, 1993). A single output plot is produced that gives the value of the error function vs position of a 9-residue sliding window of 96 reliable, high-resolution protein structures. Regions of candidate protein structures that are mis-traced or mis-registered were then identified by analysis of the pattern of non-bonded interactions from each window. Out of 50 models generated from each query sequence, one model is selected based on Errat scores for molecular docking. Errat scores for the all the models with the lowest incorrectly folded regions selected for further analysis, as well as the score of the template (1QTN) could be found in Appendix 2.

2.2.7 Ligand Structures

Virtual datasets of ligand insecticides: permethrin (ZINC01850374), deltamethrin (ZINC01997854), α -cypermethrin (ZINC1996306), DDT (ZINC01530011) and bendiocarb (ZINC02015426) were retrieved from the library of ZINC15 (<https://zinc.docking.org/>) database in MOL2 format (Irwin & Shoichet, 2005).

2.2.8 Preparation of Receptors (Models) and Ligands for Molecular Docking

MODELLER generates a model of main chain and side chain atoms devoid of hydrogen atoms and before docking simulation models were prepared by adding hydrogen atoms. This was done using the Molegro Molecular Viewer 2.5 (MMV) software from CLC bio (<http://www.clcbio.com/>) and both receptor and ligands were prepared in PDB format following the assigning of chirality to some of the insecticide ligands, e.g., permethrin.

2.2.9 Molecular Docking with Molegro Virtual Docker (MVD)

Molecular docking is basically a conformational sampling procedure in which various docked conformations are explored to attempt to predict the potential right one (Bitencourt-Ferreira & AMELIE WAMBA NDONGMO Regine/Doctorate/Ph.D. Thesis/University of Yaoundé I

de Azevedo, 2019; Ibrahim et al., 2016). Conformational sampling must be guided by a scoring or energy function (Warren et al., 2006) that is used to evaluate the fitness between the protein and the ligand. The final docked conformations are usually selected according to their scores and/or productive poses. The accepted hypothesis is that lower energy scores represent better protein-ligand bindings compared to higher energy values. A few approaches for the choice of scoring functions have been reported and can be roughly grouped into three approaches: force field methods (Goodsell et al., 1996), empirical scoring functions (Wang et al., 2007) and knowledge-based potentials (Gohlke et al., 2000). MVD is an integrated platform for predicting protein – ligand interactions which handles all aspects of the docking process from preparation of the molecules to determination of the potential binding sites of the target protein, and prediction of the binding modes of the ligands. MVD is a protein-ligand docking simulation program that allows us to carry out docking simulations in a fully integrated computational package (Bitencourt-Ferreira & de Azevedo, 2019). MVD can determine atom connectivity, assign bond orders, hybridization, add explicit hydrogens, and assign charges automatically. It is also possible subsequently to modify the various properties in the GUI (<http://molexus.io/mvd-faq>) (Rahimirad et al., 2021). MVD utilises evolutionary strategy to explore the conformational variability of a flexible ligand while simultaneously sampling available binding modes of the ligand into a partially flexible protein active site. Hydrogen bond motifs have been encoded into the MVD algorithm to search the spaces of available binding modes efficiently. Also, a simple scoring function is used to rank generated binding modes. The program has been documented to achieve up to 71% success rate of predicting correct binding mode of a ligand onto a protein when compared with the results from X-ray crystals of protein-ligand complexes (Jones et al., 1997). MVD employs artificial mimicry to simulate nature (Thomsen & Christensen, 2006); each potential docking mode (solution) is considered as a chromosome and is assigned a specific score. The chromosome contains information about the mapping of a ligand H-bond atom onto (complementary) protein H-bond atoms, mapping of hydrophobic points on the ligand onto protein hydrophobic point and the conformation around flexible ligand bonds and protein -OH groups. Sets of solutions are termed a population and corresponding chromosomes ranked according to fitness. Two individual chromosomes share the same niche if the r.m.s.d. between the coordinate of their donor and acceptor is less than 1.0Å (1.0Å = 0.1nm) apart. The population of chromosomes is iteratively optimised so that at each step of the run, a point mutation may occur in the chromosome, or two chromosomes may mate to produce a child (crossover) and migration of a population member from one island to

another can take place. The optimised chromosome then becomes a parent and selection of parent chromosome is biased towards the fitter members of the population (ligand dockings with better fitness score). For docking with MVD, ChemScore fitness function was chosen for it has been trained by regression against binding affinities data (Tripathi & Misra, 2017). The function was derived empirically from a set of 82 protein-ligand complexes for which measured binding affinities were available. ChemScore estimates the total free energy change as the ligand binds to its respective receptor. Docking was performed using the genetic algorithm (GA) protocol as implemented on the user-friendly Molegro Molecular Viewer interface of MVD. The active site of the protein was defined as a binding cavity (sphere) of 20Å radius centred on the heme-iron atom. 50 docking solutions (poses) of each ligand with respective receptor protein ranked according to their ChemScore fitness were generated. Solutions with the highest scores (best-ranked docking poses) which are in potentially productive orientations were selected for further analysis. Visualisation and preparation of figures from the docking were carried out using the PyMOL 1.7 and MMV.

2.2.10 *In silico* Analysis of Protein Pockets and Cavities

To investigate how the pyrethroid ligand could enter the active site of two models each from CYP325A (CMRCYP325A, CONCYP325A, GHACYP325A, FUMCYP325A and FANCYP325A) and how product could egress, a search of channels leading into and out of the active site to the surface of the protein (bulk solvent) was conducted using the algorithm tool CAVER 3.1 (Petřek et al., 2006). CAVER models protein body on a discrete 3-dimensional grid space with all grid nodes clustered into two classes: inside nodes (inside atomic vdW radii) and outside nodes (nodes located outside the protein body). CAVER then spans the grid nodes avoiding nodes that are in the convex hull in its calculation and then find channels by evaluating a cost-function every time a new grid node is reached (Cojocaru et al., 2007). Settings were set as described in CAVER PyMOL plugin v3.0. (http://www.caver.cz/fil/download/manual/caver_plugin_userguide.pdf):

- (i) maximum Java heap size ~6000;
- (ii) maximum probe radius which species the minimum radius a tunnel must have to be identified was set as 0.9;
- (iii) shell depth (the maximal depth of a surface region) was set as 4;

(iv) shell radius (the radius of the shell probe which will be used to define which parts of the Voronoi diagram represent the bulk solvent) was set as 3;

(v) clustering threshold which specify the level of detail at which the tree hierarchy of tunnel clusters will be cut was set as 3.5;

(vi) number of approximating balls which specify the number of balls that will be placed right under the surface of each larger atom to represent individual atoms in the input structure was set as 12. Starting points were set as x (-16.4), y (-22.6) and z (-9.6) using the input PDB file with search centre above the haem iron, and with a maximum distance of calculation starting point set as 3.0Å and desired radius of 5.0Å.

2.3 Molecular characterisation and functional validation of *CYP325A* as an insecticide resistance gene through *in vivo* and *in vitro* techniques.

2.3.1 Cloning and Co-Expression of Recombinant *CYP325A* cDNA with *An. gambiae* Cytochrome P450 Reductase (CPR)

2.3.1.1 Construction of pB13::ompA+2-CYP325A Plasmid

Four alleles each from *CYP325A* (were selected for cloning and heterologous expression (Table 10).

Table 10: Country of origin, *CYP325A* alleles selected for functional characterisation

Country	Allele	Amino Sequence Replacement Mutations in <i>CYP325A</i>
Cameroon	CMR4 <i>CYP325A</i>	L ²¹ V; K ²² R; K ²⁹ A; Q ³³¹ E;
Congo	CON1 <i>CYP325A</i>	A ²⁹ K; E ³³¹ Q; V ²¹ L; R ²² K
Fumoz	FUM <i>CYP325A</i>	A ¹¹⁷ S; L ³¹⁷ M; E ³⁴⁷ D
Ghana	GHAC <i>CYP325A</i>	S ⁹³ R; D ³⁸⁴ N; P ⁴⁷⁰ A; A ⁴⁸⁸ T
Fang	FANC <i>CYP325A</i>	

Legend: L-Leucine, K-Lysine, R-Arginine, A-Alanine, E-Glutamic acid, Q-Glutamine, S-Serine, D-Aspartic acid, P-Proline, T-Threonine, N-Asparagine

Full-length, unmodified cDNA of *CYP325A* alleles were expressed as microsomal proteins using ompA+2 strategy (Pritchard et al., 2006; Pritchard et al., 1997). cDNA fragment encoding the bacterial outer membrane protein A (ompA) leader sequence (21 amino acids) and 2 additional spacer residues (Ala-Pro linker) were introduced as signal peptide ompA+2 to the NH₂-terminus of the P450 cDNAs in frame with the P450 initiation codon as shown in scheme in Figure 32. The signal peptide directs the P450 to the membrane surface (Pritchard et al., 1997) and is thereafter cleaved upon expression in a fashion enhanced by the Ala-Pro spacer residues.

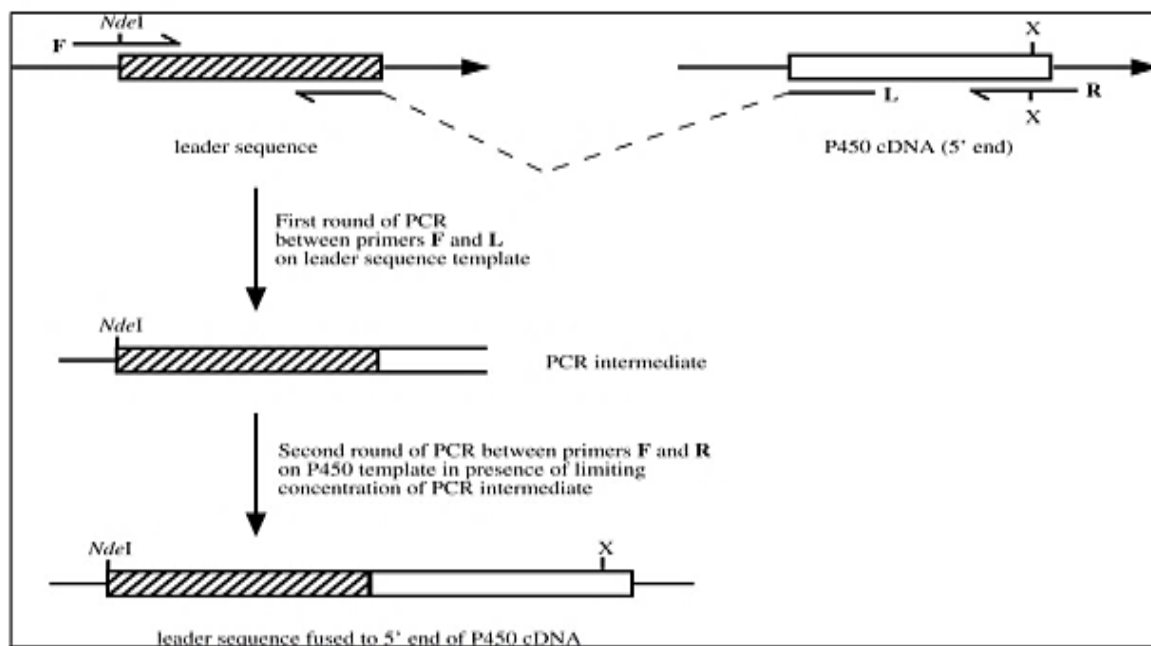


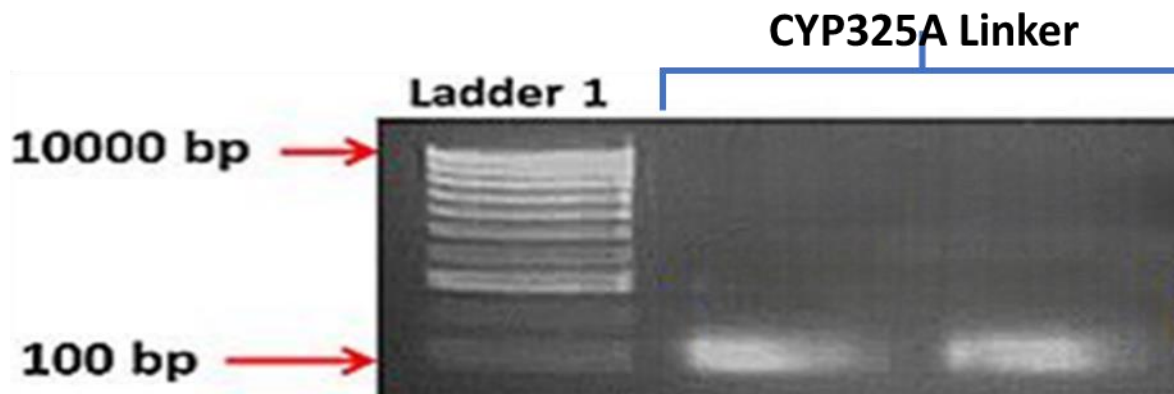
Figure 40: General scheme for the PCR-mediated fusion of bacterial leader sequences to P450 cDNAs. Adapted from (Pritchard et al., 1997).

2.3.1.2 Construction of ompA+2-CYP325A cDNA

Initially, a short DNA fragment was synthesized in a fusion PCR using 50ng *E. coli* JM109 gDNA as a template with a leader sequence-specific forward primer ompA+2F: GGAATTCCATATGAAAAAGACAGCTATCGCG (EcoRI and NdeI sites are underlined in green and purple respectively) and a reverse linker primer: ompA+2CYP325AR: CAATGAACGCTGGTAGGAAGAACATCGGAGCGGCCTGCGCTACGGTAGCGAA which is complementary to the first 24 nucleotides 5' end of CYP325A cDNA, underlined in dark red, joined to the last 21 bases linker of the leader sequence. PCR reaction mix is given in Table 11 and the High-Fidelity PCR conditions were as follows: 1 cycle at 95°C for 5 min; 35 cycles each of 94°C for 20s, 58°C for 30s, and elongation at 72 °C for 45s; and 1 cycle of final extension at 72°C for 5 min. The PCR product, an intermediate fragment (linker) of less than 100bp (containing the ompA+2 signal sequence and the first 24 nucleotides was confirmed using gel electrophoresis (Figure 33), cleaned with QIAquick® PCR Purification Kit (Qiagen) as explained earlier and its quality and quantity assessed with Nanodrop Spectrophotometer (Thermo Fisher).

Table 11: PCR reaction mix for ompA+2 intermediate linker fragment synthesis

Reagent	Final concentration	Volume (μ l)
10X Qiagen Buffer (containing 5mM MgCl ₂)	1X	5
dNTP mix (25mM)	0.66mM	0.4
ompA+2F (10 μ M)	1 μ M	1.5
ompA+2CYP325A (10 μ M)	1 μ M	1.5
JM109 gDNA template	50ng	1.0
dH ₂ O	-	39.6
HotStar Taq Polymerase	1U/ μ l	1.0
Total Volume	-	50

**Figure 41:** ~ 100 bp intermediate linker product migrated on 1.5% agarose gel stained with Midori Green

Next, cDNA minipreps of CYP325A alleles prepared in section 2.3.2.3(iii) were used as templates with limiting concentrations of the linker prepared above for second PCR, using the leader sequence-specific forward primer (ompA+2F) and reverse primers: - ompA+2CYP325AF: AAGCTTGAATTC TCACTGCAAAACATTCGGTCTAC (HINDIII and EcoRI sites in Blue and green respectively) and ompA+2CYP325AR: TCTAGAGAATTCTTACACCTTTTCTACCTTC AAG. These reverse primers designed with XbaI and EcoRI restriction sites underlined in red and green respectively are complementary to the 3'-terminus of CYP325A cDNA. PCR reaction mix is given in Table 3.3 and the High-Fidelity conditions were as follows: 1 cycle at 95°C for 15min; 35cycles each of 94°C for 20s, 50°C for 30s, and elongation at 72°C for 90s; and 1 cycle of final extension at 72°C for 5mins. The PCR product, a cDNA containing the ompA+2 signal peptide joined to the full-length cDNA (~1600bp) was confirmed using agarose gel electrophoresis, cleaned with QIAquick® PCR Purification Kit (Qiagen) and its quality and quantity assessed with Nanodrop

AMELIE WAMBA NDONGMO Regine/Doctorate/Ph.D. Thesis/University of Yaoundé I

Spectrophotometer (Thermo Fisher). 5-7ng of these PCR products were ligated into pJET1.2/blunt cloning vector using the CloneJET PCR Cloning Kit (Fermentas) as described in Table 9 and transformed into DH5 α . Positive colonies screened with pJET1.2 primers listed in Table 2.1 were minipreped overnight and sequenced using the pJET725 primers for presence of ompA+2 signal peptide sequence and restriction sites.

Table 12: PCR reaction mix for fusion of ompA+2 leader sequence to CYP325A cDNA

Reagent	Final concentration	Volume (μ l)
10X Qiagen Buffer (containing 15mM MgCl ₂)	1X	5
dNTP mix (25mM)	0.66mM	0.4
ompA+2F (10 μ M)	1 μ M	1.5
ompA+2CYP325A-R (10 μ M)	1 μ M	1.5
Linker fragment	1ng/ μ l	0.5
dH ₂ O	-	40.1
HotStar Taq Polymerase	1U/ μ l	1.0
Total Volume	-	50

1.10 Detoxification Phases of Metabolic Resistance (MR)

Insects face numerous toxins (xenobiotics) through life, some produced naturally by plants (sometimes called allelochemicals) and some produced by humans (insecticides). To survive the natural toxins, insects evolved various detoxification mechanisms which sometimes allow insects to overcome insecticides, and the level and type of mechanisms differ greatly. This results in differing toxicity among different stages, populations, and species of insects. Knowledge of detoxification allows us to better incorporate chemical resistance mechanisms in crop plants, and to better select insecticides that will be effective when applied. Normally, a lipophilic xenobiotic that enters an animal's body is rapidly detoxified in a process that could be divided into phase I (primary) and phase II (secondary) processes. Phase I reactions consist of oxidation, hydrolysis, and reduction producing metabolites which are sometimes polar enough to be excreted. These metabolites then enter the next phase where they undergo conjugation with GST becoming water soluble and easily excretable (Figure 23).

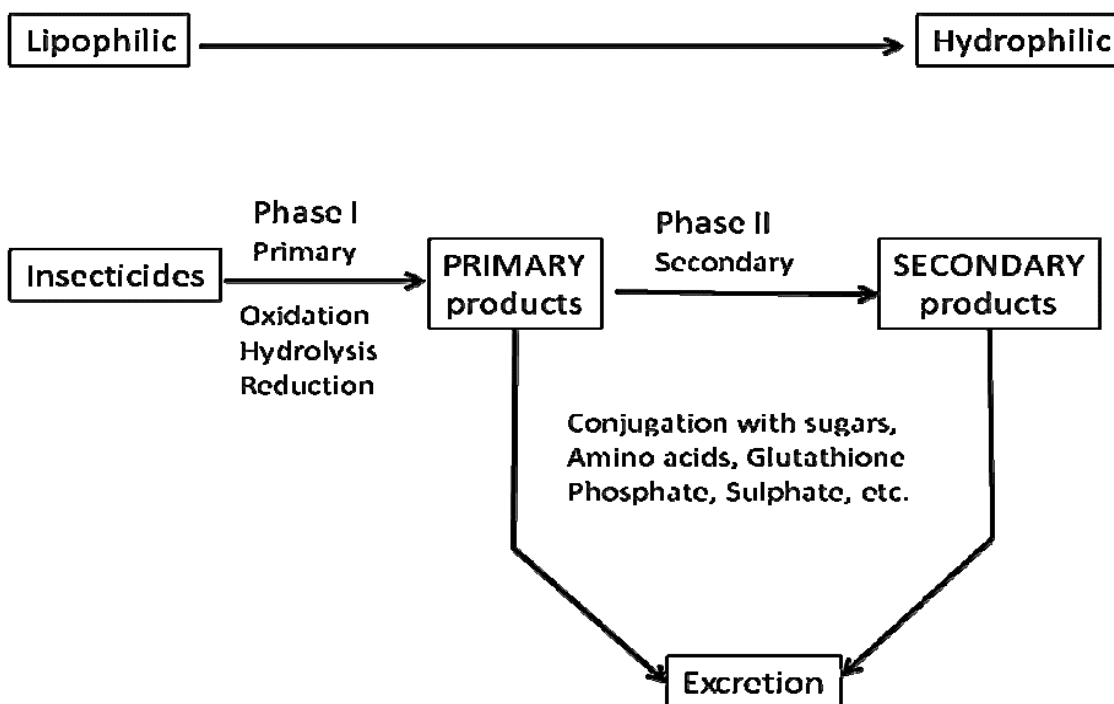


Figure 42: Xenobiotic metabolism and disposition (Corbel & N'Guessan, 2013)

2.3.1.3 Restriction Digestion of pJET1.2::ompA+2-CYP325A Construct

The pJET1.2::ompA+2-CYP325A plasmids were double-digested with restriction enzymes *NdeI* and *EcoRI* (Table 13) from Fermentas and purified by gel-extraction using the QIAquick® Gel Extraction Kit (QIAGEN). Efforts to digest pJET1.2::ompA+2CYP325A plasmids were unsuccessful and as such the cleaned PCR products from section 3.3.1.1.1 were double digested directly and used for the next step.

Table 13: Double digestion of ompA+2CYP325A and pJET1.2::ompA+2CYP325A products

Reagent	Final concentration	Volume (µl)
10X Fast Digest Green Buffer	1X	5
Fast Digest <i>NdeI</i>	-	2
Fast Digest <i>EcoRI</i>	-	2
Plasmid/ PCR product	0.1- 0.5µg	10-20
dH ₂ O	As required	20-30
Total Volume	-	50

2.3.1.4 Ligation of Restriction Digests into pCWOri+ Plasmid and Cloning into DH5 α

The ompA+2-CYP325A PCR product and plasmid digests were ligated overnight into pCWOri+ expression plasmid already linearized with NdeI and EcoRI restriction enzymes (Table 14). pCWOri+ is one of the most convenient expression vectors with two tac promoter cassettes upstream of NdeI (CA↓ TATG) restriction site coincident with initiation codon ATG (Barnes et al., 1991) as well as a gene encoding Lac repressor molecule which prevents transcription from tac promoters before addition of inducing agents. A map in Figure 34, prepared using the NEB Cutter v2.0 (Vincze et al., 2003) shows the strategy for the construction of the expression plasmid: pB13::ompACYP325A.

Table 14: Ligation of ompA+2CYP325A and pJET1.2::ompA+2CYP325A products

Reagent	Final concentration	Volume (μ l)
Restriction Digest	20-50ng	10-25
pCWOri+ Digest	5-10ng	2-4
10X T ₄ DNA Ligase Buffer	1X	1
dH ₂ O	-	As required
T ₄ DNA Ligase	1U/ μ l	1
Total Volume	-	50

Ligation condition: 16° C for 16hours

4 μ l of the ligation product was used to transform high efficiency DH5 α using the protocol outlined in section 2.3.2.3. Positive colonies were screened with forward (seqpCWF) and reverse (seqpCWR) primers (Table 15) designed within the pCWOri+ sequence approximately 100 nucleotides upstream of the NdeI restriction site and downstream of the EcoRI restriction site respectively. A band of around 1700bp comprising the insert gene (1512bp), the ompA+2 leader sequence as well as the ~200 nucleotides from pCWOri+ flanking the insert confirm the presence of the candidate genes in the expression vector. These colonies were minipreped overnight and sequenced using the ompA+2F and ompA+2CYP325AR primers as well as the seqpCWF and seqpCWR primers to confirm the presence of ompA+2 signal peptide sequence and restriction sites.

Table 15: Primers for sequencing of ompA+2-CYP325A in pCWOri+ and CPR in pACYC-184

Primer	Forward Sequence	Reverse Sequence	Product Size (bp)
SeqpCW	ATCCCCCTGTTGACAATTAATCATC	ACCTATAAAAAATAGGCGTATCACGA	~1700
SeqCPR	CTACTCGATCCATATGACGACGGTGAACAC	TACGGATCCTACAGCACATCCTCGCCCGTGCTC	~600

2.3.1.5 Construction of pACYC-184:: Cytochrome P450 Reductase Plasmid

pACYC-184 (New England Biolabs) containing the ancillary protein *An. gambiae* cytochrome P450 reductase (AgCPR) as well as the His-tagged *An. gambiae* cytochrome b₅ (Agb₅) used on the course of this study were kindly provided by Dr. M.J.I. Paine at LSTM. The P450 reductase expression cassette was prepared as described previously (Pritchard et al., 1998; Pritchard et al., 2006) with P450 reductase cDNA modified by fusing it with pelB leader sequence in a strategy like that of the ompA+2 for P450s but using the plasmid pET-20b as a template for the initial linker PCR. The pACYC-184 expression vector encodes gene for chloramphenicol resistance. More details of the engineering method of this plasmid could be found in (Pritchard et al., 2006a).

2.3.1.6 Construction of pB13:: (His) 4-Cytochrome b₅ and Purification of b₅

Agb₅ cDNA isolated by Nikou and colleagues (Nikou et al., 2003) was tagged with histidine residues in its NH₂-terminus and engineered into pB13 plasmid already linearized with NdeI and HindIII restriction sites. Expression of b₅ protein was done using A183 *E. coli* cells, harvested after 24-30 hours post-induction with 0.5mM δ -ALA and 1mM IPTG to the final concentration. The protein was prepared using the technique outlined by Holmans and colleagues (Holmans et al., 1994) in which the solubilized haemoprotein was purified by nickel affinity chromatography. Concentration of membranous b₅ was measured by determining spectral activity (Omura & Sato, 1964; Omura & TAKESUE, 1970) as difference between reduced and oxidized b₅ (OD₄₂₃ vs OD₄₉₀) using the extinction coefficient of 185mM⁻¹ cm⁻¹. Total protein was determined using Bradford assay. The enzyme was frozen in aliquot in -80° C until required.

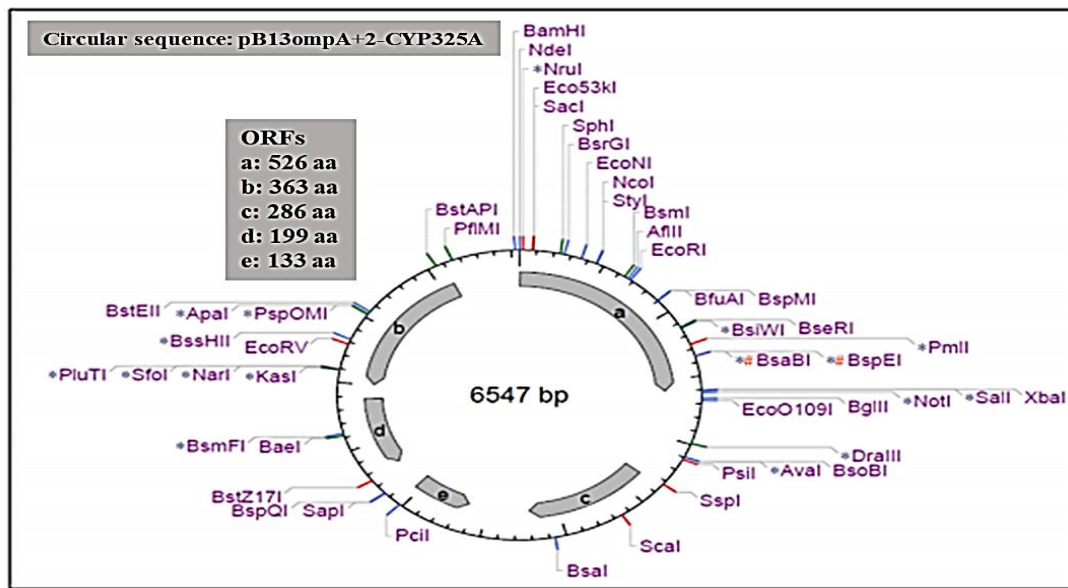


Figure 43: Map of pB13::ompA+2CYP325A showing expression plasmid construct in circular form (Ibrahim et al., 2015).

A: 21 amino acids of signal peptide plus alanine proline spacer residues, and 503 amino acids encoded by CYP325A cDNA. b. LacI repressor (NCBI: WB_002485631); c: β -lactamase (NCBI: WP_000027057); d: LacZ-alpha (GenBank: ACA638301); e: Ori+. Prepared using NEB Cutter v2. (<http://tools.neb.com/NEBcutter2/index.php>)

2.3.1.7 Co-transformation of pB13::ompA+2CYP325A with pACYC-184-*An. gambiae* CPR

High Efficiency *E. coli* JM109 cells (Promega) were co-transformed with plasmid pB13 containing *An. funestus* CYP325A and pACYC-184 bearing AgCPR in a ratio of 2:1. AgCPR was used due to the unavailability of *An. funestus* CPR cloned into pACYC vector; and because AgCPR (96% identical to *An. funestus* CPR) had been used as a surrogate redox partner with other P450s of even lower similarity like *Ae. aegypti* (87% identical) successfully (Stevenson et al., 2012). Co-transformation strategy has been described in (McLaughlin et al., 2008). 100 μ l of JM109 cells was introduced into 15ml tube chilled on ice. 4 μ l of pB13 plasmid bearing candidate P450 and 2 μ l of pACYC plasmid bearing CPR were introduced into the tubes. After 30 mins incubation on ice, cells were heat shocked for 90 seconds at 42°C and then chilled on ice for 2min. 950 μ l of S.O.C medium was added, and tubes incubated at 37°C with shaking at 200rpm for 2hours. 100 μ l of the co-transformed cells were spread onto LB plates with 100mg/ml ampicillin and 34mg/ml chloramphenicol and allowed to grow at 37°C for 16hours.

Individual colonies were suspended in 20µl distilled water the next day and screened using KAPA PCR as described earlier using the primers for pCWori+ (seqpCWF and seqPCWR) to confirm presence of candidate P450s and primers seqCPRF and seqCPRR (Table 15) for CPR. The seqCPR primers are internal primers designed inside the P450 reductase itself and produced a band of around 600bp on 1.5% agarose gel stained with ethidium bromide.

2.3.2 Heterologous co-expression of pB13::ompA+2-*An. funestus* CYP325A with pACYC-184-*An. gambiae* CPR in *E. Coli* JM109

For co-expression of CYP325A and CPR, 4µl of co-transformed colony suspended in distilled water was introduced into a 15ml tube containing 3ml LB medium, 3µl of 100mg/ml ampicillin and 5.1µl of 20mg/ml chloramphenicol. Culture could grow for 12-14 hours at 37°C with shaking at 200 rpm. The next day 1-2ml of this culture was used to inoculate 200ml of pre-warmed (37°C) TB medium containing 200µl ampicillin and 340µl chloramphenicol. This culture was grown for 3-4 hours at 37°C and 200 rpm orbital shaking until the optical density at 600nm reached 0.6-0.7. The log-phased cells were then transferred to 21°C (22°C optimal) and 150rpm orbital shaking and allowed to cool for 30 minutes. Induction was carried out by adding 1mM IPTG and 0.5mM δ-ALA to the final concentrations. Cultures were monitored for P450 activity at 6 hours interval starting from 18hours. Once P450 activity was detected cultures were then transferred into 250ml tubes chilled on ice and centrifuged at 2800rpm and 4°C for 20minutes. Detail of this protocol could be found in (McLaughlin et al., 2008; Pritchard et al., 2006; Stevenson et al., 2012) and specifically the procedure for co-expression, harvesting of cells, spheroplast preparation and isolation of membranes are given in Appendix 6.

2.3.3 Determination of concentration of *An. funestus* CYP325A proteins and *An. gambiae* cytochrome P450 reductase activity

2.3.3.1 Measurement of Total Protein, P450 and CPR Activities

Protein content of the membranes was measured calorimetrically with Bio-Rad Protein Assay Kit (Life Science Research) using the Bradford method (Bradford, 1976) with bovine serum albumin standard. The P450 concentration was quantified through spectral activity as described (Omura & Sato, 1964) by measuring the size of the peak (absorbance) at 450nm and using the absorbance at 490nm as a reference and an extinction coefficient ($\epsilon_{\text{cyt450}} = 0.091\mu\text{M}^{-1}\text{cm}^{-1}$) for P450s. 50µl of membrane was diluted in 1.5ml of P450 spectrum buffer (80% of 0.1M potassium phosphate buffer, pH 7.5, with 20% v/v glycerol). Few grains of sodium dithionate

were added, and the mix swirled gently and then divided (750µl each) into two optical cuvettes labelled E (experimental) and B (blank). After running a baseline between 500-400nm, carbon monoxide was bubbled into E for 60s. The extinction coefficient, dilution factor and the Fe²⁺ - CO (E) and Fe²⁺ (B) difference spectra were used to calculate the P450 activity.

CPR activity in the prepared membranes was measured by cytochrome c reduction assay (Strobel & Dignam, 1978). Details of the protocol for this assay could be found elsewhere (Pritchard et al., 2006). Reductase activity was measured spectrophotometrically based on extinction coefficient of reduced cytochrome c (21.4 mM⁻¹ cm⁻¹) as nmol of cytochrome c reduced/min/mg protein.

2.3.3.2 Comparative assessment of metabolic activity of CYP325A alleles with reverse-phase high-performance liquid chromatography (RPHPLC) metabolism assay

The purified CYP325A were used for metabolism assays with panel of insecticides, including representative pyrethroids (permethrin, deltamethrin and α-cypermethrin), organochlorine (DDT) and carbamates (bendiocarb and propoxur). Protocols used followed the procedure as described in previous studies (Müller et al., 2008; Stevenson et al., 2011) for metabolism assays of pyrethroids with *An. gambiae* CYP6P3 and CYP6M2 recombinant proteins, respectively

2.3.3.2.1 Substrate Depletion Assay

Initially, 2mM stock concentration of all insecticides were prepared in HPLC-grade methanol and kept in -20°C prior to use. Substrates working solution was prepared by diluting stock to 0.8mM with methanol to reduce precipitation of insecticide. The reaction mix for this protocol including the membrane expressing P450 and CPR, b₅, NADPH-regeneration system as well as the buffer used are tabulated below (Table 16). 0.2M Tris-HCl and NADPH-regeneration components (1mM glucose-6-phosphate, 0.25mM MgCl₂, 0.1mM NADP⁺ and 1U/ml glucose-6-phosphate dehydrogenase) were added to the bottom of 1.5ml tube chilled on ice.

Table 16: Reaction mix for HPLC metabolic assay

Component	Stock concentration	Final reaction concentration	Volume (µl)
Tris HCL pH 7.4	0.2M	0.2M	Varies
Membrane (P450 +CPR)	Varies (nmol/ml)	45pmol	Varies
Cytochrome b5	Varies (nmol/ml)	~180 – 500pmol	~10-20
NADPH+/- (containing 0.25mMMgCl ₂)	10X	1X	50
Incubation at 30° C and 1200rpm for 5min			
Substrate (Working)	0.8M	20µM	5.0
Total Volume			200

Membrane expressing P450 and CPR, and the b₅ proteins were added to the side of the tube and pre-incubated for 5min at 30°C, with shaking at 1200rpm to activate the membrane. 20µM of test insecticide was then added into the final volume of 0.2ml (less than 2.5% v/v methanol in final volume of reaction mix) and reaction started by vortexing at 1200rpm and 30°C for 1hour. Reactions were quenched with 0.1ml ice-cold methanol and incubated for 5 more min at 1200rpm and 30°C, to dissolve all residual insecticide. Tubes were then centrifuged at 16400rpm and 4°C for 12min and 150µl of supernatant transferred into HPLC vials for analysis. All reactions were carried out in triplicates with experimental samples (+NADPH) and negative control (-NADPH) not containing NADP. 100µl of sample was loaded into an isocratic mobile phase of Agilent 1260 Infinity with a flow rate of 1ml/min and peaks separated with a 250mm C18 column (Acclaim TM 120, Dionex) at 23°C. Details of the mobile phase composition, column temperatures, and wavelength of detection and retention time of insecticides used in this study are given in the Table 17 Enzyme activity was calculated as the percentage depletion (the difference in the quantity of insecticide(s) remaining in the +NADPH tubes compared with the -NADPH) and a paired t-test was used for statistical analysis.

Table 17: Conditions used for Reverse-Phase HPLC Analysis. Conditions used for Reverse-Phase HPLC Analysis

Insecticides	Mobile Phase (v/v)	Column Temperature (° C)	UV-Vis Wavelength (nm)	Retention time (min)
Permethrin	MeOH:H ₂ O (90:10)	23	226	cis~12, trans ~14
Deltamethrin	MeOH:H ₂ O (90:10)	23	226	cis~9, trans ~11
α -cypermethrin	MeOH:H ₂ O (90:10)	23	226	~8
Propoxur	ACN:H ₂ O (60:40)	40	270	~6
DDT	MeOH:H ₂ O (90:10)	23	232	~11

MeOH = Methanol and CAN = Acetonitrile

2.3.3.2.2 Steady-State Kinetic Parameters Analysis

Establishment of kinetic parameters for CYP325A protein variants will provide important information on turnover (the speed with which the different alleles metabolise and clear pyrethroid insecticides) and K_m (the affinity of the different alleles toward different insecticides). This will help establish differences in the catalytic efficiencies of the different alleles from resistant strain and identify whether the alleles from resistant strains differ in their pyrethroid-metabolising activity compared to alleles from susceptible strain. Enzyme response to variation in substrate concentration was determined using the pyrethroids permethrin and deltamethrin. Steady-state kinetic parameters were obtained by measuring the rate of reaction under linear conditions for 10 minutes while varying the substrate concentration from 2.5 to 20 μ M (2.5, 5.0, 7.5, 10, 12.5, 15, 17.5 and 20 μ M). Reactions were performed in triplicates with +NADPH (experimental tubes) in parallel with –NADPH (negative control). K_m and V_{max} were established from the plot of substrate concentrations against the initial velocities and fitting of the data to the Michaelis-Menten equation using the non-linear regression as implemented in the GraphPad Prism 6.03. Catalytic constants and efficiencies were automatically predicted from the steady-state parameters by the software.

2.3.3.2.3 Restriction Digestion of the Parental DNA Template

The parental plasmidic template is Dam⁺ -methylated from transformation into DH5 α . This makes it possible to cleave the unwanted template by restriction enzyme EcoRII (Thermo SCIENTIFIC, MA, USA) as described in (Zheng et al., 2004). 2 μ l of 1X Fast Digest Buffer and 1 μ l of EcoRI was added to the PCR-amplification product and incubated for one hour at 37°C. The restriction enzyme cut the parental template at position 5'...G m6 ↓ ATC...3' which is absent in the desired mutant PCR product since its newly synthesized and not passed through *E. coli* DH5 α cloning.

2.3.3.2.4 Construction of Plasmidic Expression Vector pB13::ompA+2CYP325A

4 μ l of the digest was transformed into DH5 α , positive colonies mini-prepped and sequenced on both strands with pJET725 primers to confirm presence of mutations. The PCR product was then digested with NdeI and EcoRI (see Table 13), gel extracted with QIAquick Gel Extraction Kit (QIAGEN) and then ligated into pCWori+ already linearized with the same restriction enzymes (Table 14).

2.3.3.2.5 Transformation and co-transformation of expression vector with *An. gambiae* CPR

The ligation product was then transformed into DH5 α as described in section 3.3, positive colonies mini-prepped and sequenced on both strands with seqPCW primers to confirm the presence of the ompA+2 leader and target mutations again. The miniprep was then co-transformed with AgCPR using the protocol outlined earlier into JM109 cells.

2.3.3.3 Comparative assessment of ability of allele variants of CYP325A to Confer pyrethroid resistance in *D. melanogaster* using GAL4-UAS system

Predictions of a drug's *in vivo* clearance is usually made based on kinetic parameters obtained from *in vitro* estimated intrinsic clearance (Tracy, 2003). However, *in vitro* - *in vivo* extrapolation is an assumption with some shortcomings, for *in vitro* experiments discount the influence of other metabolizing enzymes and factors within the biological system. Other proteins may be involved in binding and/or metabolism of a substrate and as such *in vitro* results may not reflect the holistic pharmacokinetics taking place. *In vitro* kinetic analyses have revealed differences in kinetic profiles between the membrane proteins from resistant and susceptible alleles of CYP325A. But, to further confirm the involvement of the resistant alleles

of these genes, a comparative analysis was conducted by introducing and expressing these genes in *D. melanogaster* using GAL4-UAS system. The transgenic flies over-expressing the genes were then screened for pyrethroid resistance. GAL4-UAS system is a veritable Swiss army knife (Duffy, 2002) which allows ectopic and targeted expression of gene of interest *in vivo* in a temporal and/or spatial fashion (Duffy, 2002; Southall et al., 2008). The technology is increasingly used to validate insecticide resistance genes as described in the background to this chapter (Daborn et al., 2007; Riveron, Ibrahim, et al., 2014; Riveron et al., 2013; Zhu et al., 2010). GAL4-UAS system is a bipartite system in which the expression of gene of interest (responder) is controlled by the presence of the UAS element, a 5 tandemly arrayed and optimized GAL4 binding sites (Duffy, 2002). Transcription of the responder requires presence of GAL4, thus the absence of GAL4 in the responder lines maintains them in a transcriptionally silent state; to activate transcription, the responder lines are mated to flies expressing GAL4 in a particular pattern termed the driver (Duffy, 2002). The progeny then expresses the responder (target gene) in a configuration that reflects the GAL4 pattern of the respective driver (Figure 44). The success of this technique is because GAL4 equivalent is absent in most species, and as such the candidate gene is only expressed in the progeny of the crosses between drivers and responder lines, when GAL4 and UAS transgenes are brought together in the same genome (Lynd & Lycett, 2012).

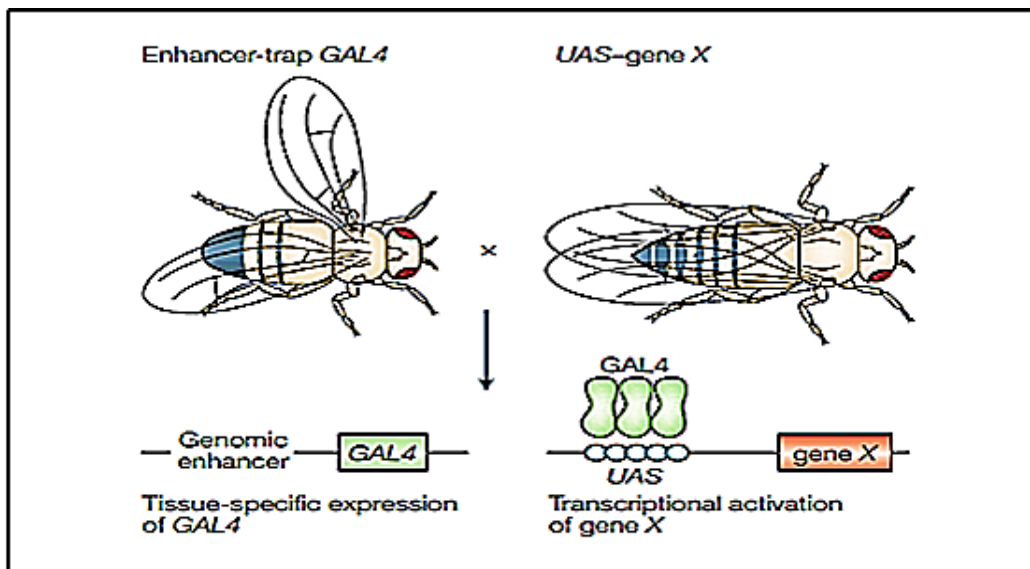


Figure 44: The GAL4-UAS system for directed gene expression.

(Adapted from (Klug et al., 2002))

2.3.3.3.1 Cloning and Construction of pUASattB::CYP325A Plasmids

Forward and reverse primers were designed for CYP325A with EcoRI restriction sites respectively to allow cloning into pUAST vector. Full length cDNA encoding CYP325A (CMRCYP325A) were amplified using HotStarTaq Polymerase (QIAGEN) and 0.5-1µg miniprep templates prepared in the cloning section earlier. Protocol for amplification (Table 18) involves initial denaturation at 95°C for 15min followed by 35 cycles each of 94°C for 30seconds: 57°C for 30seconds and 72° C for 90seconds. This is followed with final extension for 5mins at 72°C and holding at 4°C. The primers for the amplification of these genes as well as primers for qPCR validation are given in Table 19.

Table 18: PCR reaction mix for amplification of CYP325A cDNA for transgenic analysis

Reagent	Final Concentration	Volume (µl)
10X Qiagen Buffer (containing 15nM MgCl ₂)	1X	1.5
dNTP mix (25mM)	0.8mM	0.2
CYP325A_pUAS_EcoRI_F (10µM)	0.22µM	0.325
CYP325A_pUAS_NdeI_R (10µM)	0.22µM	0.325
Miniprep Template	0.5-1µg	0.5-1.0
dH ₂ O	variable	variable
HotStar Taq Polymerase	1U	0.2
Total Volume		15

PCR product was cleaned and cloned into pJET1.2 blunt, transformed into DH5α, as described previously and screened with the pJET1.2 primers. Positive colonies were minipreped overnight and sequenced on both strands to confirm presence of genes. The minipreps were then double digested with EcoRI and NdeI restriction enzymes using the protocol as described in Table 3.4. Restriction digests were then gel extracted and ligated into pUASattB vector already linearised with same restriction enzymes, overnight and at 16°C as described (Table 14). 4µl of ligation product, a construct of target genes in pUAS vector were transformed into DH5α and screened for positive colonies using the KAPPA PCR

Table 19: List of primers used

Primer	Sequences
CYP325A_pUAS_NdeI_F	<u>GAATTC</u> CATATGAAAAAGACAGCTATCGCG
CYP325A_pUAS_EcoRI_R	<u>GAATTC</u> TCACTGCAAAACATTCGGTCTAC
RPL11_F	CGATCCCTCCATCGGTATCT
RPL11_R	AACCACTTCATGGCATCCTC

EcoRI restriction site in underlined green and NdeI in underlined red

Medium scale plasmid preparation (Midiprep) was carried out using HiSpeed Plasmid Midi Kit (QIAGEN) according to manufacturer's protocol. 5ml TB medium starter culture containing 5µl of 100mg/ml ampicillin, 5µl colony in dH₂O was grown at 37°C and 300rpm for 6 hours. 4ml of the starter was transferred into a 1L flask with 150ml pre-warmed TB medium and 150µl of ampicillin and allowed to grow at 37°C and 220 rpm for 14-16 hours. Bacterial culture was then harvested and divided into three 50ml tubes chilled on ice and centrifuged for 10 mins at 4°C and 5000 rpm. Pellets were minipreped and sequenced to confirm presence of the genes. Midiprep was sent to Genetic Services, MA, USA (<http://www.geneticservices.com/>) for injection into flies. Using PhiC31 system clones were transformed into germ line of a *D. melanogaster* strain carrying the attP40 docking site on chromosome 2 ["y1w67c23; P attP40", "1; 2"]. Four transgenic lines, UAS-CMRCYP325A and UASFANCYP325A were constructed successfully.

2.3.3.3.2 Crossing and Preparation of Flies

GAL4 lines were purchased from Bloomington Stock Centre (<http://flystocks.bio.indiana.edu/>). Ubiquitous expression of candidate genes in the transgenes in adult F₁ progeny (the experimental group) was achieved after crossing homozygote males (UAS line with gene of interest) with virgin females from the driver strain Actin5C-GAL4 ["y [1] w[*]; P(Act5C-GAL4-w)E1/CyO", "1;2"]. For control group, flies with the same background as the experimental group but devoid of the UAS and the candidate genes were crossed with the driver Actin5C-GAL4 lines to generate null-Actin5C-GAL4 lines without insertion. All flies were maintained at 25°C in plastic vials with food.

2.3.3.3.3 Drosophila Insecticides Contact Assay

Insecticide papers (2% permethrin and 0.15% deltamethrin-impregnated) filter papers were prepared in acetone and Dow Corning 556 Silicone Fluid (BDH/Merk, Germany) and kept at 4° C prior to bioassay. These papers were rolled and introduced into 45cc plastic vials. The vials were then plugged with cotton wool soaked in 5% sucrose. 20-25 (2-4 days old post-eclosion females) were selected for the bioassays and introduced into the vials. Mortality plus knockdown was scored after 1 hr, 2hrs, 3hrs, 6hrs, 12hrs and 24hrs post-exposure to the discriminating doses of the insecticides. For each assay, at least six replicates were performed, and t-test was used to carry out statistical analysis of mortality plus knockdown obtained between experimental groups and control.

2.3.3.3.4 qRT-PCR validation of overexpression

To confirm relative expression of the candidate genes in the experimental flies and absence of expression in the control groups qRT-PCR was carried out as described previously (Riveron, Ibrahim, et al., 2014; Riveron et al., 2013). RNA was extracted from three pools of 5 F₁ experimental and control flies separately and cDNA synthesized as described in the section earlier. qPCR for CYP325A was conducted using the qPCR primers given in Table 8, with normalization using the housekeeping gene RPL11 (Table 19). A serial dilution of cDNA was used to establish standard curves for each gene to validate PCR efficiencies of the target and endogenous control(s) and assess quantitative differences between samples. qPCR amplification was carried using MX 3005 real-time PCR system (Agilent Technologies) with Brilliant III Ultra-Fast SYBR® Green qPCR Master Mix. 10ng of cDNA was utilised as a template in a 3-steps thermocycling involving denaturation at 95°C for 3min, followed by 40cycles each of 10seconds at 95°C and 10seconds at 60°C; this is then followed with 1min at 95°C, 30seconds at 55°C and 30seconds 95°C. The relative expression and fold-change of each target gene from the resistant and experimental and control samples was calculated using the comparative CT Method ($2^{-\Delta\Delta C T}$) as described (Schmittgen & Livak, 2008).

2.3.3.4 Comparative assessment of inhibition of CYP325A on pyrethroid resistance in *An. funestus* mosquitoes using RNA interference

Double stranded RNA-mediated interference, one of the so-called RNA-silencing mechanisms, is defined as sequence-specific RNA degradation induced by long double-stranded RNA (dsRNA). RNAi occurs in four basic steps: (i) processing of long dsRNA by RNase III Dicer

into small interfering RNA (siRNA) duplexes, (ii) loading of one of the siRNA strands on an Argonaute protein possessing endonucleolytic activity, (iii) target recognition through siRNA base pairing, and (iv) cleavage of the target by the Argonaute's endonucleolytic activity. This basic pathway diversified and blended with other RNA silencing pathways employing small RNAs. In some organisms, RNAi is extended by an amplification loop employing an RNA-dependent RNA polymerase, which generates secondary siRNAs from targets of primary siRNAs. Given the high specificity of RNAi and its presence in invertebrates, it offers an opportunity for highly selective pest control. This process was done following the updated protocol by (Kouamo et al., 2021).

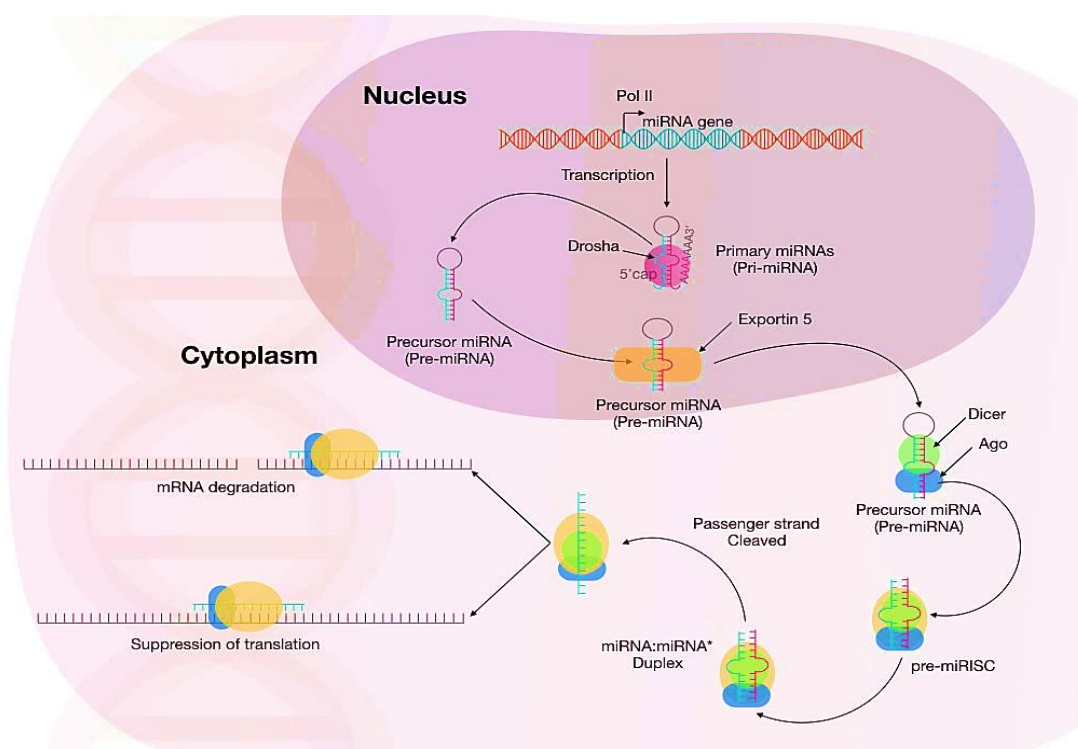


Figure 45: Principle and steps involved in RNA interference of gene expression <https://geneticeducation.co.in/rna-interference-rnai-a-process-of-gene-silencing/>

2.3.3.4.1 Double strand synthesis

Double-stranded RNAs specific to *CYP325A* of interest were synthesized for use in RNAi gene-silencing experiments. Each *CYP325A* oligonucleotide primer was designed using specific cDNA of the corresponding genes downloaded from the Vector Base (<https://vectorbase.org/vectorbase/app>). The T7 RNA polymerase promoter sequence, TAATACGACTCACTATAGGGAGA, was added to the 5' ends of each primer. Specific *CYP325A* fragments were amplified by PCR from plasmid clones using KAPA Taq Kit (Kapa AMELIE WAMBA NDONGMO Regine/Doctorate/Ph.D. Thesis/University of Yaoundé I

Biosystems, Wilmington, MA USA). Double-stranded RNA (dsRNA) was synthesized using in vitro transcription MEGAscript® T7 Kit (Ambion Inc., Austin, TX, USA) and purified using MEGAclear columns (Ambion). The purified products were concentrated by ethanol precipitation and the dsRNA was resuspended in nuclease-free water and stored at -20°C . The successful construction of dsRNA was confirmed by running 3 μL of dsRNA-diluted products in 1.5% agarose gel in a Tris-acetate-EDTA (TAE) buffer (Kouamo et al., 2021).

2.3.3.4.2 Mosquito Injection and Susceptibility Bioassay

To explore the role of CYP325A gene in conferring insecticide resistance, a trial run RNAi was performed on Elende An. funestus population, by injecting sequence-specific dsRNA to 2–3 days old F₁ female mosquitoes, followed by insecticide bioassay. A Nano injector (Nanoinject; Drummond, Burton, OH, USA) was used to inject dsCYP325A into the thorax of 2 to 3 days old female An. funestus mosquitoes as described (Blandin et al., 2002). Briefly, mosquitoes, induced to sleep with CO₂, were injected with 69 nL of either aliquot of above dsCYP325A or dsGFP (control). Four days after injection, four replicates of 20 mosquitoes for each dsRNA were exposed to permethrin (0.75%) for 1 h following the WHO testing protocol. Mosquitoes were transferred to holding tubes after exposure, supplemented with sugar and mortalities counted 24 h after the exposure. The susceptibility test was performed in triplicate with experimental mosquitoes comprising the mosquitoes injected with dsCYP325A above, whereas mosquitoes injected with dsGFP and those not injected were used as controls (Kouamo et al., 2021).

2.3.3.4.3 Quantitative RT-PCR to Confirm the Knockdown Effect

For dsCYP325A-injected and non-injected mosquitoes, RNA was extracted from 3 pools of 5 mosquitoes using TRIzol reagent (Gibco BRL, Gaithersburg, MD, USA). cDNA from each of the three biological replicates was synthesized using the Super-Script III (Invitrogen, Carlsbad, CA, USA) with oligo-dT20 and RNase H, according to the manufacturer's instructions. The cDNA from each replicate treatment was then used to assess the extent of RNAi by measuring levels of gene expression after injection by qRT-PCR. To assess the knockdown efficiency after injection and quantitative difference in the level of CYP325A expression between injected and non-injected mosquitoes, a standard curve of each gene was established using a serial dilution

of cDNA. The qPCR amplification was carried out in a MX3005 real-time PCR system using Brilliant III Ultra-Fast SYBR Green qPCR Master Mix (Agilent, Santa Clara, CA, USA). A total of 10 ng of cDNA from each sample was used as a template in a three-step program involving a denaturation at 95 °C for 3 min followed by 40 cycles of 10 s at 95 °C and 10 s at 60 °C and a last step of 1 min at 95 °C, 30 s at 55 °C and 30 s at 95 °C. The relative expression and fold-change of each target gene were calculated according to the $2^{-\Delta\Delta CT}$ Livak method, comparing expression in specific dsCYP325A-injected samples to non-injected ones, after normalization with the housekeeping genes, RPS7 (AFUN007153) and actin5C (AFUN006819), as described above.

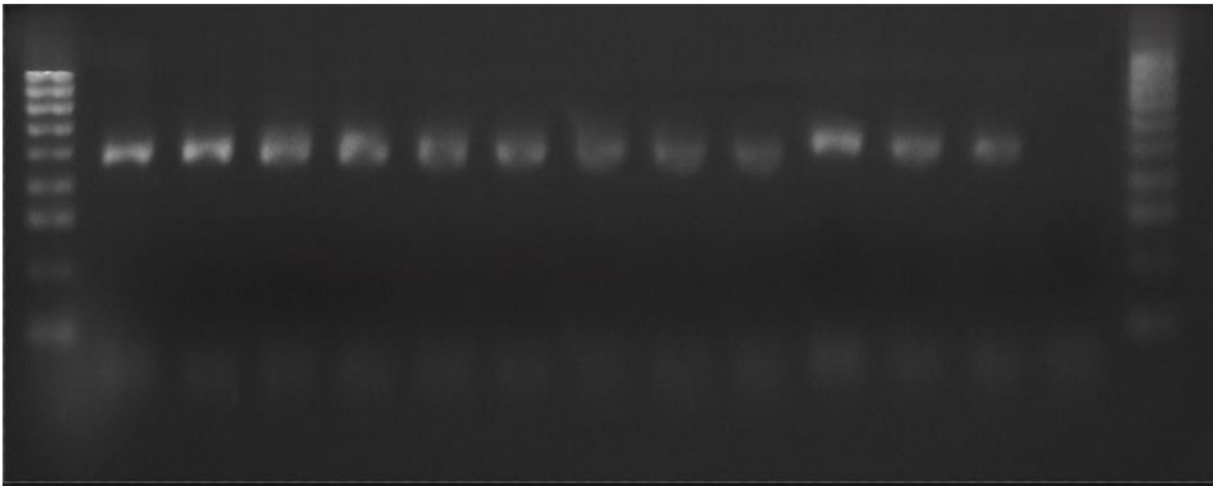
3. RESULTS

3.1 Genomic characterisation of *CYP325A* gene and investigating the role of causative mutations in the promoter region in *An. funestus* field populations across Africa

3.1.1 Mosquito collection and identification

The mosquitoes were all collected by indoor aspiration of resting blood-fed mosquitoes after which morphological identification by microscopy identified them as *Anopheles funestus*. Genomic DNA extracted from individual F₁ mosquitoes was used to perform ID species identification cocktail PCR of the indoor collected F₀ females and confirmed all mosquitoes collected at Mibellon as *An. funestus* s.s.

1kb S1 S2 S3 S4 S5 S6 S7 S8 S9 S10 S11 +ve -ve



Positive *An. funestus* s.s

Figure 46: Agarose gel picture of species identification PCR of the WHO bioassay F1 mosquitoes (S: Sample)

3.1.2 Insecticide resistance profile

The Mibellon *An. funestus* mosquitoes showed very high resistance to pyrethroids, permethrin (28.6% \pm 4.13 mortality rate after 60min and 50% \pm 17.57 mortality rate after 90min), and deltamethrin (16.8% \pm 5.05 mortality rate after 60 min and 52.3% \pm 8.3 mortality rate after 90min) (Figure 47A). Pre-exposure of mosquitoes to PBO restored partial susceptibility to both pyrethroids (mortality = 98.8% \pm 3.77 for permethrin and 96.5% \pm 1.16 for deltamethrin after 60min exposure) (Figure 47B), suggesting the role of cytochrome P450s resistance to

pyrethroids in this population. The mortality rate was significantly higher in PBO + permethrin (Mortality= 29%, $X^2 = 106.34$, $p < 0.00001$) and PBO + deltamethrin (Mortality = 17%, $X^2 = 130.56$, $p < 0.00001$). compared to permethrin and deltamethrin.

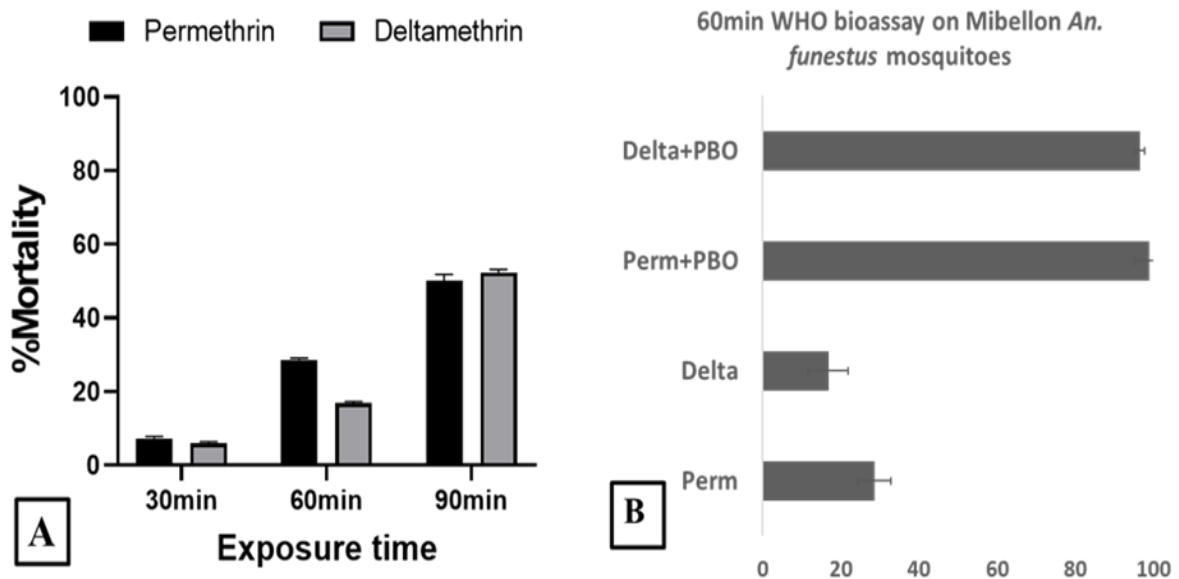


Figure 47: Susceptibility profile of *An. funestus* mosquitoes to insecticide.

A. Recorded mortalities following 30 min, 60 min, and 90 min exposure of *An. funestus* s.s. from Mibellon to different insecticides **B.** Activities of PBO combined to permethrin and deltamethrin on *An. funestus* s.s. from Mibellon, Cameroon

3.1.3 DNA and RNA extraction, cDNA synthesis, purification, and quality assessment

The RNA extraction produced was of good quality from which cDNA was synthesized and used for cloning as well as qRT-PCR. The genomic DNA extracted was also of good quality and used for species identification PCR and amplification of the putative promoter of *CYP325A*. Quality assessment was done with Nanodrop poly-analyser where the quality of 1.8 – 2 was accepted for good RNA.

3.1.4 Amplification of *CYP325A* cDNA and 1kb putative promoter region

CYP325A gene was successfully amplified by Phusion Taq PCR from the cDNA synthesized from Cameroon, DRC, Ghana, Benin, Malawi, Uganda, FANG, and FUMOZ. The bands on the agarose gel for successful amplification were at approximately 1.5kb as shown in Figure.

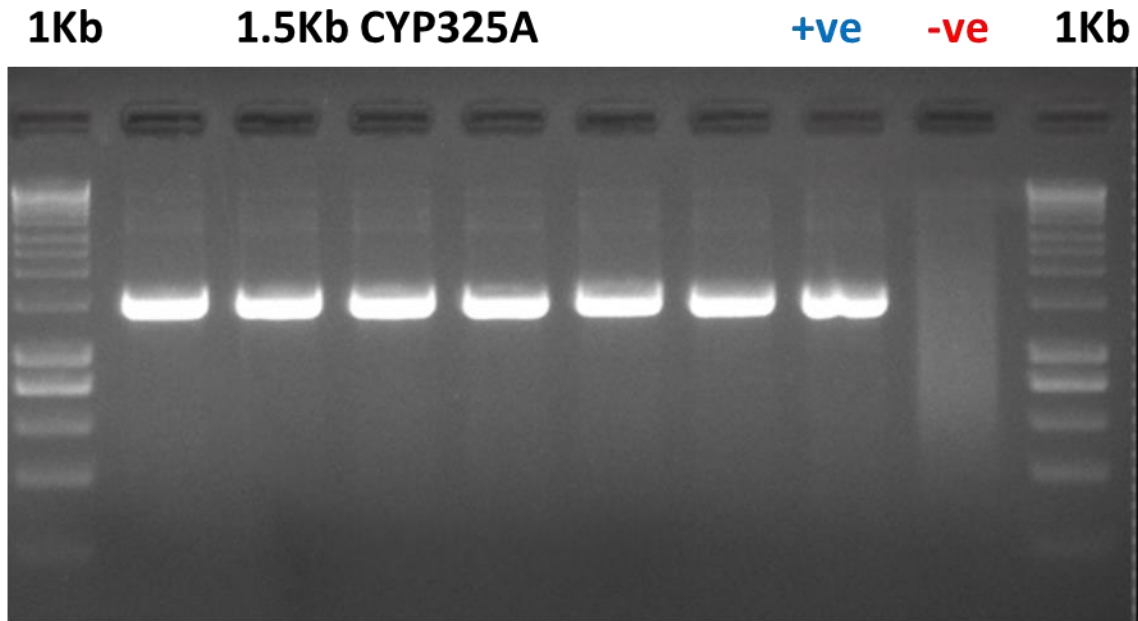


Figure 48: Phusion Taq Polymerase amplification of *CYP325A* gene. Amplification band at 1.5kb and no band in the negative control.

From the genomic DNA extracted from permethrin-exposed dead and alive mosquitoes from Mibellon, Cameroon, the 1kb putative promoter was successfully amplified through Phusion Taq PCR with a band at 1kb on the agarose gel.

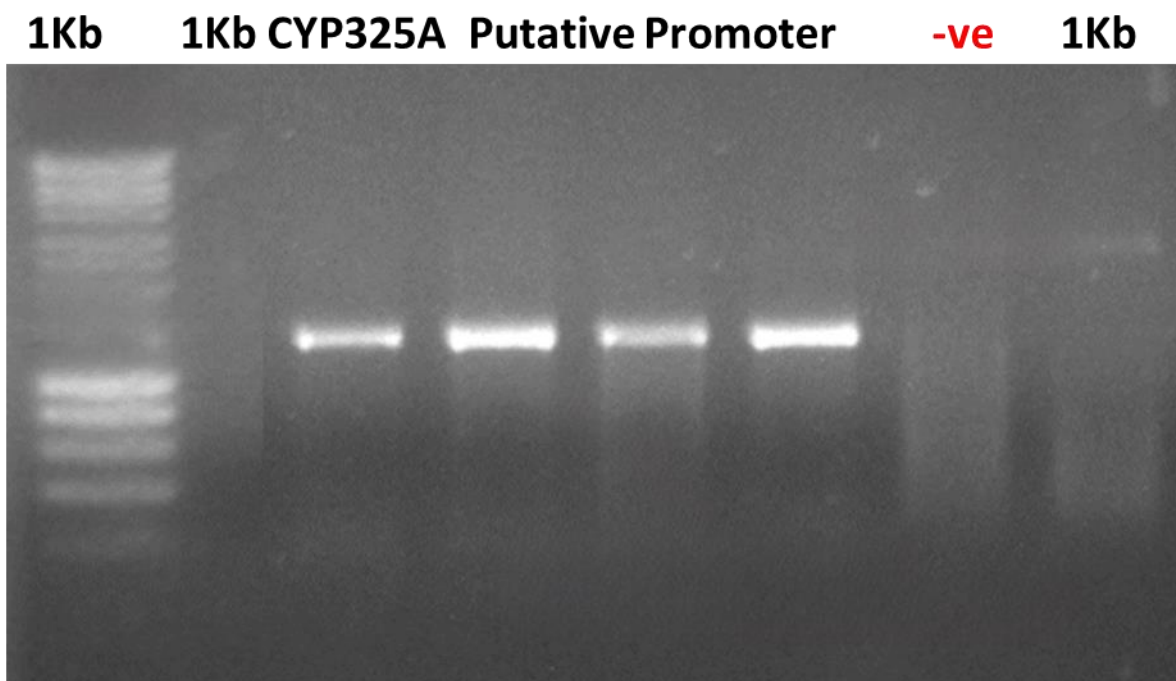


Figure 49: Phusion Taq Polymerase amplification of *CYP325A* 1kb putative promoter. Amplification band at 1kb and no band in the negative control.

Amplification with Phusion Taq polymerase yields PCR product with blunt ends which facilitates the cloning process into PJET carrier plasmid as there will be fewer complications associated with the blunting step.

3.1.5 Cloning into PJET to produce recombinant plasmid

The PCR products were purified using the Qiagen purification kit after which the quality and quantity of DNA were assessed using Nanodrop. Products with 20-25ng/μl from all localities of interest were successfully cloned into PJET carrier plasmid and transformed into DH5α competent cells. Positive colonies after screening were cultured to multiply the plasmid for harvesting and purification using the miniprep purification technique. Miniprep quality and quantity were read and those with over 100 ng/μl were sent for sequencing forward and reverse with PJET primers.

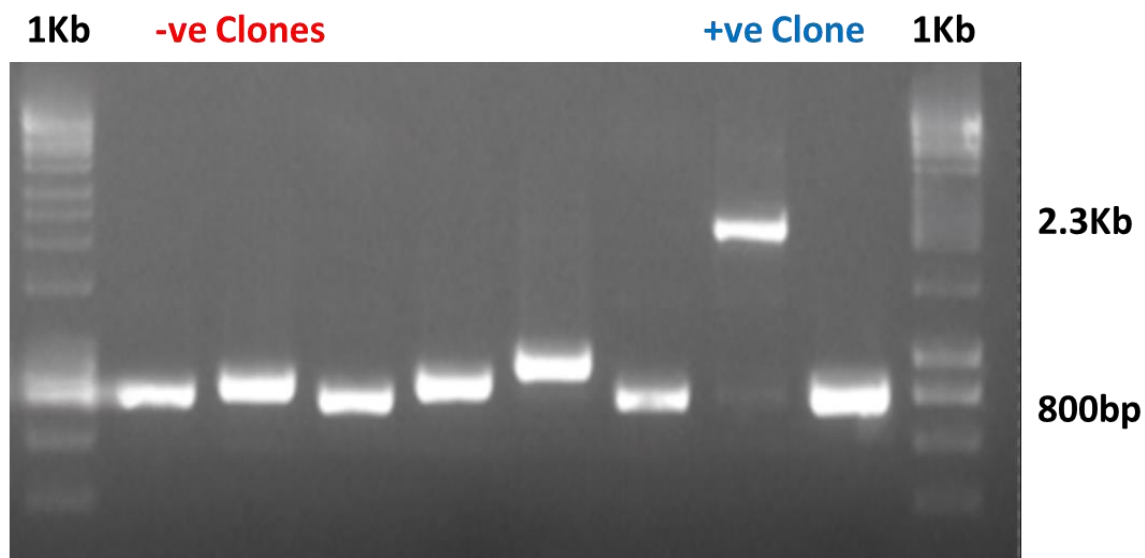


Figure 50: Kapa Taq Polymerase colony screening PCR of positive colonies with *CYP325A* insert. S: sample of PCR product.. Positive colonies have an amplification band at 2.3kb and negative colonies have a band at 800bp.

3.1.6 SANGER sequencing results

For each locality of interest, eight recombinant plasmids of *CYP325A* were aliquoted and sent for sequencing at GENEWIZ from Azenta Life Sciences. The raw sequences obtained were constructed and aligned using BioEdit. Sequences from Cameroon, FUMOZ, Uganda, Malawi, DRC, and Benin were 1532bp corresponding to the normal size of *CYP325A* cDNA. However, the sequences from FANG and Ghana were longer at 1800bp due to the intron-retention

phenomenon (Figure 50). It was confirmed by alignment with genomic DNA of *CYP325A* that the cDNA sequences from Ghana and FANG had retained all three introns of this gene. As a result, it was hypothesized that this phenomenon could be linked to the downregulation of this gene when unneeded. This hypothesis suggests that *CYP325A* is active in any native form it is secreted in as long as it doesn't retain the intron which leads to nonsense-mediated decay (NMD) and inactivity of the gene. The full alignment of the sequences highlighting all three introns retained is shown in appendix x.

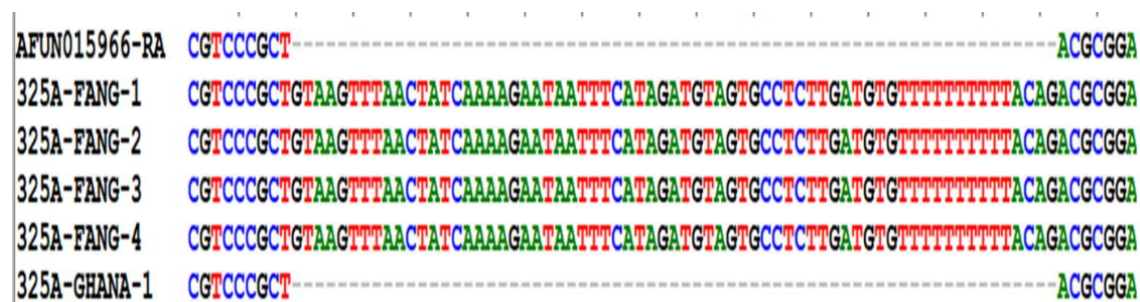


Figure 51: Intron retention example of FANG sequences compared to *CYP325A* template and Ghana sequences

In this data set, three mutations were found to be present in the resistant alleles from the Central African region compared with the susceptible FANG (Table 20). Polymorphic positions of these mutations in DNA sequences of *CYP325A*, country of origin, amino acid changes, its location in the protein sequence, and possible impact on enzyme activity are outlined in the table below.

Table 20: Nucleotide polymorphisms and amino acid substitutions between resistant alleles compared with FANG.

Amino acid substitution	Mutation	Location and potential impact
Ala ⁹¹ Ser	91:A>S	Possibly located within the hydrophobic region of the endoplasmic reticulum membrane (α B loop)
Glu ¹³ Thr	13:E>T	Found at start of the protein and possibly in the signal peptide region
Gln ¹²³ Lys	123:Q>K	SRS1 and such a mutation could influence enzyme substrate affinity

Tyr ⁷⁷ Ser	77:Y>S	Between the α A and β B loops and could influence folding of the protein
His ⁵⁶ Pro	56:H>P	Start of protein so could influence signal peptide sequence

3.1.7 Transcriptomic profile of *CYP325A* as a pyrethroid resistance gene

RNAseq data from previous studies conducted on pyrethroid-based resistance in *Anopheles funestus* across Africa already implicated a good number of overexpressed cytochrome P450s amongst which *CYP325A* and *CYP6P5* were overexpressed in Cameroon.

Present pattern of some overexpressed CYP genes in pyrethroid-resistant *An. funestus* mosquitoes from across Africa.

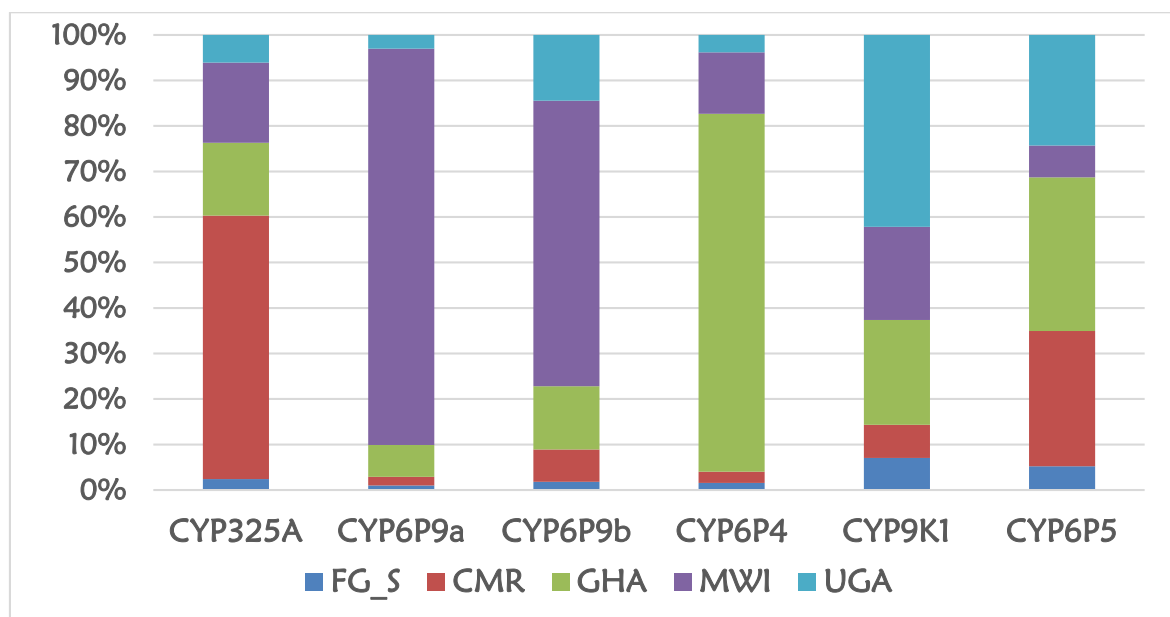


Figure 52: Expression patterns of some overexpressed CYP genes implicated in pyrethroid-based resistance across Africa.

Legend: FG: FANG, CMR: Cameroon, GHA: Ghana, MWI: Malawi and UGA: Uganda

Several studies previously conducted have shown that these overexpressed genes are circumscribed to different regions of Africa. This is the case of *CYP6P9a/b* in the southern African region, *CYP9K1* in East Africa, and *CYP6P4* in West Africa. In the central African

region, we observe a marked overexpression of two CYP gene: *CYP325A* and *CYP6P5* which could be major drivers of metabolic resistance in this region.

The RNAseq results for *CYP325A* gene which showed high overexpression of this gene have been previously published (14) and were confirmed using quantitative real-time PCR (qRT-PCR), with a significant correlation observed between the control and the permethrin-exposed, deltamethrin-exposed, DDT-exposed, and bendiocarb-exposed mosquitoes from across Africa. Permethrin-resistant mosquitoes significantly overexpressed *CYP325A* as compared to the control with $p < 0.05$ (Figure 52) as compared to deltamethrin-exposed mosquitoes.

3.1.8 Comparative investigation of the expression profile of *CYP325A* Africa-wide by qRT-PCR

qRT-PCR confirmed the overexpression of *CYP325A* in Central Africa Cameroon with a fold-change of ~45 in permethrin resistant mosquitoes. In contrast, the expression level was low in other regions of Africa, for example, the southern region (Malawi), East (Uganda), and West Africa (Ghana and Benin), with fold changes < 5 in line with prior RNA-Seq analyses (Mugenzi et al., 2019). Moreover, a greater over-expression of *CYP325A* was observed in Cameroon mosquitoes that survived exposure to permethrin than in those not exposed to insecticide (control) ($p < 0.05$) (Figure 53).

Validation of *CYP325A* expression across Africa with qRT-PCR

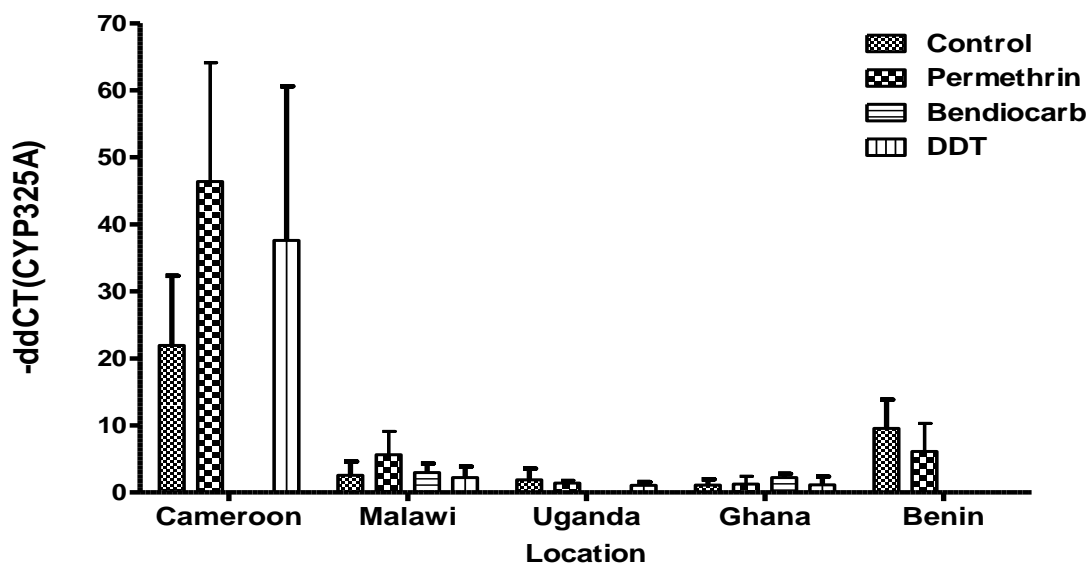


Figure 53: Differential expression of *CYP325A* in the *An. funestus* s.s. Mibellon population in Cameroon.

Measured by qRT-PCR. * $p < 0.05$, ** $p < 0.01$ and *** $p < 0.001$, $X^2 = 14.245$. The p -value is .00016 and significant at a p -value $p < 0.05$.

3.1.9. Detection of transcripts presenting a similar expression pattern to *CYP325A* in *An. funestus* populations

1. STRAND NGS software, version 3.4 (Strand Life Sciences, Bangalore, India) was used to detect the list of entities (transcripts) exhibiting a similar expression pattern to *CYP325A* and likely to be involved in the same molecular pathway. AFUN015966 (*CYP325A*) was selected in the permethrin-resistant samples and criteria of similarity index of > 0.7 was set comparing expression in mosquitoes resistant to permethrin, resistant to DDT, control mosquitoes not exposed to insecticides in Cameroon and the FANG susceptible strain. A total of 148 transcripts were found to have an index of similarity of > 0.7 with *CYP325A*. Among these, detoxification genes were detected including cytochrome P450s, glutathione S-transferases (GSTs), and ABC transporters. Among P450s, *CYP6P5* had the highest similarity expression to *CYP325A* [Similarity Index (SI) = 0.8] followed by *CYP6P9b* (SI = 0.73). The GSTs included *GSTe2* (SI = 0.75) and *GSTe6* (SI = 0.74). Two transcription factors also presented a similar expression pattern to *CYP325A*, notably CCAAT/enhancer-binding protein gamma (SI = 0.78) and transcription factor Adf-1 both known to bind to the promoter and the enhancer regions of target genes. The list also includes other genes such as serine proteases (Trypsin and Chymotrypsin 2), an ABC transporter (AFUN019220), and two microRNAs (mir-279 and mir-71).

Table 21: Similarly expressed entities to *CYP325A* and associated function

Entity	Similarity Index (SI)	Role
CYP6P5	0.8	Cytochrome P450
CYP6P9b	0.73	Cytochrome P450
GSTe2	0.75	Glutathione-S-transferase epsilon
GSTe6	0.74	Glutathione-S-transferase epsilon
CCAAT/enhancer binding protein gamma	0.78	Transcription factor

Adf-1	-	Transcription factor
Trypsin	-	Serine protease
Chymotrypsin 2	-	Serine protease
AFUN019220	-	ABC transporter
Mir-279	-	Mitochondrial RNA
Mir-71	-	Mitochondrial RNA

3.1.10 Gene Ontology Enrichment Analysis

A Gene Ontology (GO) enrichment analysis of the list of the 148 similarly expressed genes to *CYP325A* revealed an over-representation of 10 GO terms (Figure 1D) reflecting the function of those transcripts including detoxification (haem binding, tetrapyrrole binding) and serine protease activity (serine-type endopeptidase activity, serine hydrolase activity, proteolysis).

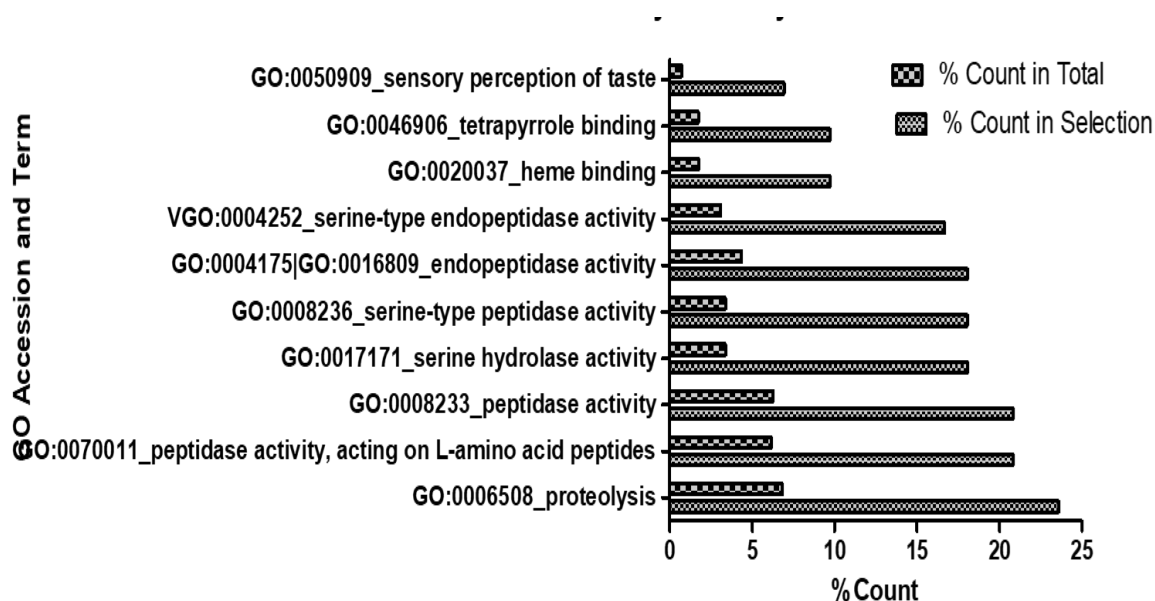


Figure 54: Gene ontology (GO) for *CYP325A* entity similarity

3.1.11 Whole genome PoolSeq analysis of selective sweep across *CYP325A*

Analyses of whole-genome PoolSeq sequences from 12 populations across Africa revealed that diversity estimates of each site type were no different between Cameroon and other populations (Figure S4). By contrast, a very clear decrease was seen in diversity in Uganda, for *CYP9K1* and in Southern African populations, and the FUMOZ resistant strain for *CYP6P9a* and *CYP6P9b*. Inspection of reading alignments in IGV did not reveal any difference between

Cameroon and other populations across the region inspected. Analyses from the Poolseq signatures revealed that diversity estimates of each site type were no different between Cameroon and other populations (Supplementary files Table 3). By contrast, we see very clear decreases in diversity in Uganda for *CYP9K1* and in Southern African populations and the FUMOZ resistant strain for *CYP6P9a* and *CYP6P9b*. Inspection of read alignments in IGV did not reveal any difference between Cameroon and other populations across the region inspected.

3.1.12 Polymorphism analysis of genetic diversity of *CYP325A* cDNA from across Africa

Screening for the genetic variability of *CYP325A* cDNA for 9 clones for FUMOZ, 6 clones for FANG, 8 clones for DRC Congo, and 16 clones for Cameroon revealed a high polymorphism of this gene, with an average of 9 polymorphic sites for each sample and 6 amino acid changes observed in total. Cameroon samples had a reduced variation in *CYP325A* when compared to the other localities with 2 haplotypes and 5 amino acid changes while samples from DRC were the most polymorphic. Tajima's D was negative for all the populations but only significant for Cameroon and FUMOZ indicating a possible recent selective sweep or a purifying selection. This is reflected in the presence of a major clade for the Cameroon samples in the maximum likelihood phylogenetic tree (Figure 55).

Table 22: Genetic parameters of *CYP325A* in laboratory and field population

Complete sequenced fragment (1512bp)												
Sample	n	S	h	Hd	Syn	Nsyn	π	D	D*	Ka	ks	Ka/ks
FUMOZ	9	13	3	0.417	5	8	0.194	-1.88947 *	-2.14486 **	0.154	0.314	0.49
FANG	7	5	2	0.286	1	4	0.094	-1.48614ns	-1.56696ns	0.099	0.081	1.22
Congo DRC	8	9	4	0.643	4	5	0.162	-1.47121 ns	-1.51047 ns	0.124	0.282	0.43
Cameroon	16	10	2	0.125	5	5	0.083	-2.18261 **	-2.98819 **	0.054	0.177	0.31
All	40	49	9	0.746	n.a	n.a	0.801	0.18277ns	-0.99808ns	0.473	1.929	0.24

N= number of sequences; S, number of polymorphic sites; Syn, Synonymous mutations; Nsyn, Non-synonymous mutations; π , nucleotide diversity; D and D* Tajima's and Fu and Li's statistics; ns, not significant; π , ka and ks are multiplied by 102, *=P < 0.05; **=P < 0.02, n.a not applicable

The significantly reduced diversity in the Cameroon cDNA sequences highlight an ongoing selection which can be clearly seen in the clustering of the Cameroon sequences shown in yellow in Figure 55 below. This clustering also highlights a polymorphism in the alignment that

is almost fixed in the Cameroon sequences but only starting in the DRC sequences. This observation suggests a directional flow of this mutation within Central Africa flowing from Cameroon to DRC.

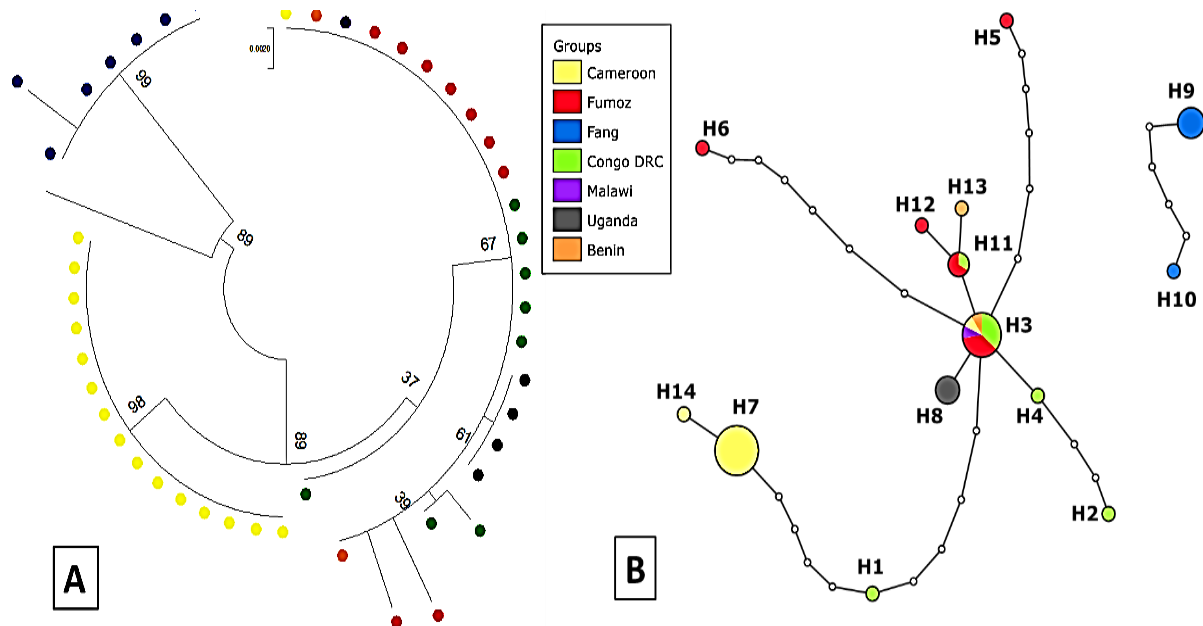


Figure 55: Population studies of *CYP325A* coding and upstream putative promoter across Africa. A. Phylogenetic tree for *CYP325A* cDNA across Africa. B. Haplotype diversity network of *CYP325A* cDNA for FANG, FUMOZ, Cameroon, Malawi, Benin, Uganda, and DRC.

Further analyses of the nucleotide and amino acid diversity in the cDNA sequences from across Africa revealed a single nucleotide polymorphism (SNP) in the Cameroon and DRC sequences G991C translated into an E331Q amino acid substitution. This SNP has a high frequency of 94% in the Cameroon sequences but only 12.5% in the DRC sequences.

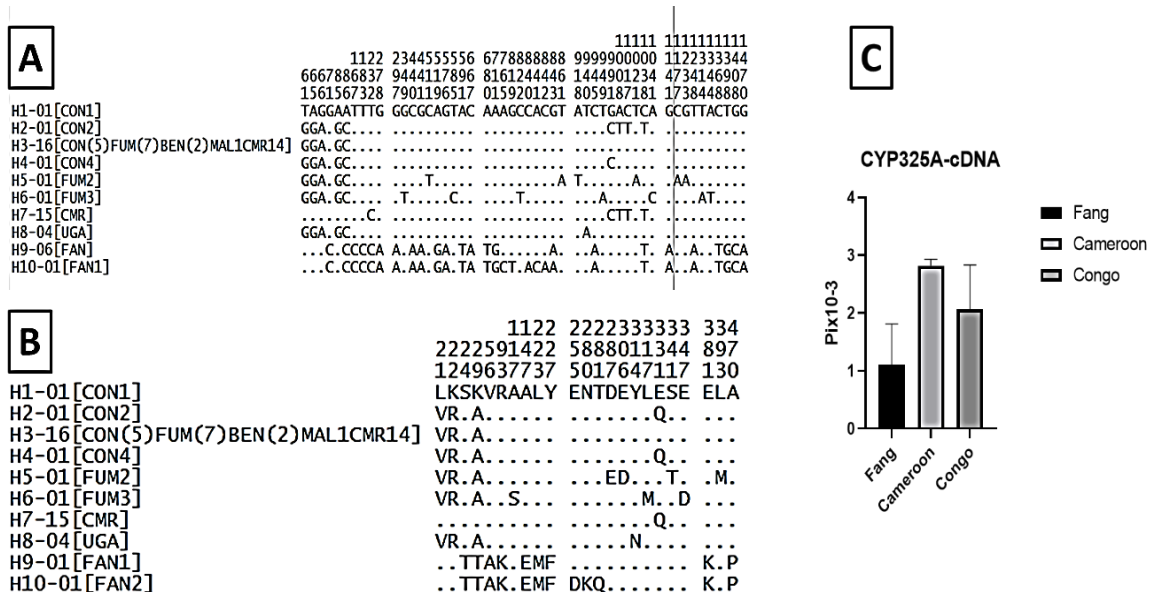


Figure 56: Genetic diversity of *CYP325A* cDNA.

A. Nucleotide diversity for *CYP325A* cDNA sequences. B. Nucleotide diversity for *CYP325A* cDNA sequences

3.1.13 Polymorphism analysis of 1kb 5'UTR region.

To further study the polymorphism patterns with insecticide selection, *An. funestus* mosquitoes from Mibellon, Cameroon exposed to permethrin were used to establish the polymorphism patterns of a 1kb promoter region upstream of the 5'-UTR of *CYP325A*. The results revealed differences between the alive and dead (Table 23).

Table 23: Genetic parameters of 1 kb 5'UTR region *CYP325A* upstream region between Permethrin alive and dead samples.

Sample	n	S	h	Hd	π	D	D*
Alive	15	13	3	0.448	0.448	0.67629 ns	1.47811 **
Dead	19	46	8	0.725	1.307	-0.09242 ns	-0.17703 ns
All	34	48	10	0.617	0.00975	-0.66073 ns	-0.35501 ns

n= number of sequences; S, the number of polymorphic sites; Syn, Synonymous mutations; Nsyn, Non-synonymous mutations; π , nucleotide diversity; D and D* Tajima's and Fu and Li's statistics; ns, not significant; π is multiplied by 102, **=P < 0.01

Analysis of the upstream region (1kb) revealed reduced diversity in the resistant samples compared to the susceptible indicated by a lower number of haplotypes (3 vs 8) and polymorphic sites (13 vs 46). The resistant samples/alive had a positive Fu and Li indicating an excess of singletons. Exploring the haplotype network (Figure 57A) and phylogenetic tree (figure 57B) showed that major haplotype (H1) was shared between the alive and dead with some haplotypes only specific to the resistant (H2 and H3) and susceptible (H4, H5, H6, H7, H8, and H10).

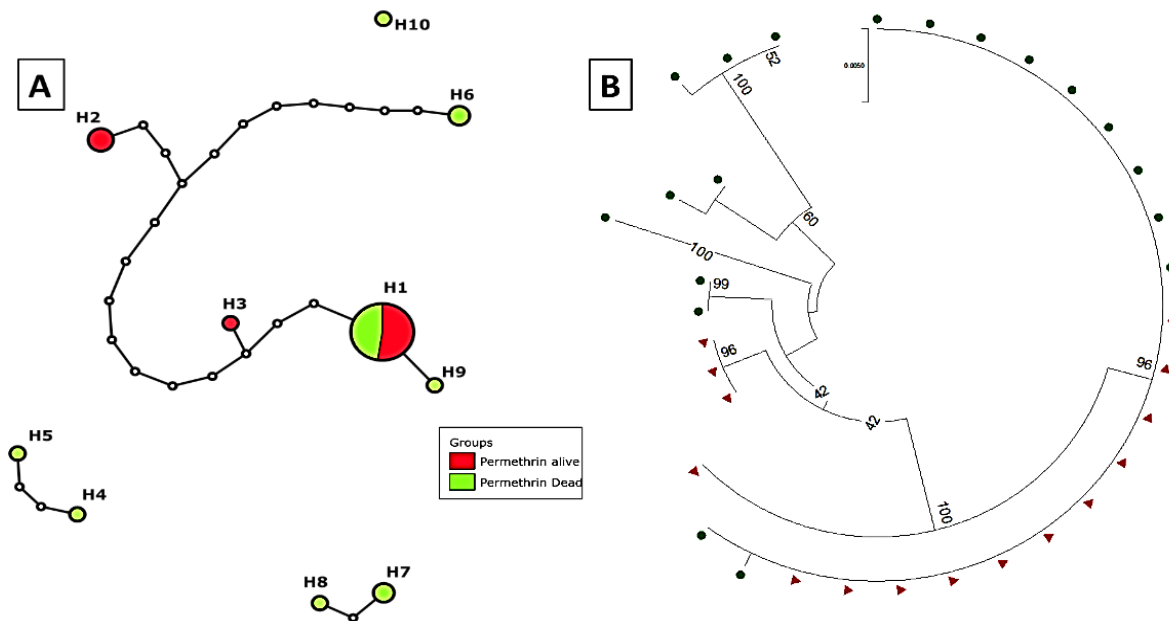


Figure 57: Haplotype network and phylogenetic tree of putative promoter sequences for permethrin dead and alive

A. Haplotype diversity network analysis of the upstream region of *CYP325A* between permethrin alive and dead samples, B. Phylogenetic tree of the upstream region of *CYP325A* between permethrin alive and dead samples revealing a dominant haplotype being shared between the resistant and the susceptible.

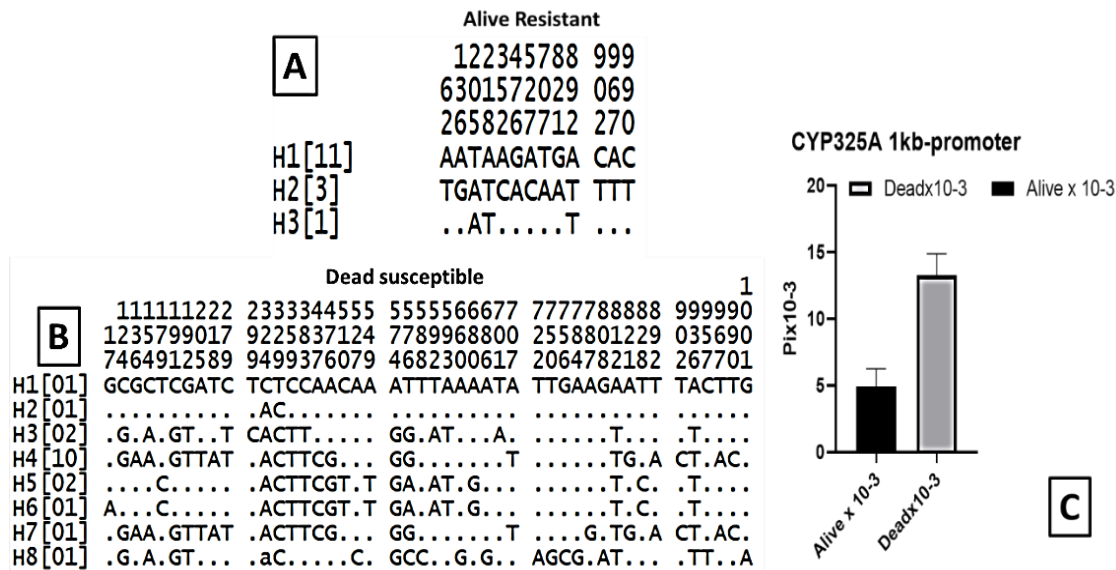


Figure 58: Genetic diversity of the 1kb putative promoter

(A) Nucleotide diversity for *CYP325A* cDNA sequences. (B) Nucleotide diversity for *CYP325A* cDNA sequences. (C) Haplotype diversity ratio of *CYP325A* cDNA for FANG, Cameroon, and Congo.

3.1.14 Amino Acid Sequence Characterisation of *An. funestus CYP325A*

3.1.14.1 With other closely related mosquito species to *An. funestus*

To assess how conserved *CYP325A* is across strains, a comparison of *An. funestus CYP325A* to other closely related sequences revealed it is 72.8% identical to its ortholog *An. gambiae CYP325A* (AGAP002208) (GenBank: AAN05727.1), 74.8% identical to *An. epiroticus CYP325A* (AEPI000241) and 81.9% identical to *An. stephensi CYP325A* (ASTE004501) (Supplementary files Figure 4). Apart from *An. epiroticus CYP325A* (499 amino acids) and *An. gambiae CYP325A* (505 amino acids), the other two P450s are made of 503 amino acids. Sequence-to-sequence mapping reveals that the WxxxR motif, the signatory oxygen-binding pocket (AGFETS)/proton transfer groove, the ExxR motif which stabilises the haem structural core, the cysteine pocket/haem-binding region (PFxxGxxxCxG), which forms the fifth axial ligand to the haem iron were all identical and conserved in the three different Anopheles sequences. Major sequence variations which could impact the activity of *An. funestus CYP325A* compared with *An. gambiae CYP325A* were observed in all the SRS and helices except α K helix and the substrate recognition site 2 (SRS-2). In the meander at positions 424 and 425, amino acid variations were observed S424Q in *An. epiroticus* and S424A in *An. gambiae*. The

conservation of this gene could suggest that its detoxification function was retained even after speciation.

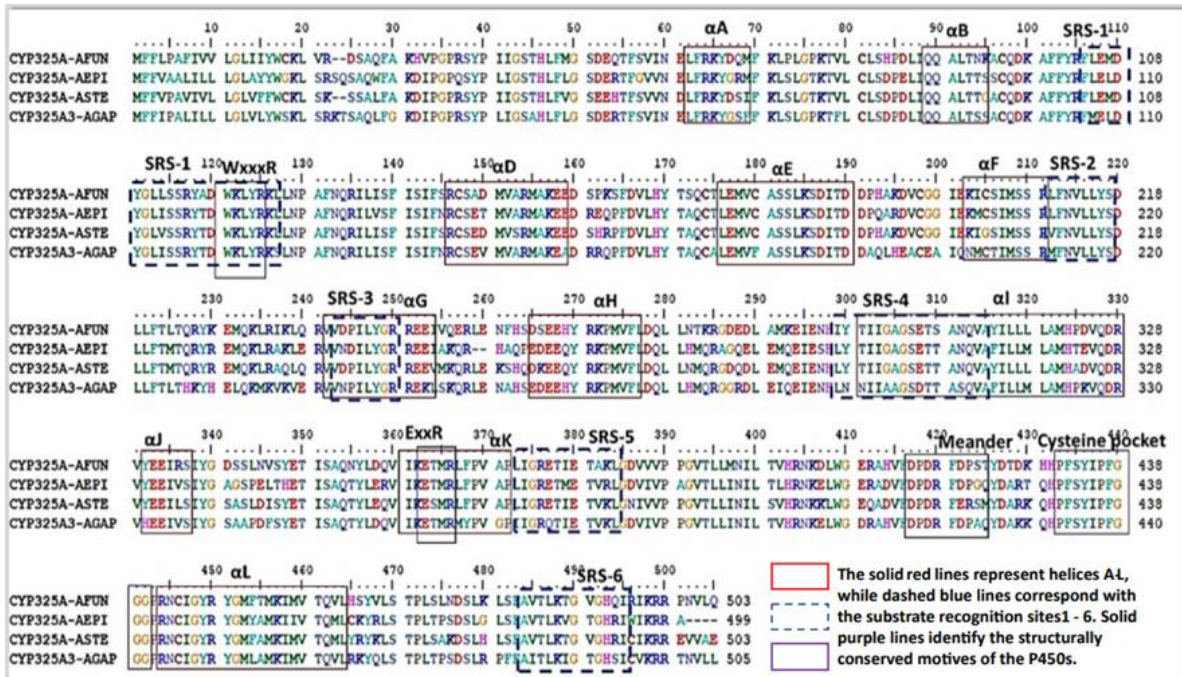


Figure 59: Comparison of *An. funestus* CYP325A amino acid sequences with orthologs from *An. gambiae*, *An. epiroticus* and *An. stephensi*.

The solid, red lines represent helices A-L, while dashed blue lines correspond to the substrate recognition sites 1-6. Solid purple lines identified the structurally conserved motifs of the P450s. Variable residues are highlighted in pink. (For interpretation of the references to colour in this figure legend, the reader is referred to the web version of this article).

3.1.14.2 Between Cameroon and DRC alleles

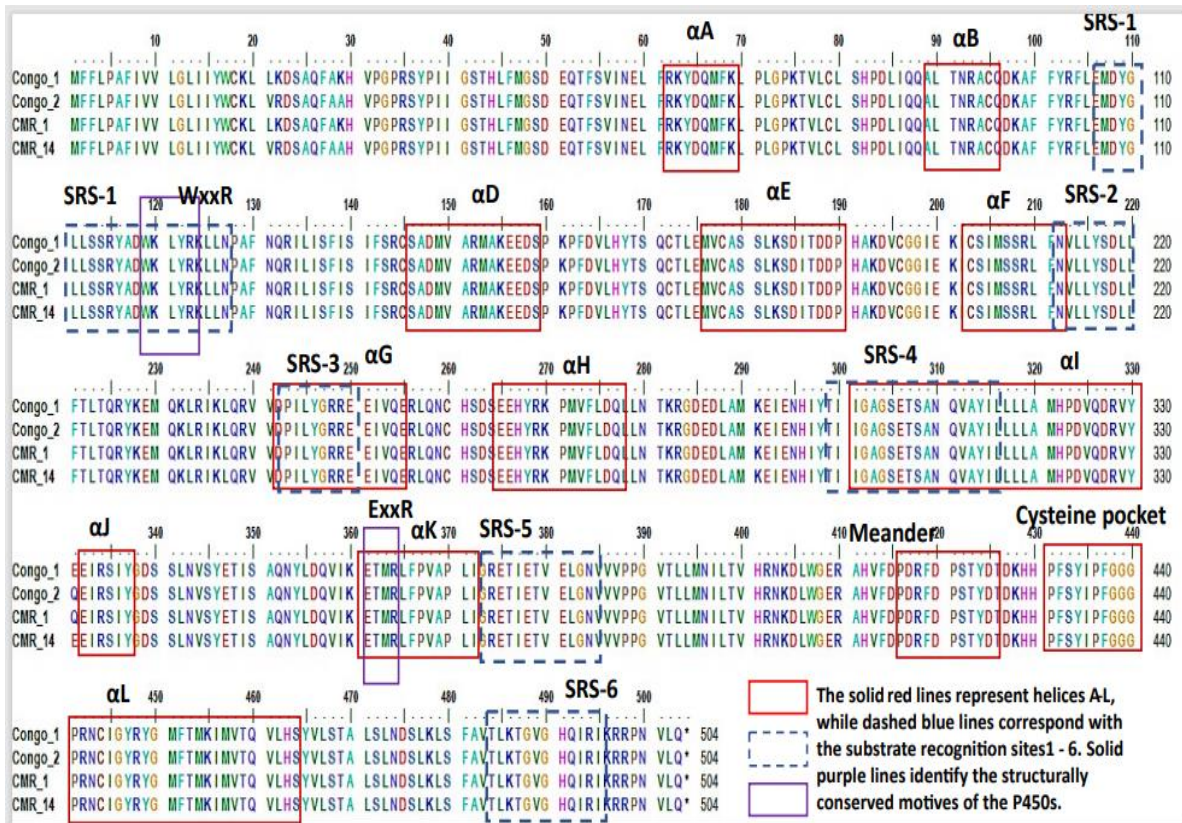


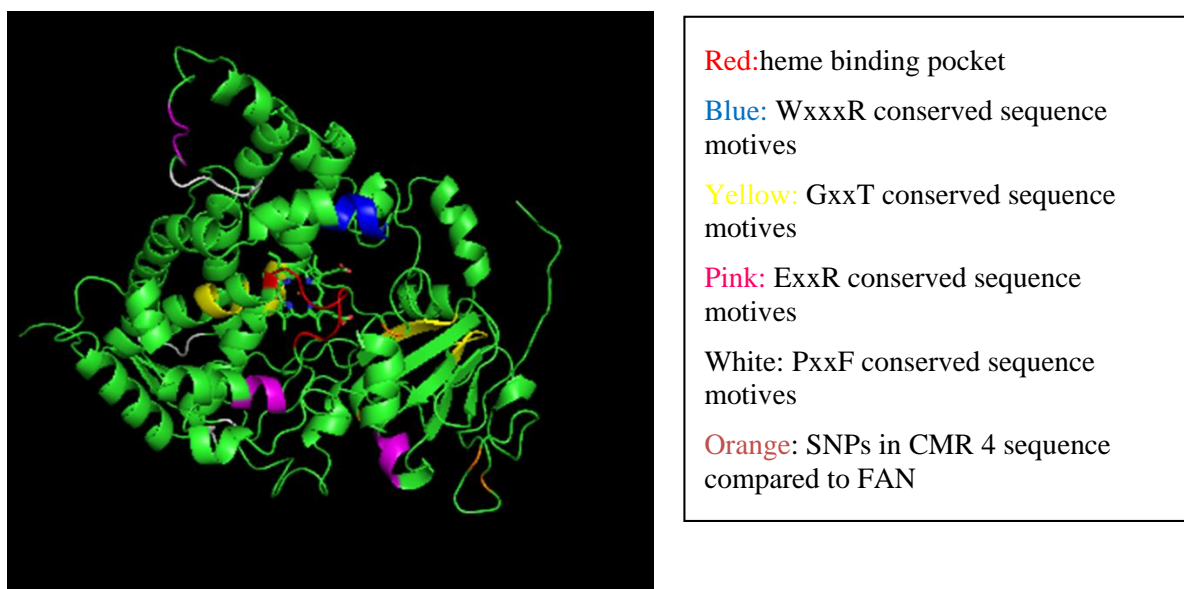
Figure 60: Comparison of *An. funestus* CYP325A amino acid sequences from Cameroon and DRC alleles.

The solid, red lines represent helices A-L, while dashed blue lines correspond to the substrate recognition sites 1-6. Solid purple lines identified the structurally conserved motifs of the P450s. Variable residues are highlighted in pink.

3.2 Perform a polymorphism survey, homology modelling, and molecular docking (in silico studies) of *CYP325A* with major classes of insecticides

3.2.1 3-D model construction of *CYP325A* alleles

3-D models of selected alleles of *CYP325A* were constructed using PyMol software to analyse the conserved regions of P450s between alleles. PyMOL is a cross-platform molecular graphics tool, widely used for three-dimensional (3D) visualization of proteins, nucleic acids, small molecules, electron densities, surfaces, and trajectories. It is also capable of editing molecules, ray tracing, and making movies. PyMOL is one of the few open-source model visualization tools available for use in structural biology. The Py part of the software's name refers to the program having been written in the programming language Python.



Legend: W: Tryptophane, R: Arginine, G: Glycine, T: Threonine, P: Proline, F: Phenylalanine, E: Glutamic acid.

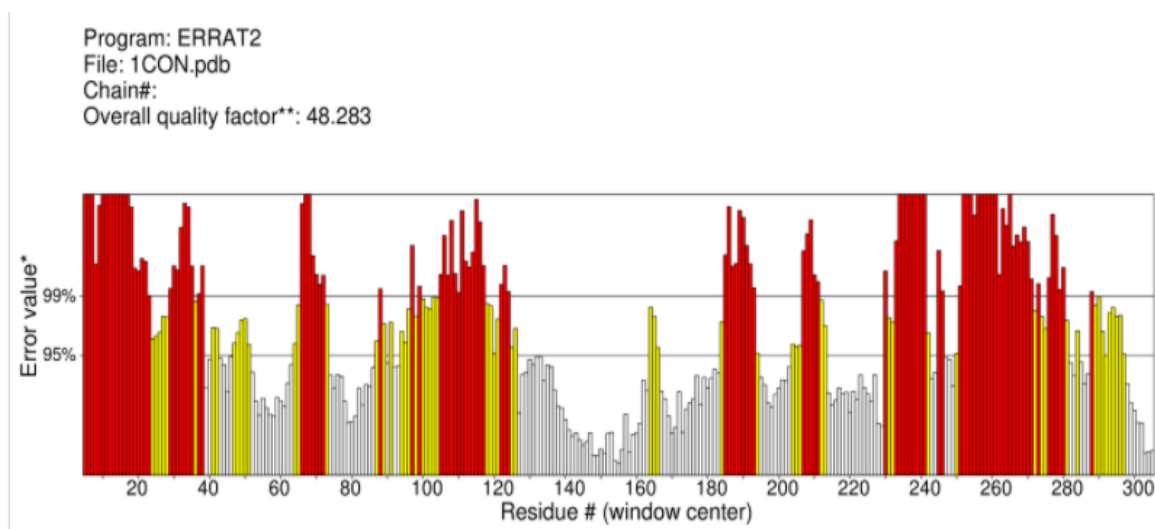
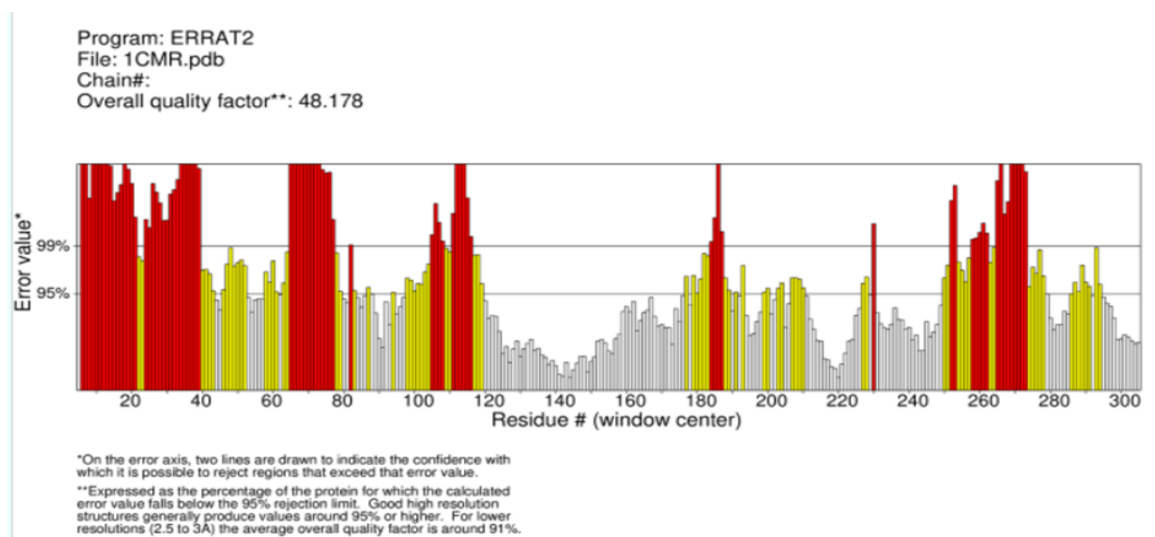
Figure 61: 3-D structural model of *CYP325A* cDNA constructed and viewed in PyMol software

Permethrin is rapidly metabolized by ester hydrolysis to inactive metabolites which are excreted primarily in the urine the cis isomer is more stable than the trans isomer, and the cis isomer yielded four faecal ester metabolites which resulted from hydroxylation at the 2'- and 4'- positions of the phenoxy group, at the trans- methyl group, and at both two latter sites. The ester-cleaved metabolites were extensively excreted into the urine, whereas the metabolites retaining ester linkage were found only in the faeces.

3.2.2 Modelling and Molecular Docking Simulation Analyses

3.2.2.1 Model production and assessment

CYP325A models were generated with haem already in place and verification with Errat v3.0 indicated that the models have reasonably good scores with the highest overall quality factor obtained for XXXCYP325A and YYYCYP325A models (Appendix x). Some regions of high disorderliness (backbone deviated from the crystal structure of the template used) shown in black (Figure x) include amino acids 20-40 corresponding to the hydrophobic terminal domains that anchor the P450 to the surface of the membrane and residues preceding the αA helix, amino acids 60 – 120 encapsulating αA helix, $\beta 1-1$, $\beta 1-2$, αB helix and $\beta 1-5$ containing the putative SRS1, amino acids 280 – 300 corresponding to the loop joining the C-terminal of αH to the N-terminus of αI .



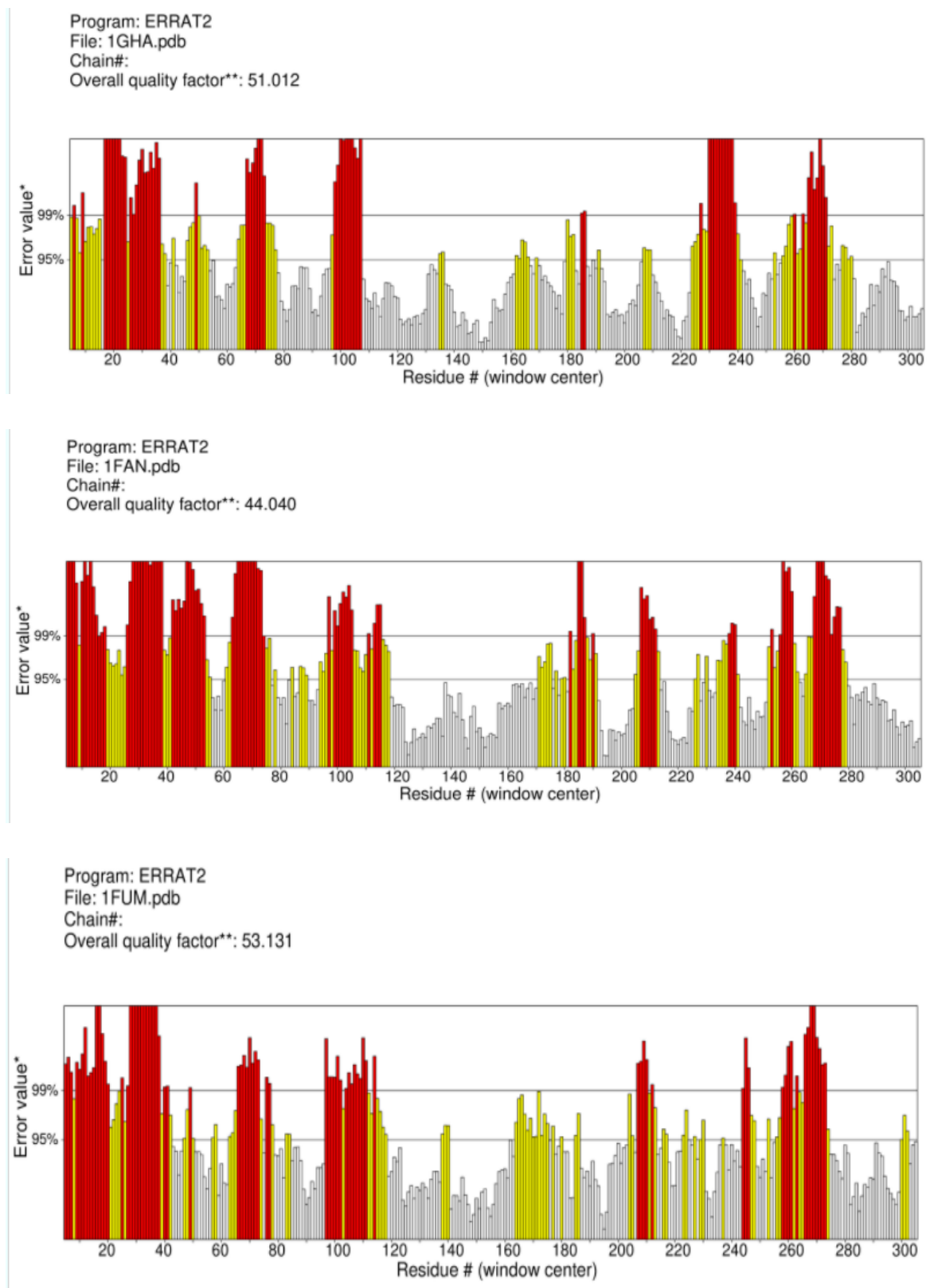


Figure 62: Errat plot for the lowest energy model.

Disordered regions are identified on the error axis*, where 2 lines are drawn to indicate the confidence with which it is possible to reject the regions that exceed the error value. The Overall

AMELIE WAMBA NDONGMO Regine/Doctorate/Ph.D. Thesis/University of Yaoundé I

Quality Factor represents the percentage of the protein within which the error value is below the 95% rejection limit as given in Appendix 2.2. A and B are plots from CMRCYP325A and FANCYP325A models, while C and D represent plots of models of FUMCYP325A and CONCYP325A.

Regions with the high disorder (backbone deviation from the folding pattern of the template) in CYP325A models (Figures C and D) include amino acids 10-40 corresponding to the sequences that constitute the hydrophobic membrane anchor, amino acids 70 – 90 corresponding to β 1-1 and β 1-2, amino acids 110-120 mapped to β 1-5 containing the putative SRS1, as well as amino acids 195 – 220 which corresponds to the F-G loop. Some models exhibited lesser backbone deviation than others though they were created with the same 1TQN template which shares 32% and 33% identity respectively.

3.2.2.2 Molecular Docking Simulations

The binding energy of a ligand is defined as the difference in free energy of the protein plus the unbound ligand, and their complex; ChemScore estimates the total free energy change that occurs on the ligand binding (Jones et al., 1997). Docking scores along with other relevant regression terms for binding of insecticide structure to *CYP325A* models are given in Tables x.x to x.y respectively. The general atom type parameters assigned to both atoms of ligand and that of receptor in contact with the ligand include S_{lipo} (lipophilic term: chlorine, bromine, and iodine atoms which are not ions; sulphurs which are not acceptors or polar types; carbons which are not polar type); H_{bond} (H bond donor: nitrogens with hydrogen attached, hydrogens attached to N or O; H-bond donor/acceptor: oxygens attached to hydrogens, imine nitrogen; H-bond acceptor, oxygens not attached to hydrogens, N with no hydrogens and one or two connections, halogens that are ions, sulphurs with one connection); S_{polar} (non H-bond: nitrogens with no hydrogens attached and more than two connections, phosphorous, sulphurs attached to one or more polar atoms 9 including H-bonding atoms and not including polar carbon atoms or fluorine atoms), carbons attached to two or more polar atoms (including H-bonding atoms and not including polar carbon atoms or fluorine atoms), carbons in nitriles or carbonyls, nitrogen atoms with no hydrogens and four connections, fluorine atoms); ΔE_{clash} (clash penalties between ligand atoms and receptor heavy atoms); S_{Metal} (contact between acceptor and/or donor atom in the receptor with the metal atom of the ligand, if any) (Baxter et al., 1998; Bitencourt-Ferreira & de Azevedo, 2019; Eldridge et al., 1997).

Detoxification of pyrethroids in insects follows two major routes: ester hydrolysis catalysed by esterases and P450s, and hydroxylation of aromatic rings or methyl groups by P450s (Gilbert & Gill, 2010). Infra-red and NMR spectroscopy and TLC analyses established that housefly P450s preferentially hydroxylate permethrin isomers at position 4' or 6 of the phenoxybenzyl ring and trans-methyl group (Shono et al., 1979), while trans-permethrin can be hydroxylated in position 6 of the benzyl ring and cis-permethrin in cis-methyl group as well as hydroxylation at 2' position. Other spectroscopic analyses, for example, an LC-MS determined metabolism of deltamethrin by *An. gambiae* CYP6M2 to proceed preferentially via 4' hydroxylation (Stevenson et al., 2011). Docking solutions obtained from this study were manually analysed, and productive poses with the highest scores and lowest free binding energy were selected for further analyses.

3.2.3 Docking of CYP325A models with different classes of insecticides

The CYP325A models docked generally with pyrethroid insecticides with a 2' position exposed for hydroxylation at 4.2Å (Figure) or with the trans methyl group oriented towards the haem at 2.6Å, 3.1Å, and 5.3Å respectively (Figure x, y, and z) indicating that except for FANCYP325A, permethrin metabolism is predicted to proceed via trans methyl group hydroxylation. However, the pose with resistant models has the lower penalty clash and higher score (Table x) indicating that the lower alleles possibly possess higher activity, compared with FANCYP325A allele whose model produced the lowest score and highest clash penalty.

3.2.3.1 Docking CYP325A Cameroon model with different insecticides

Table 24: ChemScores of the productive binding of CYP325A Cameroon model with different insecticides.

CYP325A-CMR Model	Rank	MolDock Score	Rerank Score	Internal Energy	H Bond	Docking Score
Permethrin	1 st	-125.091	-92.374	28.6653	0	-99.0195
Deltamethrin	12 th	-120.525	-98.799	30.0572	-2.5	-71.706
A-cypermethrin	3 rd	-119.237	-86.2761	16.4746	0	-81.9966
Bendiocarb	8 th	-90.3133	-63.3352	9.30258	-0.13309	-59.2159
Malathion	5 th	-101.195	-82.6868	6.39194	-2.5	-100.341
DDT	1 st	-92.1488	-71.5445	8.74404	0	-79.4646

ΔG = free energy of binding, $S(H_{\text{bond}})$ = contribution from hydrogen bonds, $S(\text{lipo})$ = lipophilic term, $\Delta E(\text{clash})$ = clash penalties between ligand and receptor heavy atoms, and $\Delta E(\text{int})$ = internal energy of the ligand and receptor.

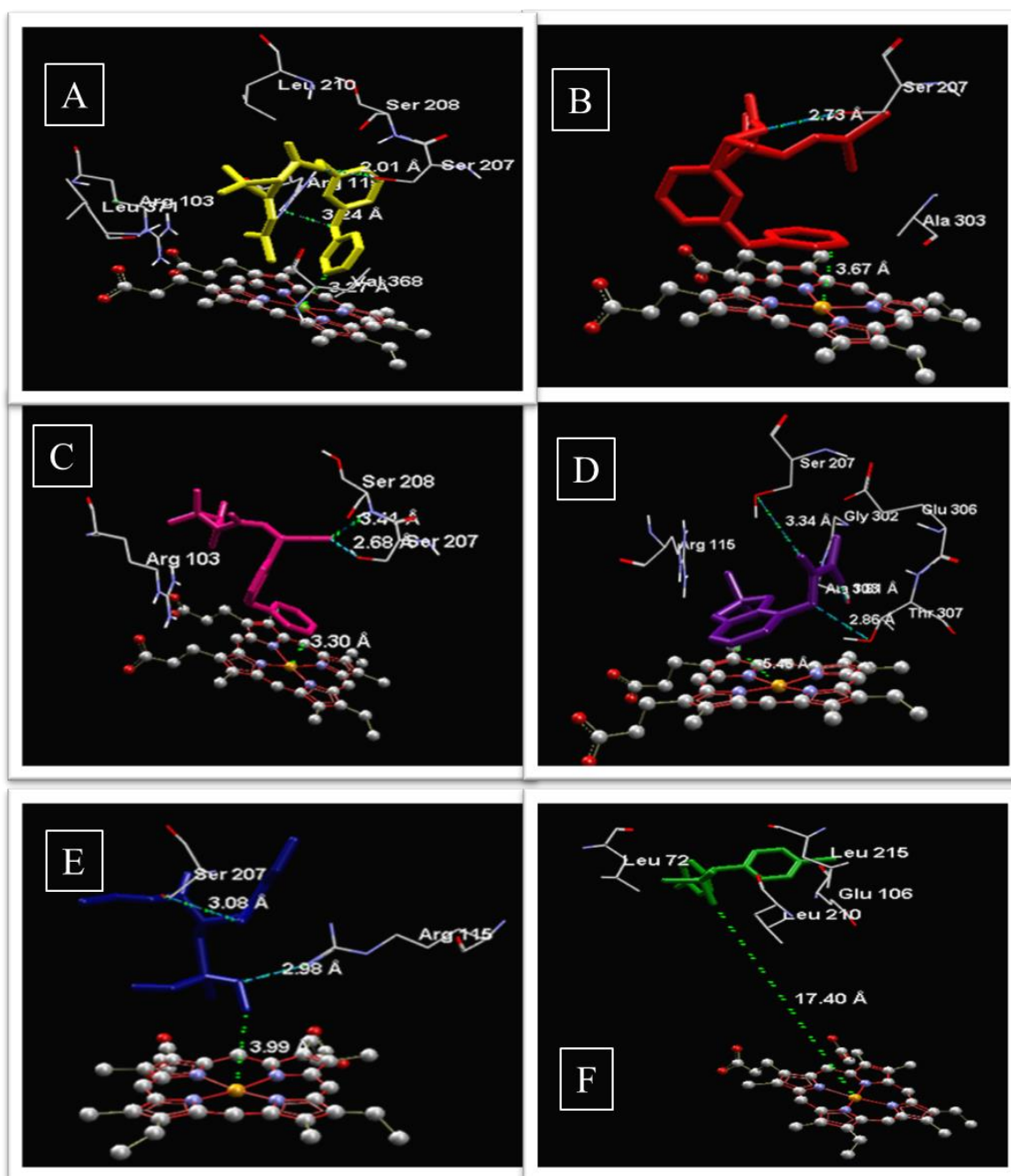


Figure 63: Binding modes of CYP325A_CMCR with insecticide models.

Binding modes of CYP325A Cameroon model with (A) Permethrin-Yellow, (B) Deltamethrin-Red, (C) α -Cypermethrin-Pink, (D) Bendiocarb-Purple, (E) Malathion-Blue, and (F) DDT-Green. Insecticides are in stick format. Haem atoms are in the spectrum. Possible sites of metabolism are indicated with yellow arrows. Showing residues involved in hydrophobic contact, within 5.0Å radius and residues from the predicted inter-molecular hydrogen bonds are annotated with numbers and haem atoms in red.

The CYP325A CMR model docked permethrin productively with the 4' spot of the phenoxy ring oriented above the haem at a distance of 3.27Å (Figure 63A) indicating with the high MolDock score (-125.091) in Table 24 that permethrin metabolism is predicted to proceed via trans methyl group hydroxylation.

Docking with deltamethrin (Figure 63B) produced similar results with the outermost benzyl ring oriented 3.67Å from the active site and a 2.73Å H-bond interaction with Ser207 in the active site. This equates to the high MolDock score (-120.525) in Table 24 predicts deltamethrin metabolism by this allele.

In the same light, α -cypermethrin docked in the pose shown (Figure 63C) proper orientation at 3.3Å from haem iron in the active site coupled to a high MolDock score (-119.237) equally predicts alpha-cypermethrin metabolism by the Cameroon allele.

Docking with bendiocarb (Figure 63D) had the benzyl ring at 6.48Å from the haem iron and therefore too far for productive binding even with a Moldock score of -90.3133. This predicts the inability of the Cameroon allele to metabolize bendiocarb.

Docking with malathion (Figure 63E), showed a very productive binding pose with the molecule at 2.99Å from the binding core and a very good Moldock score (-101.195) shown in Table 24. Contrary to the expectation that this depicts a malathion metabolising ability and subsequently a resistance to malathion, this means the opposite. The reason is that the resulting metabolite from this predicted catabolism is so much more toxic and responsible for the lethal effect of malathion on mosquitoes through its action as a potent acetylcholinesterase inhibitor. This metabolite is an oxon and in the case of malathion, a malaaxon and produced as shown in Figure 64 below. This metabolite to date is responsible for the full susceptibility observed in mosquitoes to organophosphate insecticides.

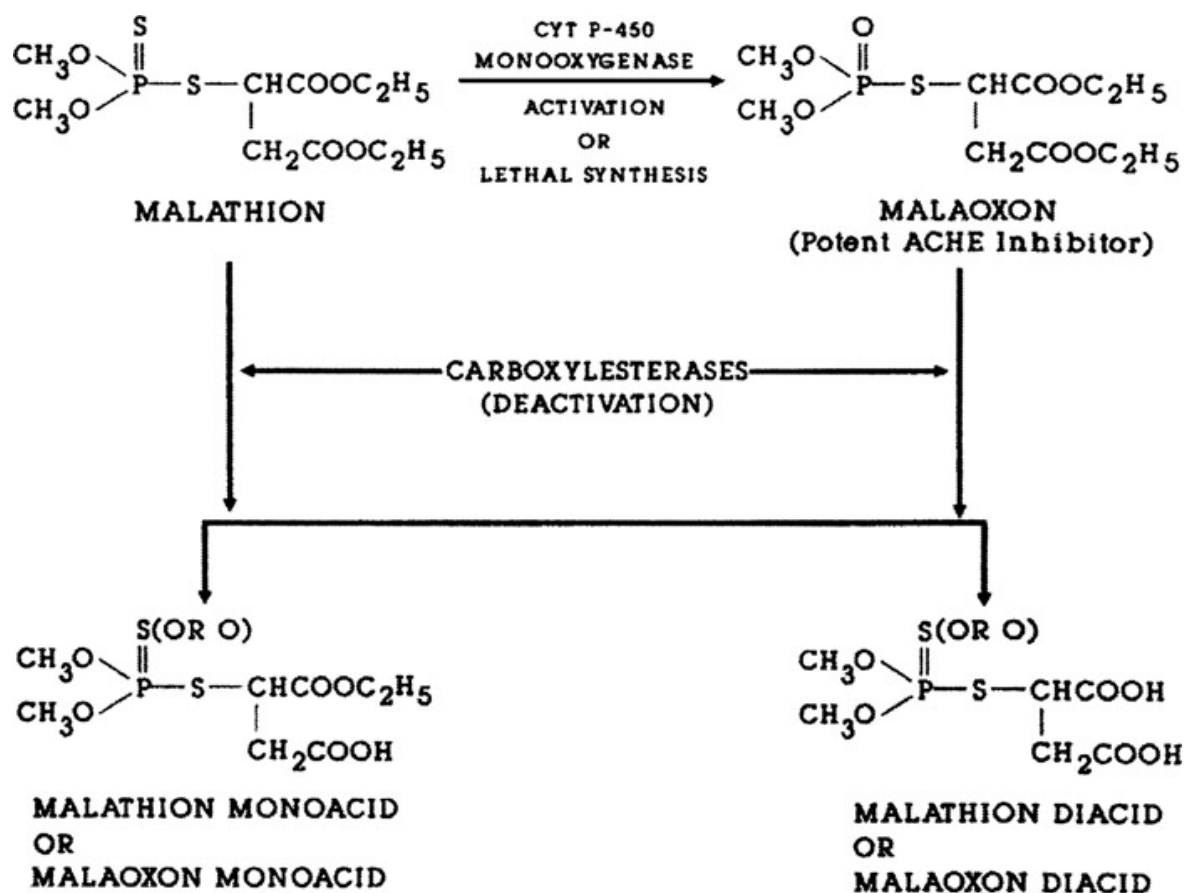


Figure 64: The activation of lethal oxon metabolite of malathion by phase I detoxification genes.

Lastly, docking with organochlorine, DDT (Figure 63F) happened very far at 17.4Å from the active site and even with a Moldock score of -92.1488, the pose is unproductive and depicts the inability of the Cameroon allele to metabolize DDT.

In summary, docking the Cameroon CYP325A allele model with pyrethroid insecticides (permethrin, deltamethrin, and α -cypermethrin) predicted the pyrethroid-metabolising ability of this allele. However, docking with non-pyrethroid insecticides (bendiocarb and DDT) predicted the inability of this allele to metabolise non-pyrethroid substrates. In the special case of organophosphate malathion, an apparent metabolising ability was observed which only reinforces the lethal effect of this insecticide on mosquitoes through the production of the toxic oxon metabolite.

3.2.3.2 Docking CYP325A DRC model with different insecticides

Table 25: ChemScores of the productive binding of CYP325A DRC model with different insecticides.

CYP325A-DRC Model	Rank	MolDock Score	Rerank Score	Internal Energy	H Bond	Docking Score
Permethrin	1st	-128.886	-68.5734	19.9098	0	-125.253
Deltamethrin	1st	-127.130	-84.2323	22.683	0	-123.1801
A-cypermethrin	4th	-139.506	-80.9886	15.0241	-0.056597	-142.006
Bendiocarb	1st	-94.336	-63.241	5.27224	0	-94.336
Malathion	5th	-111.489	-86.0216	4.95655	-2.5	109.673
DDT	5th	-101.614	-76.3423	61.11206	0	-101.357

ΔG = free energy of binding, $S(H_{\text{bond}})$ = contribution from hydrogen bonds, $S(\text{lipo})$ = lipophilic term, $\Delta E(\text{clash})$ = clash penalties between ligand and receptor heavy atoms, and $\Delta E(\text{int})$ = internal energy of the ligand and receptor.

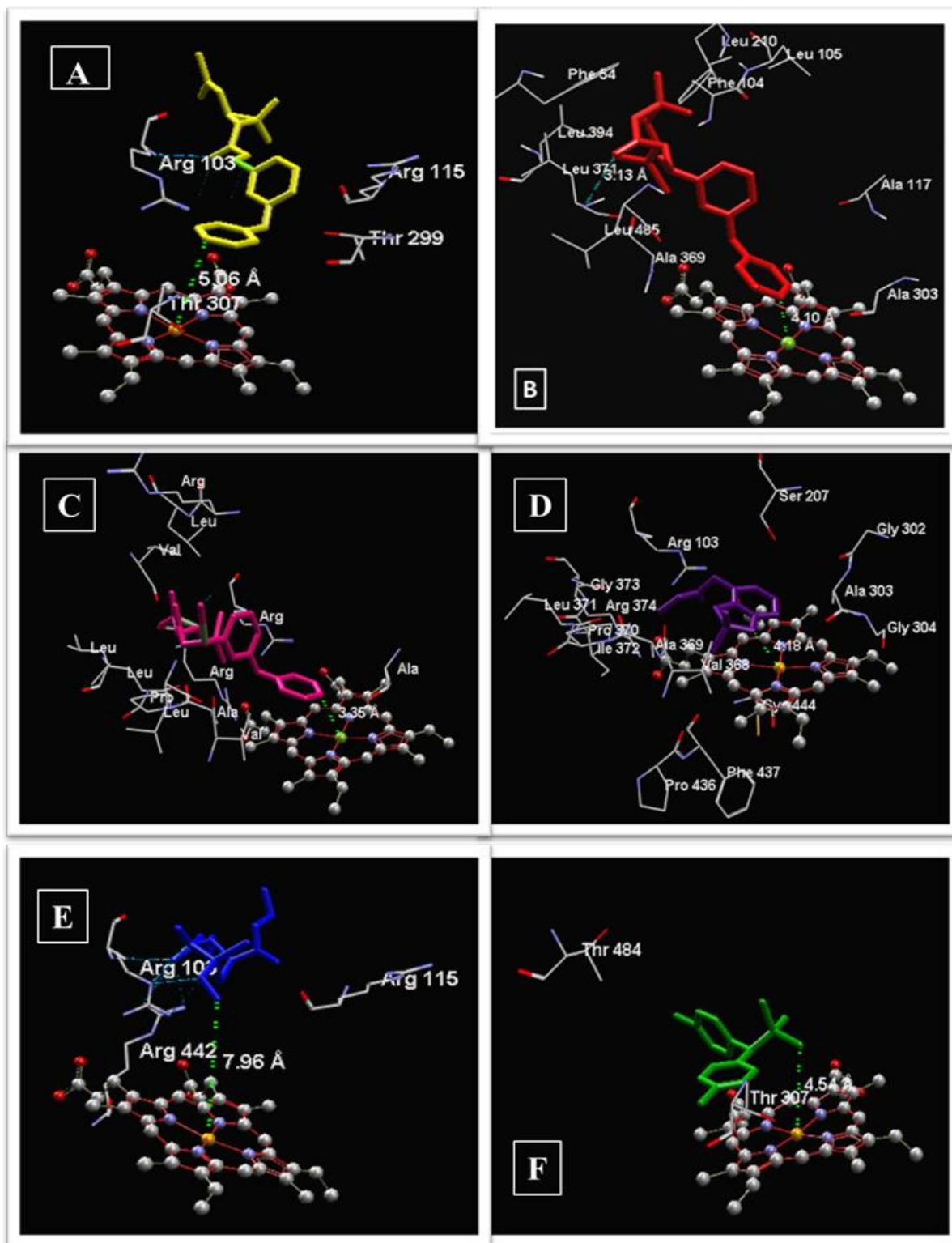


Figure 65: Binding modes of CYP325A_DRC with insecticide models.

Binding modes of CYP325A DRC model with (A) Permethrin-Yellow, (B) Deltamethrin-Red, (C) α -Cypermethrin-Pink, (D) Bendiocarb-Purple, (E) Malathion-Blue, and (F) DDT-Green. Insecticides are in stick format. Haem atoms are in spectrum. Possible sites of metabolism are indicated with yellow arrows.

Similar to the observation with the Cameroon allele, the CYP325A DRC model, docked permethrin productively with the 4' spot of the phenoxy ring oriented above the haem at a distance of 5Å (Figure 65A) indicating the high MolDock score (-128.886) in Table 25 that permethrin metabolism is predicted to metabolize permethrin though at a lower rate than the Cameroon allele due to the greater distance from the haem binding core which doesn't favour productive binding.

However, docking with deltamethrin (Figure 64B) produced similar results as seen with the Cameroon allele with the benzyl ring properly oriented in the active site at 4.1Å from the haem iron. This happened equally with the high MolDock score (-127.130) in Table 25 predicts deltamethrin metabolism by the DRC CYP325A allele.

Contrary to the observation with the Cameroon allele, α -cypermethrin docked in the pose shown (Figure 65C) with a proper orientation at 3.35Å from haem iron in the active site coupled to a high MolDock score (-139.506) but with no interaction with the amino acids in the active site making it difficult to predict alpha cypermethrin-metabolising ability of the DRC CYP325A allele.

Docking with bendiocarb (Figure 65D) had the benzyl ring at 4.1Å from the haem iron in a possible productive binding pose but with little interactions as well with the amino acids in the active site. Therefore, even with a Moldock score of -94.336, it doesn't predict the inability of the DRC allele to metabolize bendiocarb.

Docking with malathion (Figure 65E), showed a very productive binding pose with the molecule at 7.96Å from the binding core and a very good Moldock score (-111.489) shown in Table 25. This depicts an unproductive binding pose due to the great distance from the haem binding core which predicts the inability of the DRC allele to metabolize malathion.

Lastly, docking with organochlorine, DDT (Figure 65F) happened very far at 4.54Å from the active site and even with a Moldock score of -101.614, the pose is clearly unproductive due to the distance from the amino acids in the active site, lack of interaction at all which together depict the inability of the DRC allele to metabolize DDT.

To summarize, docking the DRC CYP325A allele model with pyrethroid insecticides (permethrin, deltamethrin, and α -cypermethrin) predicted the pyrethroid-metabolising ability of this allele although limited to permethrin and deltamethrin and not to α -cypermethrin. However, docking with non-pyrethroid insecticides (bendiocarb and DDT) predicted the

inability of this allele to metabolise non-pyrethroid substrates similar to the Cameroon allele. This indicates that although both alleles are similar, the Cameroon allele was predicted to have a higher metabolising ability for pyrethroid substrates compared to the DRC allele. This could be due to the structural difference observed in the E331Q SNP found to be fixed in Cameroon but only beginning in DRC.

3.2.3.3 Docking CYP325A Ghana model with different insecticides

The CYP325A Ghana model docked permethrin productively with the 4' spot of the phenoxy ring oriented above the heme at a distance of 3.3Å (Figure 2.7A), while in the active site of UGANCYP6P9b the insecticide docked with the 6 positions of the phenyl ring at a distance of 3.7Å (Figure 2.7B). Permethrin docked to the active site of FANGCYP6P9b with dihalovinyl groups approaching the heme and the possible sites of attack away from the catalytic center; trans-methyl group located 9.1Å from heme iron (Figure 2.7C) and 2' spot of phenyl ring at an 11.8Å distance. This unproductive conformation is the only pose in the ten top-ranked solutions which exhibited a very high clash penalty.

Table 26: ChemScores of the productive binding of CYP325A Ghana model with different insecticides.

CYP325A-GHA Model	Rank	MolDock Score	Rerank Score	Internal Energy	H Bond	Docking Score
Permethrin	5 th	-129.903	-76,9205	24.5679	-0.405325	-131.998
Deltamethrin	5 th	-128.716	-56.9976	26.1662	0	-128.716
A-cypermethrin	2 nd	-137.746	-90.8571	6.15174	-0.0553321	-138.359
Bendiocarb	1 st	-97.2089	-65.438	5.49802	-1.73068	-98.1862
Malathion	3 rd	-100.222	-66.1184	3.83715	0	-103.236
DDT	1 st	-104.084	-74.8352	5.56024	0	-104.084

ΔG = free energy of binding, $S(H_{\text{bond}})$ = contribution from hydrogen bonds, $S(\text{lipo})$ = lipophilic term, $\Delta E(\text{clash})$ = clash penalties between ligand and receptor heavy atoms, and $\Delta E(\text{int})$ = internal energy of the ligand and receptor.

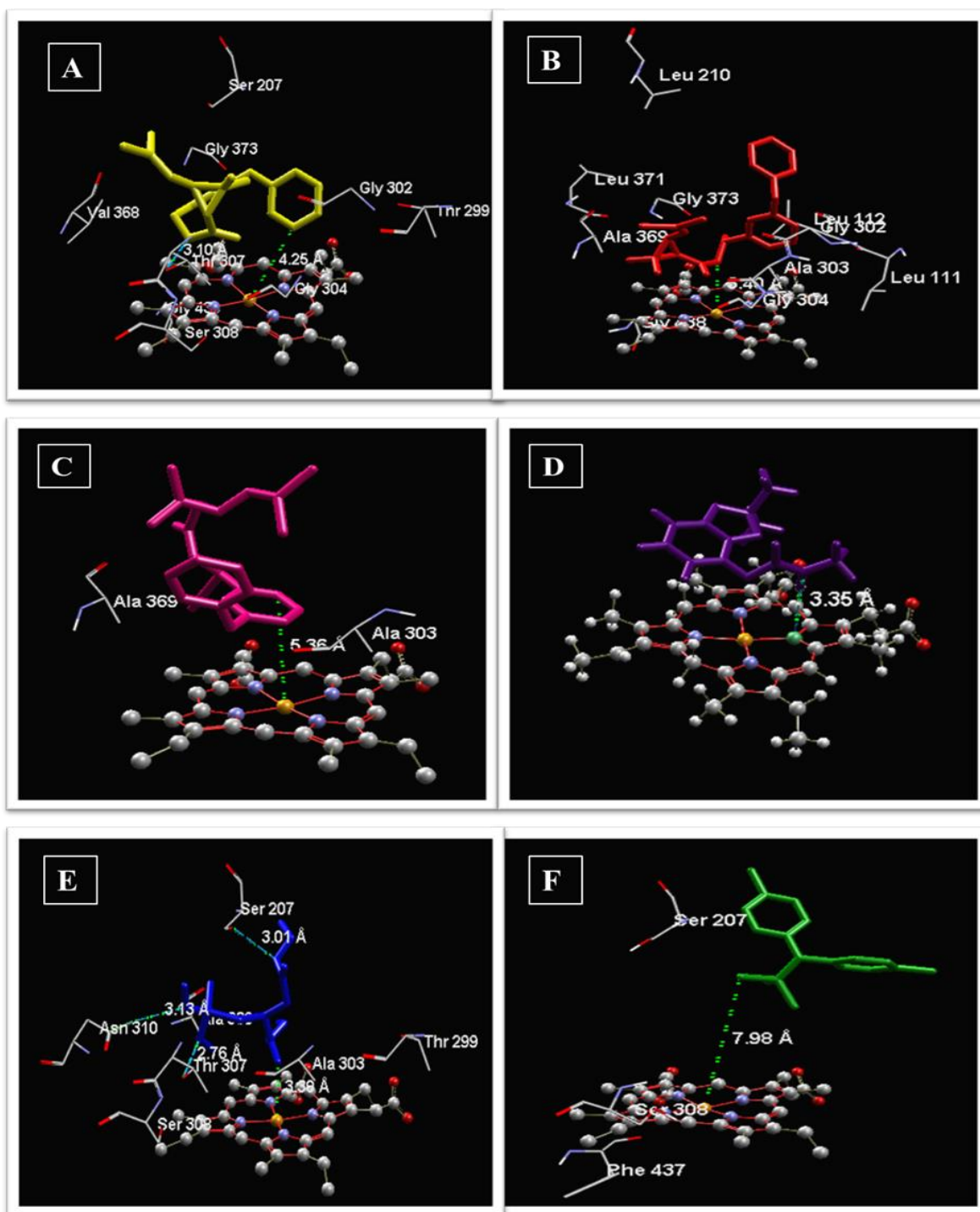


Figure 66: Binding modes of CYP325A_GHA with insecticide models.

Binding modes of CYP325A GHA model with (A) Permethrin-Yellow, (B) Deltamethrin-Red, (C) α -Cypermethrin-Pink, (D) Bendiocarb-Purple, (E) Malathion-Blue, and (F) DDT-Green. Insecticides are in stick format. Haem atoms are in the spectrum. Possible sites of metabolism are indicated with yellow arrows.

Docking with the Ghana allele was different from docking with the Cameroon and the DRC alleles primarily in the fact that the Ghana allele demonstrated the intron retention phenomenon and was therefore biologically inactive. However, cutting out the introns and docking like the other alleles was done to show that correctly spliced variants of this gene would be active and show metabolising ability towards pyrethroid substrates.

To this effect, the splice GHA_CYP325A docked permethrin productively at a distance of 4.25Å (Figure 66A) indicating with the high MolDock score (-129.903) in Table 26 with a 3.1Å H-bond interaction with Thr307 predicting that permethrin metabolism would be possible if this gene was actively secreted.

However, docking with deltamethrin and α -cypermethrin (Figure 66B and 66C respectively) showed that docking occurred too far from the haem binding core (at approximately 5.4Å) and not in the proper orientation for productive binding. Although the docking scores were relatively high (-128.716 and -137.746 respectively), the great distance from the binding core and the absence of interactions between the enzyme and the substrate predict unproductive binding for this allele.

Docking with bendiocarb (Figure 66D) happened at 3.35Å from the haem iron but with no interactions at all with the amino acids in the active site. This predicts an unproductive binding for this model with bendiocarb even with a docking score of -97.2089.

Docking with malathion (Figure 66E), showed an expected productive binding pose with a very good Moldock score (-100.222) shown in Table 26. This depicts a productive binding pose with three strong hydrogen interactions with amino acids in the active site and close proximity to the haem binding core at 3.5Å. This however facilitates the production of the oxon metabolite which will be fatal to the organism.

Lastly, docking with organochlorine, DDT (Figure 66F) happened very far at 7.98Å from the active site and even with a Moldock score of -104.084, the pose is unproductive due to the distance from the amino acids in the active site, lack of interaction at all with the amino acids in the active site which together depict the inability of the GHA allele to metabolize DDT.

In summary, docking the GHACYP325A allele model with pyrethroid insecticides (permethrin, deltamethrin, and α -cypermethrin) predicted the pyrethroid-type I metabolising ability of this allele although limited to permethrin and not to deltamethrin and α -cypermethrin. However, docking with non-pyrethroid insecticides (bendiocarb and DDT) predicted the inability of this

allele to metabolise non-pyrethroid substrates similar to the Cameroon allele. This indicates that the intron retention phenomenon could play a major role in downregulating the expression of the gene. This could also be due to the fact that there is another CYP gene CYP6P4 which is highly overexpressed in west Africa, especially in Ghana, and already strongly associated with pyrethroid resistance whence the need to downregulate similar genes.

3.2.3.4 Docking CYP325A FANG model with different insecticides

In CYP325A FANG model docked permethrin productively with the 4' spot of the phenoxy ring oriented above the heme at a distance of 3.3Å (Figure 2.7A), while in the active site of UGANCYP6P9b the insecticide docked with the 6 positions of the phenyl ring at a distance of 3.7Å (Figure 2.7B). Permethrin docked to the active site of FANGCYP6P9b with dihalovinyl groups approaching the heme and the possible sites of attack away from the catalytic center; trans-methyl group located 9.1Å from heme iron (Figure 2.7C) and 2' spot of phenyl ring at an 11.8Å distance. This unproductive conformation is the only pose in the ten top-ranked solutions which exhibited a very high clash penalty.

Table 27: ChemScores of the productive binding of CYP325A FANG model with different insecticides.

CYP325A- FAN Model	Rank	MolDock Score	Rerank Score	Internal Energy	H Bond	Docking Score
Permethrin	4 th	-129.176	-87.9296	11.19	0	-129.176
Deltamethrin	3 rd	-131.803	-94.069	14.4977	0	-133.906
A-cypermethrin	4 th	-134.065	-104.252	10.4254	0	-134.065
Bendiocarb	2 nd	-100.958	-85.0159	5.04182	-4.23613	-100.958
Malathion	1 st	-107.753	-76.2952	-9.20032	-1.76339	-108.490
DDT	5 th	-98.3846	-64.4506	7.85761	0	-98.3846

ΔG = free energy of binding, $S(H_{\text{bond}})$ = contribution from hydrogen bonds, $S(\text{lipo})$ = lipophilic term, $\Delta E(\text{clash})$ = clash penalties between ligand and receptor heavy atoms, and $\Delta E(\text{int})$ = internal energy of the ligand and receptor.

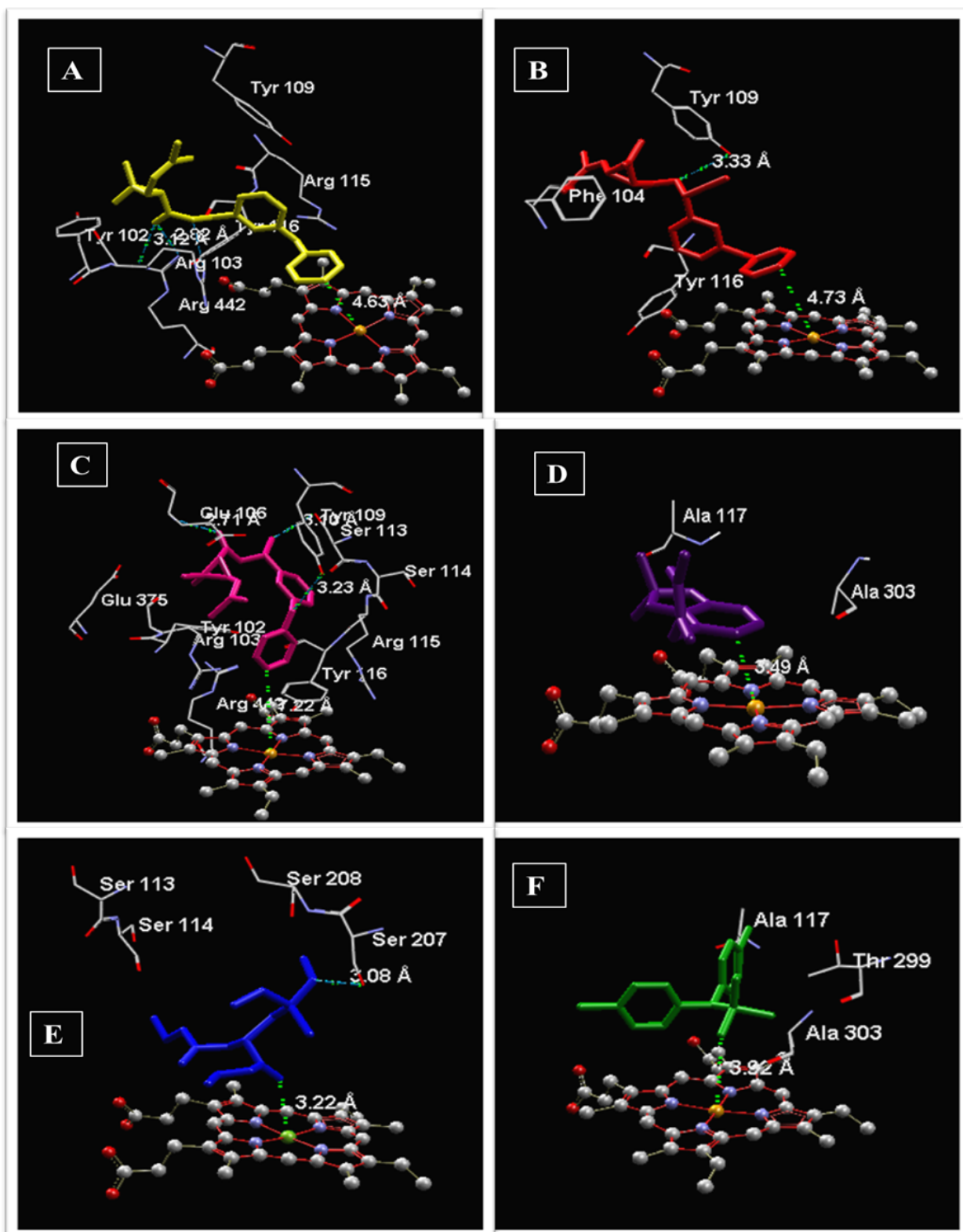


Figure 67: Binding modes of CYP325A_FAN with insecticide models.

Binding modes of CYP325A FAN model with (A) Permethrin-Yellow, (B) Deltamethrin-Red, (C) α -Cypermethrin-Pink, (D) Bendiocarb-Purple, (E) Malathion-Blue, and (F) DDT-Green. Insecticides are in stick format. Haem atoms are in the spectrum. Possible sites of metabolism are indicated with yellow arrows.

Similar to the Ghana allele, the Fang allele demonstrated the intron-retention phenomenon which was found to be fixed (100%) meaning this gene is never actively produced in the Fang strain. Cutting out the introns and docking to see if this could predict any metabolising abilities of this allele revealed little metabolising ability with the pyrethroid substrates permethrin, deltamethrin, and α -cypermethrin where we observed poor proximity to the haem binding core (above 5Å for all three) as well as with non-pyrethroid substrates (bendiocarb and DDT). This could be because this strain is from southern Africa where CYP6P9a/b is the dominant gene driving pyrethroid resistance and also due to the fully susceptible nature of this strain to insecticides in general.

3.2.3.5 Docking CYP325A FUMOZ model with different insecticides

The CYP325A FUMOZ model docked permethrin productively with the 4' spot of the phenoxy ring oriented above the heme at a distance of 3.3Å (Figure 2.7A), while in the active site of UGANCYYP6P9b the insecticide docked with the 6 positions of the phenyl ring at a distance of 3.7Å (Figure 2.7B). Permethrin docked to the active site of FANGCYYP6P9b with dihalovinyl groups approaching the heme and the possible sites of attack away from the catalytic center; trans-methyl group located 9.1Å from heme iron (Figure 2.7C) and 2' spot of phenyl ring at an 11.8Å distance. This unproductive conformation is the only pose in the ten top-ranked solutions which exhibited a very high clash penalty.

Table 28: ChemScores of the productive binding of CYP325A FUMOZ model with different insecticides.

CYP325A- Model	FUM	Rank	MolDock Score	Rerank Score	Internal Energy	H Bond	Docking Score
Permethrin		1 st	-128.659	-99.3208	18.5934	0	-132.050
Deltamethrin		1 st	-143.787	-100.14	16.3244	-0.706494	-145.653
A-cypermethrin		4 th	127.280	94.0312	17.1256	0	-131.568
Bendiocarb		1 st	-103.991	-77.7382	6.52396	0	-103.746
Malathion		5 th	-94.0123	-72.453	-0.250906	-1.32635	-96.952
DDT		1 st	-95.343	-60.4236	3.90136	0	-97.8429

ΔG = free energy of binding, $S(H_{\text{bond}})$ = contribution from hydrogen bonds, $S(\text{lipo})$ = lipophilic term, $\Delta E(\text{clash})$ = clash penalties between ligand and receptor heavy atoms, and $\Delta E(\text{int})$ = internal energy of the ligand and receptor.

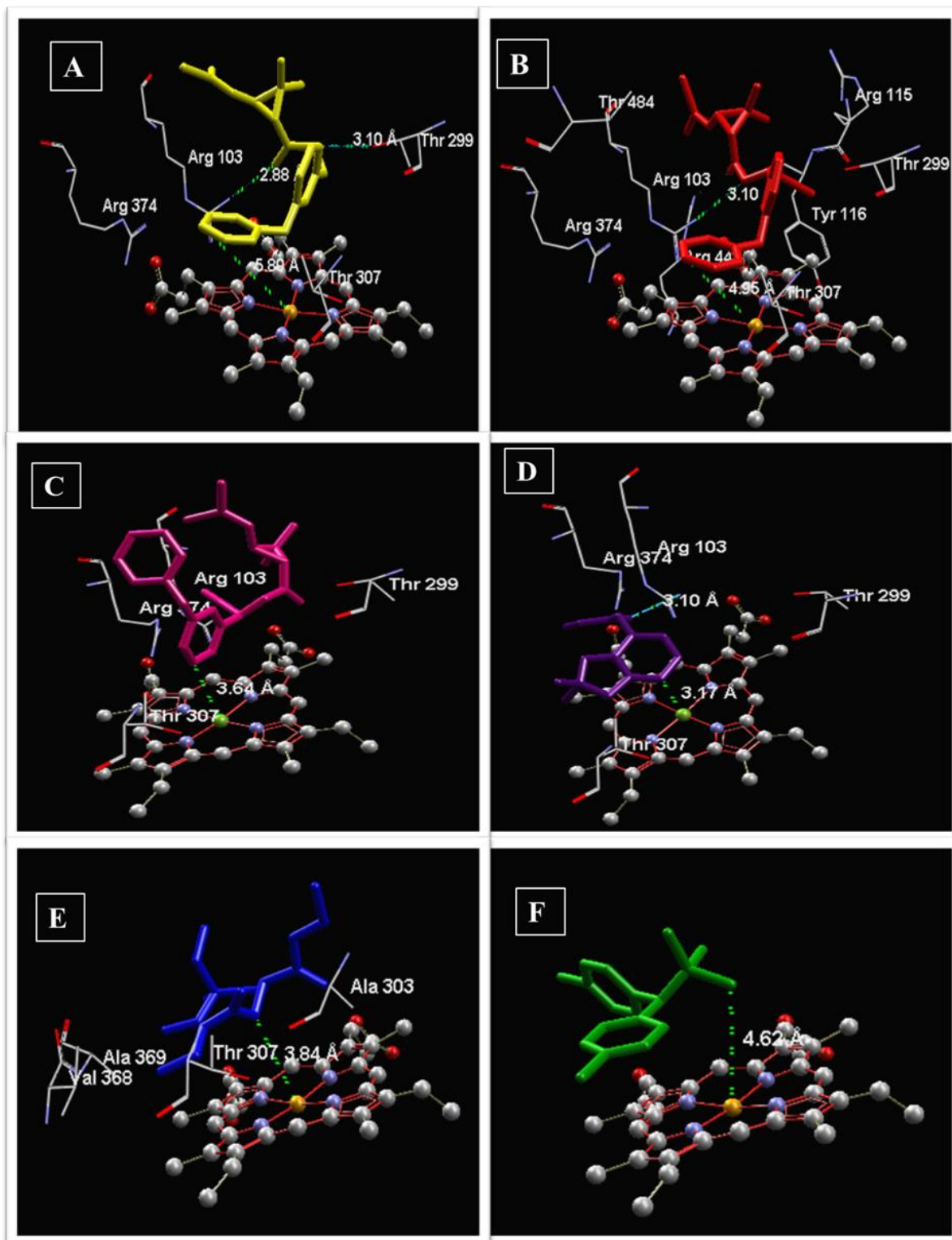


Figure 68: Binding modes of CYP325A_FUM with insecticide models.

Binding modes of CYP325A FUM model with (A) Permethrin-Yellow, (B) Deltamethrin-Red, (C) α -Cypermethrin-Pink, (D) Bendiocarb-Purple, (E) Malathion-Blue, and (F) DDT-Green. Insecticides are in stick format. Haem atoms are in the spectrum. Possible sites of metabolism are indicated with yellow arrows.

Docking the FUM CYP325A model with different insecticides predicted catabolic activity for both pyrethroid and non-pyrethroid substrates within 5Å of the active site. This also goes to stress that the active form of this gene would demonstrate metabolising activity, especially on pyrethroid substrates. This would therefore mean that the determining factor is not only the presence of the actively secreted protein but mostly the quantity secreted thereby the level of expression. Consequently, if the expression level is determinant of the gene activity and metabolising ability, it is therefore important to measure the kinetic parameters of this gene with respect to different classes of insecticides through in vitro metabolism assays.

3.2.3.2 Active Site Residues and Enzymes-Substrates Interactions

The majority of enzymes combine several strategies to enhance the rate of catalysis (Nelson et al., 2012). These include (1) covalent catalysis: acid-base catalysis involving key active sites amino acid residues, catalysis involving side chain(s)/cofactor(s) nucleophile, as well as the metal ion catalysis (metal taken up from the solution or tightly bound to the enzyme); (2) weak, non-covalent interactions: hydrophobic interactions, hydrogen bonds, vdW forces and electrostatic attractions. Evidences have shown that P450-mediated metabolism is carried out using the weak, non-covalent intra- and inter-molecular/atomic interactions to boost up the binding energy several orders of magnitude (Kenaan et al., 2011, Szklarz and Paulsen, 2002, Yoshioka et al., 2002, Paine et al., 2003). To understand the key amino acid residues lining the active/binding sites of CYP6P9a and CYP6P9b models pattern of non-bonded interaction in the binding cavities were compared between southern African alleles and FANG using the productive poses of pyrethroids in the binding cavity of the models. The southern African alleles were chosen because the highest resistance to pyrethroids was observed in southern Africa, where the two genes *CYP6P9a* and *CYP6P9b* are highly overexpressed compared with the same genes from Benin (West Africa) and Uganda (East Africa), because of the highest signature of selection from them, and because the docking with pyrethroids predicted the southern African alleles of CYP6P9a and especially CYP6P9b to possess the highest activities compared with the FANGCYP6P9a and FANGCYP6P9b.

3.3 Functional validation of CYP325A through *in vitro* and *in vivo* techniques.

In this objective, the goal was to functionally validate CYP325A as a metabolic driver of pyrethroid resistance in the major malaria vector *Anopheles funestus*. This was achieved through *in vitro* techniques involving the heterologous expression of the recombinant CYP325A in bacteria *E. coli*. The resulting protein was isolated and purified to obtain an active protein emitting a peak at 450nm by spectrophotometry. On one hand, the *in vivo* part, the recombinant CYP325A transgene was expressed in *Drosophila* flies to assess the impact of transgenic expression of this gene on the susceptibility profile of previously susceptible flies to insecticides. On the other hand, the impact of the inhibition of CYP325A on the susceptibility profile of resistant *An. funestus* mosquitoes were assessed by RNA interference.

3.3.1 *In vitro* technique by heterologous expression in *E. coli* and enzyme kinetics

An important part of this objective was the synthesis and attachment of the signal peptide outer membrane protein A + ALA-PRO (ompA+2) which is very important for the expression of cytochrome P450 genes who are membrane proteins located on the endoplasmic reticulum. In this work, the ompA+2 was synthesized and added to the gene in front of the ATG in a two-step PCR described earlier. To ensure the successful attachment of this signal peptide, digestion with DpnI was performed to screen the templates with ompA+2 which were used for subsequent *in vitro* protein expression studies.



Figure 69: Electrophoresis gel showing successful omp+2 addition to CYP325A cDNA templates

CYP325A cDNA templates with successfully attached omp+2 were then used for subcloning into pCWori+ expression plasmid. In this step, restriction enzymes were used to digest the CYP325A insert out of the carrier vector PJET and linearize the expression plasmid pCWori+. The recombinant plasmid was transformed in competent bacterial cells and after overnight culture, the colonies were screened for positive colonies as shown in the gel picture below.

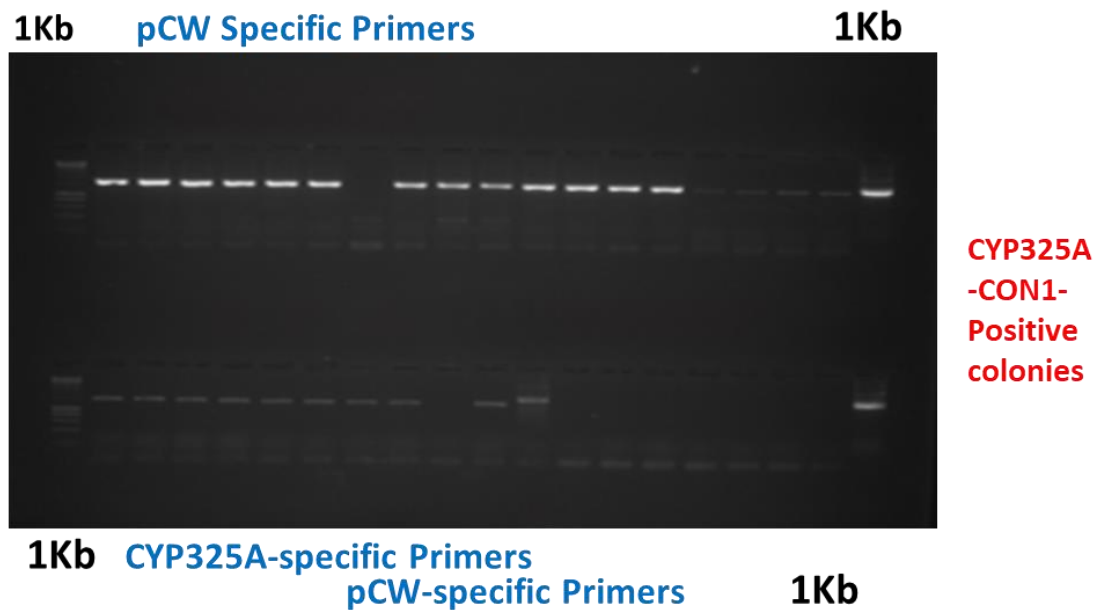


Figure 70: Colony screening PCR for positive clones with CYP325A insert omp+2-CYP325A.

The positive colonies were then isolated and co-transformed with cytochrome P450 reductase (CPR) which is an important indispensable cofactor for the physiological function of the gene. The positive colonies that co-expressed both plasmids were screened as shown below and afterward purified for the next phase.

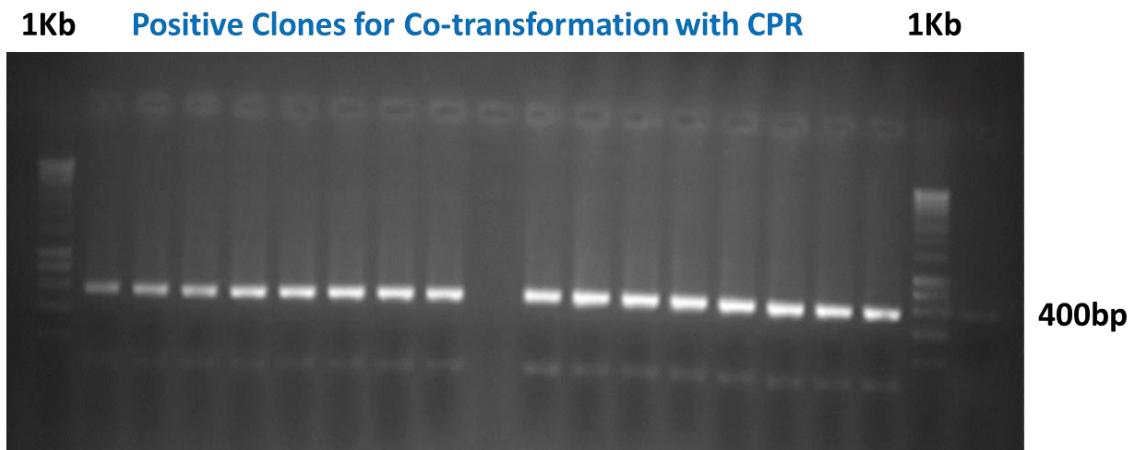


Figure 71: Colony screening gel picture for positive clones to co-transformation of recombinant pCWori+ and CPR.

The heterologous expression was carried out for three alleles from Cameroon and one allele from DRC beginning with the induction of P450 expression with ALA and IPTG. After approximately 48 – 72 hours of expression culture growth, the optical density was read after complexation with carbon monoxide until a peak at 450nm.

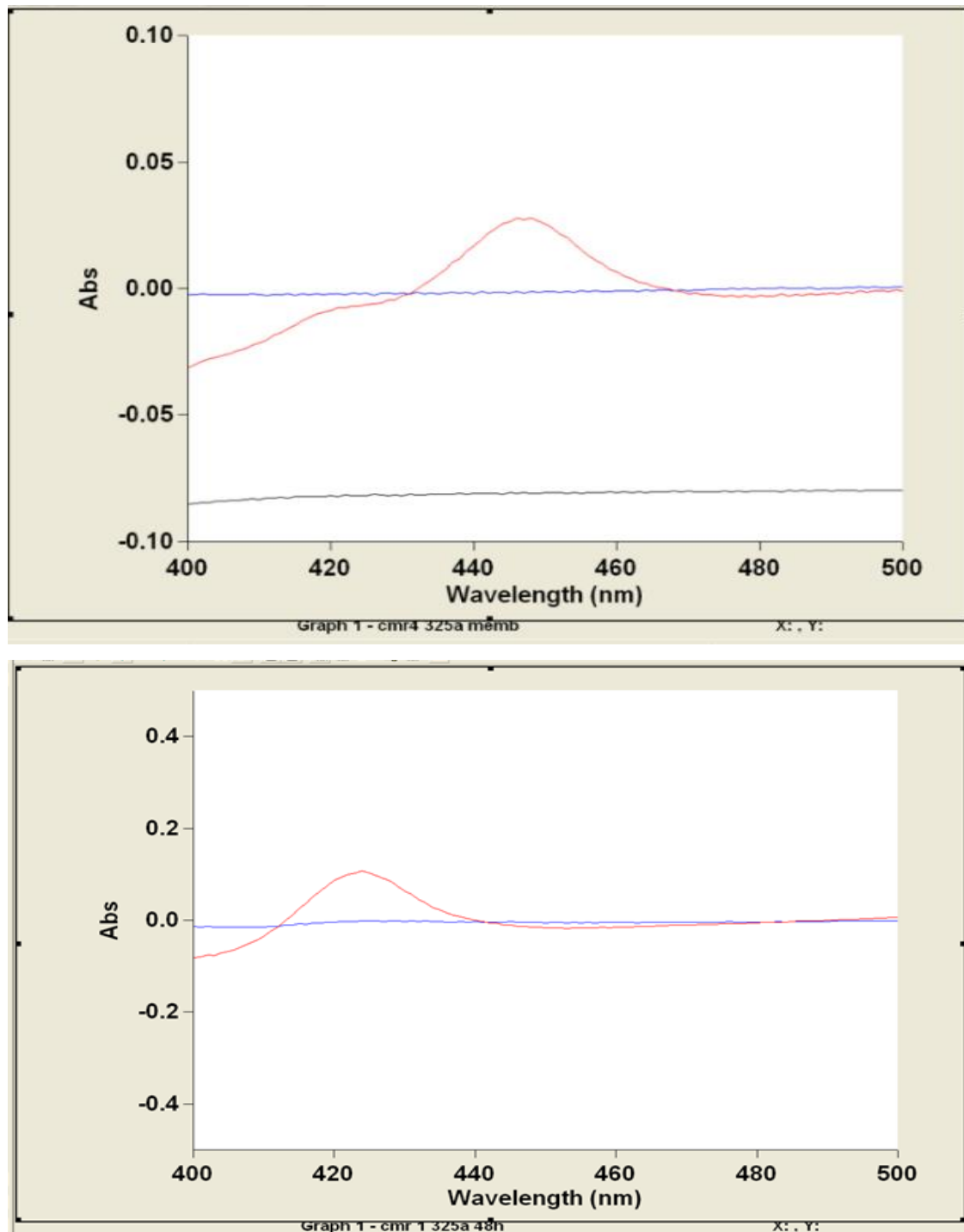


Figure 72: Spectrophotometer map showing P450 activation during culture and P450 expression

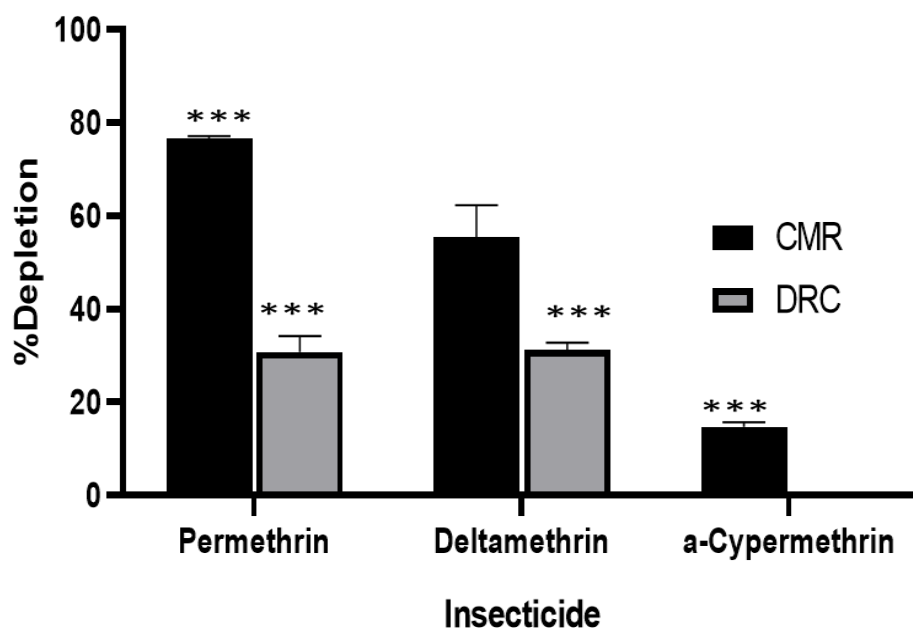


Figure 73: Cameroon and DRC CYP325A recombinant DNA depletion assays with permethrin, deltamethrin, and α -cypermethrin

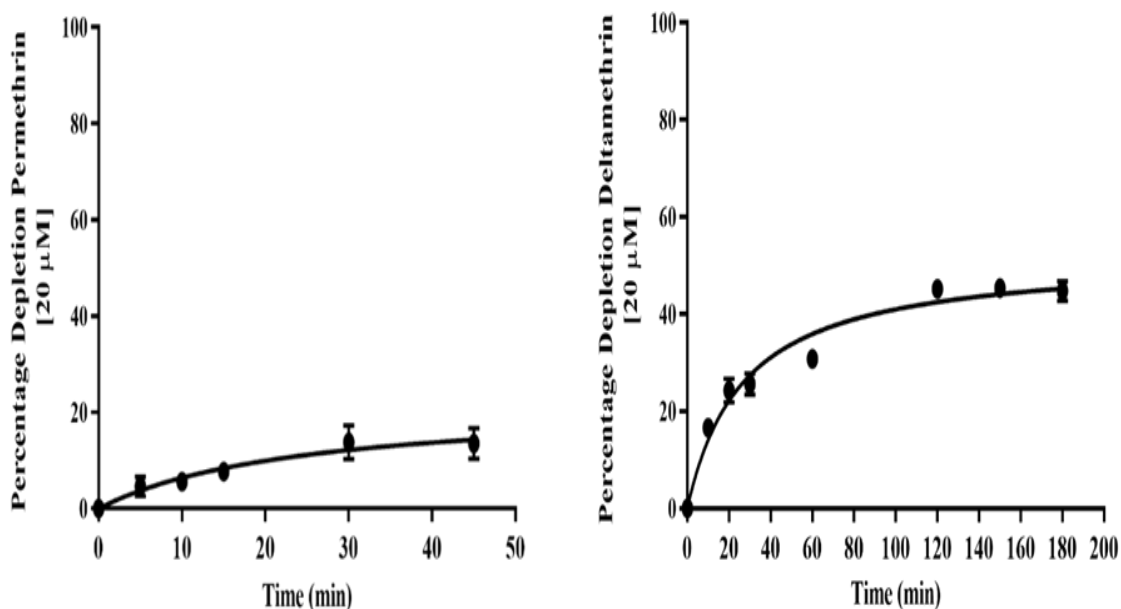


Figure 74: *In vitro* assay results. Functional confirmation of the metabolic activity of CYP325A was conducted for permethrin and deltamethrin using protein membranes.

(A) Permethrin metabolism by recombinant CYP325A-CMR (B) Deltamethrin metabolism by recombinant CYP325A-CMR. Michaelis-Menten plot of permethrin and deltamethrin metabolism by recombinant CYP325A-CMR protein. Values are mean \pm SEM of three experimental replicates compared with a negative control without NADPH (-NADPH).

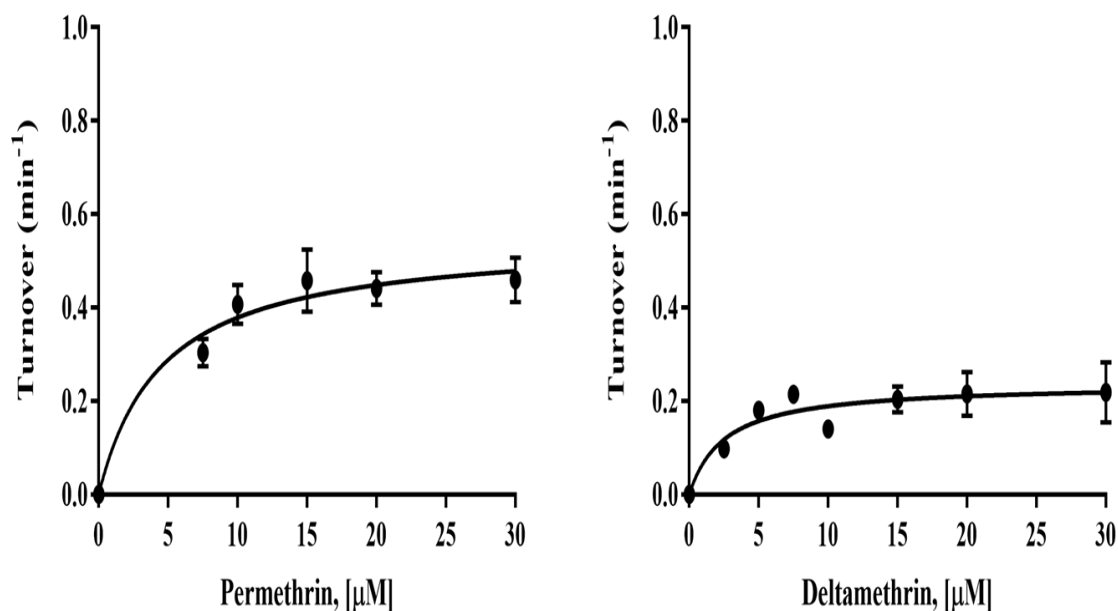


Figure 75: *In vitro* assay results. Functional confirmation of the metabolic activity of CYP325A was conducted for permethrin and deltamethrin using protein membranes.

(A) Permethrin metabolism by recombinant CYP325A-CMR (B) Deltamethrin metabolism by recombinant CYP325A-CMR. Michaelis-Menten plot of permethrin and deltamethrin metabolism by recombinant CYP325A-CMR protein. Values are mean \pm SEM of three experimental replicates compared with a negative control without NADPH (-NADPH). (C). Permethrin (D). Deltamethrin.

The *in vitro* assays performed through the heterologous expression of CYP325A in *E. coli* was successful and the harvested protein purified by ultracentrifugation was tested for activity by spectrophotometry where a peak at 450nm indicated active P450. The purified protein was then used as an enzyme to perform metabolism assays with insecticides permethrin, deltamethrin, alpha-cypermethrin, DDT and propoxur. The results of the metabolism assays were read using HPLC and the kinetics of the enzyme-substrate interaction were analyzed by drawing the Michaelis-Menten curve. The results show CYP325A preferentially metabolises the pyrethroid substrates compared to the non-pyrethroid substrates and this ties with the above *in silico* predictions.

3.3.2. *In vivo* Transgenic expression in *Drosophila* flies

In vivo expression of transgenic CYP325A in flies started with the preparation of the transgenic construct that would be injected in the flies germline cells. The results of the digestion of the plasmid and gene to produce complementary ends for ligation is shown below in Figure 76.

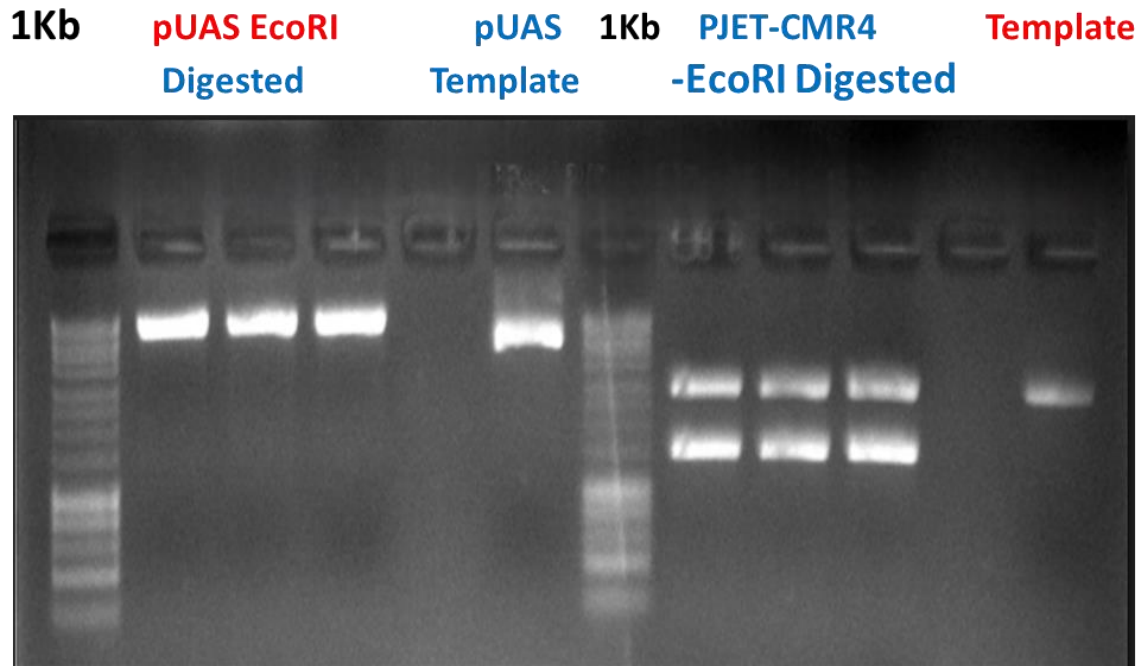
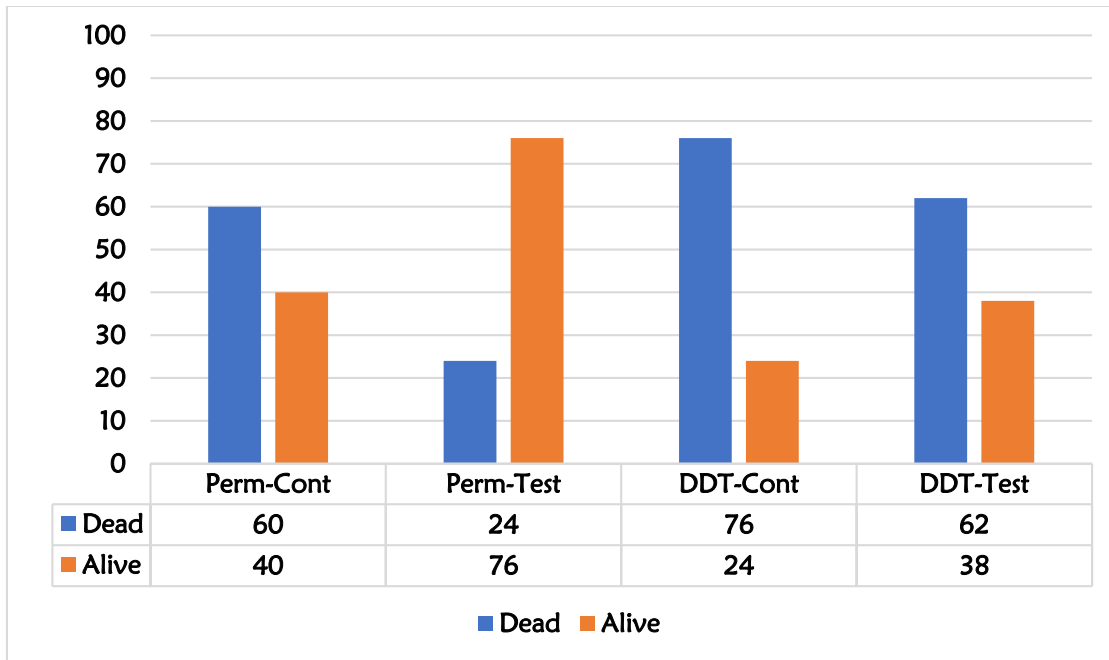


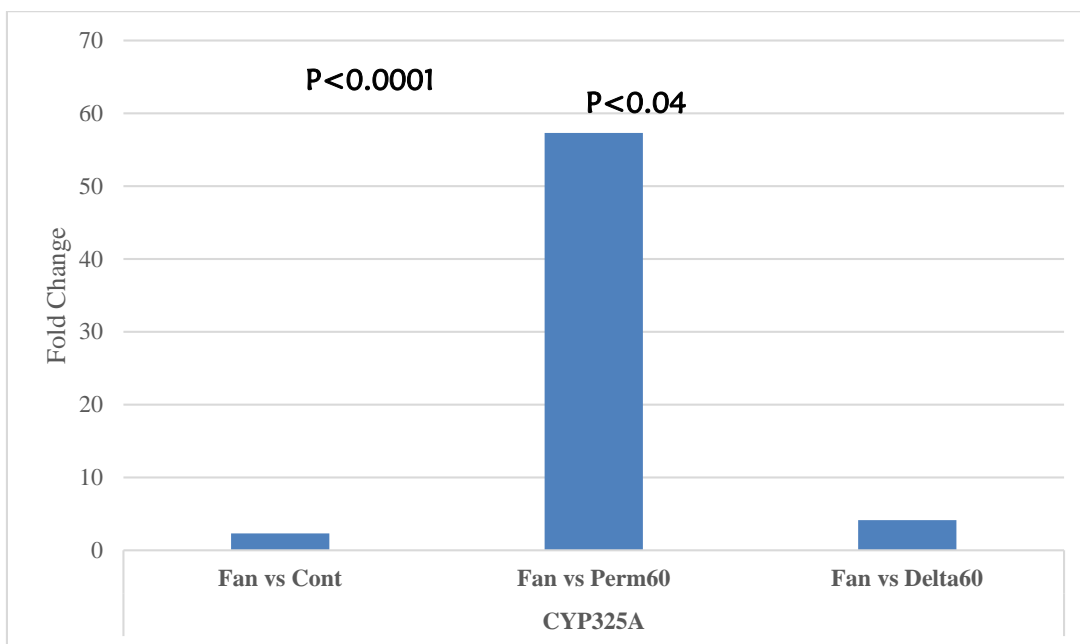
Figure 76: Endonuclease digestion of transgenic expression plasmid and PJET-CYP325A recombinant plasmid



Legend: Test – CYP325A transgenic flies line (Red eyes) Control: Flies line (White eyes)

Figure 77: Assessment of transgenic activity of CYP325A: Contact bioassay mortality results of transgenic flies with permethrin and DDT.

3.3.3. *In vivo* RNA interference by double-strand injection in *An. funestus* mosquitoes



Legend: Fan – FANG, Perm – Permethrin, Delta - Deltamethrin

Figure 78: Assessment of inhibited expression of CYP325A after injection of double strand

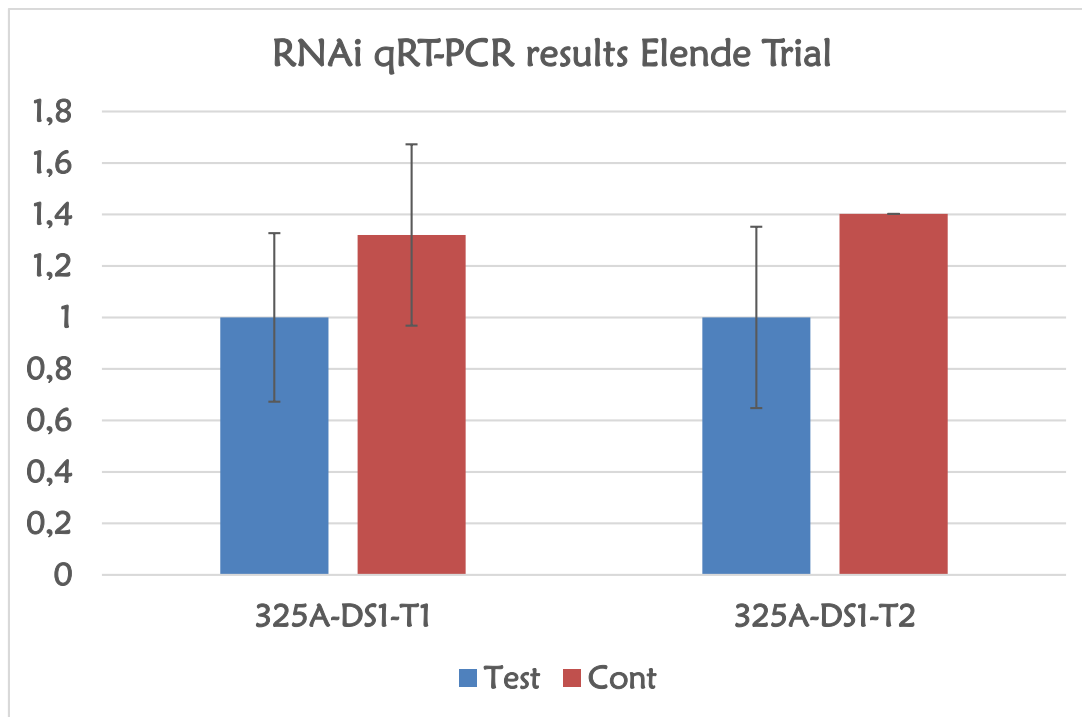


Figure 79: Assessment of expression of *CYP325A* after injection of double-strand in two trial runs

Legend: FAN:FANG, Perm: Permethrin, Delta: Deltamethrin, DS: Double strand.

DISCUSSION

Elucidation of resistance mechanisms to insecticides in mosquito vectors of tropical diseases such as malaria is a prerequisite for better management of the growing problem of resistance to existing insecticide classes. If progress has been made in elucidating the molecular basis of pyrethroid resistance in several populations of *An. funestus* in Africa like the case of CYP6P9a/b in Southern Africa, CYP6P4a/b in Western Africa, and CYP9K1 in Eastern Africa little progress has been made in the central African region in understanding the specific molecular driver of pyrethroid resistance in *Anopheles funestus*. This study investigated the role of the overexpressed CYP325A P450 in pyrethroid resistance in *An. funestus* mosquito population in Cameroon through a molecular characterization of the cDNA and a 1kb putative promoter revealing that this gene likely contributes to resistance to types I and II pyrethroids in this region.

4.1. CYP325A over-expression is observed only in Central Africa

qRT-PCR expression patterns between mosquitoes collected from Cameroon exposed to permethrin and deltamethrin with respect to a control unexposed to insecticides revealed a stark contrast in the expression pattern of CYP325A with high over-expression in Cameroon, Central Africa as previously reported by RNAseq (Mugenzi et al., 2019; Weedall et al., 2019) whereas other populations from other regions (southern and western Africa) exhibit a low expression (Nkemngbo et al., 2020). This contrasting expression profile is like that of other Africa-wide transcriptomic analyses which have consistently shown a drastic difference in expression between African regions. This is the case with the duplicated P450s CYP6P9a and CYP6P9b highly over-expressed mainly in southern Africa (Riveron et al., 2013; Weedall et al., 2019). Similarly, GSTe2 was shown to be massively over-expressed mainly in *An. funestus* populations from West Africa, notably in Benin, whereas CYP9K1 is predominantly overexpressed mainly in East Africa (Tchouakui, Miranda, et al., 2020). This contrasting expression of major resistance genes further supports evidence that pyrethroid resistance has been independently selected across these regions while also highlighting the potential restriction to gene flow between populations of *An. funestus* across the continent. Such contrast in the expression of metabolic resistance genes is also observed in other major malaria vectors including *An. gambiae*, *An. coluzzii*, *An. albimanus* and *An. arabiensis* (Dia et al., 2018; Gueye et al., 2020; Mackenzie-Impoinvil et al., 2019; Mitchell et al., 2012). Interestingly, the CYP6P5 gene was shown to have the most similar expression pattern to CYP325A in Cameroon, where

it is also overexpressed (Weedall et al., 2019). This could be linked to their potential common role in resistance as is the case in the Mibellon (Weedall et al., 2020) population. Two transcription factors CCAAT/enhancer-binding protein gamma and Adf-1 also showed a high similarity in expression to CYP325A, a possible link between gene expression and regulation (Amador et al., 2001).

4.2. CYP325A metabolism of pyrethroids establishes its role in resistance in Central African *An. funestus*

Both modelling and in vitro studies showed that CYP325A alleles from Cameroon and DRC can metabolise type I pyrethroids (permethrin) and type II pyrethroids (deltamethrin). The depletion rates observed against permethrin and deltamethrin are lower than that of other P450s previously shown to metabolise pyrethroids in *An. funestus* such as CYP6P9a (Riveron et al., 2013; Riveron, Yunta, et al., 2014), CYP6P9b (Riveron et al., 2013), CYP6M7 (Riveron, Ibrahim, et al., 2014), CYP9J11 (Riveron et al., 2017), CYP6AA1 (Ibrahim et al., 2018). This level of depletion is also like that of other genes from *An. gambiae* such as CYP6M2 and CYP6P3 found to mediate metabolic resistance to both type I and II pyrethroids (Müller et al., 2008; Wagah et al., 2021). However, the low depletion rate of CYP325A against alphacypermethrin suggests that it does not confer alphacypermethrin resistance. The inability of CYP325A to metabolise all pyrethroids is similar to previous reports that some genes could metabolise one type of pyrethroid insecticides but not the other as seen for CYP6P4's ability to metabolise permethrin but not deltamethrin in *An. arabiensis* in Chad (Ibrahim et al., 2016). The inability of CYP325A to metabolise efficiently α -cypermethrin in *An. funestus* mosquitoes could be an advantage for the use of LLINs impregnated with this insecticide such as Interceptor G2 as a vector control tool in the localities where CYP325A-based pyrethroid resistance is predominant in *An. funestus*. However, because other genes may confer alpha-cypermethrin resistance, the susceptibility of field populations to this insecticide should be monitored before making any decision. The CYP325A allele from DRC exhibited a significantly lower efficiency in breaking down pyrethroids than the CMR allele. This is likely due to the allelic variation (E331Q) observed between the sequences from Cameroon and DRC. This allelic variation is due to a key mutation E331Q observed between Cameroon and DRC alleles. The almost fixed nature of E331Q mutations in Cameroon compared to their low frequency in DRC suggests this allele is under selection and will increase over time like the case of CYP6P9a/b in southern Africa (Weedall et al., 2019) and GSTe2 in Benin (Riveron, Yunta, et al., 2014). The mutations selected and almost fixed in the Cameroon sequences are V21L, R22K, A29K, and E331Q,

however, the key mutation is at position 331 where glutamic acid (E) is replaced by glutamine (Q) in almost all the Cameroon sequences. This mutation is a major change from an acidic amino acid to a basic amino acid which could greatly impact the physio-chemical properties of this enzyme. Even though it is not located in any substrate recognition site (SRS), it is in very close proximity to the SRS-4 and the α J loop comprised in the proposed reductase interaction phase playing a role in substrate specificity and their electron transfer partners as part of the haem-binding core along with the α D, α E, α I, α L and α K loops (Sirim et al., 2010). The impact of allelic variation on the metabolic efficiency of detoxification genes has previously been shown in *An. funestus* for P450s such as CYP6P9a/b (Ibrahim et al., 2015) and for the GSTe2 for which a single L119F amino acid change was shown to drive DDT and pyrethroid resistance in West/Central Africa. Such a role of allelic variation is also similar to the case of CYP6A2 in *Drosophila melanogaster* for which three amino acid substitutions located close to the active site in the allele predominant in DDT-resistant flies, have been shown to confer the increasing metabolism of DDT (Feyereisen, 2012; Li et al., 2007). Further studies, such as site-directed mutagenesis could confirm the role of CYP325A overexpression in pyrethroid resistance and the E331Q mutation in the activity of CYP325A. Some CYP450 genes have been established as non-metabolisers of pyrethroids even though they bind productively such as *An. gambiae* CYP6Z2 for permethrin and α -cypermethrin (McLaughlin et al., 2008) and *An. arabiensis* CYP6P4. Our modelling in this study supports productive binding modes for permethrin, deltamethrin and α -cypermethrin, with possibility of binding to bendiocarb, but not DDT. However, the low similarity between CYP325A and the template, CYP3A4 could have resulted in a model with lower quality, which would impact the molecular docking resolution.

4.3. Lack of strong signatures of selective sweep around CYP325A

Polymorphism analyses of the CYP325A full-length gene in *An. funestus* mosquitoes from across Africa revealed an overall absence of selection across this gene highlighted by the lack of a predominant resistance haplotype despite the previous observation that the E331Q was conferring a greater catalytic ability to the allele from Cameroon. The absence of such positive selection could suggest that the selective pressure is still relatively recent on the population from Cameroon supported by moderate resistance levels observed in Mibellon (Menze et al., 2018). The lack of selection on CYP325A could also suggest that this gene acts through increased expression and bioavailability similar to the highly polymorphic CYP6M7 (Riveron, Ibrahim, et al., 2014), and contrary to the observation made for CYP6P9a/b for which allelic variation drives resistance through directionally selected alleles now nearly fixed in field

populations from southern Africa (Riveron et al., 2013; Weedall et al., 2019; Weedall et al., 2020). Furthermore, the regional comparison of the transcription profile of pyrethroid resistance in *An. funestus* cDNA across Africa and 1 kb putative promoter in permethrin susceptible (dead) and resistant (alive) mosquitoes from Mibellon, Cameroon revealed several facts. The polymorphism pattern analysis revealed a possible selection in the promoter region notably in Cameroon although further analyses are needed to confirm the extent of this selection and its impact on the cis-regulation of *CYP325A*. A preliminary screening of the transcription factors binding sites in this promoter region using Alggen online software revealed the presence of binding sites for Cncc/Maf, H96, Dfd-1, and AHR/Arnt; all xenobiotic sensors previously implicated in the regulation of detoxification genes like P450s (Hu et al., 2019, 2021). Further promoter activity analyses will establish the impact of these polymorphisms on the activity of *CYP325A* across Africa potentially helping to detect causative markers driving *CYP325A*-based pyrethroid resistance as done for *CYP6P9a/b* (Mugenzi et al., 2019; Weedall et al., 2019).

The *in vivo* assays trials showed the expected patterns notably an increase in susceptibility in mosquitoes injected with the double-strand inhibitor of the gene *CYP325A*. Similar results were obtained in previous studies (Kouamo et al., 2021) with GSTe genes in Benin where the inhibition of some GSTe genes in DDT-resistant mosquitoes showed a marked increase in susceptibility to DDT indicating that the successful inhibition of some GSTe genes lead to the loss of resistance to DDT conferred by gene in question. These findings are in line with what we observed in our trials where we inhibited the *CYP325A* expression in pyrethroid-resistant mosquitoes and observed an increase in susceptibility due to the loss of resistance ability conferred by *CYP325A*.

On the other hand, the expression of the transgene *CYP325A* in fruit flies resulted in a reduction in the susceptibility of the flies to insecticides to which they were previously fully susceptible. This was the case in the study conducted by Kouamo and collaborators in 2021 on transgenic GSTe expression in fruit flies (Riveron, Yunta, et al., 2014) leading to a significant decrease in susceptibility in the flies for the DDT insecticide. These findings are in line with our preliminary observation with *CYP325A* where the transgenic flies showed a reduction in susceptibility to pyrethroid insecticides.

CONCLUSION

Drawing from the findings accrued in the course of this study, the following conclusions could be made:

(i) the cytochrome P450 gene *CYP325A* is highly over-expressed in central Africa compared to the rest of Africa, does not manifest allelic variation, and is associated with pyrethroid resistance in *Anopheles funestus* mosquitoes on the field.

(ii) the *in silico* simulations of the activity of *CYP325A* models from central Africa with pyrethroid and non-pyrethroid insecticide substrates predicted the ability of *CYP325A* to metabolise pyrethroid substrates but not non-pyrethroid substrates.

(iii) the *in vitro* metabolism assays of *CYP325A* with pyrethroid insecticides confirmed its ability to metabolise permethrin and deltamethrin with the Cameroon allele demonstrating a higher metabolising ability compared to the DRC allele probably due to the E331Q SNP mutation almost fixed in Cameroon *CYP325A*. The *in vivo* trials with RNAi and transgenic expression in flies confirmed the implication of *CYP325A* in pyrethroid-based insecticide resistance.

These findings contribute to filling the knowledge gap that exists in understanding the molecular basis of insecticide resistance and elucidating the underlying biochemical mechanisms of metabolic resistance will play a major role in ensuring the continued efficacy of implemented vector control strategies as well as more informed policy making. The implication of *CYP325A* in insecticide resistance in Cameroon drives the recommendation of ITNs with PBO in the localities with such resistance to ensure the mosquitoes remain susceptible to the insecticide on the bed nets. Also, non-pyrethroid insecticide-impregnated insecticides like Interceptor G2 impregnated with alpha cypermethrin could be a plausible alternative to reduce the selection pressure on the field mosquitoes. These findings could inform policy and help the National Malaria Control Programs (NMCP) to implement more efficient vector control strategies that would foster malaria elimination.

FUTURE PERSPECTIVES

The results of our research are just a tiny part of what remains to be elucidated within the context of the molecular basis of monooxygenase-mediated insecticide resistance mechanisms. The underlying biochemical mechanisms driving metabolic resistance and especially P450-mediated insecticide could be located at many different levels of cellular function: detoxification protein gene overexpression could be due to transcriptional level changes involving higher constitutive production of transcripts, due to mutation in promoter sequences, higher inducible expression due to mutations in the trans-acting factors or greater responsiveness to transcriptional inducers. It could also be due to changes at the gene regulation level which could be understood by studying the promoters of genes. These aspects of *An. funestus* detoxification genes need to be explored further to understand how these genes are regulated and how the intron retention phenomenon is implicated in the expression of these genes during splicing, post-transcriptional and post-translational modifications especially how these relate to environmental conditions. Factors responsible for cis- or trans-regulation of P450s involved in detoxification may also be capable of regulating the expression of other P450s that are not necessarily involved in the said resistance (this is the case in houseflies). Knowing which subsets of P450s are elevated by the same regulatory factors may help to elucidate cross-resistance phenomena. Throughout this research we adopted as surrogates electron transfer partners (cytochrome P450 reductase and cytochrome b5) from *An. gambiae*. It is possible that the interaction of *An. funestus*-specific electron transfer partners may affect the qualitative and quantitative activity of its CYP450s. Potential mutations in such partners may also possibly alter their coupling with the respective *An. funestus* CYP450s. The whole picture of the resistance phenomena can only be obtained using metabolomics studies. There is an overwhelming need to find out which subsets of genes are switched on and/or off in response to insecticide exposure, and which intermediates and products are generated from insecticide metabolisms. These could be achieved using targeted transcriptomics, proteomics, and MS/MS. LC/MS could also be utilised to identify the metabolites generated by these P450s, and this could help in piecing together the pyrethroid resistance network. Modelling simulation has a great shortcoming, there is an urgent need to create a crystal structure of the P450s involved in pyrethroids metabolism with the insecticides in its active site. Also now with cryo-EM, it is possible to bypass crystallography and determine biomolecular structures of proteins more directly. This will greatly facilitate our understanding of the mechanism of action of these P450s, as well as help in the design and production of potential synergists that could be used in

combination with the insecticide to block the resistance P450s. Successful site-directed mutagenesis of the resistant allele of *CYP325A* could potentially reveal the identity of the amino acids responsible for the ability of this gene to metabolize a wide range of Type I and Type II pyrethroids. This is important, for the amino acid substitutions that could potentially impact the catalytic activity of *CYP325A* mapped to different domains of the P450 compared with the susceptible strain FANG. *CYP325A* is a similarly expressed gene to *CYP6P5* which is also overexpressed in central Africa and could be working in synergy. Understanding more about both genes could lead to detecting molecular markers that could be used to design easy DNA-based diagnostics, such as PCR-RFLP for the detection and tracking of resistance on the field in *Anopheles funestus* mosquito populations.

REFERENCES

- Ahn, S.-J., Vogel, H., & Heckel, D. G. (2012). Comparative analysis of the UDP-glycosyltransferase multigene family in insects. *Insect Biochemistry and Molecular Biology*, 42(2), 133-147.
- Akoton, R., Tchigossou, G. M., Djègbè, I., Yessoufou, A., Atoyebi, M. S., Tossou, E., Zeukeng, F., Boko, P., Irving, H., & Adéoti, R. (2018). Experimental huts trial of the efficacy of pyrethroids/piperonyl butoxide (PBO) net treatments for controlling multi-resistant populations of *Anopheles funestus* ss in Kpomè, Southern Benin. *Wellcome Open Research*, 3.
- Altschul, S. F., Gish, W., Miller, W., Myers, E. W., & Lipman, D. J. (1990). Basic local alignment search tool. *Journal of molecular biology*, 215(3), 403-410.
- Amador, A., Papaceit, M., & Juan, E. (2001). Evolutionary change in the structure of the regulatory region that drives tissue and temporally regulated expression of alcohol dehydrogenase gene in *Drosophila funebris*. *Insect Molecular Biology*, 10(3), 237-247.
- Antonio-Nkondjio, C., Ndo, C., Njiokou, F., Bigoga, J. D., Awono-Ambene, P., Etang, J., Ekobo, A. S., & Wondji, C. S. (2019). Review of malaria situation in Cameroon: technical viewpoint on challenges and prospects for disease elimination. *Parasites & vectors*, 12(1), 501.
- Antonio-Nkondjio, C., Sonhafouo-Chiana, N., Ngadjou, C., Doumbe-Belisse, P., Talipouo, A., Djamouko-Djonkam, L., Kopya, E., Bamou, R., Awono-Ambene, P., & Wondji, C. S. (2017). Review of the evolution of insecticide resistance in main malaria vectors in Cameroon from 1990 to 2017. *Parasites & vectors*, 10(1), 472.
- Aravind, L., Iyer, L. M., Wellems, T. E., & Miller, L. H. (2003). Plasmodium biology: genomic gleanings. *Cell*, 115(7), 771-785.
- Armougom, F., Moretti, S., Poirot, O., Audic, S., Dumas, P., Schaeli, B., Keduas, V., & Notredame, C. (2006). Expresso: automatic incorporation of structural information in multiple sequence alignments using 3D-Coffee. *Nucleic acids research*, 34(suppl_2), W604-W608.
- Awolola, T., Oduola, O., Strobe, C., Koekemoer, L., Brooke, B., & Ranson, H. (2009). Evidence of multiple pyrethroid resistance mechanisms in the malaria vector *Anopheles gambiae sensu stricto* from Nigeria. *Transactions of the Royal Society of Tropical Medicine and Hygiene*, 103(11), 1139-1145.
- Babić, S., Grdiša, M., Periša, M., Ašperger, D., Šatović, Z., & Kaštelan-Macan, M. (2012). Ultrasound-assisted extraction of pyrethrins from pyrethrum flowers. *Agrochimica*, 56(4/5), 193-206.
- Bai, D., Lummis, S. C., Leicht, W., Breer, H., & Sattelle, D. B. (1991). Actions of imidacloprid and a related nitromethylene on cholinergic receptors of an identified insect motor neurone. *Pesticide science*, 33(2), 197-204.
- Balabanidou, V., Grigoraki, L., & Vontas, J. (2018). Insect cuticle: a critical determinant of insecticide resistance. *Current opinion in insect science*, 27, 68-74.
- Bamou, R., Sonhafouo-Chiana, N., Mavridis, K., Tchuinkam, T., Wondji, C. S., Vontas, J., & Antonio-Nkondjio, C. (2019). Status of insecticide resistance and its mechanisms in *Anopheles gambiae* and *Anopheles coluzzii* populations from forest settings in south Cameroon. *Genes*, 10(10), 741.

- Barnes, H. J., Arlotto, M. P., & Waterman, M. R. (1991). Expression and enzymatic activity of recombinant cytochrome P450 17 alpha-hydroxylase in *Escherichia coli*. *Proceedings of the National Academy of Sciences*, 88(13), 5597-5601.
- Bass, C., Denholm, I., Williamson, M. S., & Nauen, R. (2015). The global status of insect resistance to neonicotinoid insecticides. *Pesticide Biochemistry and Physiology*, 121, 78-87.
- Baxter, C. A., Murray, C. W., Clark, D. E., Westhead, D. R., & Eldridge, M. D. (1998). Flexible docking using Tabu search and an empirical estimate of binding affinity. *Proteins: Structure, Function, and Bioinformatics*, 33(3), 367-382.
- Bayili, K., N'do, S., Namountougou, M., Sanou, R., Ouattara, A., Dabiré, R. K., Ouédraogo, A. G., Malone, D., & Diabaté, A. (2017). Evaluation of efficacy of Interceptor® G2, a long-lasting insecticide net coated with a mixture of chlorfenapyr and alpha-cypermethrin, against pyrethroid resistant *Anopheles gambiae* sl in Burkina Faso. *Malaria Journal*, 16(1), 1-9.
- Belin, P., Le Du, M. H., Fielding, A., Lequin, O., Jacquet, M., Charbonnier, J.-B., Lecoq, A., Thai, R., Courçon, M., & Masson, C. (2009). Identification and structural basis of the reaction catalyzed by CYP121, an essential cytochrome P450 in *Mycobacterium tuberculosis*. *Proceedings of the National Academy of Sciences*, 106(18), 7426-7431.
- Berman, H. M., Battistuz, T., Bhat, T. N., Bluhm, W. F., Bourne, P. E., Burkhardt, K., Feng, Z., Gilliland, G. L., Iype, L., & Jain, S. (2002). The protein data bank. *Acta Crystallographica Section D: Biological Crystallography*, 58(6), 899-907.
- Bigoga, J. D., Ndangoh, D. N., Awono-Ambene, P. H., Patchoke, S., Fondjo, E., & Leke, R. G. (2012). Pyrethroid resistance in *Anopheles gambiae* from the rubber cultivated area of Niéde, South Region of Cameroon. *Acta tropica*, 124(3), 210-214.
- Bitencourt-Ferreira, G., & de Azevedo, W. F. (2019). Molegro virtual docker for docking. In *Docking Screens for Drug Discovery* (pp. 149-167). Springer.
- Black, B. C., Hollingworth, R. M., Ahammadsahib, K. I., Kukel, C. D., & Donovan, S. (1994). Insecticidal action and mitochondrial uncoupling activity of AC-303,630 and related halogenated pyrroles. *Pesticide Biochemistry and Physiology*, 50(2), 115-128.
- Blandin, S., Moita, L. F., Köcher, T., Wilm, M., Kafatos, F. C., & Levashina, E. A. (2002). Reverse genetics in the mosquito *Anopheles gambiae*: targeted disruption of the Defensin gene. *EMBO reports*, 3(9), 852-856.
- Bloomquist, J. R. (1996). Ion channels as targets for insecticides. *Annual review of entomology*, 41(1), 163-190.
- Bradford, M. M. (1976). A rapid and sensitive method for the quantitation of microgram quantities of protein utilizing the principle of protein-dye binding. *Analytical biochemistry*, 72(1-2), 248-254.
- Braun, W., & Gö, N. (1985). Calculation of protein conformations by proton-proton distance constraints: A new efficient algorithm. *Journal of molecular biology*, 186(3), 611-626.
- Cabia, B., García, A., & Arterós, R. (2012). Humanised flies.
- Chandre, F., Darriet, F., Duchon, S., Finot, L., Manguin, S., Carnevale, P., & Guillet, P. (2000). Modifications of pyrethroid effects associated with kdr mutation in *Anopheles gambiae*. *Medical and veterinary entomology*, 14(1), 81-88.

- Chen, M. M., Coelho, P. S., & Arnold, F. H. (2012). Utilizing Terminal Oxidants to Achieve P450- Catalyzed Oxidation of Methane. *Advanced Synthesis & Catalysis*, 354(6), 964-968.
- Chery, J. (2016). RNA therapeutics: RNAi and antisense mechanisms and clinical applications. *Postdoc journal: a journal of postdoctoral research and postdoctoral affairs*, 4(7), 35.
- Clement, M., Posada, D., & Crandall, K. A. (2000). TCS: a computer program to estimate gene genealogies. *Molecular ecology*, 9(10), 1657-1659.
- Coetzee, M. (2020). Key to the females of Afrotropical Anopheles mosquitoes (Diptera: Culicidae). *Malaria Journal*, 19(1), 1-20.
- Coetzee, M., & Fontenille, D. (2004). Advances in the study of Anopheles funestus, a major vector of malaria in Africa. *Insect Biochemistry and Molecular Biology*, 34(7), 599-605.
- Coetzee, M., & Koekemoer, L. L. (2013). Molecular systematics and insecticide resistance in the major African malaria vector Anopheles funestus. *Annual review of entomology*, 58, 393-412.
- Cojocar, V., Winn, P. J., & Wade, R. C. (2007). The ins and outs of cytochrome P450s. *Biochimica et Biophysica Acta (BBA)-General Subjects*, 1770(3), 390-401.
- Colovos, C., & Yeates, T. O. (1993). Verification of protein structures: patterns of nonbonded atomic interactions. *Protein science*, 2(9), 1511-1519.
- Corbel, V., & N'Guessan, R. (2013). Distribution, mechanisms, impact and management of insecticide resistance in malaria vectors: a pragmatic review. In *Anopheles mosquitoes- New insights into malaria vectors*. IntechOpen.
- Curtis, C., & Hill, N. (1993). Are there effective resistance management strategies for vectors of human disease? *Biological journal of the Linnean Society*, 48(1), 3-18.
- D Menze, B., Wondji, M. J., Tchapa, W., Tchoupo, M., Riveron, J. M., & Wondji, C. S. (2018). Bionomics and insecticides resistance profiling of malaria vectors at a selected site for experimental hut trials in central Cameroon. *Malaria Journal*, 17(1), 1-10.
- Daborn, P. J., Lumb, C., Boey, A., Wong, W., & Batterham, P. (2007). Evaluating the insecticide resistance potential of eight Drosophila melanogaster cytochrome P450 genes by transgenic over-expression. *Insect Biochemistry and Molecular Biology*, 37(5), 512-519.
- Davidson, G. (1957). Insecticide resistance in Anopheles sudaicus. *Nature*, 180(4598).
- Davies, T., Field, L., Usherwood, P., & Williamson, M. (2007). DDT, pyrethrins, pyrethroids and insect sodium channels. *IUBMB life*, 59(3), 151-162.
- De Montellano, P. R. O. (2005). *Cytochrome P450: structure, mechanism, and biochemistry* (Vol. 115). Springer.
- Dennig, A., Kuhn, M., Tassoti, S., Thiessenhusen, A., Gilch, S., Bülter, T., Haas, T., Hall, M., & Faber, K. (2015). Oxidative decarboxylation of short- chain fatty acids to 1- alkenes. *Angewandte Chemie International Edition*, 54(30), 8819-8822.
- Dia, A. K., Guèye, O. K., Niang, E. A., Diédhiou, S. M., Sy, M. D., Konaté, A., Samb, B., Diop, A., Konaté, L., & Faye, O. (2018). Insecticide resistance in Anopheles arabiensis populations from Dakar and its suburbs: role of target site and metabolic resistance mechanisms. *Malaria Journal*, 17(1), 1-9.

- Dia, I., Guelbeogo, M. W., & Ayala, D. (2013). Advances and Perspectives in the Study of the Malaria Mosquito *Anopheles funestus*. *Anopheles mosquitoes-New insights into malaria vectors*, 10, 55389.
- Djouaka, R., Irving, H., Tukur, Z., & Wondji, C. S. (2011). Exploring mechanisms of multiple insecticide resistance in a population of the malaria vector *Anopheles funestus* in Benin. *PLoS one*, 6(11), e27760.
- Du, W., Awolola, T., Howell, P., Koekemoer, L., Brooke, B., Benedict, M., Coetzee, M., & Zheng, L. (2005). Independent mutations in the Rdl locus confer dieltrin resistance to *Anopheles gambiae* and *An. arabiensis*. *Insect Molecular Biology*, 14(2), 179-183.
- Duffy, J. B. (2002). GAL4 system in *Drosophila*: a fly geneticist's Swiss army knife. *genesis*, 34(1- 2), 1-15.
- Edi, C. V., Djogbenou, L., Jenkins, A. M., Regna, K., Muskavitch, M. A., Poupardin, R., Jones, C. M., Essandoh, J., Ketoh, G. K., & Paine, M. J. (2014). CYP6 P450 enzymes and ACE-1 duplication produce extreme and multiple insecticide resistance in the malaria mosquito *Anopheles gambiae*. *PLoS Genet*, 10(3), e1004236.
- Elanga-Ndille, E., Nouage, L., Ndo, C., Binyang, A., Assatse, T., Nguiffo-Nguete, D., Djonabaye, D., Irving, H., Tene-Fossog, B., & Wondji, C. S. (2019). The G119S acetylcholinesterase (Ace-1) target site mutation confers carbamate resistance in the major malaria vector *Anopheles gambiae* from Cameroon: A challenge for the coming IRS Implementation. *Genes*, 10(10), 790.
- Elbashir, A. B., Abdelbagi, A. O., Hammad, A. M., Elzorgani, G. A., & Laing, M. D. (2015). Levels of organochlorine pesticides in the blood of people living in areas of intensive pesticide use in Sudan. *Environmental monitoring and assessment*, 187(3), 1-10.
- Eldridge, M. D., Murray, C. W., Auton, T. R., Paolini, G. V., & Mee, R. P. (1997). Empirical scoring functions: I. The development of a fast empirical scoring function to estimate the binding affinity of ligands in receptor complexes. *Journal of computer-aided molecular design*, 11(5), 425-445.
- Etang, J., Manga, L., Toto, J.-C., Guillet, P., Fondjo, E., & Chandre, F. (2007). Spectrum of metabolic-based resistance to DDT and pyrethroids in *Anopheles gambiae* sl populations from Cameroon. *Journal of Vector Ecology*, 32(1), 123-133.
- Fadel, A. N., Ibrahim, S. S., Tchouakui, M., Terence, E., Wondji, M. J., Tchoupo, M., Wanji, S., & Wondji, C. S. (2019). A combination of metabolic resistance and high frequency of the 1014F kdr mutation is driving pyrethroid resistance in *Anopheles coluzzii* population from Guinea savanna of Cameroon. *Parasites & Vectors*, 12(1). <https://doi.org/10.1186/s13071-019-3523-7>
- Farnham, A. W., Murray, A. W., Sawicki, R. M., Denholm, I., & White, J. C. (1987). Characterization of the structure- activity relationship of kdr and two variants of super-kdr to pyrethroids in the housefly (*Musca domestica* L.). *Pesticide science*, 19(3), 209-220.
- Farnsworth, C. A., Teese, M. G., Yuan, G., Li, Y., Scott, C., Zhang, X., Wu, Y., Russell, R. J., & Oakeshott, J. G. (2010). Esterase-based metabolic resistance to insecticides in heliothine and spodopteran pests. *Journal of Pesticide Science*, 35(3), 275-289.
- Feyereisen, R. (2012). Insect CYP genes and P450 enzymes. In *Insect molecular biology and biochemistry* (pp. 236-316). Elsevier.

- Fiser, A., Do, R. K. G., & Šali, A. (2000). Modeling of loops in protein structures. *Protein science*, 9(9), 1753-1773.
- Fiser, A., & Sali, A. (2003). ModLoop: automated modeling of loops in protein structures. *Bioinformatics*, 19(18), 2500-2501.
- Fiser, A., & Šali, A. (2003a). Modeller: generation and refinement of homology-based protein structure models. In *Methods in enzymology* (Vol. 374, pp. 461-491). Elsevier.
- Fiser, A., & Šali, A. (2003b). Modeller: generation and refinement of homology-based protein structure models. *Methods in enzymology*, 374, 461-491.
- Forgash, A. J. (1984). History, evolution, and consequences of insecticide resistance. *Pesticide Biochemistry and Physiology*, 22(2), 178-186.
- Fournier, D. (2005). Mutations of acetylcholinesterase which confer insecticide resistance in insect populations. *Chemico-biological interactions*, 157, 257-261.
- Fujita, M., Mizukado, S., Fujita, Y., Ichikawa, T., Nakazawa, M., Seki, M., Matsui, M., Yamaguchi-Shinozaki, K., & Shinozaki, K. (2007). Identification of stress-tolerance-related transcription-factor genes via mini-scale Full-length cDNA Over-eXpressor (FOX) gene hunting system. *Biochemical and biophysical research communications*, 364(2), 250-257.
- Fukuto, T. R. (1990). Mechanism of action of organophosphorus and carbamate insecticides. *Environmental health perspectives*, 87, 245-254.
- Funhoff, E. G., Bauer, U., García-Rubio, I., Witholt, B., & van Beilen, J. B. (2006). CYP153A6, a soluble P450 oxygenase catalyzing terminal-alkane hydroxylation. *Journal of bacteriology*, 188(14), 5220-5227.
- Gareth D. Weedall, L. M. J. M., Benjamin D. Menze, Magellan Tchouakui, Sulaiman S. Ibrahim, Nathalie Amvongo-Adjia, Helen Irving, Murielle J. Wondji, Micareme Tchoupo, Rousseau Djouaka, Jacob M. Riveron, Charles S. Wondji. (2019). A cytochrome P450 allele confers pyrethroid resistance on a major African malaria vector, reducing insecticide-treated bednet efficacy. *Science Translational Medicine*, 11(7386).
- Gilbert, L. I., & Gill, S. S. (2010). *Insect control: biological and synthetic agents*. Academic Press.
- Gillies, M., & Coetzee, M. (1987). A supplement to the Anophelinae of Africa South of the Sahara. *Publ S Afr Inst Med Res*, 55, 1-143.
- Gillies, M. T., & De Meillon, B. (1968). The Anophelinae of Africa south of the Sahara (Ethiopian zoogeographical region). *The Anophelinae of Africa south of the Sahara (Ethiopian Zoogeographical Region)*.
- Girhard, M., Kunigk, E., Tihovsky, S., Shumyantseva, V. V., & Urlacher, V. B. (2013). Light-driven biocatalysis with cytochrome P 450 peroxygenases. *Biotechnology and applied biochemistry*, 60(1), 111-118.
- Gohlke, H., Hendlich, M., & Klebe, G. (2000). Knowledge-based scoring function to predict protein-ligand interactions. *Journal of molecular biology*, 295(2), 337-356.
- Goodsell, D. S., Morris, G. M., & Olson, A. J. (1996). Automated docking of flexible ligands: applications of AutoDock. *Journal of molecular recognition*, 9(1), 1-5.

- Grant, J. L., Hsieh, C. H., & Makris, T. M. (2015). Decarboxylation of fatty acids to terminal alkenes by cytochrome P450 compound I. *Journal of the American Chemical Society*, *137*(15), 4940-4943.
- Grant, J. L., Mitchell, M. E., & Makris, T. M. (2016). Catalytic strategy for carbon– carbon bond scission by the cytochrome P450 OleT. *Proceedings of the National Academy of Sciences*, *113*(36), 10049-10054.
- Graziadei, P., & Metcalf, J. (1971). Autoradiographic and ultrastructural observations on the frog's olfactory mucosa. *Zeitschrift für Zellforschung und mikroskopische Anatomie*, *116*(3), 305-318.
- Gubler, D. (2009). Vector-borne diseases. *Revue scientifique et technique (International Office of Epizootics)*, *28*(2), 583-588.
- Guerra, C. A., Gikandi, P. W., Tatem, A. J., Noor, A. M., Smith, D. L., Hay, S. I., & Snow, R. W. (2008). The limits and intensity of Plasmodium falciparum transmission: implications for malaria control and elimination worldwide. *PLoS Med*, *5*(2), e38.
- Gueye, O., Tchouakui, M., Dia, A. K., Faye, M. B., Ahmed, A. A., Wondji, M. J., Nguiffo, D. N., Mugenzi, L., Tripet, F., & Konaté, L. (2020). Insecticide Resistance Profiling of Anopheles coluzzii and Anopheles gambiae Populations in the Southern Senegal: Role of Target Sites and Metabolic Resistance Mechanisms. *Genes*, *11*(12), 1403.
- Gupta, R. C., Malik, J. K., & Milatovic, D. (2011). Organophosphate and carbamate pesticides. In *Reproductive and Developmental Toxicology* (pp. 471-486). Elsevier.
- Gupta, R. C., Mukherjee, I. R. M., Malik, J. K., Doss, R. B., Dettbarn, W.-D., & Milatovic, D. (2019). Insecticides. In *Biomarkers in toxicology* (pp. 455-475). Elsevier.
- Hall, T. A. (1999). BioEdit: a user-friendly biological sequence alignment editor and analysis program for Windows 95/98/NT. *Nucleic acids symposium series*,
- Harbach, R. E., & Kitching, I. J. (2016). The phylogeny of Anophelinae revisited: inferences about the origin and classification of Anopheles (Diptera: Culicidae). *Zoologica Scripta*, *45*(1), 34-47.
- Harrison, G. (1978). Mosquitoes, malaria and man: A history of the hostilities since 1880. *Mosquitoes, malaria and man: a history of the hostilities since 1880*.
- Hematpoor, A., Liew, S. Y., Azirun, M. S., & Awang, K. (2017). Insecticidal activity and the mechanism of action of three phenylpropanoids isolated from the roots of Piper sarmentosum Roxb. *Scientific Reports*, *7*(1), 1-13.
- Hemingway, J. (2014). The role of vector control in stopping the transmission of malaria: threats and opportunities. *Philosophical Transactions of the Royal Society B: Biological Sciences*, *369*(1645), 20130431.
- Hemingway, J., Hawkes, N. J., McCarroll, L., & Ranson, H. (2004). The molecular basis of insecticide resistance in mosquitoes. *Insect Biochemistry and Molecular Biology*, *34*(7), 653-665. <https://doi.org/10.1016/j.ibmb.2004.03.018>
- Hemingway, J., & Ranson, H. (2000). Insecticide resistance in insect vectors of human disease. *Annual review of entomology*, *45*(1), 371-391.
- Holmans, P. L., Shet, M. S., Martinwixtrom, C. A., Fisher, C. W., & Estabrook, R. W. (1994). The high-level expression in Escherichia coli of the membrane-bound form of human

- and rat cytochrome b5 and studies on their mechanism of function. *Archives of Biochemistry and Biophysics*, 312(2), 554-565.
- Huang, S.-W., Li, W.-Y., Wang, W.-H., Lin, Y.-T., Chou, C.-H., Chen, M., Huang, H.-D., Chen, Y.-H., Lu, P.-L., & Wang, S.-F. (2017). Characterization of the drug resistance profiles of patients infected with CRF07_BC using phenotypic assay and ultra-deep pyrosequencing. *PloS one*, 12(1), e0170420.
- Hunt, R., Brooke, B., Pillay, C., Koekemoer, L., & Coetzee, M. (2005). Laboratory selection for and characteristics of pyrethroid resistance in the malaria vector *Anopheles funestus*. *Medical and veterinary entomology*, 19(3), 271-275.
- Ibrahim, S. S., Amvongo-Adjia, N., Wondji, M. J., Irving, H., Riveron, J. M., & Wondji, C. S. (2018). Pyrethroid resistance in the major malaria vector *Anopheles funestus* is exacerbated by overexpression and overactivity of the P450 CYP6AA1 across Africa. *Genes*, 9(3), 140.
- Ibrahim, S. S., Fadel, A. N., Tchouakui, M., Terence, E., Wondji, M. J., Tchoupo, M., Kérah-Hinzoumbé, C., Wanji, S., & Wondji, C. S. (2019). High insecticide resistance in the major malaria vector *Anopheles coluzzii* in Chad Republic. *Infectious Diseases of Poverty*, 8(1). <https://doi.org/10.1186/s40249-019-0605-x>
- Ibrahim, S. S., Mukhtar, M. M., Datti, J. A., Irving, H., Kusimo, M. O., Tchapgá, W., Lawal, N., Sambo, F. I., & Wondji, C. S. (2019). Temporal escalation of Pyrethroid Resistance in the major malaria vector *Anopheles coluzzii* from Sahelo-Sudanian Region of northern Nigeria. *Scientific Reports*, 9(1), 7395. <https://doi.org/10.1038/s41598-019-43634-4>
- Ibrahim, S. S., Riveron, J. M., Bibby, J., Irving, H., Yunta, C., Paine, M. J., & Wondji, C. S. (2015). Allelic variation of cytochrome P450s drives resistance to bednet insecticides in a major malaria vector. *PLoS genetics*, 11(10), e1005618.
- Ibrahim, S. S., Riveron, J. M., Stott, R., Irving, H., & Wondji, C. S. (2016). The cytochrome P450 CYP6P4 is responsible for the high pyrethroid resistance in knockdown resistance-free *Anopheles arabiensis*. *Insect Biochemistry and Molecular Biology*, 68, 23-32.
- Ihling, C., Tanzler, D., Hagemann, S., Kehlen, A., Huttelmaier, S., Arlt, C., & Sinz, A. (2020). Mass spectrometric identification of SARS-CoV-2 proteins from gargle solution samples of COVID-19 patients. *Journal of proteome research*, 19(11), 4389-4392.
- Iorio, F., Bosotti, R., Scacheri, E., Belcastro, V., Mithbaokar, P., Ferriero, R., Murino, L., Tagliaferri, R., Brunetti-Pierri, N., & Isacchi, A. (2010). Discovery of drug mode of action and drug repositioning from transcriptional responses. *Proceedings of the National Academy of Sciences*, 107(33), 14621-14626.
- Irwin, J. J., & Shoichet, B. K. (2005). ZINC— a free database of commercially available compounds for virtual screening. *Journal of chemical information and modeling*, 45(1), 177-182.
- Jefferies, P. R., Toia, R. F., Brannigan, B., Pessah, I., & Casida, J. E. (1992). Ryania insecticide: analysis and biological activity of 10 natural ryanoids. *Journal of Agricultural and Food Chemistry*, 40(1), 142-146.
- Jefferies, P. R., Toia, R. F., & Casida, J. E. (1991). Ryanodol 3-(pyridine-3-carboxylate): a novel ryanoid from *Ryania* insecticide. *Journal of natural products*, 54(4), 1147-1149.

- Jones, G., Willett, P., Glen, R. C., Leach, A. R., & Taylor, R. (1997). Development and validation of a genetic algorithm for flexible docking. *Journal of molecular biology*, 267(3), 727-748.
- Joó, B., & Clark, M. A. (2012). Lattice QCD on GPU clusters, using the QUDA library and the Chroma software system. *The International Journal of High Performance Computing Applications*, 26(4), 386-398.
- Kaviraj, A., Unlu, E., Gupta, A., & El Nemr, A. (2014). Biomarkers of environmental pollutants. In: Hindawi.
- Kazachkova, N. (2007). *Genotype analysis and studies of pyrethroid resistance of the oilseed rape (Brassica napus) insect pest-pollen beetle (Meligethes aeneus)* (Vol. 2007).
- Kettler, L. (2020). SEZIONE VII—La cirrosi epatica. In *Trattato di anatomia patologica speciale Vol. 2, 2* (pp. 293-374). De Gruyter.
- Kiszewski, A., Mellinger, A., Spielman, A., Pia, M., Sachs, E., & Sachs, J. (2004). Global distribution (Robinson Projection) of dominant or potentially important malaria vectors. *American Journal of Tropical Medicine and Hygiene*, 70(5), 486-498.
- Klueg, K. M., Alvarado, D., Muskavitch, M. A., & Duffy, J. B. (2002). Creation of a GAL4/UAS- coupled inducible gene expression system for use in Drosophila cultured cell lines. *genesis*, 34(1- 2), 119-122.
- Koekemoer, L., Kamau, L., Hunt, R., & Coetzee, M. (2002). A cocktail polymerase chain reaction assay to identify members of the Anopheles funestus (Diptera: Culicidae) group. *The American journal of tropical medicine and hygiene*, 66(6), 804-811.
- Kopeć, A., Skoczylas, J., Jędrszczyk, E., Francik, R., Bystrowska, B., & Zawistowski, J. (2020). Chemical composition and concentration of bioactive compounds in garlic cultivated from air bulbils. *Agriculture*, 10(2), 40.
- Kouamo, M. F., Ibrahim, S. S., Hearn, J., Riveron, J. M., Kusimo, M., Tchouakui, M., Ebai, T., Tchapgá, W., Wondji, M. J., & Irving, H. (2021). Genome-Wide Transcriptional Analysis and Functional Validation Linked a Cluster of Epsilon Glutathione S-Transferases with Insecticide Resistance in the Major Malaria Vector Anopheles funestus across Africa. *Genes*, 12(4), 561.
- Krieger, R. (2010). *Hayes' handbook of pesticide toxicology* (Vol. 1). Academic press.
- Kulkarni, A. P., & Hodgson, E. (1980). Metabolism of insecticides by mixed function oxidase systems. *Pharmacology & therapeutics*, 8(2), 379-475.
- Kumar, S., Stecher, G., Li, M., Knyaz, C., & Tamura, K. (2018). MEGA X: molecular evolutionary genetics analysis across computing platforms. *Molecular biology and evolution*, 35(6), 1547-1549.
- Kumari, M. (2015). *The molecular target and mode of action of the acylurea insecticide, diflubenzuron*. Kansas State University.
- Kwiatkowska, R. M., Platt, N., Poupardin, R., Irving, H., Dabire, R. K., Mitchell, S., Jones, C. M., Diabaté, A., Ranson, H., & Wondji, C. S. (2013). Dissecting the mechanisms responsible for the multiple insecticide resistance phenotype in Anopheles gambiae ss, M form, from Vallee du Kou, Burkina Faso. *Gene*, 519(1), 98-106.
- Lai, F., Misra, M., Xu, L., Smith, H., & Meissner, G. (1989). The ryanodine receptor-Ca²⁺ release channel complex of skeletal muscle sarcoplasmic reticulum: evidence for a

- cooperatively coupled, negatively charged homotetramer. *Journal of Biological Chemistry*, 264(28), 16776-16785.
- Lesk, A. M., & Chothia, C. (1980). How different amino acid sequences determine similar protein structures: the structure and evolutionary dynamics of the globins. *Journal of molecular biology*, 136(3), 225-270.
- Li, A., Wang, B., Ilie, A., Dubey, K. D., Bange, G., Korendovych, I. V., Shaik, S., & Reetz, M. T. (2017). A redox-mediated Kemp eliminase. *Nature communications*, 8(1), 1-8.
- Li, X., Schuler, M. A., & Berenbaum, M. R. (2007). Molecular mechanisms of metabolic resistance to synthetic and natural xenobiotics. *Annu. Rev. Entomol.*, 52, 231-253.
- Liu, Y., Wang, C., Yan, J., Zhang, W., Guan, W., Lu, X., & Li, S. (2014). Hydrogen peroxide-independent production of α -alkenes by OleT JE P450 fatty acid decarboxylase. *Biotechnology for biofuels*, 7(1), 1-12.
- Livak, K. J., & Schmittgen, T. D. (2001). Analysis of relative gene expression data using real-time quantitative PCR and the $2^{-\Delta\Delta CT}$ method. *methods*, 25(4), 402-408.
- Lynd, A., & Lycett, G. J. (2012). Development of the bi-partite Gal4-UAS system in the African malaria mosquito, *Anopheles gambiae*. *PloS one*, 7(2), e31552.
- Ma, J., Wu, G., Li, S., Tan, W., Wang, X., Li, J., & Chen, L. (2018). Magnetic solid-phase extraction of heterocyclic pesticides in environmental water samples using metal-organic frameworks coupled to high performance liquid chromatography determination. *Journal of Chromatography A*, 1553, 57-66.
- Mackenzie-Impoinvil, L., Weedall, G. D., Lol, J. C., Pinto, J., Vizcaino, L., Dzuris, N., Riveron, J., Padilla, N., Wondji, C., & Lenhart, A. (2019). Contrasting patterns of gene expression indicate differing pyrethroid resistance mechanisms across the range of the New World malaria vector *Anopheles albimanus*. *PloS one*, 14(1), e0210586.
- MacKerell Jr, A. D., Bashford, D., Bellott, M., Dunbrack Jr, R. L., Evanseck, J. D., Field, M. J., Fischer, S., Gao, J., Guo, H., & Ha, S. (1998). All-atom empirical potential for molecular modeling and dynamics studies of proteins. *The journal of physical chemistry B*, 102(18), 3586-3616.
- Manoj, K. M., Gade, S. K., & Mathew, L. (2010). Cytochrome P450 reductase: a harbinger of diffusible reduced oxygen species. *PloS one*, 5(10), e13272.
- Mansuy, I. M., Mayford, M., Jacob, B., Kandel, E. R., & Bach, M. E. (1998). Restricted and regulated overexpression reveals calcineurin as a key component in the transition from short-term to long-term memory. *Cell*, 92(1), 39-49.
- Martinez- Torres, D., Chandre, F., Williamson, M., Darriet, F., Bergé, J. B., Devonshire, A. L., Guillet, P., Pasteur, N., & Pauron, D. (1998). Molecular characterization of pyrethroid knockdown resistance (kdr) in the major malaria vector *Anopheles gambiae* ss. *Insect Molecular Biology*, 7(2), 179-184.
- Matsuda, K., Buckingham, S. D., Kleier, D., Rauh, J. J., Grauso, M., & Sattelle, D. B. (2001). Neonicotinoids: insecticides acting on insect nicotinic acetylcholine receptors. *Trends in pharmacological sciences*, 22(11), 573-580.
- Matthews, S., Tee, K. L., Rattray, N. J., McLean, K. J., Leys, D., Parker, D. A., Blankley, R. T., & Munro, A. W. (2017). Production of alkenes and novel secondary products by P450 Ole TJE using novel H₂O₂- generating fusion protein systems. *FEBS letters*, 591(5), 737-750.

- McClements, D. J., Zou, L., Zhang, R., Salvia-Trujillo, L., Kumosani, T., & Xiao, H. (2015). Enhancing nutraceutical performance using excipient foods: Designing food structures and compositions to increase bioavailability. *Comprehensive Reviews in Food Science and Food Safety*, 14(6), 824-847.
- McHugh, M. L. (2013). The chi-square test of independence. *Biochemia medica*, 23(2), 143-149.
- McLaughlin, L., Niazi, U., Bibby, J., David, J. P., Vontas, J., Hemingway, J., Ranson, H., Sutcliffe, M., & Paine, M. (2008). Characterization of inhibitors and substrates of *Anopheles gambiae* CYP6Z2. *Insect Molecular Biology*, 17(2), 125-135.
- McLean, K. J., Carroll, P., Lewis, D. G., Dunford, A. J., Seward, H. E., Neeli, R., Cheesman, M. R., Marsollier, L., Douglas, P., & Smith, W. E. (2008). Characterization of active site structure in CYP121: A cytochrome P450 essential for viability of *Mycobacterium tuberculosis* H37Rv. *Journal of Biological Chemistry*, 283(48), 33406-33416.
- Mellanby, K. (1992). *The DDT story*. The British Crop Protection Council.
- Menze, B. D., Wondji, M. J., Tchapgá, W., Tchoupo, M., Riveron, J. M., & Wondji, C. S. (2018). Bionomics and insecticides resistance profiling of malaria vectors at a selected site for experimental hut trials in central Cameroon. *Malaria Journal*, 17(1), 1-10.
- Metcalf, R. L., Sangha, G. K., & Kapoor, I. P. (1971). Model ecosystem for the evaluation of pesticide biodegradability and ecological magnification. *Environmental Science & Technology*, 5(8), 709-713.
- Mitchell, S. N., Stevenson, B. J., Müller, P., Wilding, C. S., Egyir-Yawson, A., Field, S. G., Hemingway, J., Paine, M. J., Ranson, H., & Donnelly, M. J. (2012). Identification and validation of a gene causing cross-resistance between insecticide classes in *Anopheles gambiae* from Ghana. *Proceedings of the National Academy of Sciences*, 109(16), 6147-6152.
- Moiroux, N., Gomez, M. B., Pennetier, C., Elanga, E., Djènonatin, A., Chandre, F., Djègbé, I., Guis, H., & Corbel, V. (2012). Changes in *Anopheles funestus* biting behavior following universal coverage of long-lasting insecticidal nets in Benin. *The Journal of infectious diseases*, 206(10), 1622-1629.
- Morgan, J. C., Irving, H., Okedi, L. M., Steven, A., & Wondji, C. S. (2010). Pyrethroid resistance in an *Anopheles funestus* population from Uganda. *PLoS one*, 5(7), e11872.
- Moyes, C. L., Lees, R., Yunta, C., Walker, K., Hemmings, K., Oladepo, F., Hancock, P., Weetman, D., Paine, M., & Ismail, H. (2021). Assessing cross-resistance within the pyrethroids in terms of their interactions with key cytochrome P450 enzymes and resistance in vector populations. *Parasites & vectors*, 14(1), 1-13.
- Mugenzi, L. M., Menze, B. D., Tchouakui, M., Wondji, M. J., Irving, H., Tchoupo, M., Hearn, J., Weedall, G. D., Riveron, J. M., & Wondji, C. S. (2019). Cis-regulatory CYP6P9b P450 variants associated with loss of insecticide-treated bed net efficacy against *Anopheles funestus*. *Nature communications*, 10(1), 1-11.
- Müller, P., Warr, E., Stevenson, B. J., Pignatelli, P. M., Morgan, J. C., Steven, A., Yawson, A. E., Mitchell, S. N., Ranson, H., & Hemingway, J. (2008). Field-caught permethrin-resistant *Anopheles gambiae* overexpress CYP6P3, a P450 that metabolises pyrethroids. *PLoS Genet*, 4(11), e1000286.

- Munro, A. W., McLean, K. J., Grant, J. L., & Makris, T. M. (2018). Structure and function of the cytochrome P450 peroxygenase enzymes. *Biochemical Society Transactions*, 46(1), 183-196.
- Nikou, D., Ranson, H., & Hemingway, J. (2003). An adult-specific CYP6 P450 gene is overexpressed in a pyrethroid-resistant strain of the malaria vector, *Anopheles gambiae*. *Gene*, 318, 91-102.
- Nkemngo, F. N., Mugenzi, L. M., Terence, E., Niang, A., Wondji, M. J., Tchoupo, M., Nguete, N. D., Tchapgá, W., Irving, H., & Ntabi, J. D. (2020). Elevated Plasmodium sporozoite infection and multiple insecticide resistance in the principal malaria vectors *Anopheles funestus* and *Anopheles gambiae* in a forested locality close to the Yaoundé airport, Cameroon. *Wellcome Open Research*, 5.
- Notredame, C., Higgins, D. G., & Heringa, J. (2000). T-Coffee: A novel method for fast and accurate multiple sequence alignment. *Journal of molecular biology*, 302(1), 205-217.
- Nwane, P., Etang, J., Chouaibou, M., Toto, J. C., Kerah-Hinzoumbé, C., Mimpfoundi, R., Awono-Ambene, H. P., & Simard, F. (2009). Trends in DDT and pyrethroid resistance in *Anopheles gambiae* ss populations from urban and agro-industrial settings in southern Cameroon. *BMC Infectious Diseases*, 9(1), 1-10.
- Omura, T., & Sato, R. (1964). The carbon monoxide-binding pigment of liver microsomes I. Evidence for its hemoprotein nature. *Journal of Biological Chemistry*, 239(7), 2370-2378.
- Omura, T., & TAKESUE, S. (1970). A new method for simultaneous purification of cytochrome b 5 and NADPH-cytochrome c reductase from rat liver microsomes. *The Journal of Biochemistry*, 67(2), 249-257.
- Onoda, H., Shoji, O., & Watanabe, Y. (2015). Acetate anion-triggered peroxygenation of non-native substrates by wild-type cytochrome P450s. *Dalton Transactions*, 44(34), 15316-15323.
- Perry, A. (2018). Gene drives accelerate evolution—but we need brakes.
- Petřek, M., Otyepka, M., Banáš, P., Košinová, P., Koča, J., & Damborský, J. (2006). CAVER: a new tool to explore routes from protein clefts, pockets and cavities. *BMC bioinformatics*, 7(1), 316.
- Plapp, F. W., & FW, P. (1976). Biochemical genetics of insecticide resistance.
- PNLP, C. (2018). *Profil Entomologique Du Paludisme Au Cameroun* [Unpublished].
- Pritchard, M. P., Glancey, M. J., Blake, J., Gilham, D. E., Burchell, B., Wolf, C. R., & Friedberg, T. (1998). Functional co-expression of CYP2D6 and human NADPH-cytochrome P450 reductase in *Escherichia coli*. *Pharmacogenetics*, 8(1), 33-42.
- Pritchard, M. P., McLaughlin, L., & Friedberg, T. (2006). Establishment of functional human cytochrome P450 monooxygenase systems in *Escherichia coli*. In *Cytochrome P450 Protocols* (pp. 19-29). Springer.
- Pritchard, M. P., Ossetian, R., Li, D. N., Henderson, C. J., Burchell, B., Wolf, C. R., & Friedberg, T. (1997). A General Strategy for the Expression of Recombinant Human Cytochrome P450s in *Escherichia coli* Using Bacterial Signal Peptides: Expression of CYP3A4, CYP2A6, and CYP2E1. *Archives of Biochemistry and Biophysics*, 345(2), 342-354.

- Rahimirad, S., Fard, N. A., Mirzabeygi, R., & Mortazavi, B. (2021). The concurrent mutations of C26 N/N53F can reduce the antigenic propensity of nsLTP2 as an anti-tumor or viral drug carrier. *Informatics in Medicine Unlocked*, 22, 100510.
- Ranson, H., & Hemingway, J. (2005). Mosquito glutathione transferases. *Methods in enzymology*, 401, 226-241.
- Ranson, H., Jensen, B., Vulule, J., Wang, X., Hemingway, J., & Collins, F. (2000). Identification of a point mutation in the voltage-gated sodium channel gene of Kenyan *Anopheles gambiae* associated with resistance to DDT and pyrethroids. *Insect Molecular Biology*, 9(5), 491-497.
- Rendic, S., & Carlo, F. J. D. (1997). Human cytochrome P450 enzymes: a status report summarizing their reactions, substrates, inducers, and inhibitors. *Drug metabolism reviews*, 29(1-2), 413-580.
- Riveron, J. M., Chiumia, M., Menze, B. D., Barnes, K. G., Irving, H., Ibrahim, S. S., Weedall, G. D., Mzilahowa, T., & Wondji, C. S. (2015). Rise of multiple insecticide resistance in *Anopheles funestus* in Malawi: a major concern for malaria vector control. *Malaria Journal*, 14(1), 344.
- Riveron, J. M., Ibrahim, S. S., Chanda, E., Mzilahowa, T., Cuamba, N., Irving, H., Barnes, K. G., Ndula, M., & Wondji, C. S. (2014). The highly polymorphic CYP6M7 cytochrome P450 gene partners with the directionally selected CYP6P9a and CYP6P9b genes to expand the pyrethroid resistance front in the malaria vector *Anopheles funestus* in Africa. *BMC genomics*, 15(1), 817.
- Riveron, J. M., Ibrahim, S. S., Mulamba, C., Djouaka, R., Irving, H., Wondji, M. J., Ishak, I. H., & Wondji, C. S. (2017). Genome-wide transcription and functional analyses reveal heterogeneous molecular mechanisms driving pyrethroids resistance in the major malaria vector *Anopheles funestus* across Africa. *G3: Genes, Genomes, Genetics*, 7(6), 1819-1832.
- Riveron, J. M., Irving, H., Ndula, M., Barnes, K. G., Ibrahim, S. S., Paine, M. J., & Wondji, C. S. (2013). Directionally selected cytochrome P450 alleles are driving the spread of pyrethroid resistance in the major malaria vector *Anopheles funestus*. *Proceedings of the National Academy of Sciences*, 110(1), 252-257.
- Riveron, J. M., Tchouakui, M., Mugenzi, L., Menze, B. D., Chiang, M.-C., & Wondji, C. S. (2018). Insecticide resistance in malaria vectors: an update at a global scale. In *Towards malaria elimination-a leap forward*. IntechOpen.
- Riveron, J. M., Yunta, C., Ibrahim, S. S., Djouaka, R., Irving, H., Menze, B. D., Ismail, H. M., Hemingway, J., Ranson, H., & Albert, A. (2014). A single mutation in the GSTe2 gene allows tracking of metabolically based insecticide resistance in a major malaria vector. *Genome biology*, 15(2), R27.
- Roberts, D. R., Chareonviriyaphap, T., Harlan, H. H., & Hsieh, P. (1997). Methods of testing and analyzing excito-repellency responses of malaria vectors to insecticides. *Journal of the American Mosquito Control Association*, 13(1), 13-17.
- Rozas, J., Sánchez-DelBarrio, J. C., Messeguer, X., & Rozas, R. (2003). DnaSP, DNA polymorphism analyses by the coalescent and other methods. *Bioinformatics*, 19(18), 2496-2497.

- Russell, T., Govella, N., Azizi, S., Drakeley, C., & Kachur, S. (2011). Increased proportions of outdoor feeding among residual malaria vector populations following increased use of insecticide-- treated nets in rural Tanzania. *Malar J*, 10, 80.
- Sadasivaiah, S., Tozan, Y. i., & Breman, J. G. (2007). Dichlorodiphenyltrichloroethane (DDT) for indoor residual spraying in Africa: how can it be used for malaria control? *Defining and Defeating the Intolerable Burden of Malaria III: Progress and Perspectives: Supplement to Volume 77 (6) of American Journal of Tropical Medicine and Hygiene*.
- Šali, A., & Blundell, T. L. (1993). Comparative protein modelling by satisfaction of spatial restraints. *Journal of molecular biology*, 234(3), 779-815.
- Schleier III, J. J., & Peterson, R. K. (2011). *Pyrethrins and pyrethroid insecticides* (Vol. 11). Royal Society of Chemistry London.
- Schleier III, J. J., & Peterson, R. K. (2012). The joint toxicity of type I, II, and nonester pyrethroid insecticides. *Journal of economic entomology*, 105(1), 85-91.
- Schmittgen, T. D., & Livak, K. J. (2008). Analyzing real-time PCR data by the comparative C T method. *Nature protocols*, 3(6), 1101.
- Shaik, S., Kumar, D., de Visser, S. P., Altun, A., & Thiel, W. (2005). Theoretical perspective on the structure and mechanism of cytochrome P450 enzymes. *Chemical reviews*, 105(6), 2279-2328.
- Sherman, I. W. (1979). Biochemistry of Plasmodium (malarial parasites). *Microbiological reviews*, 43(4), 453.
- Shoji, O., Fujishiro, T., Nagano, S., Tanaka, S., Hirose, T., Shiro, Y., & Watanabe, Y. (2010). Understanding substrate misrecognition of hydrogen peroxide dependent cytochrome P450 from Bacillus subtilis. *JBIC Journal of Biological Inorganic Chemistry*, 15(8), 1331-1339.
- Shono, T., Ohsawa, K., & Casida, J. E. (1979). Metabolism of trans-and cis-permethrin, trans-and cis-cypermethrin, and decamethrin by microsomal enzymes. *Journal of Agricultural and Food Chemistry*, 27(2), 316-325.
- Simon-Delso, N., Amaral-Rogers, V., Belzunces, L. P., Bonmatin, J.-M., Chagnon, M., Downs, C., Furlan, L., Gibbons, D. W., Giorio, C., & Girolami, V. (2015). Systemic insecticides (neonicotinoids and fipronil): trends, uses, mode of action and metabolites. *Environmental Science and Pollution Research*, 22(1), 5-34.
- Singh, P., Shukla, R., & Yadav, N. (2012). Bio-efficacy of some insecticides against *H. armigera* (Hubner) on chickpea (*Cicer arietinum* L.). *Journal of food legumes*, 25(4), 291-293.
- Sinka, M. E., Bangs, M. J., Manguin, S., Coetzee, M., Mbogo, C. M., Hemingway, J., Patil, A. P., Temperley, W. H., Gething, P. W., & Kabaria, C. W. (2010). The dominant Anopheles vectors of human malaria in Africa, Europe and the Middle East: occurrence data, distribution maps and bionomic précis. *Parasites & vectors*, 3(1), 1-34.
- Sinka, M. E., Bangs, M. J., Manguin, S., Rubio-Palis, Y., Chareonviriyaphap, T., Coetzee, M., Mbogo, C. M., Hemingway, J., Patil, A. P., & Temperley, W. H. (2012). A global map of dominant malaria vectors. *Parasites & vectors*, 5(1), 1-11.
- Sippl, M. J. (1993). Recognition of errors in three- dimensional structures of proteins. *Proteins: Structure, Function, and Bioinformatics*, 17(4), 355-362.

- Sirim, D., Widmann, M., Wagner, F., & Pleiss, J. (2010). Prediction and analysis of the modular structure of cytochrome P450 monooxygenases. *BMC structural biology*, *10*(1), 1-12.
- Southall, T. D., Elliott, D. A., & Brand, A. H. (2008). The GAL4 system: a versatile toolkit for gene expression in *Drosophila*. *Cold Spring Harbor Protocols*, *2008*(7), pdb. top49.
- Sparks, T. C., & Nauen, R. (2015). IRAC: Mode of action classification and insecticide resistance management. *Pesticide Biochemistry and Physiology*, *121*, 122-128.
- Stevenson, B. J., Bibby, J., Pignatelli, P., Muangnoicharoen, S., O'Neill, P. M., Lian, L.-Y., Müller, P., Nikou, D., Steven, A., & Hemingway, J. (2011). Cytochrome P450 6M2 from the malaria vector *Anopheles gambiae* metabolizes pyrethroids: sequential metabolism of deltamethrin revealed. *Insect Biochemistry and Molecular Biology*, *41*(7), 492-502.
- Stevenson, B. J., Pignatelli, P., Nikou, D., & Paine, M. J. (2012). Pinpointing P450s associated with pyrethroid metabolism in the dengue vector, *Aedes aegypti*: developing new tools to combat insecticide resistance. *PLoS Negl Trop Dis*, *6*(3), e1595.
- Strobel, H. W., & Dignam, J. D. (1978). [7] Purification and properties of NADPH-Cytochrome P-450 reductase. In *Methods in enzymology* (Vol. 52, pp. 89-96). Elsevier.
- Tchakounte, A., Tchouakui, M., Mu-Chun, C., Tchapgga, W., Kopia, E., Soh, P. T., Njiokou, F., Riveron, J. M., & Wondji, C. S. (2019). Exposure to the insecticide-treated bednet PermaNet 2.0 reduces the longevity of the wild African malaria vector *Anopheles funestus* but GSTe2-resistant mosquitoes live longer. *PLoS one*, *14*(3), e0213949.
- Tchouakui, M., Miranda, J. R., Mugenzi, L. M., Djonabaye, D., Wondji, M. J., Tchoupo, M., Tchapgga, W., Njiokou, F., & Wondji, C. S. (2020). Cytochrome P450 metabolic resistance (CYP6P9a) to pyrethroids imposes a fitness cost in the major African malaria vector *Anopheles funestus*. *Heredity*, *124*(5), 621-632.
- Tchouakui, M., Riveron Miranda, J., Mugenzi, L. M. J., Djonabaye, D., Wondji, M. J., Tchoupo, M., Tchapgga, W., Njiokou, F., & Wondji, C. S. (2020). Cytochrome P450 metabolic resistance (CYP6P9a) to pyrethroids imposes a fitness cost in the major African malaria vector *Anopheles funestus*. *Heredity*, *124*(5), 621-632. <https://doi.org/10.1038/s41437-020-0304-1>
- Thatheyus, A., & Selvam, A. D. G. (2013). Synthetic pyrethroids: toxicity and biodegradation. *Appl Ecol Environ Sci*, *1*(3), 33-36.
- Thompson, J. D., Gibson, T. J., & Higgins, D. G. (2003). Multiple sequence alignment using ClustalW and ClustalX. *Current protocols in bioinformatics*(1), 2.3. 1-2.3. 22.
- Thomsen, R., & Christensen, M. H. (2006). MolDock: a new technique for high-accuracy molecular docking. *Journal of medicinal chemistry*, *49*(11), 3315-3321.
- Tonye, S. G. M., Kouambeng, C., Wounang, R., & Vounatsou, P. (2018). Challenges of DHS and MIS to capture the entire pattern of malaria parasite risk and intervention effects in countries with different ecological zones: the case of Cameroon. *Malaria Journal*, *17*(1), 156.
- Tracy, T. S. (2003). Atypical enzyme kinetics: their effect on in vitro-in vivo pharmacokinetic predictions and drug interactions. *Current drug metabolism*, *4*(5), 341-346.
- Tripathi, A., & Misra, K. (2017). Molecular Docking: A structure-based drug designing approach. *JSM Chem*, *5*(2), 1042-1047.

- van den Berg, H., Zaim, M., Yadav, R. S., Soares, A., Ameneshewa, B., Mnzava, A., Hii, J., Dash, A. P., & Ejov, M. (2012). Global trends in the use of insecticides to control vector-borne diseases. *Environmental health perspectives*, *120*(4), 577-582.
- Vincze, T., Posfai, J., & Roberts, R. J. (2003). NEBcutter: a program to cleave DNA with restriction enzymes. *Nucleic acids research*, *31*(13), 3688-3691.
- Vontas, J., David, J. P., Nikou, D., Hemingway, J., Christophides, G., Louis, C., & Ranson, H. (2007). Transcriptional analysis of insecticide resistance in *Anopheles stephensi* using cross-species microarray hybridization. *Insect Molecular Biology*, *16*(3), 315-324.
- Wagah, M. G., Korlević, P., Clarkson, C., Miles, A., Lawniczak, M. K., & Makunin, A. (2021). Genetic variation at the Cyp6m2 putative insecticide resistance locus in *Anopheles gambiae* and *Anopheles coluzzii*. *Malaria Journal*, *20*(1), 1-13.
- Wamba, A. N., Ibrahim, S. S., Kusimo, M. O., Muhammad, A., Mugenzi, L. M., Irving, H., Wondji, M. J., Hearn, J., Bigoga, J. D., & Wondji, C. S. (2021). The cytochrome P450 CYP325A is a major driver of pyrethroid resistance in the major malaria vector *Anopheles funestus* in Central Africa. *Insect Biochemistry and Molecular Biology*, *138*, 103647.
- Wang, B., Westerhoff, L. M., & Merz, K. M. (2007). A critical assessment of the performance of protein–ligand scoring functions based on NMR chemical shift perturbations. *Journal of medicinal chemistry*, *50*(21), 5128-5134.
- Warren, G. L., Andrews, C. W., Capelli, A.-M., Clarke, B., LaLonde, J., Lambert, M. H., Lindvall, M., Nevins, N., Semus, S. F., & Senger, S. (2006). A critical assessment of docking programs and scoring functions. *Journal of medicinal chemistry*, *49*(20), 5912-5931.
- Waterhouse, A. L., Holden, I., & Casida, J. E. (1985). Ryanoid insecticides: structural examination by fully coupled two-dimensional ¹H–¹³C shift correlation nuclear magnetic resonance spectroscopy. *Journal of the Chemical Society, Perkin Transactions* *2*(7), 1011-1016.
- Weedall, G. D., Mugenzi, L. M., Menze, B. D., Tchouakui, M., Ibrahim, S. S., Amvongo-Adjia, N., Irving, H., Wondji, M. J., Tchoupo, M., & Djouaka, R. (2019). A cytochrome P450 allele confers pyrethroid resistance on a major African malaria vector, reducing insecticide-treated bednet efficacy. *Science translational medicine*, *11*(484).
- Weedall, G. D., Riveron, J. M., Hearn, J., Irving, H., Kamdem, C., Fouet, C., White, B. J., & Wondji, C. S. (2020). An Africa-wide genomic evolution of insecticide resistance in the malaria vector *Anopheles funestus* involves selective sweeps, copy number variations, gene conversion and transposons. *PLoS genetics*, *16*(6), e1008822.
- Weill, M., Lutfalla, G., Mogensen, K., Chandre, F., Berthomieu, A., Berticat, C., Pasteur, N., Philips, A., Fort, P., & Raymond, M. (2003). Insecticide resistance in mosquito vectors. *Nature*, *423*(6936), 136-137.
- Weill, M., Malcolm, C., Chandre, F., Mogensen, K., Berthomieu, A., Marquine, M., & Raymond, M. (2004). The unique mutation in ace-1 giving high insecticide resistance is easily detectable in mosquito vectors. *Insect Molecular Biology*, *13*(1), 1-7.
- Werck-Reichhart, D., & Feyereisen, R. (2000). Cytochromes P450: a success story. *Genome biology*, *1*(6), 1-9.
- Wéry, M. (1995). *Protozoologie médicale*. De Boeck Université.

- WHO. (2016). Test procedures for insecticide resistance monitoring in malaria vector mosquitoes.
- WHO. (2020a). *World Malaria Report*.
- WHO. (2020b). World malaria report 2020: 20 years of global progress and challenges.
- WHO. (2020c). World malaria report 2020: 20 years of global progress and challenges. In *World malaria report 2020: 20 years of global progress and challenges*.
- WHO. (2021). World malaria report 2020. 2020. Available at: <https://www.who.int/publications/i/item/9789240015791> (Accessed: 1 June 2021).
- Wilkes, T., Matola, Y., & Charlwood, J. (1996). *Anopheles rivulorum*, a vector of human malaria in Africa. *Medical and veterinary entomology*, 10(1), 108-110.
- Winder, D. G., Mansuy, I. M., Osman, M., Moallem, T. M., & Kandel, E. R. (1998). Genetic and pharmacological evidence for a novel, intermediate phase of long-term potentiation suppressed by calcineurin. *Cell*, 92(1), 25-37.
- Wondji, C., Simard, F., Petrarca, V., Etang, J., Santolamazza, F., Torre, A. D., & Fontenille, D. (2005). Species and populations of the *Anopheles gambiae* complex in Cameroon with special emphasis on chromosomal and molecular forms of *Anopheles gambiae* ss. *Journal of medical entomology*, 42(6), 998-1005.
- Wondji, C. S., Coleman, M., Kleinschmidt, I., Mzilahowa, T., Irving, H., Ndula, M., Rehman, A., Morgan, J., Barnes, K. G., & Hemingway, J. (2012). Impact of pyrethroid resistance on operational malaria control in Malawi. *Proceedings of the National Academy of Sciences*, 109(47), 19063-19070.
- Wondji, C. S., Dabire, R. K., Tukur, Z., Irving, H., Djouaka, R., & Morgan, J. C. (2011). Identification and distribution of a GABA receptor mutation conferring dieltrin resistance in the malaria vector *Anopheles funestus* in Africa. *Insect Biochemistry and Molecular Biology*, 41(7), 484-491.
- Wondji, C. S., Irving, H., Morgan, J., Lobo, N. F., Collins, F. H., Hunt, R. H., Coetzee, M., Hemingway, J., & Ranson, H. (2008). Two duplicated P450 genes are associated with pyrethroid resistance in *Anopheles funestus*, a major malaria vector. *Genome Research*, 19(3), 452-459. <https://doi.org/10.1101/gr.087916.108>
- Wood, O., Hanrahan, S., Coetzee, M., Koekemoer, L., & Brooke, B. (2010). Cuticle thickening associated with pyrethroid resistance in the major malaria vector *Anopheles funestus*. *Parasites & vectors*, 3(1), 1-7.
- Wooding, M., Naudé, Y., Rohwer, E., & Bouwer, M. (2020). Controlling mosquitoes with semiochemicals: a review. *Parasites & vectors*, 13(1), 1-20.
- Yamauchi, T., Kamon, J., Waki, H., Imai, Y., Shimosawa, N., Hioki, K., Uchida, S., Ito, Y., Takakuwa, K., & Matsui, J. (2003). Globular adiponectin protected ob/ob mice from diabetes and ApoE-deficient mice from atherosclerosis. *Journal of Biological Chemistry*, 278(4), 2461-2468.
- Yano, J. K., Wester, M. R., Schoch, G. A., Griffin, K. J., Stout, C. D., & Johnson, E. F. (2004). The structure of human microsomal cytochrome P450 3A4 determined by X-ray crystallography to 2.05-Å resolution. *Journal of Biological Chemistry*, 279(37), 38091-38094.

- Zhang, Y., Yan, H., Lu, W., Li, Y., Guo, X., & Xu, B. (2013). A novel Omega-class glutathione S-transferase gene in *Apis cerana cerana*: molecular characterisation of GSTO2 and its protective effects in oxidative stress. *Cell Stress and Chaperones*, 18(4), 503-516.
- Zheng, L., Baumann, U., & Reymond, J.-L. (2004). An efficient one-step site-directed and site-saturation mutagenesis protocol. *Nucleic acids research*, 32(14), e115-e115.
- Zhu, F., Parthasarathy, R., Bai, H., Woithe, K., Kausmann, M., Nauen, R., Harrison, D. A., & Palli, S. R. (2010). A brain-specific cytochrome P450 responsible for the majority of deltamethrin resistance in the QTC279 strain of *Tribolium castaneum*. *Proceedings of the National Academy of Sciences*, 107(19), 8557-8562.
- Zilly, F. E., Acevedo, J. P., Augustyniak, W., Deege, A., Häusig, U. W., & Reetz, M. T. (2011). Tuning a P450 enzyme for methane oxidation. *Angewandte Chemie International Edition*, 50(12), 2720-2724.

APPENDICES

Appendix 1: Python script used to build models using the MODELLER 9v2.0

```
from modeller import * # Load the automodel class
from modeller.automodel import *
log.verbose() # request verbose output
env = environ () # create a new MODELLER environment to build this model in
env.io.atom_files_directory = '/directory/folder/subfolder'
env.io.hetatm = True
a = automodel(env,
              alnfile = '/directory/folder/subfolder/alignment.ali',
              knowns = ('1TQN'), # codes of the templates
              sequence = 'SEQUENCE NAME')
# code of the target
a.starting_model= 1          # index of the first model
a.ending_model = 50         # index of the last model
a.make()                    # do the actual homology modelling
```

Appendix 2: Errat profiles of CYP325A models and CYP3A4 (PDB:1TQN)

Serial Number	Model Name	Overall Quality Factor (%)
1	CMRCYP325A.pdb	48.178
2	GHACYP325A.pdb	51.012
3	DRCCYP325A.pdb	48.283
4	FANCYP325A.pdb	44.040
5	FUMCYP325A.pdb	53.131

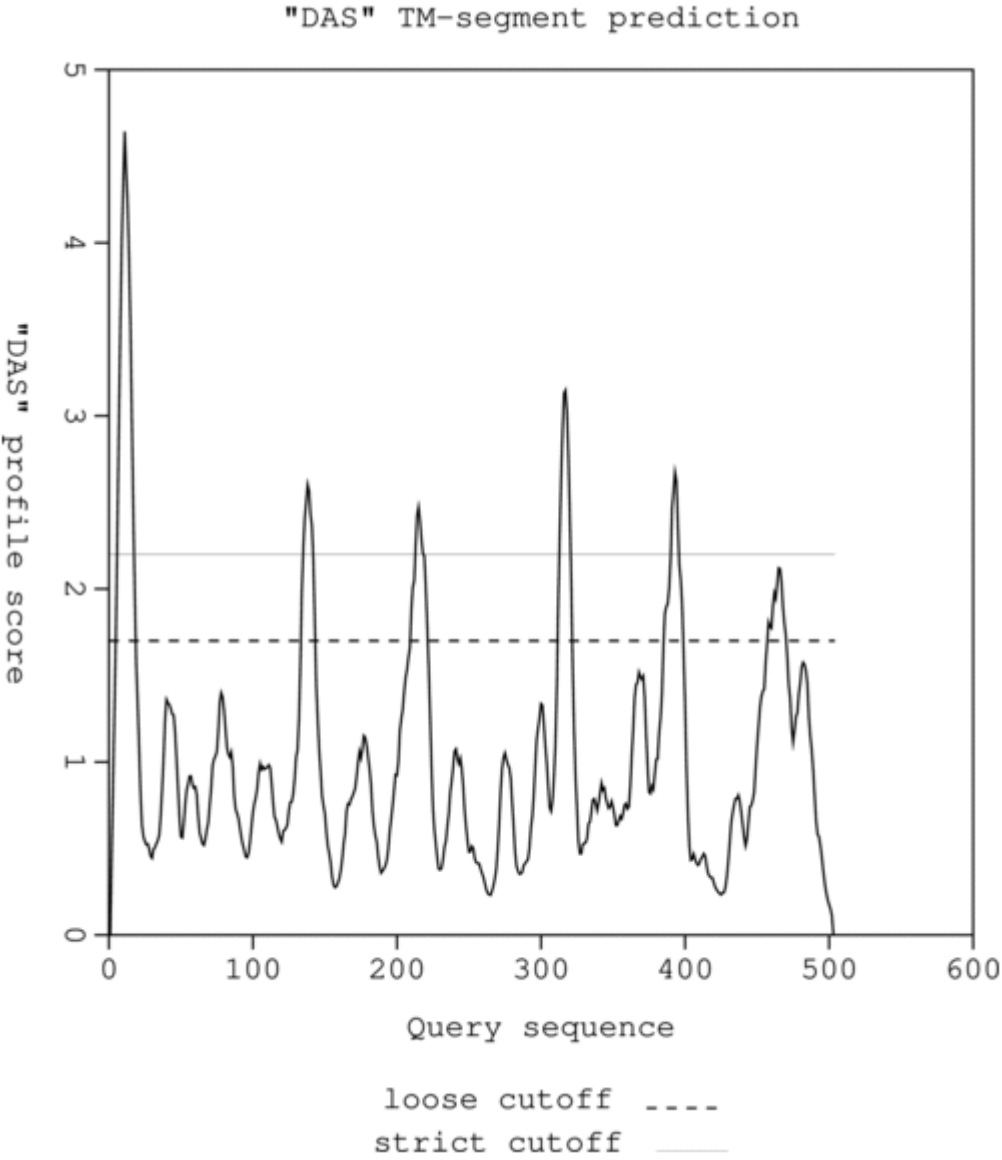
Appendix 3: Potential transmembrane segments and DAS plot of transmembrane domains of CYP325A protein sequence

A. Potential transmembrane segments

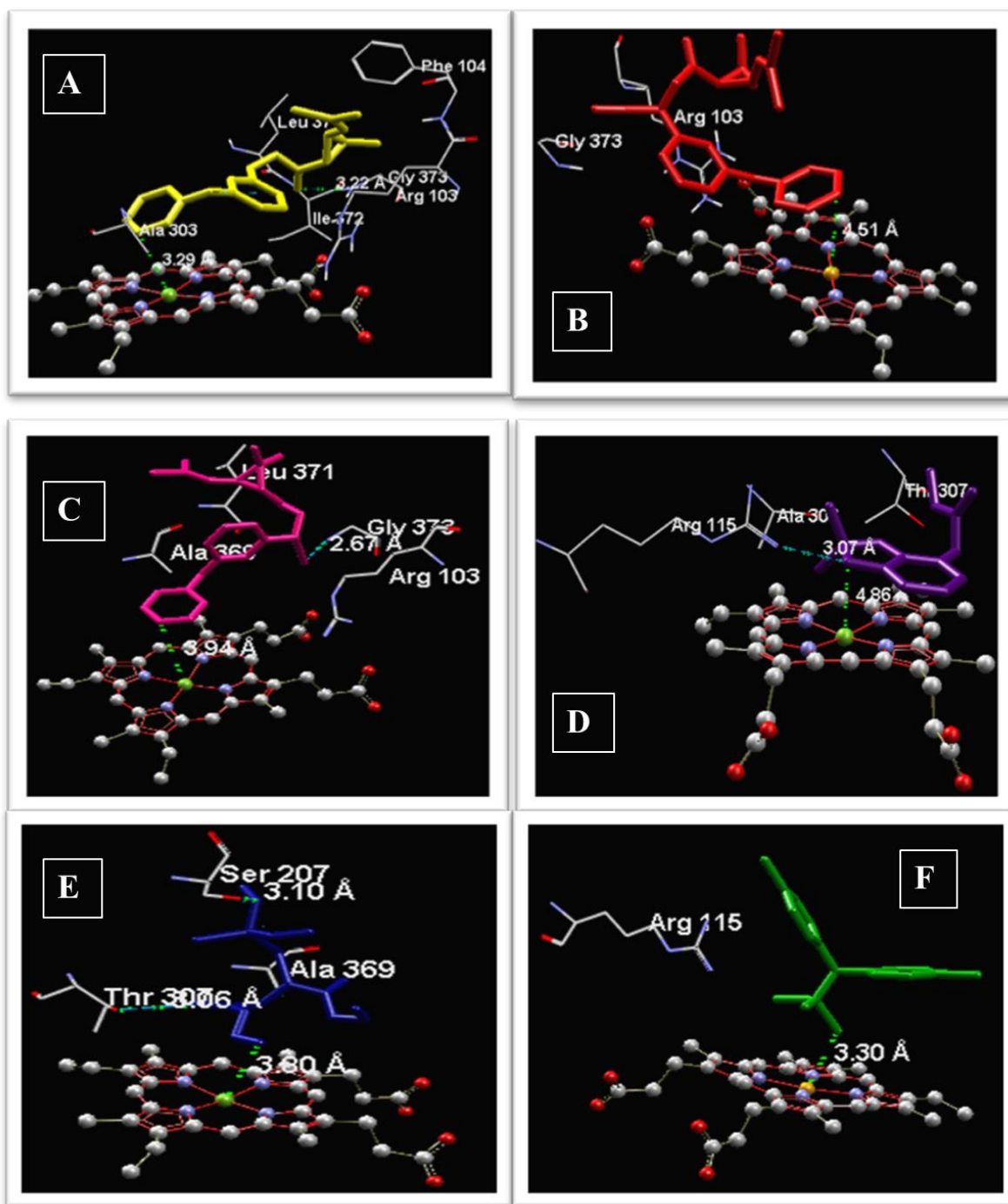
Start	Stop	Length	~	Cutoff
5	18	14	~	1.7
6	17	12	~	2.2
134	143	10	~	1.7
135	141	7	~	2.2
210	221	12	~	1.7
213	218	6	~	2.2
312	321	10	~	1.7
313	320	8	~	2.2
386	398	13	~	1.7
391	395	5	~	2.2
458	470	13	~	1.7

The 2.2 strict cut off is informative score in terms of matching segment while the loose score of 1.7 gives the actual location of the transmembrane segment.

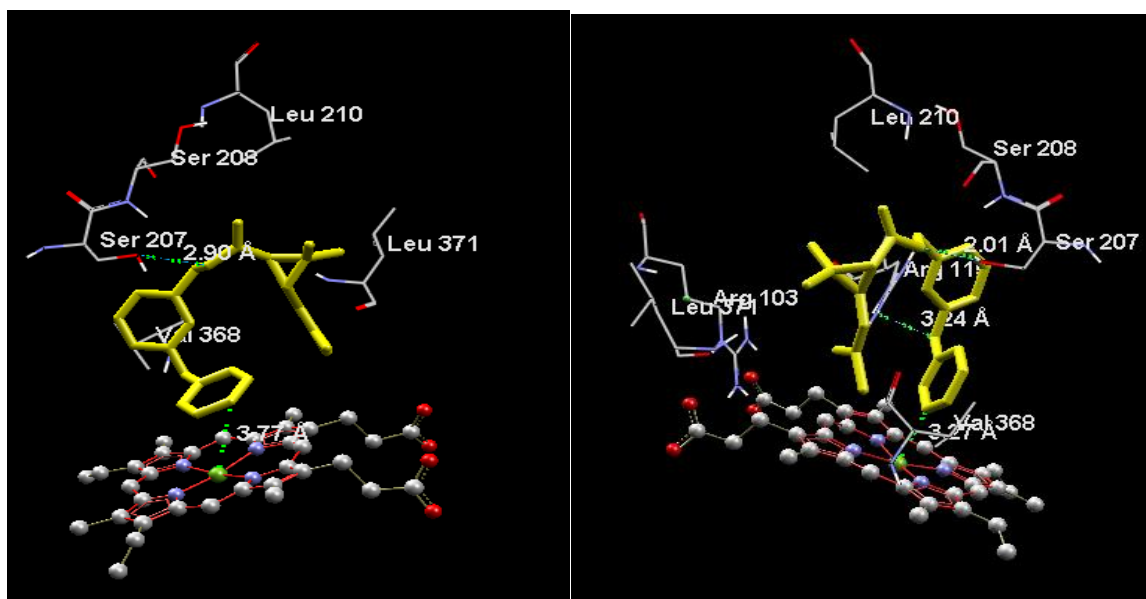
B. DAS plot of transmembrane domains of CYP325A protein sequence



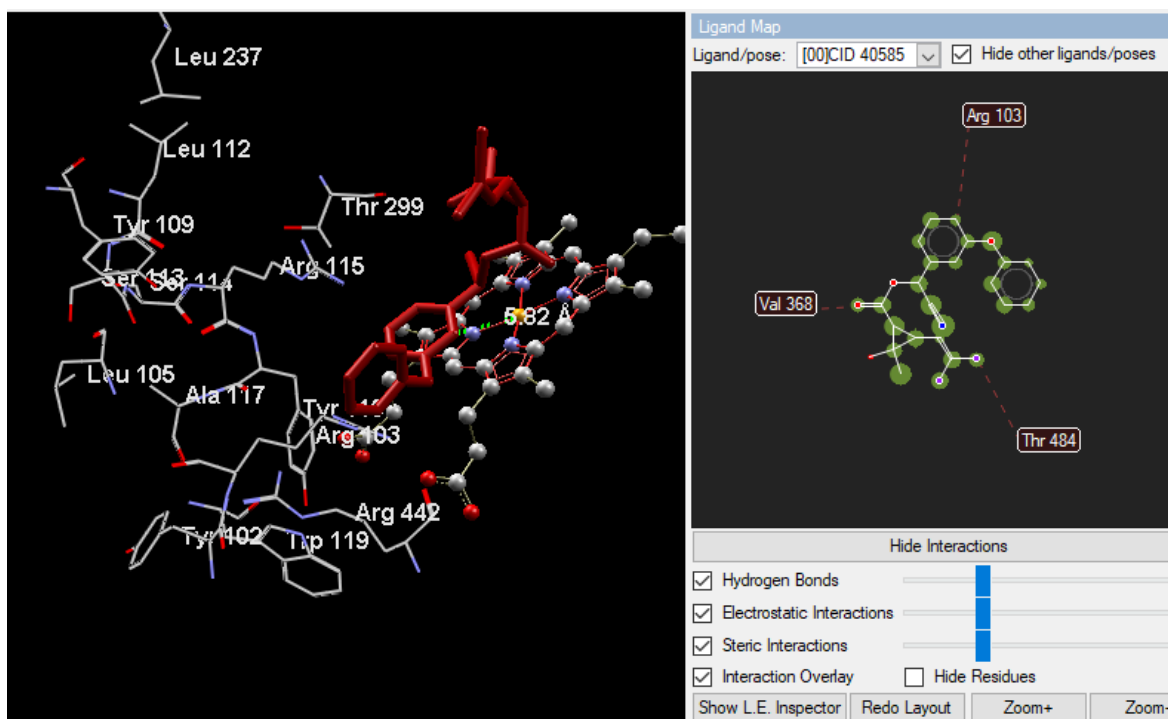
APPENDIX 4: Binding modes of permethrin in CMRCYP325A model.



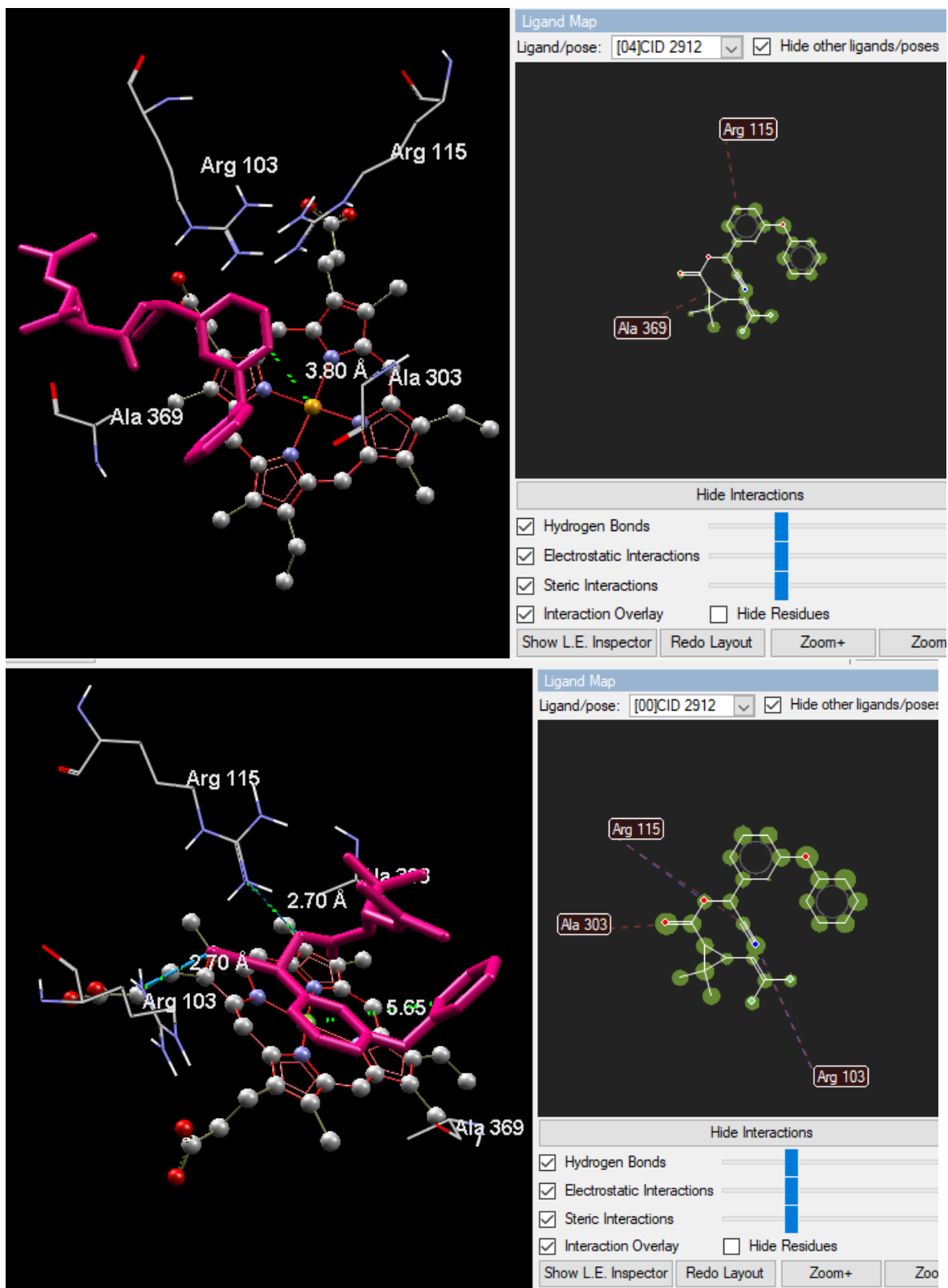
A. Binding modes of permethrin in CMRCYP325A model showing different binding poses. Permethrin is in stick format and yellow colour. Heme atoms are in stick and spectrum. Possible sites of metabolism are indicated with blue interrupted lines.



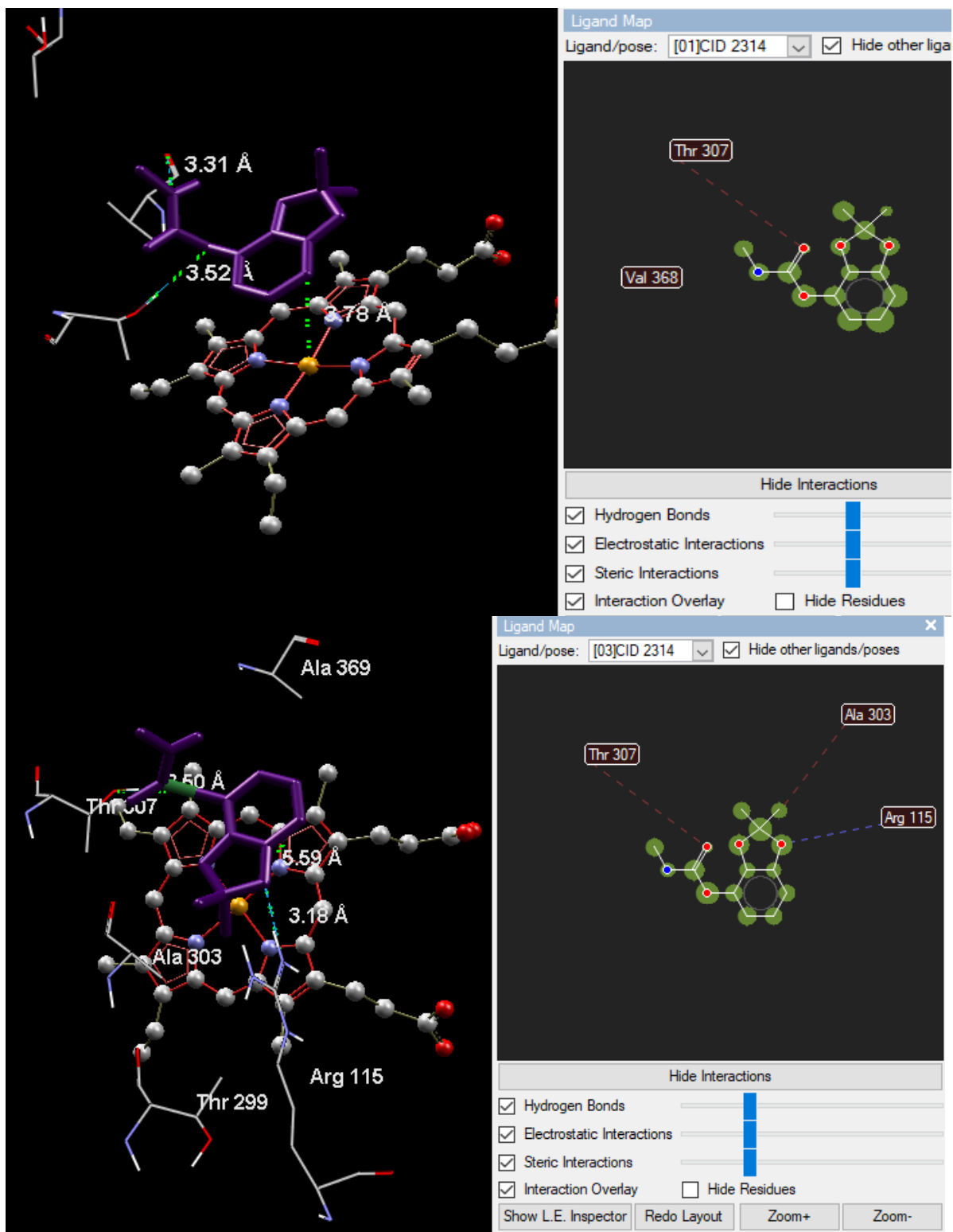
B. Binding modes of permethrin in CMRCYP325A model showing different binding poses. Permethrin is in stick format and yellow colour. Heme atoms are in stick and spectrum. Possible sites of metabolism are indicated with blue interrupted lines. On the right is the MVD ligand map showing different interactions between ligand and receptor.



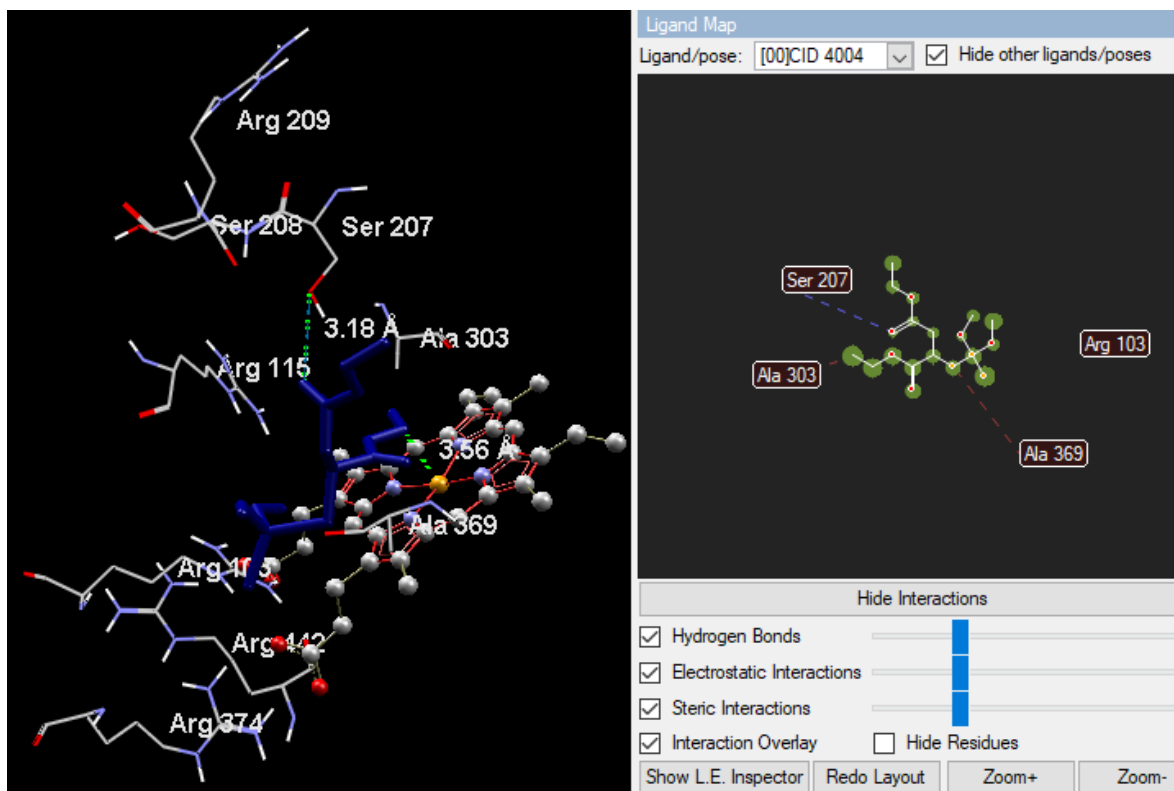
C. Binding modes of deltamethrin in CMRCYP325A model showing different binding poses. Deltamethrin is in stick format and red colour. Heme atoms are in stick and spectrum. Possible sites of metabolism are indicated with blue interrupted lines. On the right is the MVD ligand map showing different interactions between ligand and receptor.



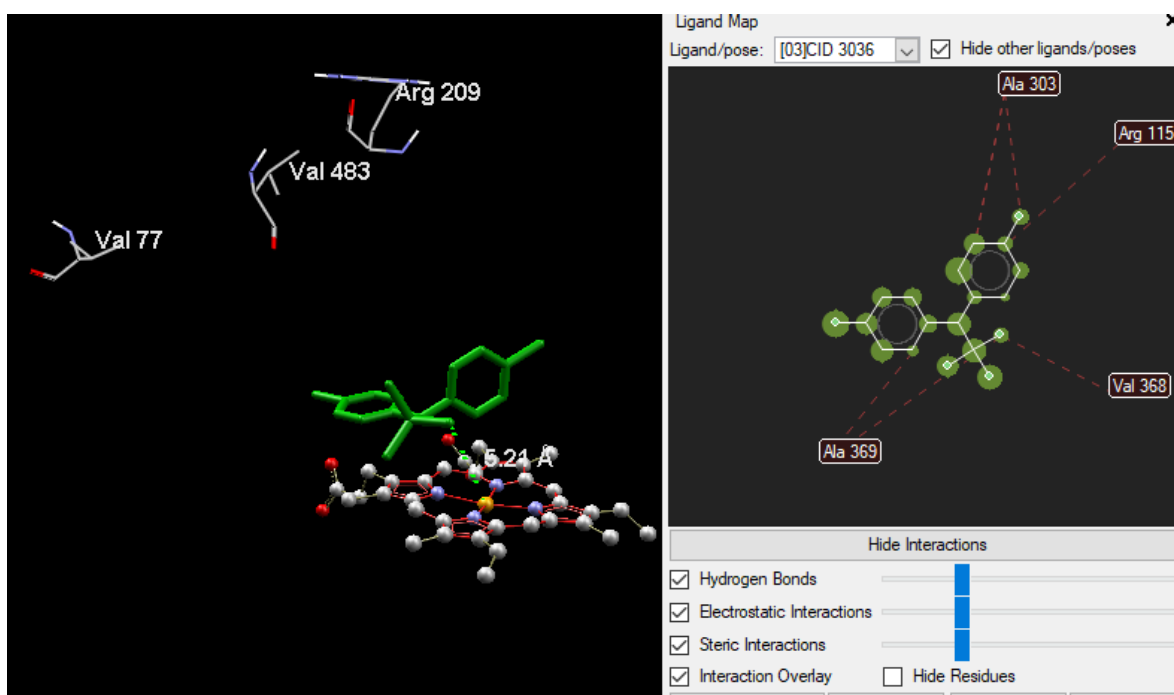
D. Binding modes of alpha cypermethrin in CMRCYP325A model showing different binding poses. Alpha cypermethrin is in stick format and pink colour. Heme atoms are in stick and spectrum. Possible sites of metabolism are indicated with blue interrupted lines. On the right is the MVD ligand map showing different interactions between ligand and receptor.



E. Binding modes of bendiocarb in CMRCYP325A model showing different binding poses. Bendiocarb is in stick format and purple colour. Heme atoms are in stick and spectrum. Possible sites of metabolism are indicated with blue interrupted lines. On the right is the MVD ligand map showing different interactions between ligand and receptor.



F. Binding modes of malathion in CMRCYP325A model showing different binding poses. Malathion is in stick format and blue colour. Heme atoms are in stick and spectrum. Possible sites of metabolism are indicated with blue interrupted lines. On the right is the MVD ligand map showing different interactions between ligand and receptor.



G. Binding modes of DDT in CMRCYP325A model showing different binding poses. DDT is in stick format and green colour. Heme atoms are in stick and spectrum. Possible sites of metabolism are indicated with blue interrupted lines. On the right is the MVD ligand map showing different interactions between ligand and receptor.

Appendix 5: Molecular docking scores with other docking parameters

Permethrin	Ligand	MolDock Score	Rerank Score	RMSD	Internal	HBond
[00]CID 40326	CID 40326	-141.574	-107.518	32.8029	17.124	0
[01]CID 40326	CID 40326	-134.984	-89.5888	31.7522	6.07168	0
[02]CID 40326	CID 40326	-129.337	-88.137	32.0208	8.8009	0
[03]CID 40326	CID 40326	-129.161	-91.1833	31.4049	11.7025	-0.83866
[05]CID 40326	CID 40326	-128.739	-103.232	32.1892	20.6422	-0.00099
[08]CID 40326	CID 40326	-127.802	-92.6201	33.802	25.2141	0
[04]CID 40326	CID 40326	-126.967	-89.1593	31.8921	20.0902	0
[10]CID 40326	CID 40326	-125.717	-91.99	31.7737	10.8227	-0.62696
[06]CID 40326	CID 40326	-125.506	-82.3034	31.9548	0.615086	0
[09]CID 40326	CID 40326	-124.363	-67.5753	32.7078	15.7453	-2.46617
[07]CID 40326	CID 40326	-123.343	-83.4894	33.2539	17.0335	0
[12]CID 40326	CID 40326	-120.82	-93.7383	32.6708	17.5928	0
[11]CID 40326	CID 40326	-120.624	-81.3163	32.2591	8.31863	-0.81789
[13]CID 40326	CID 40326	-116.871	-97.418	26.0137	15.8183	0
[15]CID 40326	CID 40326	-115.44	-92.3696	32.5447	20.8303	0
[14]CID 40326	CID 40326	-114.077	-78.8734	32.3654	2.11233	-0.81678
[16]CID 40326	CID 40326	-113.98	-46.8951	33.1863	18.2448	0
Name	Ligand	MolDock Score	Rerank Score	Internal	HBond	Docking Score
[02]CID 2314	CID 2314	-95.673	-79.4438	4.4624	0	-95.673
[00]CID 2314	CID 2314	-94.8094	-78.2971	6.51578	-0.452098	-99.3242
[04]CID 2314	CID 2314	-94.5305	-81.1344	10.1469	-1.35836	-94.5305
[01]CID 2314	CID 2314	-93.2217	-64.5815	6.97375	-0.670508	-95.9531
[03]CID 2314	CID 2314	-92.571	-55.6228	4.797	-1.28297	-95.5553
[00]CID 2912	CID 2912	-152.782	-92.1015	-10.2462	-1.08307	-155.282
[01]CID 2912	CID 2912	-141.666	-106.573	15.4619	0	-141.666

[02]CID 2912	CID 2912	-139.505	-95.8863	7.29913	-3.60297	-139.505
[03]CID 2912	CID 2912	-138.971	-107.634	14.6228	0	-138.971
[04]CID 2912	CID 2912	-136.809	-95.0716	14.5049	0	-136.809
[00]CID 3036	CID 3036	-98.3565	-74.8163	7.6911	0	-98.3565
[01]CID 3036	CID 3036	-97.5174	-54.3973	10.6369	0	-97.5174
[02]CID 3036	CID 3036	-96.9452	-73.3332	9.08998	0	-96.9452
[03]CID 3036	CID 3036	-96.7163	-59.7273	12.3871	0	-96.7163
[04]CID 3036	CID 3036	-96.0009	-63.9538	19.4041	0	-96.0009
[00]CID 4004	CID 4004	-108.671	-72.5121	-4.74356	-0.739978	-110.015
[03]CID 4004	CID 4004	-103.557	-76.173	-1.89353	-4.47526	-105.294
[02]CID 4004	CID 4004	-103.553	-72.8016	3.16469	-3.23455	-106.632
[04]CID 4004	CID 4004	-102.128	-72.7896	3.34842	-1.70126	-103.955
[01]CID 4004	CID 4004	-97.6419	-65.1058	-2.73573	-1.96313	-108.892
[00]CID 40326	CID 40326	-152.59	-121.478	16.1728	0	-152.59
[01]CID 40326	CID 40326	-133.085	-98.0038	14.4441	0	-133.085
[02]CID 40326	CID 40326	-130.015	-42.4363	1.94482	-0.2497	-132.266
[03]CID 40326	CID 40326	-127.866	-89.5066	14.9769	0	-129.832
[04]CID 40326	CID 40326	-124.843	-77.6797	20.1369	-2.77103	-128.287
[00]CID 40585	CID 40585	-143.824	-101.409	19.8135	0	-143.824
[01]CID 40585	CID 40585	-133.334	-91.7251	8.37111	0	-135.834
[02]CID 40585	CID 40585	-132.633	-95.7183	17.1897	0	-132.633
[04]CID 40585	CID 40585	-131.982	-97.2835	25.4034	0	-131.982
[03]CID 40585	CID 40585	-129.69	-85.2184	8.90607	-0.256256	-132.19

Appendix 6: Preparation of CYP450 Expressing Bacterial Membranes

A. MATERIALS

- ❖ 50 mg/ml ampicillin in water (filter-sterilized and stored in aliquots at -20°C).
- ❖ 34 mg/ml chloramphenicol in ethanol (if expressing P450 reductase as well: cotransformation).
- ❖ 2 X Tris-Sucrose –EDTA (TSE) buffer: 0.1M Tris-acetate at pH 7.6 with 0.5M sucrose and 0.5mM EDTA-filter-sterilize and store at 4°C. 1X TSE is equivalent quantity of 2X TSE + equivalent quantity of distilled water.
- ❖ Spheroplast Resuspension (SR) buffer: 0.1M potassium phosphate at pH 7.6, 6mM magnesium acetate and 20% (v/v) glycerol-filter-sterilized. Add dithiothreitol immediately before use for a final concentration of 0.1mM using a 100mM filter-sterilized stock solution stored in aliquots at -20°C.

B. CULTURES FOR P450 EXPRESSION

1. Transform JM109 cells with the plasmid that express the P450 and the plasmid which express the P450 reductase. You need to have fresh LB+AMP+Chloramphenicol plates.
2. Pick a single colony from the transformation and inoculate 3ml of LB with antibiotics (50µg/ml ampicillin and 34µg/ml chloramphenicol).
3. Incubate this culture overnight (16 hours) at 37°C with 150-200 rpm shaking.
4. Use 2 ml of the overnight culture to inoculate 200ml of Terrific Broth in a 1L flask. The media should be pre-warmed to 37°C, to avoid shocking cells, and include antibiotics as for the overnight culture.
5. Incubate the culture at 37°C with 200 rpm shaking.
6. Monitor the absorption at of the culture at 595-600 nm (plate reader) and when this value has reached about 0.7-0.8, after ~4 hours, transfer the culture to a 21 or 25°C incubator and continue with 150 rpm shaking.
7. After 30 min at 21/25°C (allowing for the culture to cool) add IPTG for a final concentration of 1mM and ALA for 0.5mM (16,759 mg ALA and 47,66 mg IPTG).
8. Continue incubating at 25°C until the culture is ready for harvesting.

Note: several variables can be optimised for P450 expression: incubation time, incubation temperature, induction time (adding IPTG/ALA), and IPTG or ALA concentration. Cultures should be monitored daily for P450/P420 production using CO difference spectra. Some P450 require only 1 day at 25°C whereas others need 3-4 days.

C. SPHEROPLAST PREPARATION

1. Pour the 200 ml bacterial culture into a 250 ml centrifuge bottle. Chill the bottles on ice for at least 10 minutes while checking and preparing the centrifuge and rotor. Centrifuge the cultures at 2800 x g for 20 minutes at 4°C.
2. Discard the supernatant and retain the pellet
3. Re-suspend the cell pellets in 20 ml of 1x TSE with a 25ml transfer pipette while keeping the bottles on ice (use automatic machine for the pipetting).
4. Add 10 ml dH₂O and mix and mix again (on ice)
5. Prepare a solution of 20mg/mL lysozyme in dH₂O and store on ice. Add 250µl of this lysozyme solution to give 0.25 mg/mL lysozyme in 20 ml of cell suspension.
6. Pipette the mix into 50ml Nalgene centrifuge tube (already chilled on ice)
7. Keep the centrifuge bottles in a polystyrene container with ice, and place the container on a rocking platform to allow gentle mixing for 60 minutes while the cell walls are degraded to allow spheroplast to form.
8. Load the 50mL bottles into the JA 25.50 rotor (Beckman) and centrifuge at 2800xg for 25 minutes at 4°C. Discard supernatant and retain pellet.
9. Add 8mL of spheroplast re-suspension buffer and 8µl of 0.1M DTT. 10. Proceed to the next step or store the spheroplast in -80 °C

D. FROM SPHEROPLASTS TO MEMBRANES

1. Remove the spheroplast from -80°C and thaw it on ice. Add the following items to 8 mL of spheroplasts: a. 40 µl of 0.2 M PMSF (dissolved in ethanol and usually stored in the freezer) b. 0.8 µl of 10 mg/mL aprotinin (make aliquots and keep in freezer and use each aliquot only once). c. 0.8 µl of 10 mg/mL leupeptin (usually stored in the freezer)

2. Sonicate the suspension three times for 30 seconds with the sonicator (30 seconds on and 30 seconds off/intervals) at about 70% power (this may need optimising) and tip should be kept submerged in the suspension to avoid frothing. Keep the sample on ice between the bursts of sonication. The sample will initially become viscous during sonication as DNA is released, but this viscosity should drop as the DNA is sheared by the sonication.
3. Dry and balance the weight of the tubes with dH₂O.
4. Load the 50 ml Nalgene tube with the sonicated sample into the JA 25.50 rotor (Beckman Avanti TM JM 25) along with a balance tube (+/-0.01g). Centrifuge at 30,000 x g for 20 minutes at 4°C.
5. Transfer the supernatant to a 26.3 ml ultracentrifuge bottles (transparent) on ice. These bottles must not be centrifuged when less than half full, can only be used up to 50000 rpm when over half full, and can only be centrifuged at their maximum rate, 60000 rpm, when full. Therefore, add 8 ml of ice-cold water to the 8 ml sample and make sure the bottles are not full to the neck. Prepare a balanced tube (+/-0.005 g) with ice-cold water.
6. Dry and load the balanced ultracentrifuge bottles in the 70Ti rotor and centrifuge at 49600 rpm (180000 x g), for 1 hour at 4°C.
7. Remove the tubes and discard the supernatant using a transfer pipette. The membranes should appear as a translucent red-brown pellet. Transfer the majority of this pellet to a 1mL Dounce homogeniser on ice using a glass Pasteur pipette to lightly scrape the pellet. Avoid blocking up the pipette with the membrane pellet by using the side of the tip to scrape and transfer bits of the pellet into the Dounce homogeniser. Once most of the pellet has been transferred, add 0.5 ml of ice-cold 1 X TSE buffer and 0.5ml of water and use the same Pasteur pipette to re-suspend the remaining pellet and transfer this to the Dounce homogeniser. Load the liquid from the bottom of the homogeniser to avoid bubbles. Alternatively, 250uL of both 1X TSE and 250uL of ddH₂O should be used and then later the same amounts to wash the homogeniser and transfer the contents into the Eppendorf.
8. Aliquot the homogenised membrane into small plastic tubes (100-200µl) and store at -80°C.

Appendix 7: Kinetic Constants of Recombinant P450 CYP325A for Pyrethroids, Bendiocarb, propoxur and DDT

A. Kinetic Constants for Recombinant CYP325A

Metabolism of Permethrin, Deltamethrin and alpha cypermethrin

Insecticide	Kcat (min ⁻¹)	KM (μM)	Kcat/KM (min ⁻¹ μM ⁻¹)
Permethrin	0.613 ± 0.005939	4.597 ± 1.819	0.1333 ± 0.0527
Deltamethrin	0.2571 ± 0.0290	2.349 ± 1.261,	0.109 ± 0.060
Alpha cypermethrin	0	0	0
Bendiocarb	0	0	0
Propoxur	0	0	0
DDT	0	0	0

Values are mean ±S.D. of three replicates Apparent Kcat was calculated as pmol/min/pmol P450; Catalytic efficiency was calculated as Kcat/KM

Appendix 8: Binding parameters template of the productive mode of permethrin, deltamethrin, alpha cypermethrin, bendiocarb and DDT docked to the active sites of CYP325A models

Insecticide	Rank	ChemScore (kJ/mol)	ΔG (kJ/mol)	S(hbond)	S(metal)	S(lipo)	ΔE(clash)
Cameroon							
Permethrin							
Deltamethrin							
Alpha cypermethrin							
Bendiocarb							
DDT							
DRC							
Permethrin							
Deltamethrin							

Alpha cypermethrin							
Bendiocarb							
DDT							
GHANA							
Permethrin							
Deltamethrin							
Alpha cypermethrin							
Bendiocarb							
DDT							
FANG							
Permethrin							
Deltamethrin							
Alpha cypermethrin							
Bendiocarb							
DDT							
FUMOZ							
Permethrin							
Deltamethrin							
Alpha cypermethrin							
Bendiocarb							
DDT							

Appendix 9: List of some important reagents used in this study

Reagent	Name Brand		Product Code
DNA/RNA extraction			
Ethanol 100%	Ethanol, Absolute (200 Proof), Molecular Biology Grade, Fisher BioReagents™	Fisher Bioreagents BP2818-500	10644795

Alcohol	Hexeal IPA 100% 1L Lab Grade Isopropyl Alcohol/Isopropanol (99%) Brand	Hexeal	B079YVPZDF
RNA later	Invitrogen™ RNAlater™ Stabilization Solution	Invitrogen™ AM7021	10427114
PBS 10X	PBS, Phosphate Buffered Saline, 10X Solution, Fisher BioReagents	Fisher Bioreagents BP399-4	12899712
RNA Isolation kit	QIAamp Viral RNA Mini Kit (250)	QIAGEN	52906
Silicagel	Silicagel orange, for drying purposes, non-toxic grade, ACROS Organics™	Acros Organics392030010	10647444
NaCl	Analysis, meets analytical specification of Ph.Eur, Fisher Chemical	Fisher Chemical S/3160/60	10428420
Sucrose	Sucrose, Certified AR for Analysis, meets analytical specification of Ph.Eur., BP, Fisher Chemical	Fisher Chemical S/8600/63	10254590
EDTA	Invitrogen™ UltraPure™ 0.5M EDTA, pH 8.0	Invitrogen™15575020	11568896
SDS	Sulfate Solution, Molecular Biology/Electrophoresis, Fisher BioReagents™	Fisher Bioreagents BP1311-1	10607443
PCR amplification			
Nuclease-Free Water	Invitrogen™ Nuclease-Free Water (not DEPC-Treated)	Invitrogen™ 4387936	10793837

KAPA Taq PCR Kit	KAPA Taq PCR Kit, Kapa Biosystems	Roche	BK1002
Phusion Hot Start II	Thermo Scientific™ Phusion Hot Start II DNA Polymerase (2 U/μL)	Thermo Scientific™ F549L	10628439
dNTP mix	Bioline dNTP Mix 100mM Final Conc. 50umol dNTP (500uL)		BIO39053
Electrophoresis			
	Agarose Agarose (Low-EEO/MultiPurpose/Molecular Biology Grade), Fisher BioReagents	Fisher Bioreagents BP160-500	10366603
Ladder 100bp	Thermo Scientific™ GeneRuler 100 bp Plus DNA Ladder, ready-to-use	Thermo Scientific™ SM0324	10181260
Ladder 1kb	Thermo Scientific™ GeneRuler 1 kb DNA Ladder	Thermo Scientific™ SM0312	11833963
Loading dye	Thermo Scientific™ TriTrack DNA Loading Dye (6X)	Thermo Scientific™ R1161	11581575
TAE 50X TAE Buffer	Tris-Acetate-EDTA, 50X Solution, Electrophoresis, Fisher BioReagents	Fisher Bioreagents BP1332-4	10542985
Staining	Bulldog Bio IncSupplier MIDORI GREEN ADVANCE DNA STAIN	Bulldog Bio IncSupplier MG04	NC0434746
qRT-PCR			
Sensimix	SensiMixTMSyBr® & Fluorescent kit	Bioline ReagentsLtd. QT615-05(500RXN)	208

SybrGreen	KiCqStart SYBR GREEN qPCR ReadyMix	Sigma-Aldrich KCQS0	
-----------	---------------------------------------	------------------------	--

Appendix 10: Intron retention phenomenon observed in CYP325A Ghana and FANG sequences (spliced out manually for in silico studies)

CYP325A Intron 1

```

340      350      360      370      380      390      400      410
|.....|.....|.....|.....|.....|.....|.....|.....|
AFUN015966-RA 5TCCCGCT-----AC
325A-FANG-1 5TCCCGCTGTAAGTTTAACTATCAAAGAATAATTTCATAGATGTAGTGCCTCTTGATGTGTTTTTTTTTACAGAC
325A-FANG-2 5TCCCGCTGTAAGTTTAACTATCAAAGAATAATTTCATAGATGTAGTGCCTCTTGATGTGTTTTTTTTTACAGAC
325A-FANG-3 5TCCCGCTGTAAGTTTAACTATCAAAGAATAATTTCATAGATGTAGTGCCTCTTGATGTGTTTTTTTTTACAGAC
325A-FANG-4 5TCCCGCTGTAAGTTTAACTATCAAAGAATAATTTCATAGATGTAGTGCCTCTTGATGTGTTTTTTTTTACAGAC
325A-GHANA-1 5TCCCGCT-----AC
325A-GHANA-2 5TCCCGCTGTAAGTTTAACTATCAAATGATTAATTTCATAGATGTAGTGCCTCTTGATGTGTTTTTTTTTACAGAC
325A-GHANA-3 5TCCCGCTGTAAGTTTAACTATCAAATGATTAATTTCATAGATGTAGTGCCTCTTGATGTGTTTTTTTTTACAGAC
325A-GHANA-4 5TCCCGCTGTAAGTTTAACTATCAAATGATTAATTTCATAGATGTAGTGCCTCTTGATGTGTTTTTTTTTACAGAC
325A-GHANA-5 5TCCCGCTGTAAGTTTAACTATCAAATGATTAATTTCATAGATGTAGTGCCTCTTGATGTGTTTTTTTTTACAGAC

```

CYP325A Intron 2

```

      R00      R10      R20      R30      R40      R50      R60      R70
|.....|.....|.....|.....|.....|.....|.....|.....|
AFUN015966-RA 1CCT-----ATCT
325A-FANG-1 1CCTGTAAGTGCTACCAATGACATGGTTACAGTTAAAACGAAATGATTTTTAAATTGTTTTATATTTCCGTCACAGATCT
325A-FANG-2 1CCTGTAAGTGCTACCAATGACATGGTTACAGTTAAAACGAAATGATTTTTAAATTGTTTTATATTTCCGTCACAGATCT
325A-FANG-3 1CCTGTAAGTGCTACCAATGACATGGTTACAGTTAAAACGAAATGATTTTTAAATTGTTTTATATTTCCGTCACAGATCT
325A-FANG-4 1CCTGTAAGTGCTACCAATGACATGGTTACAGTTAAAACGAAATGATTTTTAAATTGTTTTATATTTCCGTCACAGATCT
325A-GHANA-1 1CCT-----ATCT
325A-GHANA-2 1CCTGTAAGTGCTAACCAATGACATGGTTACAGTCAAACGAAAAGATTTTTAAATTGTTTTATATTTCCGTCACAGATCT
325A-GHANA-3 1CCTGTAAGTGCTAACCAATGACATGGTTACAGTCAAACGAAAAGATTTTTAAATTGTTTTATATTTCCGTCACAGATCT
325A-GHANA-4 1CCTGTAAGTGCTAACCAATGACATGGTTACAGTCAAACGAAAAGATTTTTAAATTGTTTTATATTTCCGTCACAGATCT
325A-GHANA-5 1CCTGTAAGTGCTAACCAATGACATGGTTACAGTCAAACGAAAAGATTTTTAAATTGTTTTATATTTCCGTCACAGATCT

```

CYP325A Intron 3

```

      1050      1060      1070      1080      1090      1100      1110      1120
|.....|.....|.....|.....|.....|.....|.....|.....|
AFUN015966-RA 8GCTG-----GCAGT(
325A-FANG-1 8GCTGTAAGTTGCTACACAACAAAAGAACATGACCAATTCAGTTATTTTGACATTTGTTCTTTGTTTCTAGGGCAGT(
325A-FANG-2 8GCTGTAAGTTGCTACACAACAAAAGAGCATGACCAATTCAGTTATTTTGACATTTGTTCTTTGTTTCTAGGGCAGT(
325A-FANG-3 8GCTGTAAGTTGCTACACAACAAAAGAACATGACCAATTCAGTTATTTTGACATTTGTTCTTTGTTTCTAGGGCAGT(
325A-FANG-4 8GCTGTAAGTTGCTACACAACAAAAGAACATGACCAATTCAGTTATTTTGACATTTGTTCTTTGTTTCTAGGGCAGT(
325A-GHANA-1 8GCTG-----GCAGT(
325A-GHANA-2 8GCTGTAAGTTGGCTACACAACAAAAGAACATGACCAATTCAGTTATTTTGACATTTGTTCTTCTTTCTAGGGCAGT(
325A-GHANA-3 8GCTGTAAGTTGGCTACACAACAAAAGAACATGACCAATTCAGTTATTTTGACATTTGTTCTTCTTTCTAGGGCAGT(
325A-GHANA-4 8GCTGTAAGTTGGCTACACAACAAAAGAACATGACCAATTCAGTTATTTTGACATTTGTTCTTCTTTCTAGGGCAGT(
325A-GHANA-5 8GCTGTAAGTTGGCTACACAACAAAAGAACATGACCAATTCAGTTATTTTGACATTTGTTCTTCTTTCTAGGGCAGT(

```

PUBLICATION



The cytochrome P450 *CYP325A* is a major driver of pyrethroid resistance in the major malaria vector *Anopheles funestus* in Central Africa

Amelie N.R. Wamba^{a,b,*}, Sulaiman S. Ibrahim^{c,d}, Michael O. Kusimo^a,
Abdullahi Muhammad^{c,g}, Leon M.J. Mugenzi^{a,f}, Helen Irving^c, Murielle J. Wondji^{a,c},
Jack Hearn^c, Jude D. Bigoga^{c,e}, Charles S. Wondji^{a,c,**}

^a Centre for Research in Infectious Diseases (CRID), P.O. BOX 13591, Yaoundé, Cameroon

^b Faculty of Science, Department of Biochemistry, University of Yaoundé I, P.O. Box 812, Yaoundé, Cameroon

^c Vector Biology Department, Liverpool School of Tropical Medicine (LSTM), Pembroke Place, Liverpool, L3 5QA, UK

^d Department of Biochemistry, Bayero University, PMB, 3011, Kano, Nigeria

^e Laboratory for Vector Biology and Control, National Reference Unit for Vector Control, The Biotechnology Centre, Nkolbisson – University of Yaoundé I, P.O. Box 3851, Messa, Yaoundé, Cameroon

^f Department of Biochemistry and Molecular Biology, Faculty of Science, University of Buea, P.O. Box 63, Buea, Cameroon

^g Centre for Biotechnology Research, Bayero University, Kano, PMB, 3011, Kano Nigeria

ARTICLE INFO

Keywords:

Anopheles funestus
Malaria
Pyrethroids
Metabolic resistance
Cytochrome P450– *CYP325A*
Central Africa

ABSTRACT

The overexpression and overactivity of key cytochrome P450s (*CYP450*) genes are major drivers of metabolic resistance to insecticides in African malaria vectors such as *Anopheles funestus* s.s. Previous RNAseq-based transcription analyses revealed elevated expression of *CYP325A* specific to Central African populations but its role in conferring resistance has not previously been demonstrated. In this study, RT-qPCR consistently confirmed that *CYP325A* is highly over-expressed in pyrethroid-resistant *An. funestus* from Cameroon, compared with a control strain and insecticide-unexposed mosquitoes. A synergist bioassay with PBO significantly recovered susceptibility for permethrin and deltamethrin indicating P450-based metabolic resistance. Analyses of the coding sequence of *CYP325A* Africa-wide detected high-levels of polymorphism, but with no predominant alleles selected by pyrethroid resistance. Geographical amino acid changes were detected notably in Cameroon. *In silico* homology modelling and molecular docking simulations predicted that *CYP325A* binds and metabolises type I and type II pyrethroids. Heterologous expression of recombinant *CYP325A* and metabolic assays confirmed that the most-common Cameroonian haplotype metabolises both type I and type II pyrethroids with depletion rate twice that of the DR Congo haplotype. Analysis of the 1 kb putative promoter of *CYP325A* revealed reduced diversity in resistant mosquitoes compared to susceptible ones, suggesting a potential selective sweep in this region. The establishment of *CYP325A* as a pyrethroid resistance metabolising gene further explains pyrethroid resistance in Central African populations of *An. funestus*. Our work will facilitate future efforts to detect the causative resistance markers in the promoter region of *CYP325A* to design field applicable DNA-based diagnostic tools.

1. Introduction

Malaria remains a major cause of death in Africa which shoulders about 94% of the global burden with 229 million malaria cases and 409,000 deaths recorded worldwide in 2019, mostly among pregnant

women and children under five years of age (WHO, 2020). Cameroon bears approximately 3% of this global burden accounting for 23.6% of consultations in health centres, 68.7% of deaths in children below five years and 16.9% of deaths in pregnant women (Diengou et al., 2020; Tonye et al., 2018). Major vectors of malaria across Africa and in

* Corresponding author. Centre for Research in Infectious Diseases (CRID), P.O. BOX 13591, Yaoundé, Cameroon.

** Corresponding author. Vector Biology Department, Liverpool School of Tropical Medicine (LSTM), Pembroke Place, Liverpool, L3 5QA, UK.

E-mail addresses: amelie.wamba@crid-cam.net (A.N.R. Wamba), charles.wondji@lstmed.ac.uk (S.S. Ibrahim), gkusimo@gmail.com (M.O. Kusimo), abdullahi.muhammad@lstmed.ac.uk (A. Muhammad), leon.mugenzi@crid-cam.net (L.M.J. Mugenzi), helen.irving@lstmed.ac.uk (H. Irving), murielle.wondji@lstmed.ac.uk (M.J. Wondji), jack.hearn@lstmed.ac.uk (J. Hearn), judebigoga@yahoo.com (J.D. Bigoga), charles.wondji@lstmed.ac.uk (C.S. Wondji).

<https://doi.org/10.1016/j.ibmb.2021.103647>

Received 15 July 2021; Received in revised form 20 August 2021; Accepted 7 September 2021

Available online 14 September 2021

0965-1748/© 2021 Published by Elsevier Ltd.

Cameroon are *An. gambiae* s.l. and *An. funestus*, which are both widely distributed (Antonio-Nkondjio et al., 2012), have high vector competences for *Plasmodium*, are highly anthropophilic (Tchuinkam et al., 2015) and thrive in urban and rural environments (Djouaka et al., 2016). The relative abundance of these vectors due to favourable climatic conditions and abundant breeding sites, is directly linked to malaria incidence rates in endemic areas and therefore a major public health concern (Antonio-Nkondjio et al., 2011).

Malaria prevention relies heavily on the use of insecticide-based interventions such as long lasting insecticidal nets (LLINs) and IRS (Indoor Residual Spraying) (Mendis et al., 2009). Pyrethroids remain the most widely used and main class of insecticides recommended by WHO for adult vector control through bed net treatment and IRS (WHO, 2020). However an alarmingly rapid increase and spread of pyrethroid resistance in malaria vectors *An. gambiae* and *An. funestus* poses a huge threat to the continued efficacy of current pyrethroid-based interventions (Riveron et al., 2013).

The two major mechanisms of insecticide resistance in mosquitoes are target-site resistance in the voltage-gated sodium channel (*kdr*) and metabolic resistance (Riveron et al., 2018a). Cytochrome P450 monooxygenase (CYP)-mediated detoxification is a major mechanism driving pyrethroid resistance in mosquitoes (Riveron et al., 2016), more so, in *An. funestus* where there is currently no evidence of target-site resistance (*kdr*) implying the resistance mechanism is principally metabolic (Hemingway, 2014; Moyes et al., 2020). Several studies already confirmed through QTL mapping and other analyses, the role of CYP6 cluster genes in *An. funestus* (Wondji et al., 2007) and *An. gambiae* (Nikou et al., 2003) pyrethroid-based resistance. Genome-wide transcriptomic analyses have implicated many over-expressed CYP450s in metabolic resistance in *An. funestus* across Africa (Riveron et al., 2017). The over-expression of these P450s has been characterised by a regional split as specific genes are over-expressed in different regions (Riveron et al., 2017; Weedall et al., 2019). This is supported by the massive over-expression of *CYP6P9a/b* duplicated genes in southern Africa which does not occur in other regions. Recent progress has led to extensive characterisation of the *CYP6P9a/b* driven resistance with detection of DNA-based markers driving this resistance (Mugenzi et al., 2019; Weedall et al., 2019) allowing the use of PCR-based assays to detect such resistance in individual mosquitoes. However, separate assays must be designed for other regions such as Central Africa where different genes have been shown to be over-expressed. Among CYP450s, *CYP325A* has been shown to have the greatest fold change among P450s in the Central Africa region versus a susceptible strain of *An. funestus* (Mugenzi et al., 2019; Weedall et al., 2020). Several studies have characterised the role of *Anopheles* CYP450s in insecticide resistance, using *in silico* homology modelling/substrate docking, in addition to heterologous expression of recombinant CYP450s and activity assays. For example, *CYP6P3* and *CYP6M2* shown to confer pyrethroid resistance in *Anopheles gambiae* (Müller et al., 2008; Stevenson, B. et al., 2011; Stevenson, Bradley J et al., 2011) and *CYP6Z1* shown to metabolise DDT in the same species (Chiu et al., 2008). In *An. funestus* previous study has used docking and activity assays to establish allelic variation impacting pyrethroid resistance in the resistance genes, *CYP6P9a* and *CYP6P9b* (Ibrahim et al., 2015) as well as the role of the *CYP6Z1* in cross-resistance to pyrethroid and bendiocarb (Ibrahim et al., 2016a). Also, *in silico* analysis of the 5'UTR regulatory element of the major *An. funestus* pyrethroid resistance gene *CYP6P9a*, coupled with promoter activity assay (dual luciferase reporter assay) has recently led to the discovery of the first metabolic resistance marker in CYP450s (Mugenzi et al., 2019; Weedall et al., 2019). However, the ability of this gene *CYP325A* to confer pyrethroid resistance and the underlying molecular process remain uncharacterised.

Therefore, to fill this gap in knowledge, we investigated the role played by *CYP325A* in pyrethroid resistance in resistant populations of *An. funestus* from Cameroon, Central Africa. Up-regulation of this gene is highly associated with resistance to both type I and II pyrethroids in field

populations of *An. funestus* in Cameroon. Through *in vitro* recombinant protein expression, metabolic assays, and modelling and molecular docking simulations we showed that *CYP325A* can metabolise both type I and II pyrethroids, albeit with greater efficiency against type I.

2. Materials and methods

2.1. Study sites

Blood-fed female *Anopheles* mosquitoes were collected from Mibellon (6°46'N, 11° 70'E), a rural village in Cameroon, Adamawa Region, (Fig. S1A). This region forms a transition between forested south and northern savannah of Cameroon and comprises of several water bodies such as lakes and swamplands which act as suitable breeding sites for mosquitoes (Menze et al., 2018). Major activities in this region include subsistence farming, fishing, and hunting. Menze et al. (2018) identified high use of insecticides in agriculture, mainly pyrethroids, neonicotinoids and carbamates in this region (Menze et al., 2018). Other mosquito samples used in this study are samples collected during previous studies conducted across Africa (Fig. S1B) (Ibrahim et al., 2016a, 2019; Menze et al., 2018; Riveron et al., 2015, 2016, 2017, 2018b). Field mosquitoes from four different regions of Africa with different resistant profiles were utilized, together with the susceptible laboratory strain FANG, originally from Angola, as well as the resistant laboratory strain FUM0Z originating from Mozambique. The field resistant mosquitoes were from Southern Africa: Chikwawa in Malawi (Barnes et al., 2017); East Africa: Tororo in Uganda (Okia et al., 2018); West Africa: Kpome in Benin (Tchigossou et al., 2018) and Obuasi in Ghana (Riveron et al., 2016); Central Africa: Mibellon in Cameroon (Menze et al., 2018) and Kinshasa in DRC. The pyrethroid resistance profiles of these mosquito populations have been previously established.

2.2. Mosquito collection and rearing

Blood fed, indoor resting female *An. funestus* mosquitoes were collected early in the morning, between 06:00 and 11:00 in the houses after verbal consent was obtained from household heads. Mosquitoes were collected in Mibellon in March 2018 using the Prokopack electrical aspirator (John W. Hook, Gainesville, FL, USA) and kept in netted paper cups that were stored in a cool box. Samples were transported to the insectary of Centre for Research in Infectious Disease (CRID) Yaoundé, Cameroon. Fully gravid mosquitoes, obtained after 4–5 days were induced to lay eggs using the forced egg-laying method (Morgan et al., 2010) in cups containing mineral water for hatching. After hatching, the larvae were reared to adult and mosquitoes mixed in cages (Cuamba et al., 2010; Morgan et al., 2010).

2.2.1. Species identification

All female mosquitoes used for individual ovipositing were morphologically identified as belonging to the *An. funestus* group according to the identification key of Coetzee (2020). The genomic DNA was extracted using the Livak method (Livak, 1984; Livak and Schmittgen, 2001) and a cocktail PCR assay (Koekemoer et al., 2002) was used to confirm that all females that laid eggs were *An. funestus* *sensu stricto*.

2.3. Insecticide resistance profile of field population of *An. funestus* in Mibellon

Insecticide susceptibility bioassays were conducted using 2- to 5-day-old F₁ adult female mosquitoes from pooled F₁ mosquitoes, following the WHO protocol (WHO, 2016). For each insecticide approximately 20–25 female mosquitoes per tube were exposed to either permethrin (0.75%) or deltamethrin (0.05%) impregnated papers for 30 min, 1 h and 1.5 h, and transferred to a clean holding tube immediately, supplied with 10% sugar solution, and mortality determined 24 h later. For each

test, mosquitoes exposed to untreated papers were used as controls. The assay was carried out at temperatures of $25\text{ }^{\circ}\text{C} \pm 2$ and $80\% \pm 10$ relative humidity.

As P450 monooxygenases have previously been involved in pyrethroid resistance in *An. funestus* (Riveron et al., 2013) their potential involvement in resistance was assessed in the Mibellon mosquito population using PBO (piperonyl butoxide), a synergist/inhibitor of P450s (Feyereisen, 2012; Menze et al., 2018). 100 female mosquitoes were pre-exposed to 4% PBO papers for 1 h and immediately exposed to 0.75% permethrin or 0.05% deltamethrin for 1 h. Mortality was assessed after 24 h and compared to the results obtained without PBO (Menze et al., 2018). Significance levels were assessed using the chi-squared test at $p < 0.05$ (McHugh, 2013).

2.4. Comparative investigation of expression profile of CYP325A Africa-wide

The expression profile of CYP325A was investigated by qRT-PCR using mosquitoes from six different locations in Africa, to confirm its higher overexpression in Central Africa (Cameroon and DRC) compared with East (Uganda) and southern Africa (Malawi) (Weedall et al., 2019). Primers used are listed in Table 1 in Fig. S2. Total RNA was extracted from three biological replicates (three pools of 10 females) of the mosquitoes that survived exposure following the WHO test procedures for insecticide resistance monitoring in malaria vector mosquitoes (WHO, 2016) to permethrin and DDT from Cameroon, Malawi, Uganda, Ghana, and Benin; and bendiocarb from Malawi and Ghana. For each insecticide/location a control of same replicates of unexposed females were used. The FANG susceptible strain was used as control susceptible *An. funestus* population. One microgram of the RNA was used for cDNA synthesis using SuperScript III (Invitrogen) with oligo-dT20 and RNAase H following the manufacturer's instructions. Using the standard protocol (Kwiatkowska et al., 2013; Riveron et al., 2013) for qRT-PCR, the amplification was conducted after establishing the standard curve for CYP325A. Relative expression and fold change of CYP325A for the test sample and control were established by comparisons to expression levels from FANG susceptible colony, after normalization with the house-keeping genes ribosomal protein S7 (RSP7; AFUN007153) and actin 5C (AFUN002505).

2.5. Africa-wide genetic polymorphism analysis of CYP325A

2.5.1. Polymorphism analysis of CYP325A alleles

cDNA of permethrin-resistant samples from Cameroon, Benin, Uganda, Malawi, DRC, the resistant FUMOZ laboratory colony and the susceptible FANG laboratory colony were used to assess the role of allelic variation in resistance.

The amplification was done with the cDNA from section 2.4, using Phusion Taq polymerase. Primers are provided in Table 1 of Fig. S2. The PCR products were cloned into PJET1.2 blunt end vector, miniprep and plasmids sequenced using the above primers. The sequences were cleaned using Chromas version 2.6.2 (Joó and Clark, 2012) and BioEdit (Hall, 1999) then aligned in multiple alignments using ClustalW

(Thompson et al., 2003). Population genetic parameters, including nucleotide diversity and haplotype diversity were assessed using DnaSP version 6.12.03 (Rozas et al., 2003). A haplotype network was built using the TCS program (Clement et al., 2000) and a maximum likelihood phylogenetic tree was constructed using MEGA X (Kumar et al., 2018).

In addition, to assess the potential association between polymorphisms in the promoter region and pyrethroid resistance, a 1 kb genomic fragment upstream of CYP325A was amplified, cloned as above, and sequenced in 19 susceptible (dead after 30 min exposure to permethrin) and 16 resistant (alive after 90 min exposure to permethrin) mosquitoes from Cameroon. The primers used are listed in Fig. S2.

2.6. Prediction of activity of CYP325A using in silico analysis

2.6.1. Homology modelling and docking

To predict the potential pyrethroid metabolising capability of CYP325A, models were created using MODELLER 9v25 (Fiser and Šali, 2003; Webb and Sali, 2014), using human CYP3A4 (PDB: 1TQN) (Yano et al., 2004), which shares 25.63% identity, as a template. 20 models were generated for each sequence and the most qualitative models selected based on Errat version 2.0 (Colovos and Yeates, 1993) assessment. Ligand structures were retrieved from ZINC¹⁵ library (<https://zinc.docking.org/>) (Sterling and Irwin, 2015). The 3D protein models and ligands were prepared for docking using Molegro Molecular Viewer 2.5 (<http://www.clcbio.com/>). To predict the pattern of interactions between the enzymes and insecticides, docking was carried out with Molegro Virtual Docker 7.0.0 (Bitencourt-Ferreira and de Azevedo, 2019), with MolScore scoring function (Eldridge et al., 1997) and active site defined as a cavity of 20 Å radius centred above the haem iron. 50 binding poses were obtained for each ligand for 1R-cis permethrin (ZINC01850374), deltamethrin (ZINC01997854) α -cypermethrin (ZINC2526765), bendiocarb (ZINC02015426), and DDT (ZINC01530011), which were sorted according to hybrid MolDock_{GRID} score (Korb et al., 2009) and the conformation of ligands in the active site of CYP325A. Figures were prepared using the PyMOL 2.4 (DeLano and Bromberg, 2004) and Molegro Molecular Viewer 7 (<http://www.clcbio.com/>).

2.7. Comparative sequence characterisation of *An. funestus* CYP325A to its orthologs

Additionally, to identify the features of CYP325A which could impact its activity, its coding sequence was compared to other closely related P450s. Putative substrate recognition sites 1 to 6 of *An. funestus* CYP325A, *An. gambiae* CYP325A (AGAP002208), *An. stephensi* CYP325A (ASTE004501) and *An. epiroticus* CYP325A (AEPI000241) were compared by mapping their amino acid sequences to that of *Pseudomonas putida* CYP101A (P450cam) (Ibrahim et al., 2016a; Poulos et al., 1987). The locations of amino acid differences in the sequences were mapped by identifying helices A-L and substrate recognition sites (SRS1-6) using crystal structures of CYP2 family (Gotoh, 1992), and structurally conserved regions of the were also predicted using an online tool, CYPED (<http://www.cyped.uni-stuttgart.de/>) (Poulos et al., 1985;

Table 1
Genetic parameters of CYP325A in laboratory and field population no selective sweep in CYP325A.

Complete sequenced fragment (1512bp)												
Sample	n	S	h	Hd	Syn	Nsyn	π	D	D*	Ka	Ks	Ka/Ks
FUMOZ	9	13	3	0.417	5	8	0.194	-1.88947 *	-2.14486 **	0.154	0.314	0.49
FANG	7	5	2	0.286	1	4	0.094	-1.48614ns	-1.56696ns	0.099	0.081	1.22
DRC	8	9	4	0.643	4	5	0.162	-1.47121 ns	-1.51047 ns	0.124	0.282	0.43
Cameroon	16	10	2	0.125	5	5	0.083	-2.18261 **	-2.98819 **	0.054	0.177	0.31
All	40	49	9	0.746	n.a	n.a	0.801	0.18277ns	-0.99808ns	0.473	1.929	0.24

n, number of sequences; S, number of polymorphic sites; Syn, Synonymous mutations; Nsyn, Non-synonymous mutations; π , nucleotide diversity; D and D* Tajima's and Fu and Li's statistics; ns, not significant; π , ka and ks are multiplied by 10^2 , * = $P < 0.05$; ** = $P < 0.02$, n.a not applicable.

Šali et al., 1995; Sirim et al., 2010a).

2.8. Assessment of metabolic activity of CYP325A

2.8.1. Heterologous expression of recombinant CYP325A in *E. coli* and metabolic assays

A recombinant CYP325A gene was expressed for the predominant haplotypes where this gene was differentially expressed (Cameroon and DR Congo). Expression plasmids pB13:ompA+2-CYP325A were prepared for Cameroon-CYP325A (hereby CMR-CYP325A) and DRC-CYP325A (DRC-CYP325A). The CYP325A sequences from the susceptible colony, FANG could not be expressed because the sequences retained all three introns. The recombinant plasmids were constructed by fusing cDNA fragment from a bacterial *ompA*+2 leader sequence with its downstream ala-pro linker to the NH₂-terminus of the CYP325A cDNA, in frame with the P450 initiation codon, as described (Pritchard et al., 1997); and then cloned into *Nde*I- and *Eco*RI-linearised pCW-ori + vector (McLaughlin et al., 2008). Details of PCR conditions used to create this type of expression plasmid cassettes have already been described (Ibrahim et al., 2015; Riveron et al., 2013) and list of primers are provided in Fig. S2. The *E. coli* JM109 cells were co-transformed with the P450 expression cassettes and a plasmid containing the *An. gambiae* cytochrome P450 reductase in pACYC-184 expression vector (pACYC-AgCPR) fused to pelB leader sequence (Pritchard et al., 1997; Willats et al., 1999). Membrane expression and preparations, measurement of P450 content, measurement of cytochrome *c* reductase activity, cytochrome *b*₅ expression and measurement of its content were carried out as previously described (Guengerich et al., 2009; Omura and Sato, 1964; Sato, 1964; Stevenson, Bradley J. et al., 2011). Metabolic assays were conducted as previously described (Ibrahim et al., 2015; Riveron et al., 2014a). 0.2 M Tris-HCl and NADPH regeneration components (1 mM glucose-6-phosphate, 0.25 mM MgCl₂, 0.1 mM NADP and 1 U/ml glucose-6-phosphate dehydrogenase) were added to the bottom of 1.5 ml tube chilled on ice. Membrane expressing recombinant CYP325A and AgCPR, and reconstituted cytochrome *b*₅ were added to the side of the tube and pre-incubated for 5 min at 30 °C, with shaking at 1200 rpm to activate the membrane. 20 μM of test insecticides (permethrin or deltamethrin) was added into the final volume of 0.2 ml (~2.5% v/v methanol), and reaction started by vortexing at 1200 rpm and 30 °C for 1 h. Reactions were quenched with 0.1 ml ice-cold methanol and incubated for 5 more min. Tubes were then centrifuged at 16,000 rpm and 4 °C for 15 min, and 150 μl of supernatant transferred into HPLC vials for analysis. Reactions were carried out in triplicates with experimental samples (+NADPH) and negative controls (-NADPH). 100 μl of sample was loaded onto an isocratic mobile phase (90:10 v/v methanol to water) with a flow rate of 1 ml/min, monitoring wavelength of 226 nm and peaks separated with a 250 mm C18 column (Acclaim 120, Dionex) on Agilent 1260 Infinity at 23 °C. Enzyme activity was calculated as percentage depletion (the difference in the quantity of insecticide(s) remaining in the +NADPH tubes compared with the -NADPH) and a *t*-test used to assess significance (Kim, 2015). For permethrin, deltamethrin and α-cypermethrin using the Cameroon and DRC recombinant CYP325A, steady state kinetic parameters were determined by measuring the rate reaction for 20 min at varying substrate concentrations (0–30 μM) in presence of 50 pmol recombinant CYP325A. Reactions were replicated in triplicate for both + NADPH and -NADPH at each concentration. *K*_m and *V*_{max} were established from the plot of substrate concentrations against the initial velocities and fitting of the data to the Michaelis-Menten module using the least squares non-linear regression in GraphPad Prism 6.03 Software (Swift, 1997).

2.9. Analysis of selective sweep spanning CYP325A using PoolSeq

2.9.1. Genetic diversity of CYP325A

Reads from pooled population data were aligned to the AfunF₁ chromosomal assembly of *Anopheles funestus* (Ghurye et al., 2019) using

bwa (Li and Durbin, 2009). Variants were called at a minor allele frequency of 0.01 in Varscan (Koboldt et al., 2009) and SNPs within 20bp of indels removed using bcftools (Li et al., 2009). Variants were annotated in snpEff (Cingolani et al., 2012) and coding sequence SNP variants for CYP325A input to SNPGenie (Nelson et al., 2015). Non-synonymous site diversity (π_n) and synonymous diversity (π_s) were extracted from SNPGenie results per population for CYP325A (AFUN015966), and diversity estimates compared between populations. We compared diversity estimates at CYP325A with three genes CYP9K1, CYP6P9a and CYP6P9b, which we know to have undergone selective sweeps across Africa (Mugenzi et al., 2019; Weedall et al., 2019, 2020). Alignments were also inspected visually in IGV (Robinson et al., 2011) for a region 10,000bp up- and down-stream of the CYP325A to identify any structural variation and gene duplication events.

2.10. Polymorphism analysis of 1 kb putative promoter in Cameroon in relation to resistance phenotype

Assessment of the correlation of polymorphism of CYP325A and pyrethroid resistance was conducted by individually amplifying and direct sequencing a 5'UTR segment of the promoter region of CYP325A, 1061 bp upstream of the ATG codon. This was done using 19 mosquitoes dead after 30 min exposure to permethrin (susceptible) and 15 mosquitoes alive after 90 min exposure to permethrin (resistant) from Mibellon. Amplification was carried out using the following conditions: initial denaturation of one cycle at 94 °C for 3 min; followed by 35 cycles each of 95 °C for 30 s (denaturation), 60 °C for 30 s (annealing), and extension at 72 °C for 1 min; and one cycle at 72 °C for 5 min (final elongation). PCR products were cleaned individually with QIAquick® PCR Purification Kit (QIAGEN, Hilden, Germany) and cloned into pJET1.2/blunt according to manufacturer's protocol (ThermoFisher Scientific, MA, USA). These were then used to transform in *Escherichia coli* DH5α, plasmids miniprep with the QIAprep Miniprep Kit (QIAGEN, Hilden, Germany). Three clones per sample were sequenced on both strands using the pJET1.2 sequencing primers. The polymorphic positions were detected through a manual analysis of sequence traces using BioEdit 7.2.5 (Hall et al., 2011) and sequence differences and multiple alignments using ClustalW, DnaSP 6.12.03 (Rozas et al., 2017) was used to define and to assess genetic parameters, such as nucleotide diversity (π), haplotype diversity and the D and D* selection estimates. A maximum likelihood tree of the haplotypes for both cDNA and genomic amplifications was constructed using MEGA 10.0.4 (Kumar et al., 1994), and a haplotype network was built using the TCS program (95% connection limit, gaps treated as a fifth state) to assess the potential connection between haplotypes and resistance phenotypes (Clement et al., 2002). The data was represented in histograms using GraphPad Prism 7.0 (Swift, 1997).

3. Results

3.1. Characterisation of the *Anopheles funestus* population from Mibellon

3.1.1. Mosquito identification and insecticide resistance profile

Cocktail PCR of the indoor collected F₀ females confirmed all 288 mosquitoes collected at Mibellon as *An. funestus* s.s.

The Mibellon *An. funestus* mosquitoes showed very high resistance to permethrin (mortality = 28.6% ± 4.13 for 60 min exposure and 50% ± 17.57 for 90 min) and deltamethrin (mortality = 16.8% ± 5.05 for 60 min and 52.3% ± 8.3 for 90 min) (Fig. 1A). Pre-exposure of mosquitoes to PBO restored full susceptibility to both pyrethroids (mortality = 98.8% ± 3.77 for permethrin and 96.5% ± 1.16 for deltamethrin at 60 min exposure, respectively) (Fig. 1B), suggesting the role of cytochrome P450s resistance to pyrethroids in this population.

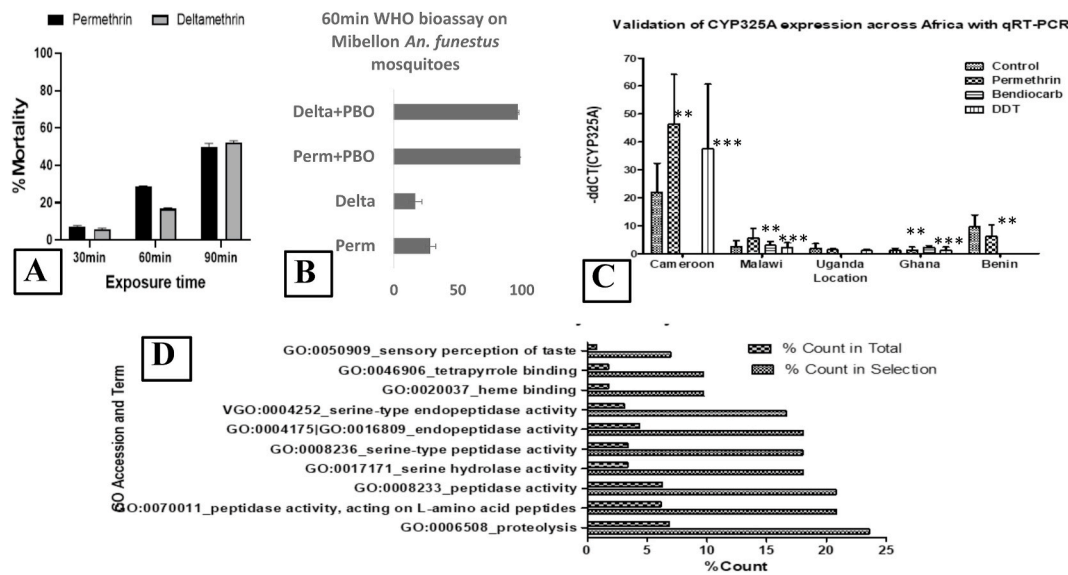


Fig. 1. Susceptibility profile of *An. funestus* mosquitoes to insecticide. **A.** Recorded mortalities following 30 min, 60 min and 90 min exposure of *An. funestus* s.s. from Mibellon to different insecticides **B.** Activities of PBO combined to permethrin and deltamethrin on *An. funestus* s.s. from Mibellon, Cameroon **C.** Differential expression of *CYP325A* in the *An. funestus* s.s. Mibellon population in Cameroon, measured by qRT-PCR. * $p < 0.05$, ** $p < 0.01$ and *** $p < 0.001$, $X^2 = 14.245$. The p -value is 0.00016 and significant at p -value $p < 0.05$ **D.** Gene ontology (GO) for *CYP325A* entity similarity.

3.2. Expression profile of *CYP325A*

3.2.1. Pattern of expression of *CYP325A* across Africa

qRT-PCR confirmed the overexpression of *CYP325A* in Central Africa, Cameroon with fold-change of ~45 in permethrin resistant mosquitoes. In contrast the expression level was low in other regions of Africa, for example, southern region (Malawi), East (Uganda) and West Africa (Ghana and Benin), with fold changes < 5 in line with prior RNA-Seq analyses (Mugenzi et al., 2019). Moreover, a greater over-expression of *CYP325A* was observed in Cameroonian mosquitoes that survived exposure to permethrin than in those not exposed to insecticide (control) ($p < 0.05$) (Fig. 1C).

3.2.2. Detection of transcripts presenting a similar expression pattern to *CYP325A* in *An. funestus* populations

STRAND NGS software, version 3.4 (Strand Life Sciences, Bangalore, India) was used to detect the list of entities (transcripts) exhibiting a similar expression pattern to *CYP325A* and likely to be involved in the same molecular pathway. AFUN015966 (*CYP325A*) was selected in the permethrin-resistant samples and a criteria of similarity index of > 0.7 was set comparing expression in mosquitoes resistant to permethrin, resistant to DDT, control mosquitoes not exposed to insecticides in Cameroon and to the FANG susceptible strain. A total of 148 transcripts were found to have index of similarity of > 0.7 with *CYP325A*. Among these, detoxification genes were detected including cytochrome P450s, glutathione S-transferases (GSTs), ABC transporters. Among P450s, *CYP6P5* had the highest similarity expression to *CYP325A* [Similarity Index (SI) = 0.8] followed by *CYP6P9b* (SI = 0.73). The GSTs included *GSTe2* (SI = 0.75) and *GSTe6* (SI = 0.74). Two transcription factors also presented a similar expression pattern to *CYP325A*, notably CCAAT/enhancer-binding protein gamma (SI = 0.78) and transcription factor Adf-1 both known to bind to the promoter and the enhancer regions of target genes. The list also includes other genes such as serine proteases (Trypsin and Chymotrypsin 2), an ABC transporter (AFUN019220) and two microRNAs (mir-279 and mir-71).

A Gene Ontology (GO) enrichment analysis of the list of the 148 similarly expressed genes to *CYP325A* revealed an over-representation of 10 GO terms (Fig. 1D) reflecting the function of those transcripts including detoxification (haem binding, tetrapyrrole binding) and serine protease activity (serine-type endopeptidase activity, serine hydrolase

activity, proteolysis).

3.3. Africa-wide genetic polymorphism analysis of *CYP325A*

3.3.1. Polymorphism analysis of cDNA

Screening for the genetic variability of 1512 bp *CYP325A* cDNA for 9 clones for FUM0Z, 7 clones for FANG, 8 clones for DRC and 16 clones for Cameroon revealed a relatively high polymorphism in this gene (Table 1). The Cameroon samples had a reduced variation when compared to the other localities with 2 haplotypes and the lowest haplotype diversity (Hd) (Fig. 2B, Table 1) and nucleotide diversity (Fig. S3), while samples from DRC were the most polymorphic. Tajima's D was negative for all the populations but significantly so only for Cameroon and FUM0Z suggesting a recent population expansion possibly after a bottleneck or a selective sweep. This is reflected in the presence of a major clade for the Cameroon samples (which cluster separately from field sequences from resistant populations in all the other countries) in the maximum likelihood phylogenetic tree (Fig. 2A).

3.3.2. Whole genome PoolSeq analysis of selective sweep across *CYP325A*

Analyses of whole genome PoolSeq sequences from 12 populations across Africa revealed that diversity estimates of each site type were no different between Cameroon and other populations (Fig. S4). By contrast a very clear decrease was seen in diversity in Uganda, for *CYP9K1* and in Southern African populations and the FUM0Z resistant strain for *CYP6P9a* and *CYP6P9b*. Inspection of read alignments in IGV did not reveal any difference between Cameroon and other populations across the region inspected.

3.3.3. Polymorphism analysis of 1 kb putative promoter

An. funestus mosquitoes from Mibellon, Cameroon exposed to permethrin were used to establish the polymorphism patterns of a 1 kb promoter region upstream of the 5'-UTR of *CYP325A*. The results revealed significant differences between alive and dead mosquitoes (Table 2). Analysis of the upstream region (1 kb) showed reduced diversity in the resistant samples compared to the susceptible. This is evident in a lower number of haplotypes (3 vs 8) and polymorphic sites (13 vs 46) suggesting a possible ongoing directional selection in resistant mosquitoes, although the positive values obtained for the Tajima's D and Fu and Li statistics points towards a balancing selection. The

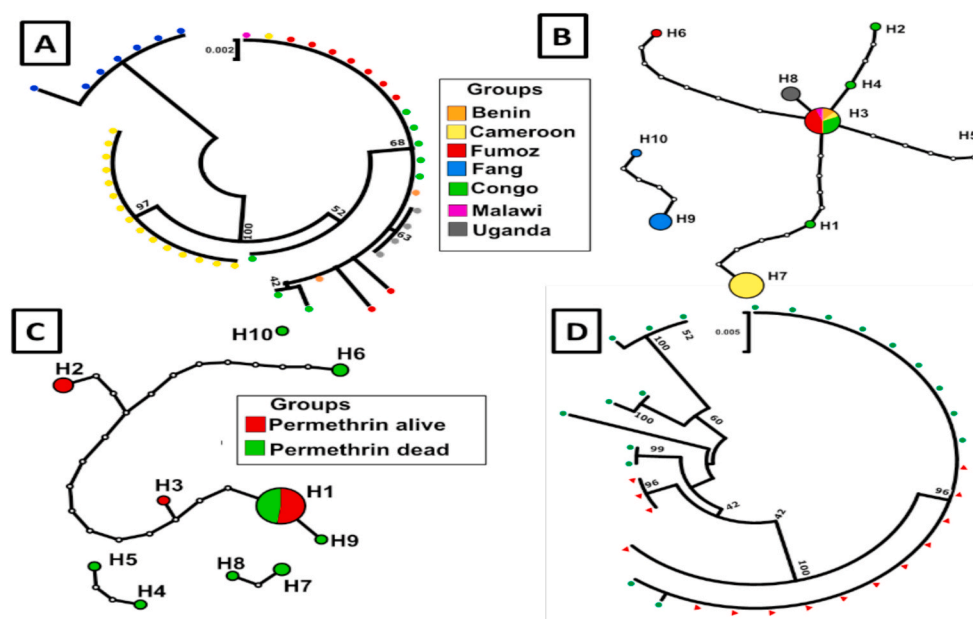


Fig. 2. Population studies of *CYP325A* coding sequences across Africa and a 1kb putative promoter from Cameroon. **A.** Phylogenetic tree for *CYP325A* cDNA across Africa. **B.** Haplotype diversity network of *CYP325A* cDNA for FANG, FUMOS, Cameroon, Malawi, Benin, Uganda, and DRC. **C.** Haplotype diversity network analysis of 1kb putative promoter of *CYP325A* between permethrin alive and dead samples. **D.** Phylogenetic tree of 1kb putative promoter of *CYP325A* between permethrin alive and dead samples revealing a dominant haplotype being shared between the resistant and the susceptible.

Table 2

Genetic parameters of a 1 kb putative promoter of *CYP325A* upstream of ATG between permethrin alive and dead samples.

Sample	n	S	h	Hd	π	D	D*
Alive	15	13	3	0.448	0.448	0.67629 ns	1.47811 **
Dead	19	46	8	0.725	1.307	-0.09242 ns	-0.17703 ns
All	34	48	10	0.617	0.975	-0.66073 ns	-0.35501 ns

n = number of sequences; S, number of polymorphic sites; Syn, Synonymous mutations; Nsyn, Non-synonymous mutations; π , nucleotide diversity; D and D* Tajima's and Fu and Li's statistics; ns, not significant; π is multiplied by 10^2 , ** = $P < 0.01$.

haplotype network (Fig. 2C) and phylogenetic tree (Fig. 2D) showed a predominance of haplotype H1 (73%) in the alive mosquitoes compared to the dead ones with a marked difference in haplotype diversity (Fig. S5C). Other haplotypes were only specific to the resistant (H2 and H3) and susceptible (H4, H5, H6, H7, and H8) (Figure S5, A and B) with susceptible haplotypes presenting the highest number of mutational steps (5 haplotypes with >20 mutational steps) to the major H1 haplotype further supporting the reduced diversity in resistant mosquitoes.

3.4. Amino acid sequence characterisation of *An. funestus* *CYP325A*

Comparison of *An. funestus* *CYP325A* to other closely related sequences revealed it is 72.8% identical to *An. gambiae* *CYP325A* (AGAP002208), 74.8% identical to *An. epiroticus* *CYP325A* (AEPI000241) and 81.9% identical to *An. stephensi* *CYP325A* (ASTE004501) (Fig. S6). Apart from *An. epiroticus* *CYP325A* (499 amino acids) and *An. gambiae* *CYP325A* (505 amino acids), the other two P450s are made of 503 amino acids. Sequence-to-sequence mapping reveals that the WxxxR motif, the signatory oxygen-binding pocket (AGFETS)/proton transfer groove, the ExxR motif which stabilises the haem structural core, the cysteine pocket/haem-binding region (PFxxGxxxCxG), which forms the fifth axial ligand to the haem iron were all identical and conserved in the three different *Anopheles* sequences. Major variations which could impact the activity of *An. funestus* *CYP325A* compared with *An. gambiae* *CYP325A* were not observed in all the substrate recognition sites (SRSs) and helices except the α K helix (Ala³⁷¹ in *An. funestus* *CYP325A* and Gly³⁷¹ in *An. gambiae*) and the SRS-2 (Gly²⁰⁵ in *An. stephensi* and Cys²⁰⁵ in the others). In the meander at

positions 424 and 425, amino acid variations were observed S⁴²⁴Q in *An. epiroticus* and S⁴²⁴A in *An. gambiae*.

3.5. Prediction of activity of *CYP325A* using in silico analysis

3.5.1. Homology modelling and docking

The models of *CYP325A* alleles from Cameroon and DRC were used to predict ability to metabolise insecticides. Docking simulation was carried out using permethrin, α -cypermethrin, deltamethrin, bendiocarb and DDT. The calculated binding parameters for each insecticide, demonstrating their most favourable, productive, and properly oriented poses, are given in Fig. S8.

Permethrin, deltamethrin and α -cypermethrin exhibited high scores compared to bendiocarb and DDT consistent with the resistance profile in Mibellon population, where DDT resistance has been shown to be driven by *GSTe2* (D Menze et al., 2018; Menze et al., 2018; Riveron et al., 2014b). Comparison of the different conformations of the insecticide molecules in the active site of *CYP325A* revealed the possible mechanisms through which this gene could drive pyrethroid resistance. For permethrin, the CMR_ *CYP325A* model was exhibited in the correct orientation with the benzyl ring located within 3-5 Å of the haem catalytic site as shown in the binding pose (Fig. 3A and Fig. 3B). These poses predict a ring hydroxylation to produce 2-hydroxypermethrin. The permethrin productive poses show two major amino acids involved, namely Serine²⁰⁸ and Serine²⁰⁷, with the latter forming a H-bond interactions with the ester oxygen, at 2-4 Å.

For type II pyrethroids deltamethrin and α -cypermethrin, a different pattern was observed. Deltamethrin docked with the phenoxy ring above the haem and the 4' spot located within 4.5 Å from the haem iron (Fig. 3C and Fig. S9B). In this posture, the ring hydroxylation to generate 4'-hydroxydeltamethrin is possible. Also, the benzyl ring docked within 5 Å of the haem iron with the possibility of hydroxylation. Like the permethrin docking, deltamethrin and α -cypermethrin were found to dock productively in several binding modes mainly interacting with Ser²⁰⁷, Ser²⁰⁸ and Arg¹¹⁵ with strong H-bonds and near the haem catalytic site. (Fig. 3D and Fig. S9C).

Bendiocarb docked very close (3 Å), with the aromatic ring oriented to the haem catalytic site and forms very strong H-bond interactions with the Ser²⁰⁷, Ser²⁰⁸ and Arg¹¹⁵ in some suggestively productive poses in the proper orientation. The carbamic ester group oriented away from the haem iron (Fig. 3E and Fig. S9D).

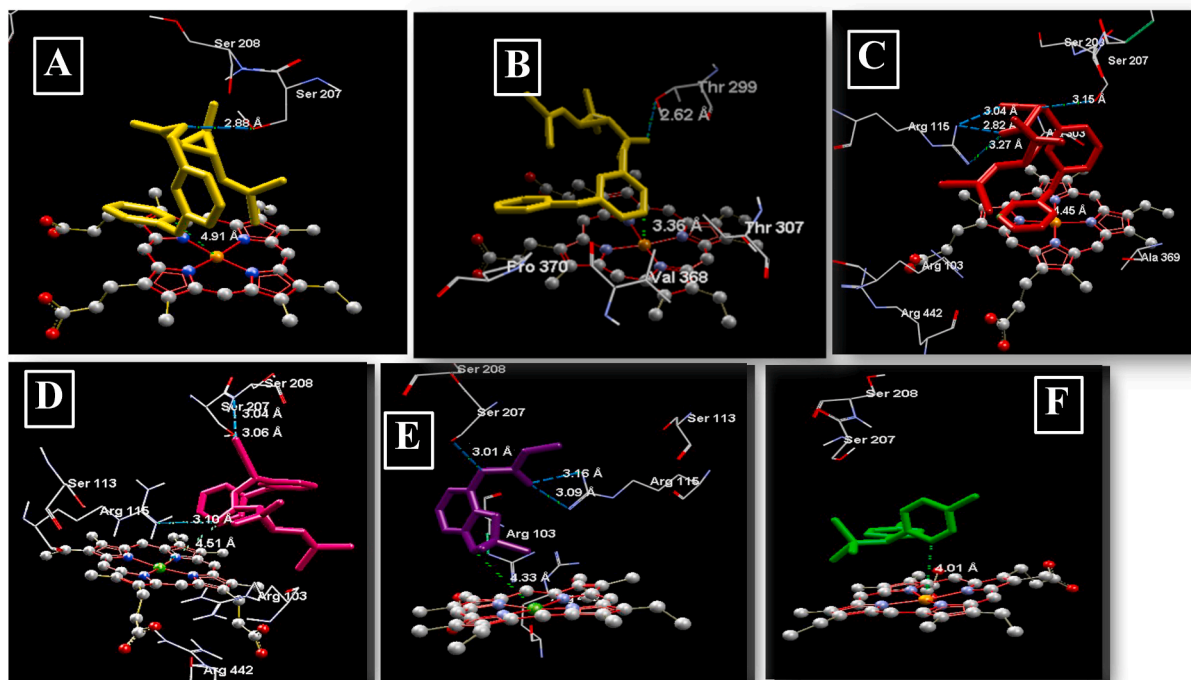


Fig. 3. Comparative *in silico* docking of (A) Permethrin_CMR, (B) Permethrin_DRC, (C) Deltamethrin_CMR, (D) α -Cypermethrin_CMR, (E) Bendiocarb_CMR and (F) DDT_CMR to CYP325A Cameroon model. Poses showing permethrin and deltamethrin in the active site of CYP325A. Permethrin (yellow) and deltamethrin (red), α -cypermethrin (pink), bendiocarb (purple) and DDT (green) is in stick format while CYP325A amino acids are in white stick format. Haem atoms are in stick format and grey/red/blue. Distance between possible sites of metabolism and haem iron is annotated in Angstrom. (For interpretation of the references to colour in this figure legend, the reader is referred to the Web version of this article.)

DDT docked in the CYP325A Cameroon model unproductively with the trichloromethyl group positioned approximately 7 Å away from the haem catalysis centre. No non-bonded interactions, e.g., H-bond or VDW interactions were observed between DDT and the nearby amino acids

(Fig. 3F and Fig. S9E). The postures show there is a very low possibility of reductive dichlorination to produce DDE due to the distance from the haem catalysis site.

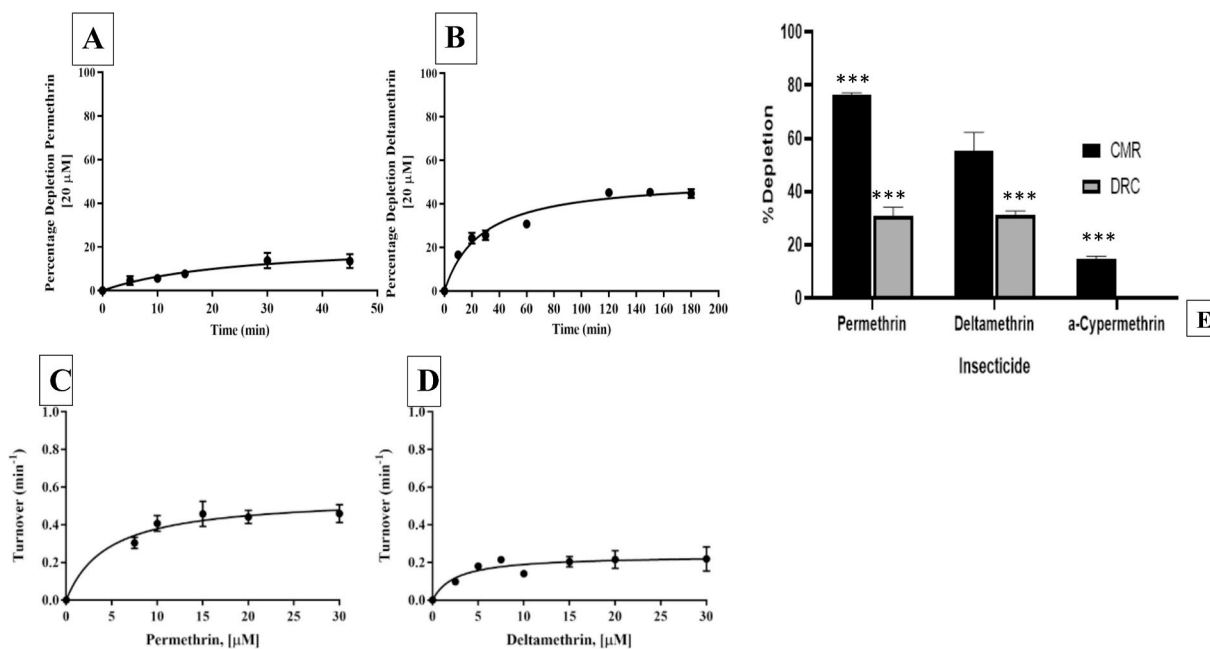


Fig. 4. *In vitro* assay results. Functional confirmation of the metabolic activity of CYP325A conducted for permethrin and deltamethrin using protein membranes. (A) Permethrin metabolism by recombinant CYP325A-CMR (B) Deltamethrin metabolism by recombinant CYP325A-CMR. Michaelis-Menten plot of permethrin and deltamethrin metabolism by recombinant CYP325A-CMR protein. Values are mean \pm SEM of three experimental replicates compared with negative control without NADPH (-NADPH). (C). Permethrin (D). Deltamethrin *** $p < 0.0001$.

3.6. Assessment of metabolic activity of CYP325A

3.6.1. Protein expression pattern of CYP325A

CYP325A expressed with concentrations of 9.606 ± 0.071 nmol protein for Cameroon and 2.29 ± 0.40 nmol protein for DRC.

3.6.2. Validation of the role of *An. funestus* CYP325A in metabolism of insecticides using *in vitro* metabolism assays

Disappearance of 20 μ M insecticides substrates was determined after 90 min of incubation with the recombinant CYP325A in the presence of cytochrome b_5 and NADPH regeneration system. CYP325A-CMR significantly metabolized permethrin with depletion of $76.5\% \pm 0.6$ ($p < 0.0001$), deltamethrin at $55.4\% \pm 6.9$ ($p < 0.0634$) and α -cypermethrin at $14.7\% \pm 1.0$ ($p < 0.0001$), while CYP325A-DRC metabolized permethrin with only a depletion of $30.8\% \pm 3.4$ ($p < 0.0001$) and deltamethrin at $31.2\% \pm 1.6$ ($p < 0.0001$) but showed no activity towards α -cypermethrin (Fig. 4E). For the non-pyrethroid (bendiocarb and propoxur), no depletion was observed indicating lack of enzymatic activity toward carbamate insecticides. Initial analysis of reaction rates established that the CYP325A-CMR metabolized both permethrin and deltamethrin with turnovers of $K_{cat} = 0.613 \text{ min}^{-1} \pm 0.005939$ (95% CI (0.4815–0.8163)) and $K_{cat} = 0.2571 \text{ min}^{-1} \pm 0.0290$ (95% CI (0.199–0.3458)), respectively (Fig. 4A and B). Reaction follows Michaelis-Menten pattern, with a low catalytic rate; $K_{cat} = 0.613 \text{ min}^{-1} \pm 0.006$ and $K_{cat} = 0.2571 \text{ min}^{-1} \pm 0.03$ respectively, for permethrin and deltamethrin (Fig. 4C and D). Reaction speed was more than double for permethrin compared to deltamethrin. However, the affinity (K_m) for deltamethrin was double that of permethrin; $K_m = 4.597 \mu\text{M} \pm 1.819$ and $K_m = 2.349 \mu\text{M} \pm 1.261$, respectively. The K_m values were within the normal range of 1–50 μM , associated with substrate binding and P450 metabolism (Stevenson et al., 2012). Turnover kinetic studies determined K_m and V_{max} values of CYP325A showing enzyme-substrate affinity for pyrethroid however, K_{cat} values obtained for CYP325A are lower than those obtained for CYP6P9a ($5.77 \pm 1.48 \text{ min}^{-1}$ and $5.91 \pm 1.64 \text{ min}^{-1}$ for permethrin and deltamethrin, respectively), CYP6P9b ($6.43 \pm 1.40 \text{ min}^{-1}$ and $7.041 \pm 1.98 \text{ min}^{-1}$ with permethrin and deltamethrin, respectively), CYP6M7 ($5.71 \pm 1.52 \text{ min}^{-1}$ for permethrin and $6.25 \pm 1.67 \text{ min}^{-1}$ for deltamethrin) and CYP6AA1 (K_{cat}) of $11.99 \text{ min}^{-1} \pm 2.17$ and $15.65 \text{ min}^{-1} \pm 2.642$, respectively for permethrin and deltamethrin (Ibrahim et al., 2018; Riveron et al., 2014a).

Thus, the recombinant CYP325A exhibited comparable catalytic efficiency (K_{cat}/K_m) of $0.1333 \text{ min}^{-1}\mu\text{M}^{-1} \pm 0.0527$ for permethrin and $0.109 \text{ min}^{-1}\mu\text{M}^{-1} \pm 0.060$ for deltamethrin.

In this study, it was impossible to use FANG as control because all six FANG sequences obtained had retained all three introns possessed by this gene (Fig. S10).

4. Discussion

Elucidation of resistance mechanisms to insecticides in mosquito vectors of tropical diseases such as malaria is a prerequisite for better management of the growing problem of resistance to existing insecticide classes. If progress has been made in elucidating the molecular basis of pyrethroid resistance in southern African populations of *An. funestus*, little progress has been made in other African regions, most notably Central Africa. This study investigated the role of the overexpressed CYP325A P450 in pyrethroid resistance in *An. funestus* mosquito population in Cameroon, revealing that this gene likely contributes to resistance to types I and II pyrethroids in this region.

4.1. CYP325A over-expression is observed only in Central Africa

qRT-PCR expression patterns revealed a stark contrast in the expression pattern of CYP325A with high over-expression in Cameroon, Central Africa as previously reported by RNAseq (Mugenzi et al., 2019;

Weedall et al., 2019) whereas other populations from other regions exhibit a low expression (Nkemngo et al., 2020). This contrasting expression profile is like that of other Africa-wide transcriptomic analyses which have consistently shown a drastic difference of expression between African regions. This is the case with the duplicated P450s CYP6P9a and CYP6P9b highly over-expressed mainly in southern Africa (Riveron et al., 2013; Weedall et al., 2019). Similarly, GSTe2 was shown to be massively over-expressed mainly in *An. funestus* populations from West Africa, notably in Benin, whereas CYP9K1 is predominantly overexpressed mainly in East Africa (Tchouakui et al., 2021). This contrasting expression of major resistance genes further support evidence that pyrethroid resistance has been independently selected across these regions while also highlighting the potential restriction to gene flow between populations of *An. funestus* across the continent. Such contrast in expression of metabolic resistance genes is also observed in other major malaria vectors including *An. gambiae*, *An. coluzzii*, *An. albimanus* and *An. arabiensis* (Dia et al., 2018; Gueye et al., 2020; Mackenzie-Impoinvil et al., 2019; Mitchell et al., 2012). Interestingly, the CYP6P5 gene was shown to have the most similar expression pattern to CYP325A in Cameroon, where it is also overexpressed (Weedall et al., 2019). This could be linked to their potential common role in resistance as is the case in the Mibellon (Weedall et al., 2020) population. Two transcription factors CCAAT/enhancer binding protein gamma and Adf-1 also showed a high similarity in expression to CYP325A, a possible link between gene expression and regulation (Amador et al., 2001).

4.2. CYP325A metabolism of pyrethroids establishes its role in resistance in Central African *An. funestus*

Both modelling and *in vitro* studies showed that CYP325A alleles from Cameroon and DRC can metabolise type I pyrethroids (permethrin) and type II pyrethroids (deltamethrin). The depletion rates observed against permethrin and deltamethrin are lower than that of other P450s previously shown to metabolise pyrethroids in *An. funestus* such as CYP6P9a (Riveron et al., 2014a), CYP6P9b (Riveron et al., 2013), CYP6M7 (Riveron et al., 2014a), CYP9J11 (Riveron et al., 2017), CYP6AA1 (Ibrahim et al., 2018). This level of depletion is also like that of other genes from *An. gambiae* such as CYP6M2 and CYP6P3 found to mediate metabolic resistance to both type I and II pyrethroids (Müller et al., 2008; Wagah et al., 2021). However, the low depletion rate of CYP325A against alphacypermethrin suggests that it does not confer alphacypermethrin resistance. The inability of CYP325A to metabolise all pyrethroids is similar to previous reports that some genes could metabolise one type of pyrethroid insecticides but not the other as seen for CYP6P4's ability to metabolise permethrin but not deltamethrin in *An. arabiensis* in Chad (Ibrahim et al., 2016b). The inability of CYP325A to metabolise efficiently α -cypermethrin in *An. funestus* mosquitoes could be an advantage for the use of LLINs impregnated with this insecticide such as Interceptor G2 as a vector control tool in the localities where CYP325A-based pyrethroid resistance is predominant in *An. funestus*. However, because other genes may confer alpha-cypermethrin resistance, the susceptibility of field populations to this insecticide should be monitored before making any decision. The CYP325A allele from DRC exhibited a significantly lower efficiency in breaking down pyrethroids than the CMR allele. This is likely due to the allelic variation (E³³¹Q) observed between the sequences from Cameroon and DRC. This allelic variation is due to a key mutation E³³¹Q observed between Cameroon and DRC alleles. The almost fixed nature of E³³¹Q mutations in Cameroon compared to their low frequency in DRC suggests this allele is under selection and will increase over time like the case of CYP6P9a/b in southern Africa (Weedall et al., 2019) and GSTe2 in Benin (Riveron et al., 2014b). The mutations selected and almost fixed in the Cameroon sequences are V²¹L, R²²K, A²⁹K and E³³¹Q, however, the key mutation is at position 331 where glutamic acid (E) is replaced by glutamine (Q) in almost all the Cameroon sequences. This mutation is a major change from an acidic amino acid to a basic amino acid which could greatly

impact the physio-chemical properties of this enzyme. Even though it is not located in any substrate recognition site (SRS), it is in very close proximity to the SRS-4 and the α J loop comprised in the proposed reductase interaction phase playing a role in substrate specificity and their electron transfer partners as part of the haem-binding core along with the α D, α E, α I, α L and α K loops (Sirim et al., 2010b). The impact of allelic variation on the metabolic efficiency of detoxification genes has previously been shown in *An. funestus* for P450s such as *CYP6P9a/b* (Ibrahim et al., 2015) and for the *GSTe2* for which a single L119F amino acid change was shown to drive DDT and pyrethroid resistance in West/central Africa. Such a role of allelic variation is also similar to the case of *CYP6A2* in *Drosophila melanogaster* for which three amino acid substitutions located close to the active site in the allele predominant in DDT-resistant flies, have been shown to confer the increasing metabolism of DDT (Feyereisen, 2012; Li et al., 2007). Further studies, such as site-directed mutagenesis could confirm the role of *CYP325A* over-expression in pyrethroid resistance and the E³³¹Q mutation in the activity of *CYP325A*. Some *CYP450* genes have been established as non-metabolisers of pyrethroids even though they bind productively such as *An. gambiae* *CYP6Z2* for permethrin and α -cypermethrin (McLaughlin et al., 2008) and *An. arabiensis* *CYP6P4*. Our modelling in this study supports productive binding modes for permethrin, deltamethrin and α -cypermethrin, with possibility of binding to bendiocarb, but not DDT. However, the low similarity between *CYP325A* and the template, *CYP3A4* could have resulted in a model with lower quality, which would impact the molecular docking resolution.

4.3. Lack of strong signatures of selective sweep around *CYP325A*

Polymorphism analyses of the *CYP325A* full-length gene in *An. funestus* mosquitoes from across Africa revealed an overall absence of selection across this gene highlighted by the lack of a predominant resistance haplotype despite the previous observation that the E³³¹Q was conferring a greater catalytic ability to the allele from Cameroon. The absence of such positive selection could suggest that the selective pressure is still relatively recent on the population from Cameroon supported by moderate resistance levels observed in Mibellon (Menze et al., 2018). The lack of selection on *CYP325A* could also suggest that this gene acts through increased expression and bioavailability similar to the highly polymorphic *CYP6M7* (Riveron et al., 2014a), and contrary to the observation made for *CYP6P9a/b* for which allelic variation drives resistance through directionally selected alleles now nearly fixed in field populations from southern Africa (Riveron et al., 2013; Weedall et al., 2019, 2020).

Furthermore, the regional comparison of the transcription profile of pyrethroid resistance in *An. funestus* cDNA across Africa and 1 kb putative promoter in permethrin susceptible (dead) and resistant (alive) mosquitoes from Mibellon, Cameroon revealed several facts. The polymorphism pattern analysis revealed a possible selection in the promoter region notably in Cameroon although further analyses are needed to confirm the extent of this selection and its impact on the cis regulation of *CYP325A*. A preliminary screening of the transcription factors binding sites in this promoter region using Alggen online software revealed the presence of binding sites for Cncc/Maf, H96, Dfd-1 and AHR/Arnt; all xenobiotic sensors previously implicated in regulation of detoxification genes like P450s (Hu et al., 2019, 2021). Further promoter activity analyses will establish the impact of these polymorphisms on the activity of *CYP325A* across Africa potentially helping to detect causative markers driving *CYP325A*-based pyrethroid resistance as done for *CYP6P9a/b* (Mugenzi et al., 2019; Weedall et al., 2019).

5. Conclusion

Knowledge of the underlying mechanisms and molecular drivers of insecticide resistance is crucial in the efficient management of insecticide resistance in malaria vectors. However, such knowledge requires

understanding the molecular basis of the resistance which can then be applied by vector control programs for more effective intervention and management strategies. Here, we established that the P450 *CYP325A* is highly implicated in the resistance against the bed net insecticides permethrin and deltamethrin in the *An. funestus* mosquito population in Cameroon, Central Africa. These findings will help pave the way to detect the associated molecular markers to facilitate the design of DNA-based diagnostic tools to track this resistance in the field.

Author contributions

CSW conceived and designed the study. JDB was the academic supervisor of the study and reviewed the manuscript; ANRW performed the molecular and biochemical experiments with contributions from SSI and MOK; ANRW, SSI and AM conducted the *in vitro* assays; JH performed the Poolseq analyses and writeup, MJW provided the qRT-PCR data and handled the sequencing process at CRID, HI helped acquire pCW plasmid for the enzyme characterization work and handled the sequencing process at LSTM, LMJM contributed to the population genetics analyses, ANRW analysed the data with contributions from CSW, JH, LMJM, SSI and MOK; ANRW, SSI, JH, and CSW wrote the manuscript with contributions from all authors.

Accession numbers

CYP325A sequences- GenBank MW542209-MW542311 for the 1 kb putative promoter and cDNA. Data analysed in this study are available in public repositories (ENA archive for Cameroon PoolSeq: PRJEB24384) or available within the article and its Supplementary Information files. Further details are available from the authors upon request.

Funding

This work was supported by a Wellcome Trust Senior Research Fellowship in Biomedical Sciences to CSW (101893/Z/13/Z and 217188/Z/19/Z).

Declaration of competing interest

The authors declare no competing interests.

Acknowledgements

We thank Dr Magellan Tchouakui, Williams Tchappa, Tchoupa Micareme, Ebai Terence, Doumani Djonabaye, Mangoua Mersimine, Fotso Toguem Yvan, Dr Tresor Melachio, and Dr Daniel Nguete from CRID, for assistance in optimisation, logistics and data analyses. A special thanks to Dr Mark Paine (LSTM) for providing the pCW-ori + plasmid used in enzyme characterization in this study.

Appendix A. Supplementary data

Supplementary data to this article can be found online at <https://doi.org/10.1016/j.ibmb.2021.103647>.

References

- Amador, A., Papaceit, M., Juan, E., 2001. Evolutionary change in the structure of the regulatory region that drives tissue and temporally regulated expression of alcohol dehydrogenase gene in *Drosophila funebris*. *Insect Mol. Biol.* 10 (3), 237–247.
- Antonio-Nkondjio, C., Defo-Talom, B., Tagne-Fotso, R., Tene-Fossog, B., Ndo, C., Lehman, L.G., Awono-Ambene, P., 2012. High mosquito burden and malaria transmission in a district of the city of Douala, Cameroon. *BMC Infect. Dis.* 12 (1), 275.
- Antonio-Nkondjio, C., Fossog, B.T., Ndo, C., Djantio, B.M., Togouet, S.Z., Awono-Ambene, P., Ranson, H., 2011. *Anopheles gambiae* distribution and insecticide resistance in the cities of Douala and Yaoundé (Cameroon): influence of urban agriculture and pollution. *Malar. J.* 10 (1), 154.

- Barnes, K.G., Irving, H., Chiumia, M., Mzilahowa, T., Coleman, M., Hemingway, J., Wondji, C.S., 2017. Restriction to gene flow is associated with changes in the molecular basis of pyrethroid resistance in the malaria vector *Anopheles funestus*. *Proc. Natl. Acad. Sci. Unit. States Am.* 114 (2), 286–291.
- Bitencourt-Ferreira, G., de Azevedo, W.F., 2019. Molegro Virtual Docker for Docking *Docking Screens For Drug Discovery*. Springer, pp. 149–167.
- Chiu, T.-L., Wen, Z., Rupasinghe, S.G., Schuler, M.A., 2008. Comparative molecular modeling of *Anopheles gambiae* CYP6Z1, a mosquito P450 capable of metabolizing DDT. *Proc. Natl. Acad. Sci. Unit. States Am.* 105 (26), 8855–8860.
- Cingolani, P., Platts, A., Wang, L.L., Coon, M., Nguyen, T., Wang, L., Ruden, D.M., 2012. A program for annotating and predicting the effects of single nucleotide polymorphisms, SnpEff: SNPs in the genome of *Drosophila melanogaster* strain w1118; iso-2; iso-3. *Fly* 6 (2), 80–92.
- Clement, M., Posada, D., Crandall, K.A., 2000. TCS: a computer program to estimate gene genealogies. *Mol. Ecol.* 9 (10), 1657–1659.
- Clement, M., Snell, Q., Walker, P., Posada, D., Crandall, K., 2002. TCS: estimating gene genealogies. Paper presented at the Parallel and Distributed Processing Symposium. International 3, 0184-0184.
- Coetzee, M., 2020. Key to the females of Afrotropical *Anopheles* mosquitoes (Diptera: Culicidae). *Malar. J.* 19 (1), 1–20.
- Colovos, C., Yeates, T.O., 1993. Verification of protein structures: patterns of nonbonded atomic interactions. *Protein Sci.* 2 (9), 1511–1519.
- Cuamba, N., Morgan, J.C., Irving, H., Steven, A., Wondji, C.S., 2010. High level of pyrethroid resistance in an *Anopheles funestus* population of the Chokwe District in Mozambique. *PLoS One* 5 (6), e11010.
- D Menze, B., Wondji, M.J., Tchappa, W., Tchoupo, M., Riveron, J.M., Wondji, C.S., 2018. Bionomics and insecticides resistance profiling of malaria vectors at a selected site for experimental hut trials in central Cameroon. *Malar. J.* 17 (1), 1–10.
- DeLano, W.L., Bromberg, S., 2004. PyMOL User's Guide. DeLano Scientific LLC, p. 629.
- Dia, A.K., Guèye, O.K., Niang, A.E., Diédhiou, S.M., Sy, M.D., Konaté, A., Faye, O., 2018. Insecticide resistance in *Anopheles arabiensis* populations from Dakar and its suburbs: role of target site and metabolic resistance mechanisms. *Malar. J.* 17 (1), 1–9.
- Diengou, N.H., Cumber, S.N., Nkfusai, C.N., Mbinyui, M.S., Viyoff, V.Z., Bede, F., Judith, A.-K., 2020. Factors associated with the uptake of intermittent preventive treatment of malaria in pregnancy in the Bamenda health districts, Cameroon. *The Pan African Medical Journal* 35.
- Djouaka, R., Riveron, J.M., Yessoufou, A., Tchigossou, G., Akoton, R., Irving, H., Tamò, M., 2016. Multiple insecticide resistance in an infected population of the malaria vector *Anopheles funestus* in Benin. *Parasites Vectors* 9 (1), 1–12.
- Eldridge, M.D., Murray, C.W., Auton, T.R., Paoloni, G.V., Mee, R.P., 1997. Empirical scoring functions: I. The development of a fast empirical scoring function to estimate the binding affinity of ligands in receptor complexes. *J. Comput. Aided Mol. Des.* 11 (5), 425–445.
- Feyereisen, R., 2012. Insect CYP Genes and P450 Enzymes *Insect Molecular Biology and Biochemistry*. Elsevier, pp. 236–316.
- Fiser, A., Sali, A., 2003. Modeller: Generation and Refinement of Homology-Based Protein Structure Models Methods in Enzymology, vol. 374. Elsevier, pp. 461–491.
- Ghurye, J., Koren, S., Small, S.T., Redmond, S., Howell, P., Phillippy, A.M., Besansky, N. J., 2019. A chromosome-scale assembly of the major African malaria vector *Anopheles funestus*. *GigaScience* 8 (6), giz063.
- Gotoh, O., 1992. Substrate recognition sites in cytochrome P450 family 2 (CYP2) proteins inferred from comparative analyses of amino acid and coding nucleotide sequences. *J. Biol. Chem.* 267 (1), 83–90.
- Guengerich, F.P., Martin, M.V., Sohl, C.D., Cheng, Q., 2009. Measurement of cytochrome P450 and NADPH-cytochrome P450 reductase. *Nat. Protoc.* 4 (9), 1245–1251.
- Gueye, O., Tchouakui, M., Dia, A.K., Faye, M.B., Ahmed, A.A., Wondji, M.J., Konaté, L., 2020. Insecticide resistance profiling of *Anopheles coluzzii* and *Anopheles gambiae* populations in the southern Senegal: role of target sites and metabolic resistance mechanisms. *Genes* 11 (12), 1403.
- Hall, T., Bioinformatics, I., Carlsbad, C., 2011. BioEdit: an important software for molecular biology. *GERF Bull. Biosci.* 2 (1), 60–61.
- Hall, T.A., 1999. BioEdit: a User-Friendly Biological Sequence Alignment Editor and Analysis Program for Windows 95/98/NT. In: Paper Presented at the Nucleic Acids Symposium Series.
- Hemingway, J., 2014. The role of vector control in stopping the transmission of malaria: threats and opportunities. *Phil. Trans. Biol. Sci.* 369 (1645), 20130431.
- Hu, B., Huang, H., Hu, S., Ren, M., Wei, Q., Tian, X., Reddy Palli, S., 2021. Changes in both trans- and cis-regulatory elements mediate insecticide resistance in a lepidopteran pest, *Spodoptera exigua*. *PLoS Genet.* 17 (3), e1009403.
- Hu, B., Huang, H., Wei, Q., Ren, M., Mburu, D.K., Tian, X., Su, J., 2019. Transcription factors CncC/Maf and AhR/ARNT coordinately regulate the expression of multiple GSTs conferring resistance to chlorpyrifos and cypermethrin in *Spodoptera exigua*. *Pest Manag. Sci.* 75 (7), 2009–2019.
- Ibrahim, S.S., Amvongo-Adjia, N., Wondji, M.J., Irving, H., Riveron, J.M., Wondji, C.S., 2018. Pyrethroid resistance in the major malaria vector *Anopheles funestus* is exacerbated by overexpression and overactivity of the P450 CYP6AA1 across Africa. *Genes* 9 (3), 140.
- Ibrahim, S.S., Mukhtar, M.M., Datti, J.A., Irving, H., Kusimo, M.O., Tchappa, W., Wondji, C.S., 2019. Temporal escalation of Pyrethroid Resistance in the major malaria vector *Anopheles coluzzii* from Sahelo-Sudanian Region of northern Nigeria. *Sci. Rep.* 9 (1), 7395. <https://doi.org/10.1038/s41598-019-43634-4>.
- Ibrahim, S.S., Ndula, M., Riveron, J.M., Irving, H., Wondji, C.S., 2016a. The P450 CYP 6Z1 confers carbamate/pyrethroid cross-resistance in a major African malaria vector beside a novel carbamate-insensitive N485I acetylcholinesterase-1 mutation. *Mol. Ecol.* 25 (14), 3436–3452.
- Ibrahim, S.S., Riveron, J.M., Bibby, J., Irving, H., Yunta, C., Paine, M.J., Wondji, C.S., 2015. Allelic variation of cytochrome P450s drives resistance to bednet insecticides in a major malaria vector. *PLoS Genet.* 11 (10), e1005618.
- Ibrahim, S.S., Riveron, J.M., Stott, R., Irving, H., Wondji, C.S., 2016b. The cytochrome P450 CYP6P4 is responsible for the high pyrethroid resistance in knockdown resistance-free *Anopheles arabiensis*. *Insect Biochem. Mol. Biol.* 68, 23–32.
- Joó, B., Clark, M.A., 2012. Lattice QCD on GPU clusters, using the QUDA library and the Chroma software system. *Int. J. High Perform. Comput. Appl.* 26 (4), 386–398.
- Kim, T.K., 2015. T test as a parametric statistic. *Korean journal of anesthesiology* 68 (6), 540.
- Koboldt, D.C., Chen, K., Wylie, T., Larson, D.E., McLellan, M.D., Mardis, E.R., Ding, L., 2009. VarScan: variant detection in massively parallel sequencing of individual and pooled samples. *Bioinformatics* 25 (17), 2283–2285.
- Koekemoer, L., Kamau, L., Hunt, R., Coetzee, M., 2002. A cocktail polymerase chain reaction assay to identify members of the *Anopheles funestus* (Diptera: Culicidae) group. *Am. J. Trop. Med. Hyg.* 66 (6), 804–811.
- Korb, O., Stutzle, T., Exner, T.E., 2009. Empirical scoring functions for advanced protein–ligand docking with PLANTS. *J. Chem. Inf. Model.* 49 (1), 84–96.
- Kumar, S., Stecher, G., Li, M., Niyaz, C., Tamura, K., 2018. MEGA X: molecular evolutionary genetics analysis across computing platforms. *Mol. Biol. Evol.* 35 (6), 1547–1549.
- Kumar, S., Tamura, K., Nei, M., 1994. MEGA: molecular evolutionary genetics analysis software for microcomputers. *Bioinformatics* 10 (2), 189–191.
- Kwiatkowska, R.M., Platt, N., Poupardin, R., Irving, H., Dabire, R.K., Mitchell, S., Wondji, C.S., 2013. Dissecting the mechanisms responsible for the multiple insecticide resistance phenotype in *Anopheles gambiae* ss, M form, from Vallee du Kou, Burkina Faso. *Gene* 519 (1), 98–106.
- Li, H., Durbin, R., 2009. Fast and accurate short read alignment with Burrows–Wheeler transform. *Bioinformatics* 25 (14), 1754–1760.
- Li, H., Handsaker, B., Wysoker, A., Fennell, T., Ruan, J., Homer, N., Durbin, R., 2009. The sequence alignment/map format and SAMtools. *Bioinformatics* 25 (16), 2078–2079.
- Li, X., Schuler, M.A., Berenbaum, M.R., 2007. Molecular mechanisms of metabolic resistance to synthetic and natural xenobiotics. *Annu. Rev. Entomol.* 52, 231–253.
- Livak, K.J., 1984. Organization and mapping of a sequence on the *Drosophila melanogaster* X and Y chromosomes that is transcribed during spermatogenesis. *Genetics* 107 (4), 611–634.
- Livak, K.J., Schmittgen, T.D., 2001. Analysis of relative gene expression data using real-time quantitative PCR and the 2⁻ΔΔCT method. *Methods* 25 (4), 402–408.
- Mackenzie-Impoinvil, L., Weedall, G.D., Lol, J.C., Pinto, J., Viccaino, L., Dzuris, N., Lenhart, A., 2019. Contrasting patterns of gene expression indicate differing pyrethroid resistance mechanisms across the range of the New World malaria vector *Anopheles albimanus*. *PLoS One* 14 (1), e0210586.
- McHugh, M.L., 2013. The chi-square test of independence. *Biochem. Med.* 23 (2), 143–149.
- McLaughlin, L., Niazi, U., Bibby, J., David, J.P., Vontas, J., Hemingway, J., Paine, M., 2008. Characterization of inhibitors and substrates of *Anopheles gambiae* CYP6Z2. *Insect Mol. Biol.* 17 (2), 125–135.
- Mendis, K., Rietveld, A., Warsame, M., Bosman, A., Greenwood, B., Wernsdorfer, W.H., 2009. From malaria control to eradication: the WHO perspective. *Trop. Med. Int. Health* 14 (7), 802–809.
- Menze, B.D., Wondji, M.J., Tchappa, W., Tchoupo, M., Riveron, J.M., Wondji, C.S., 2018. Bionomics and insecticides resistance profiling of malaria vectors at a selected site for experimental hut trials in central Cameroon. *Malar. J.* 17 (1), 1–10.
- Mitchell, S.N., Stevenson, B.J., Müller, P., Wilding, C.S., Egyri-Yawson, A., Field, S.G., Donnelly, M.J., 2012. Identification and validation of a gene causing cross-resistance between insecticide classes in *Anopheles gambiae* from Ghana. *Proc. Natl. Acad. Sci. Unit. States Am.* 109 (16), 6147–6152.
- Morgan, J.C., Irving, H., Okedi, L.M., Steven, A., Wondji, C.S., 2010. Pyrethroid resistance in an *Anopheles funestus* population from Uganda. *PLoS One* 5 (7), e11872.
- Moyes, C.L., Lees, R.S., Yunta, C., Walker, K.J., Hemmings, K., Oladepo, F., Ismail, H.M., 2020. Evaluating the Evidence from Molecular Structure and Population Studies for Cross-Resistance to the Pyrethroids Used in Malaria Vector Control.
- Mugenzi, L.M., Menze, B.D., Tchouakui, M., Wondji, M.J., Irving, H., Tchoupo, M., Wondji, C.S., 2019. Cis-regulatory CYP6P9b P450 variants associated with loss of insecticide-treated bed net efficacy against *Anopheles funestus*. *Nat. Commun.* 10 (1), 1–11.
- Müller, P., Warr, E., Stevenson, B.J., Pignatelli, P.M., Morgan, J.C., Steven, A., Hemingway, J., 2008. Field-caught permethrin-resistant *Anopheles gambiae* overexpress CYP6P3, a P450 that metabolises pyrethroids. *PLoS Genet.* 4 (11), e1000286.
- Nelson, C.W., Moncla, L.H., Hughes, A.L., 2015. SNPGenie: estimating evolutionary parameters to detect natural selection using pooled next-generation sequencing data. *Bioinformatics* 31 (22), 3709–3711.
- Nikou, D., Ranson, H., Hemingway, J., 2003. An adult-specific CYP6 P450 gene is overexpressed in a pyrethroid-resistant strain of the malaria vector, *Anopheles gambiae*. *Gene* 318, 91–102.
- Nkemngbo, F.N., Mugenzi, L.M., Terence, E., Niang, A., Wondji, M.J., Tchoupo, M., Ntahi, J.D., 2020. Elevated Plasmodium sporozoite infection and multiple insecticide resistance in the principal malaria vectors *Anopheles funestus* and *Anopheles gambiae* in a forested locality close to the Yaoundé airport, Cameroon. *Wellcome Open Research* 5.
- Okia, M., Hoel, D.F., Kirunda, J., Rwakimari, J.B., Mpeka, B., Ambayo, D., Govere, J., 2018. Insecticide resistance status of the malaria mosquitoes: *Anopheles gambiae* and *Anopheles funestus* in eastern and northern Uganda. *Malar. J.* 17 (1), 1–12.

- Omura, T., Sato, R., 1964. The carbon monoxide-binding pigment of liver microsomes: I. Evidence for its hemoprotein nature. *J. Biol. Chem.* 239 (7), 2370–2378.
- Poulos, T.L., Finzel, B., Gunsalus, I., Wagner, G.C., Kraut, J., 1985. The 2.6-Å crystal structure of *Pseudomonas putida* cytochrome P-450. *J. Biol. Chem.* 260 (30), 16122–16130.
- Poulos, T.L., Finzel, B.C., Howard, A.J., 1987. High-resolution crystal structure of cytochrome P450cam. *J. Mol. Biol.* 195 (3), 687–700.
- Pritchard, M.P., Ossetian, R., Li, D.N., Henderson, C.J., Burchell, B., Wolf, C.R., Friedberg, T., 1997. A general strategy for the expression of recombinant human cytochrome P450s in *Escherichia coli* using bacterial signal peptides: expression of CYP3A4, CYP2A6, and CYP2E1. *Arch. Biochem. Biophys.* 345 (2), 342–354.
- Riveron, J.M., Chiumia, M., Menze, B.D., Barnes, K.G., Irving, H., Ibrahim, S.S., Wondji, C.S., 2015. Rise of multiple insecticide resistance in *Anopheles funestus* in Malawi: a major concern for malaria vector control. *Malar. J.* 14 (1), 344.
- Riveron, J.M., Ibrahim, S.S., Chanda, E., Mzilahowa, T., Cuamba, N., Irving, H., Wondji, C.S., 2014a. The highly polymorphic CYP6M7 cytochrome P450 gene partners with the directionally selected CYP6P9a and CYP6P9b genes to expand the pyrethroid resistance front in the malaria vector *Anopheles funestus* in Africa. *BMC Genom.* 15 (1), 817.
- Riveron, J.M., Ibrahim, S.S., Mulamba, C., Djouaka, R., Irving, H., Wondji, M.J., Wondji, C.S., 2017. Genome-wide transcription and functional analyses reveal heterogeneous molecular mechanisms driving pyrethroids resistance in the major malaria vector *Anopheles funestus* across Africa. *G3: Genes, Genomes, Genetics* 7 (6), 1819–1832.
- Riveron, J.M., Irving, H., Ndula, M., Barnes, K.G., Ibrahim, S.S., Paine, M.J., Wondji, C.S., 2013. Directionally selected cytochrome P450 alleles are driving the spread of pyrethroid resistance in the major malaria vector *Anopheles funestus*. *Proc. Natl. Acad. Sci. Unit. States Am.* 110 (1), 252–257.
- Riveron, J.M., Osaie, M., Egyir-Yawson, A., Irving, H., Ibrahim, S.S., Wondji, C.S., 2016. Multiple insecticide resistance in the major malaria vector *Anopheles funestus* in southern Ghana: implications for malaria control. *Parasites Vectors* 9 (1), 504.
- Riveron, J.M., Tchouakui, M., Mugenzi, L., Menze, B.D., Chiang, M.-C., Wondji, C.S., 2018a. Insecticide Resistance in Malaria Vectors: an Update at a Global Scale *Towards Malaria Elimination-A Leap Forward*. IntechOpen.
- Riveron, J.M., Watsenga, F., Irving, H., Irish, S.R., Wondji, C.S., 2018b. High Plasmodium infection rate and reduced bed net efficacy in multiple insecticide-resistant malaria vectors in Kinshasa, Democratic Republic of Congo. *J. Infect. Dis.* 217 (2), 320–328.
- Riveron, J.M., Yunta, C., Ibrahim, S.S., Djouaka, R., Irving, H., Menze, B.D., Albert, A., 2014b. A single mutation in the GSTe2 gene allows tracking of metabolically based insecticide resistance in a major malaria vector. *Genome Biol.* 15 (2), R27.
- Robinson, J., Thorvaldsdottir, H., Winckler, W., Guttman, M., Lander, E., 2011. Etx G, Mesirov JP, Integrative genomics viewer. *Nat. Biotechnol.* 29, 24–26.
- Rozas, J., Ferrer-Mata, A., Sánchez-DelBarrio, J.C., Guirao-Rico, S., Librado, P., Ramos-Onsins, S.E., Sánchez-Gracia, A., 2017. DnaSP 6: DNA sequence polymorphism analysis of large data sets. *Mol. Biol. Evol.* 34 (12), 3299–3302.
- Rozas, J., Sánchez-DelBarrio, J.C., Messeguer, X., Rozas, R., 2003. DnaSP, DNA polymorphism analyses by the coalescent and other methods. *Bioinformatics* 19 (18), 2496–2497.
- Šali, A., Pottert, L., Yuan, F., van Vlijmen, H., Karplus, M., 1995. Evaluation of comparative protein modeling by MODELLER. *Proteins: Structure, Function, and Bioinformatics* 23 (3), 318–326.
- Sato, T.O.a.R., 1964. The carbon monoxide-binding pigment of liver microsomes. *J. Biol. Chem.* 239 (7).
- Sirim, D., Widmann, M., Wagner, F., Pleiss, J., 2010a. Prediction and analysis of the modular structure of cytochrome P450 monooxygenases. *BMC Struct. Biol.* 10 (1), 34.
- Sirim, D., Widmann, M., Wagner, F., Pleiss, J., 2010b. Prediction and analysis of the modular structure of cytochrome P450 monooxygenases. *BMC Struct. Biol.* 10 (1), 1–12.
- Sterling, T., Irwin, J.J., 2015. ZINC 15—ligand discovery for everyone. *J. Chem. Inf. Model.* 55 (11), 2324–2337.
- Stevenson, B., Bibby, J., Pignatelli, P., Muangnoicharoen, S., O'Neill, P.M., Lian, L.-Y., Hemingway, J., 2011. Cytochrome P450 6M2 from the malaria vector *Anopheles gambiae* metabolizes pyrethroids: sequential metabolism of deltamethrin revealed. *Insect Biochem. Mol. Biol.* 41 (7), 492–502.
- Stevenson, B.J., Bibby, J., Pignatelli, P., Muangnoicharoen, S., O'Neill, P.M., Lian, L.-Y., Hemingway, J., 2011. Cytochrome P450 6M2 from the malaria vector *Anopheles gambiae* metabolizes pyrethroids: sequential metabolism of deltamethrin revealed. *Insect Biochem. Mol. Biol.* 41 (7), 492–502.
- Stevenson, B.J., Bibby, J., Pignatelli, P., Muangnoicharoen, S., O'Neill, P.M., Lian, L.-Y., Paine, M.J.I., 2011. Cytochrome P450 6M2 from the malaria vector *Anopheles gambiae* metabolizes pyrethroids: sequential metabolism of deltamethrin revealed. *Insect Biochem. Mol. Biol.* 41 (7), 492–502. <https://doi.org/10.1016/j.ibmb.2011.02.003>.
- Stevenson, B.J., Pignatelli, P., Nikou, D., Paine, M.J., 2012. Pinpointing P450s associated with pyrethroid metabolism in the dengue vector, *Aedes aegypti*: developing new tools to combat insecticide resistance. *PLoS Neglected Trop. Dis.* 6 (3), e1595.
- Swift, M.L., 1997. GraphPad prism, data analysis, and scientific graphing. *J. Chem. Inf. Comput. Sci.* 37 (2), 411–412.
- Tchigossou, G., Djouaka, R., Akoton, R., Riveron, J.M., Irving, H., Atoyebi, S., Wondji, C.S., 2018. Molecular basis of permethrin and DDT resistance in an *Anopheles funestus* population from Benin. *Parasites Vectors* 11 (1), 1–13.
- Tchouakui, M., Mugenzi, L.M., D Menze, B., Khauka, J.N., Tchappa, W., Tchoupe, M., Wondji, C.S., 2021. Pyrethroid resistance aggravation in Ugandan malaria vectors is reducing bednet efficacy. *Pathogens* 10 (4), 415.
- Tchuinkam, T., Nyih-Kong, B., Fopa, F., Simard, F., Antonio-Nkondjio, C., Awono-Ambene, H.-P., Mpoame, M., 2015. Distribution of *Plasmodium falciparum* gametocytes and malaria-attributable fraction of fever episodes along an altitudinal transect in Western Cameroon. *Malar. J.* 14 (1), 96.
- Thompson, J.D., Gibson, T.J., Higgins, D.G., 2003. Multiple sequence alignment using ClustalW and ClustalX. *Current protocols in bioinformatics* (1), 2.3. 1–32.3. 22.
- Tonye, S.G.M., Kouambeng, C., Wounang, R., Vounatsou, P., 2018. Challenges of DHS and MIS to capture the entire pattern of malaria parasite risk and intervention effects in countries with different ecological zones: the case of Cameroon. *Malar. J.* 17 (1), 156.
- Wagah, M.G., Korlević, P., Clarkson, C., Miles, A., Lawnczak, M.K., Makunin, A., 2021. Genetic variation at the Cyp6m2 putative insecticide resistance locus in *Anopheles gambiae* and *Anopheles coluzzii*. *Malar. J.* 20 (1), 1–13.
- Webb, B., Sali, A., 2014. Protein Structure Modeling with MODELLER *Protein Structure Prediction*. Springer, pp. 1–15.
- Weedall, G.D., Mugenzi, L.M., Menze, B.D., Tchouakui, M., Ibrahim, S.S., Amvongo-Adjia, N., Djouaka, R., 2019. A cytochrome P450 allele confers pyrethroid resistance on a major African malaria vector, reducing insecticide-treated bednet efficacy. *Sci. Transl. Med.* 11 (484).
- Weedall, G.D., Riveron, J.M., Hearn, J., Irving, H., Kamdem, C., Fouet, C., Wondji, C.S., 2020. An Africa-wide genomic evolution of insecticide resistance in the malaria vector *Anopheles funestus* involves selective sweeps, copy number variations, gene conversion and transposons. *PLoS Genet.* 16 (6), e1008822.
- WHO, 2016. Test Procedures for Insecticide Resistance Monitoring in Malaria Vector Mosquitoes.
- WHO, 2020. World Malaria Report 2020: 20 Years of Global Progress and Challenges.
- Willits, W.G., Gilmartin, P.M., Mikkelsen, J.D., Knox, J.P., 1999. Cell wall antibodies without immunization: generation and use of de-esterified homogalacturonan block-specific antibodies from a naive phage display library. *Plant J.* 18 (1), 57–65.
- Wondji, C.S., Morgan, J., Coetzee, M., Hunt, R.H., Steen, K., Black, W.C., Ranson, H., 2007. Mapping a quantitative trait locus (QTL) conferring pyrethroid resistance in the African malaria vector *Anopheles funestus*. *BMC Genom.* 8 (1), 1–14.
- Yano, J.K., Wester, M.R., Schoch, G.A., Griffin, K.J., Stout, C.D., Johnson, E.F., 2004. The structure of human microsomal cytochrome P450 3A4 determined by X-ray crystallography to 2.05-Å resolution. *J. Biol. Chem.* 279 (37), 38091–38094.